An Approach for Upscaling the Flow Effects of Multiple Deep-Water Genetic Units

Jiangchen Han

Submitted for the degree of Doctor of Philosophy

Heriot-Watt University

Institute of Petroleum Engineering
School of Energy, Geoscience, Infrastructure and Society

July 2015

Abstract

Developing a deep-water basin raises many issues and challenges; one of the most significant and necessary issues is overpressure prediction. Basin modelling to construct full scale models is an effective way to find out overpressure distribution in many conditions. However, with current modelling and other methods, it is difficult to obtain data about highly heterogeneous complex structures, which involve coupling between hydraulics and geo-mechanics (compaction) in a system with spatial complexity and temporal evolution of geological bodies, termed as genetic units (GUs). The data collection is difficult and costly in both economic and time aspects.

Understanding the role of the interactions between GUs could play a major role in helping to simplify the highly heterogeneous complex structures. The aim of this thesis is to develop the understanding that can underpin the creation of a workflow to be used to assess the role of interactions between GUs, in relation to predicting overpressure in deep-water sedimentary basins.

Tilted sandy aquifers enclosed in muddy sediments (block rotation) are a good reference case which is not uncommon in deep-water basins worldwide. This thesis shows that, by applying basin modelling and response surface methodology, not only is a parameterised prediction possible but also the uncertainty of the parameters can be taken into consideration at the same time.

A tilted aquifer, however, rarely exists alone within a 'featureless' mud background, but occurs along with other geological architectures of sediment units of the same genetic origins, deposited later. These genetic units may be channels and levees. The GUs could allow the fluid energy to dissipate more easily and therefore can reduce the overpressure at the crest. However, the existence of additional GUs complicates the prediction of the overpressure, as the dimensions of parameter space increases dramatically. This poses a big challenge to extend the prediction, and therefore calls for development of appropriate parameterised overpressure-prediction techniques. This thesis reports the development of parameterised overpressure-prediction techniques in the presence of multiple channels. This result forms the basis for follow-on research that can seek to further generalise the approach to a wider set of systems and their associated descriptive parameters.

Acknowledgement

I would like to thank my supervisors, Prof. Gary. D. Couples and Dr Jingsheng Ma with deepest gratitude, for providing me the opportunity to pursue PhD degree in The Institute of Petroleum Engineering (IPE), Heriot-Watt University, UK. My research work would not have been completed without their continuous guidance, fantastic advices, hard push and effective encouragement.

I would also like to acknowledge my appreciation to "Caprocks" project sponsors for their financial support in 2011-2012. Although the project had finished since two years ago, I still would like to express extraordinary appreciations to members in "Caprocks" research group for their unconditional help and kind encouragements.

I am very grateful to the research staff, secretaries, and all other supporting staff of IPE. I thank all my friends for technical discussions and social interactions – especially those whom I met regularly at lunch at Energy Academy.

Last but not least, my special thanks go to my parents who are willing to share happiness with me and to support me with their selfless love.

Contents

Figure Content

Table Content

Nomenclature

Symbol	Description
R(T)	Unknown true overpressure at a reference point in a basin
F(Y)	Overpressure value from basin modelling method prediction
F(X)	Unknown functional relationship between parameters in space X and the true response
F(x)	Overpressure value from basin modelling method prediction without CLS influence
G(XCLS), G(Z)	Channel-levee systems fluid interaction influence on overpressure at RP
G(X*,z), g(z)	Channel-levee systems fluid interaction influence on overpressure at RP with parameters R,C,D,H are constant
f(X)	Fitting result for F(X) from response surface methodology
h(z)	Fitting result for g(z) from response surface methodology
gg(z)	Upscaling fitting results of two CLS cluster fluid interaction on overpressure from response surface methodology
T	Parameters can influence overpressure in nature
Y	Parameters can influence overpressure in basin modelling
X	Belong to Y which was simplified to predict overpressure in RP
Z	Parameters can influence overpressure in channel-levee systems fluid interaction
X*	Constant value of influence parameters R,C,D,H
z	Influence parameters in channel-levee systems fluid interaction which removed parameters R,C,D,H
R	Influence parameter in X: Sedimentation rate
C, r	Influence parameter in X: Overburden mud clay content
D	Influence parameter in X: Reference point depth
H	Influence parameter in X: Relief of aquifer
B	Influence parameter in X: Bending of aquifer
S	Influence parameter in z: Area of channel-levee system
L	Influence parameter in z: Horizontal position of channel-levee system
d	Influence parameter in z: Vertical position of channel-levee system
E(), ε()	Error items in each parts

W	Vertical thickness of overlying sediments
b	Average bulk density
P	Fluid pressure
P*	Fluid overpressure
P_{ms}	Mudstone pressure
B_P	Pore pressure build-up coefficient
K	Hydraulic conductivity
S_t	Storage
T	Temperature
P_{clay}	Clay dehydration pressure component
K_{hh}	Horizontal permeability
K_{vh}	Vertical permeability
$\boldsymbol{\sigma}$, S_v	Overburden stress
$\boldsymbol{\sigma}'$	Effective stress
β	Bulk compressibility
β_f	Fluid compressibility
Φ_η	Porosity in compacted reference
ρ_f	Fluid density
σ_L	Lithostatic stress
α_m	Matrix thermal expansion coefficient
δ	Decay constant
e	Void ratio
e_{100}	Initial void ratio
Φ	Porosity
Φ_0	Initial porosity at sea floor
Φ_1	Average porosity
a	Anisotropy factor

Chapter 1. INTRODUCTION

1.1 Background

Continuing depletion of so-called easy oil and gas reservoirs in the world, coupled with the increasing worldwide demand for energy, is driving the oil and gas industry to look for petroleum resources in frontier basins where the geologies are more complex and conditions for petroleum production are more hostile. Of these frontier regions, deep-water basins, which are widely distributed along continental margins, have been a major focus of exploration by the industry. In the last two decades, major discoveries have been reported in deep-water settings in the Gulf of Mexico, Angola, Brazil, Nigeria and the Mediterranean [1, 2].

Although they may have formed and evolved up to the present day under very different conditions (e.g. tectonic settings or sources of sediments), deep-water basins comprise sediment packages of similar geological architectures, referred to as Genetic Units (GUs) (Figure 1-1): these include sand bodies/sheets, channel-levee systems, hemipelagics and mass transport deposits (MTDs) composed of transported pieces of previously-deposited GUs from one of these original components. The coarser-grained components of these sediments are usually considered to create flow pathways that can be used in the de-watering of the whole sediment package, which is a critical process that governs compaction. The flow rates of de-watering are normally thought to be slow, and thus, even poor-quality GUs that contains coarse materials can be significant for this slow flow, as compared to the mud-rich background sediments. The coarser flow-significant components are often called aquifers.

Basin development involves tectonic movements that may rotate the initially-horizontal depositional units. If the rotated rock package contains aquifer units, the tectonics leads to a significant hydraulic re-arrangement, in which the aquifers can connect deep down-dip regions with up-dip, shallow crests. Such a dipping sandstone body, and overlying mud-rich units, are the focus of this thesis. The geological conditions which could give rise to a dipping aquifer in a sedimentary basin include salt intrusion[3], sand injections and rotated fault blocks [4] [5]. In this thesis, the case of a tilted block (nominally, associated with bounding faults, but faults are not included in this analysis) is the prototype situation, creating a tilted aquifer and over-lying mud-rich rocks that were deposited during the period of block rotation.

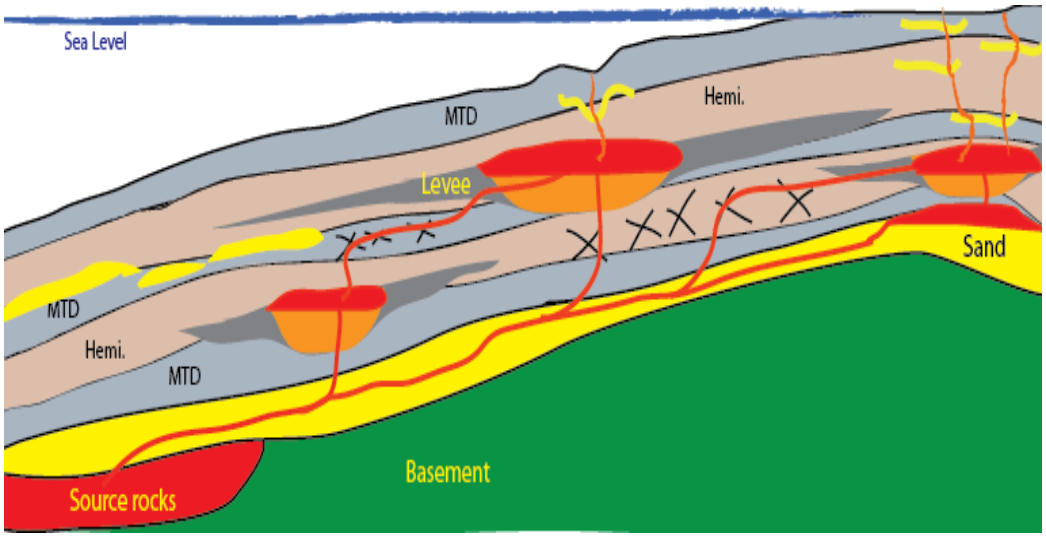

Figure 1-1 A graphic of the complex architecture of a deep-water basin with multiple genetic units deposited, which from unpublished work by Jingsheng Ma). In the graphic, MTD is hemipelagics and MTD is mass transport deposit.

A continuing challenge in deep-water locations, amongst others, is the occurrence of high overpressure. Overpressure conditions of the formation fluids have to be managed by adjusting the mud weight so as to ensure that the borehole fluid energy exceeds that of the formation fluids. This may require the installation of additional casing strings that enable mud weight to be increased in some sections of the hole to a density that would be impossible to sustain in shallower, open-hole sections. Even where the pressures can be managed, excess fluid pressure is associated with issues such as borehole stability, slow rates of penetration, and other types of drilling risk. These issues are problematic enough, even when the conditions are expected, such as in field development, but they introduce even wider concerns in exploration, where pore pressures are only predicted and not known in advance of drilling.

It is the issue of overpressure prediction that motivates the research reported in this thesis. There are several methods that can be used to predict the distribution of overpressure in basins. Geophysics (seismic velocity data) and petro-physics (well log data) are widely used in the industry. Pre-drill prediction of overpressure is usually achieved through manipulation of seismic data, founded on the empirical relationship between effective stress and seismic velocity. However, velocity-based pore pressure prediction methods are not reliable under all geological conditions [6]. Furthermore, understanding fluid interaction and overpressure distribution analysis between GUs in heterogeneous formations have limitation in both of them. So some of failed exploration

usually occurs in shallow burial depositions in deep water basins, because of overpressure and pressure prediction failed in heterogeneous formations. This situation results in loss of both time and money.

Basin modelling to construct full scale models is an effective way to discover overpressure distribution and GU interaction in any conditions. This method is based on parameterization of different geological conditions, and is also able to take into account the overpressure mechanisms.

However, current modelling and other methods are not satisfactory. Frequently, the current basin modelling techniques produce highly heterogeneous geological models with complex geological structures, which involve coupling between hydraulics and geo-mechanics (compaction) in a system with spatial complexity and temporal evolution of GUs. The collection of data is difficult, with a high cost in terms of the economic and time aspects.

Understanding the role of these GU interactions could greatly help to simplify the complexity of heterogeneous geological models on overpressure prediction. This is because such genetic units could form different flow-significant elements in a deep-water basin and their interaction can introduce alterations to the source and drainage of fluids in a deep-water sedimentary basin, affecting function, in terms of fluid flow with implications for overpressure in the basin processes. This is basically a problem of the upscaling type, in which smaller-scale heterogeneities need to be combined in an effective way to answer a practical question in a coarse-model fashion, without the cost and complexity of undertaking full simulation of the detailed specific arrangement.

Overpressure may be generated by multiple mechanisms which could also be taken into account in basin modelling. Among these are thermal expansion of pore water [7]; digenetic clay dehydration reactions [8], [9]; hydrocarbon generation [10]; cementation of pore space [11]; chemical reactions [12]; disequilibrium compaction [13], [14] and fluid lateral transfer [15]. Fluid lateral transfer (LT) and disequilibrium compaction are the two reasons considered in basin modelling in this thesis.

A tilted aquifer deposited during the period of block rotation, which was only filled by mechanical compaction in the basin process is an ideal reference case for expressing overpressure characteristics, and can allow the research to focus on both fluid flow and the mechanical compaction process, which are the main concerns of the industry (LT

model). In addition, if GUs is added in the overburden, this could be a good case to assess the role of GU heterogeneity on overpressure.

The LT model could give rise to high overpressure in structure by disequilibrium compaction and LT. When a dipping sandstone body is formed by block rotation, at the bottom of an aquifer, disequilibrium compaction in the overburden mud can generate a pore pressure gradient between the sand body and the overburden mud, which could drive the fluid to flow into the aquifer, which would then flow as lateral transfer (LT) to the crest and be expelled at that region, leading to high pore pressure in the aquifer crest (Figure 1-2). In this way, overpressure can be enhanced at structural crests by the fluid lateral transfer and disequilibrium compaction in such conditions. Such overpressures are not uncommon and examples are found in the Central North Sea (Figures 1-3), and the Gulf of Mexico[4]. It is such systems which are of concern in this work.

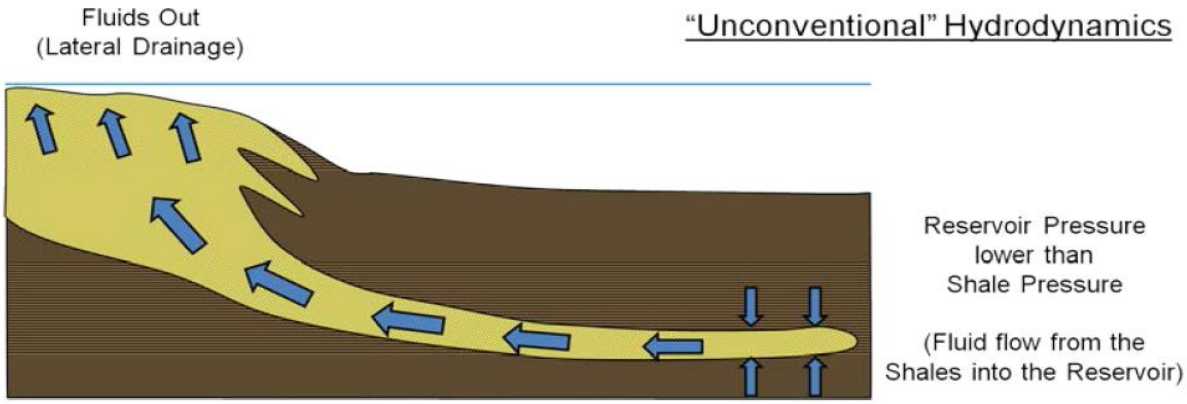

Figure 1-2 Schematic diagram of an fluid LT hydrodynamic system. The blue line in top is sea level. [16]

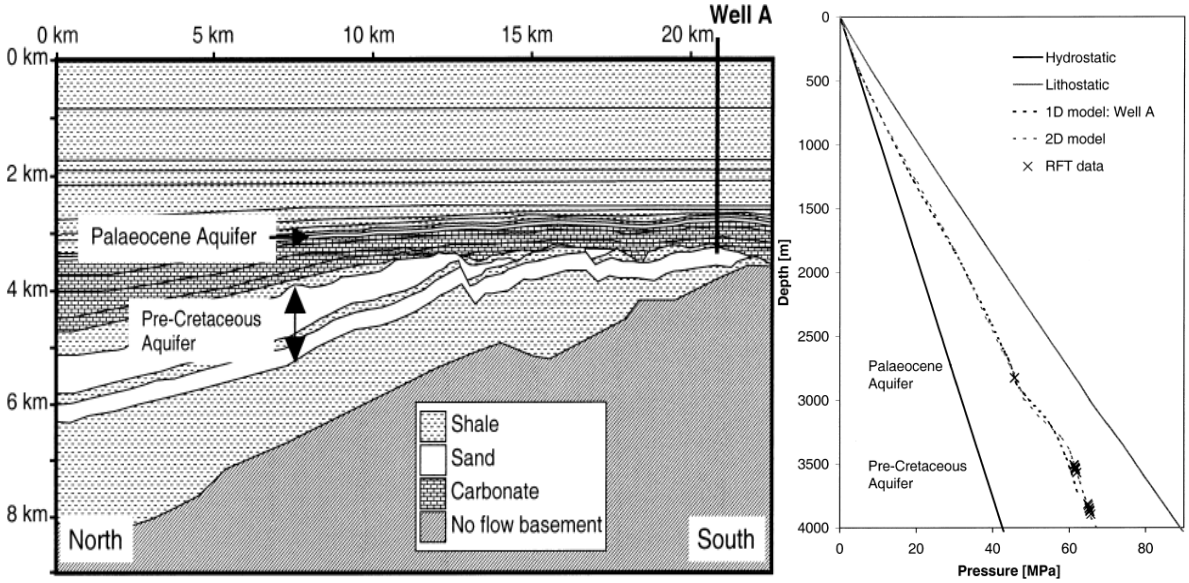

Figure 1-3 Fluid LT hydrodynamics in Central North Sea: because of the effect of LT, high pore pressure occurred at the crest of the aquifer. The pre-cretaceous aquifer is reservoir and the plot in right side is about pressure/depth plot of well-A.

However, accurately estimating overpressure in the LT model is challenging, even when mechanical compaction is the sole mechanism to be considered in a progressive fill-and-burial evolution process of a basin, because such a process may only be characterised by a set of multiple controlling parameters. These consist of overburden sedimentation rate [17], depth of tilted sand aquifer, dipping sandstone relief [15], property of over-burden mud [15, 17] and aquifer geology shape [5], as will be detailed in a later chapter.

It is not uncommon for a basin to comprise a sand-body overlain by zero or more GUs surrounded by otherwise muddy sediments. The choice is to consider the role of the spatial arrangements of GU elements in the overburden, which here are selected to be channel-levee systems (CLs). The spatial arrangements of these CLs could be distributed in different combinations– scattered from each other or two or three clustered, with different characteristics (size, location and depth). Examples of such cases are found in Indus [18, 19] (Figure 1-4), West Africa [20] and the Gulf of Mexico[1].

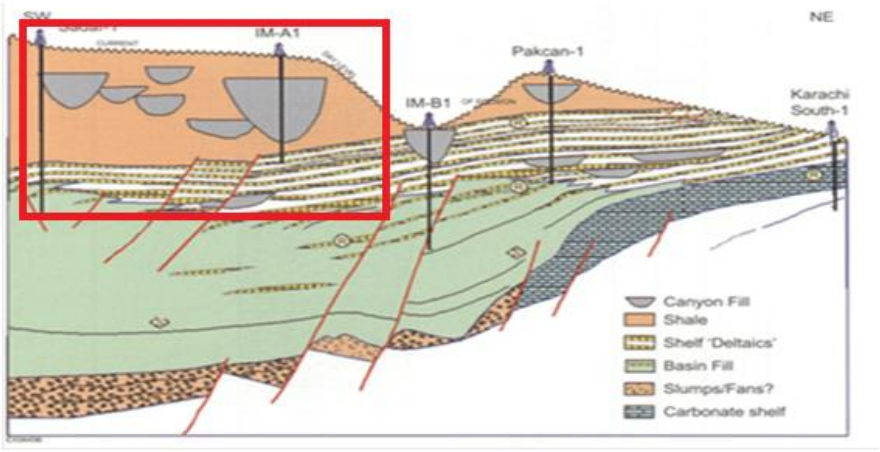

Figure 1-4 A cross-section of the Indus Basin, showing multiple-channel levee systems distributed irregularly above lateral sand layers. Some of these channel-levee systems are connective and some of them are separate [19]. The area within the red rectangle shows multiple channel-levee systems deposited above several sand bodies, and with different combinations and characteristics.

When these are added to the overburden of the LT model, the hydrodynamic system is altered, affecting the compaction processes, and hence feeding back to the hydrodynamics, and the whole system thus evolves along a path that is not easily predicted. Because the channel-levee (CL) systems may form connected paths for fluids to flow away from the muddy sediments and even from the dipping sand-body to the surfaces, they allow the fluid energy to dissipate more easily and can therefore reduce the overpressure at the structure crest. The CLs could influence fluid and overpressure distribution in a deep-water basin, as demonstrated with numerical modelling, by Binh [1].

1.2 Problem and Motivation

Overpressure prediction may be notionally expressed as:

$$R(T) = F(Y) + \sigma(T)$$

where R(T) is the unknown, true overpressure at a reference point (or, in general terms, any set of such reference points) in a basin , determined by a possibly very large number of physicochemical processes and factors, represented by the comprehensive set T. F(Y) is the overpressure that is predicted by considering only a smaller set of specific physicochemical processes and key factors, Y, which are, in principle, capable of being known or estimated with sufficient accuracy. σ(T) is the error of the calculated

overpressure with respect to its true value. In practical terms, R(T) can never be predicted to absolute accuracy, due to the complexity of natural systems, and our inability to determine all possible parameters across a huge space and time range. Nevertheless, the idea of R(T) represents the low-error overpressure estimate that could, in principle, be derived, at high cost, by use of a highly involved numerical approach and the largest possible set of data.

This “high-cost” estimation of overpressure is considered to be the output of a type of basin modelling simulation. Given a basin with an incomplete evolutionary history and largely unknown true overpressure distributions, basin modelling has widely been used to model overpressure, as it allows the identification and testing of the physicochemical processes and the constraints exerted on those processes, which, together, may be responsible for the current basin configurations and dynamics indicated by observations such as seismic data and well-logs. However, the complex evolution of a typical basin means that accurate modelling demands a large collection of the variety of data available, and such data are typically expensive and time-consuming to obtain, and they remain incomplete, even in the best of cases. So what is needed by the petroleum industry is a quick method to develop the understanding of role of GU interaction relative to predicting overpressure, without so much cost, based on simplifying the complex heterogeneity.

The main motivation that inspires this research is to develop the understanding that can underpin creation of a workflow to be used to assess the role of interactions between GUs, in relation to prediction of overpressure in deep-water sedimentary basins. This is basically a problem of the upscaling type, in which smaller-scale heterogeneities need to be combined in an effective way to answer a practical question in a coarse-model fashion, without the cost and complexity of undertaking full simulation of the detailed specific arrangements. The research demonstrates that the target function, i.e. the prediction of overpressure at a certain reference location, defined after simplifying the complex influence of parameters and developing an understanding of the interaction of the GU, can be estimated with sufficient accuracy over a wide range of parameters that define the spatial arrangements of the system, while demonstrating credible GU interaction relative to predicting overpressure in such a case. This result forms the basis for follow-on research that can seek to further generalise the approach to a wider set of systems and cases and their associated descriptive parameters.

1.3 Objectives

The main objectives of the work in this thesis are:

1) To demonstrate that such a quick method can be developed based on well-established scientific methodologies, using the tilted-aquifer example that is usually associated with the Lateral Transfer concept;

2) To derive models for estimating overpressure at a chosen (single) reference point at the crest of the system, taking into account for a set of mainly geometric parameters that describe the aquifer itself, AND the presence of higher-permeability GUs in the overburden, according to the assessment of their interaction;

3) To create a workflow for basin modellers to develop understanding of GU interaction relative to overpressure prediction in such a case, which could be extended to other cases to help indecision making when detailed modelling is necessary.

1.4 Approach

To developing understanding the role of GU interaction relative to overpressure prediction by basin modelling, choosing a suitable reference case is the first consideration. A dipping tilted aquifer case (LT) is the ideal reference case to express the overpressure characteristics, focusing on both fluid flow and mechanical compaction in the basin formation process. Moreover, if genetic units are added in the over-burden, it could effectively assess the role of GU interaction in relation to prediction of overpressure. Hence, overpressure prediction for a chosen (single) reference point is necessary for assessing the GU interaction in such a case. But the case overpressure involves coupling influence parameters between hydraulics and geo-mechanics in a system with spatial complexity and temporal evolution. The approach adopted here is one in which the task is simplified in such a way that it can be assessed whether it is possible, under model arrangements that are plausibly realistic, to find ways to reduce the system complexity to a small number of "key" parameters, while still making a sufficiently accurate prediction of overpressure. In this way, we are able to gain an approximate estimate of overpressure distributions using proxy models, with an understood level of error, and based on the results, to develop understanding of GU interaction and to make a decision as to whether detailed basin modelling is warranted in this case. In this respect, simplifying the complexity of the parameters and

assessment of the effect of GU interaction on over-pressure prediction are two main difficulties to be solved.

The choice taken in this research is to consider the role of the spatial arrangements of GU in the overburden, which are selected to be a channel-levee system (CLSs) or multiple channel-levee systems (CLSs). A CLS is a cluster of channel-levees of spatial proximate and treated in this work as an individual entity. When these are added to the overburden of the LT model, the hydrodynamic system is altered, affecting the compaction processes, and hence feeding back to the hydrodynamics, and the whole system evolves along a path that is not easily predicted.

1.4.1 Process and Challenges

For the cases where CLSs are scattered in terms of relative distance from each other and from the aquifer, one could imagine that the overall influence of CLSs on the overpressure may be sufficiently approximated by the simple summation of influence of individual CLS. However, for the cases where CLSs are clustered and close to the aquifer, the simple linear decomposition is unlikely to work, given the expected stronger interactions among them. However, if each cluster of CLSs is further apart from another cluster and each cluster could be treated as an upscaled super CLS, the simple linear decomposition can be applied on the clusters. In this case, one would imagine that the contribution of each cluster may be estimated by a weighed linear decomposition of the contribution of each CL in that cluster. This suggests hierarchical unweighted and weighted linear decompositions. What are the physical criteria to define whether CLs are scattered or clustered? How would the weighting factors be determined for each cluster? Would this approach work over the whole parameter space or not? If so, can predictive models be constructed in a similar way as discussed for LT basins without any CLS? These questions will be answered in Chapter 4. In the process, the understanding of interaction between each CLS and the aquifer can be developed, for judging in which conditions the complex heterogeneity could be simplified and how in relation to predicting overpressure in a deep-water sedimentary basin. The derivation of predictive functions of GU interactions demonstrate GU interaction reliability and the work flow assessment will be discussed in Chapter 5.

1.4.2 Methodologies

For modelling the LT reference cases, mechanical compaction is chosen as the only mechanism that needs to be considered, and therefore, by reducing the number of model

parameters, the objectives can be achieved. Let us assume F(Y) as the estimated overpressure at the crest, from a proxy model of a set of parameters Y, and F(X) being the estimated overpressure at the same reference point, from a model of reduced parameters X (Y = X + others), and this gives F(Y) = F(X) + e(Y) where e(Y) is the error term. Given Y, it is of interest to know what parameters are necessary to form X. These important parameters, after being simplified in the LT model, are variable rates of overburden sedimentation [17], depth of tilted sand aquifer, dipping sand relief [15], and aquifer geology shape [5], so that the error term is within an acceptable limit and what degree of influence each parameter has on the overpressure at the reference point. This idea is considered as parameter screening in this thesis, and it has been done on a set of model parameter points $\{X_i\}$ by basin simulations. At the same time, the model responses, i.e. the overpressure at certain reference points can be determined, and from these a predictive model, denoted as f(.) can be constructed to approximate F(X) and therefore F(Y), i.e. to estimate the overpressure at the reference point from the reduced parameters X, without resorting to basin simulations. Note that a capital letter, being used to define a function, e.g. F(X), expresses a unknown functional relationship between parameters in the space X and the true responses, while the small letter, e.g. f(X), expresses an approximation of F(X) estimated from samples $\{X_i\}$ in the space X in and the simulated responses on the corresponding models.

Chapter 3 will show that for the LT model exist alone. In this case X needs to contain a minimum of 5 parameters for the procedure described here to work well. Nevertheless, this approach would not work well if X contains a large number of parameters; parameter screening may be become prohibited computationally, let alone building a model to capture all important cross-interactions. For LT basins with CLSs the number of parameters in X would increase dramatically with the number of CLSs, as mechanical and fluid interactions occur between a CLS and the aquifer, and also between one CLS and another CLS. These interactions influence the fluid drainage from the crest of the aquifer and thus the overpressure at the reference point. They also introduce alterations of the source and drainage of fluids in the overburden, and between them and the aquifer, at various locations. Let us assume that these aspects are expressed by a set of additional parameters, denoted as XCLS. If their influence on the overpressure, referred to as G(XCL), in addition to f(X), is a good approximation of F(Y), that is, F(Y) = f(X) + G(XCLS) + E(Y), the same approach for the case without

any CLS can be extended by decomposing the sub-parameter spaces, X and XCLS, in turn, for modelling G(XCLS) and estimating E(Y).

In order to support parameter screening and predictive model building as outlined above, a large number of models must be constructed and simulated. This demands the utilisation of well-developed methods to minimise the number of samples, which here means parameterised models need to be constructed and calculated. It is well-known that the Design of Experiment (DoE) approach has been developed to deal with this situation, while the response surface methodology (RSM), which employs the DoE approach, enables parameter screening, and the construction of predictive models in the form of response surfaces. This study uses 2^k factorial design to screen a set of variables, and examines the significance of them before carrying out the D-optimal design of response surface analysis.

1.5 The Outline of Thesis

This chapter has introduced the background of off-shore heterogeneity depositional basin features and their importance of fluid migration. The current overpressure prediction methods are not sufficient and main reasons were outlined. Meaning of Genetic Units interaction upscale was expressed obviously in this chapter. The objective of this thesis work is to develop a new workflow for predicting overpressure in highly heterogeneity and complex architecture in deep-water basins

The remaining chapters are as follows. In chapter 2, a review of important literature related to this thesis work is presented. It covers basic geology on depositional and sedimentary aspects of basin types of concern, basin modelling approaches, methods and techniques, and Design and Experiment and Response Surface Methodology needed, in this work. .

Chapter 3 is concerned mainly with the characterisation of overpressure in a basis reference case – LT model with respect the reference point at the crest of aquifer. It shows how a high-dimensional parameters space in Y can be screened to reduce to “X” with only 5 key parameter. Then it shows the use of Response Surface Methodology to define an optimal number of simulation cases to derive overpressure relationships in reference point (f(X)). The outcome response surfaces are mathematical models derived using “design expert” software package. The sensitivity of parameters, both individually

and jointly, on the overpressure in this case was assessed. An error analysis and application of this process will be showed in a later chapter.

In chapter 4, channel-levee GUs will be introduced into the overburden of the LT model, and their impact on overpressure at the same references will be studied by considering the interactions between aquifer and CLSs as well as between CLSs. For LT-type basins with CLSs, additional number of parameters is needed to be brought into X and the number would increase with the number of CLS dramatically to capture mechanical and fluid interactions. This interaction would reduce the overpressure at the reference point, given that CLS contains sandier than muddy deposits as the background of LT. Let assume the additional impact over f(X) is encapsulated by function G(XCLS) that is, F(Y) = f(X) + G(XCLS) + E(Y) This chapter concerns modelling G(XCLS) and estimating E(Y) and analysis of parameter space in which estimates of E(Y) fall with an acceptable range.

In Chapter 5, the target function which contains CLS fluid interaction experience and parameter simplification will be examined. Fluid interaction impact on overpressure between CLSs and aquifer, and each CLSs will be demonstrate by examples. Further explanation the complexity heterogeneity of CLSs spatial arrangement could be simplified relative to overpressure prediction in which condition and how. The work flow which could extend to other fields and reference cases to develop role of GU for helping simplify their heterogeneity will also be summarized.

In Chapter 6, Conclusion and future work

Main process of overpressure prediction in chosen reference point (technical process) in thesis is showed in Figure 1-5

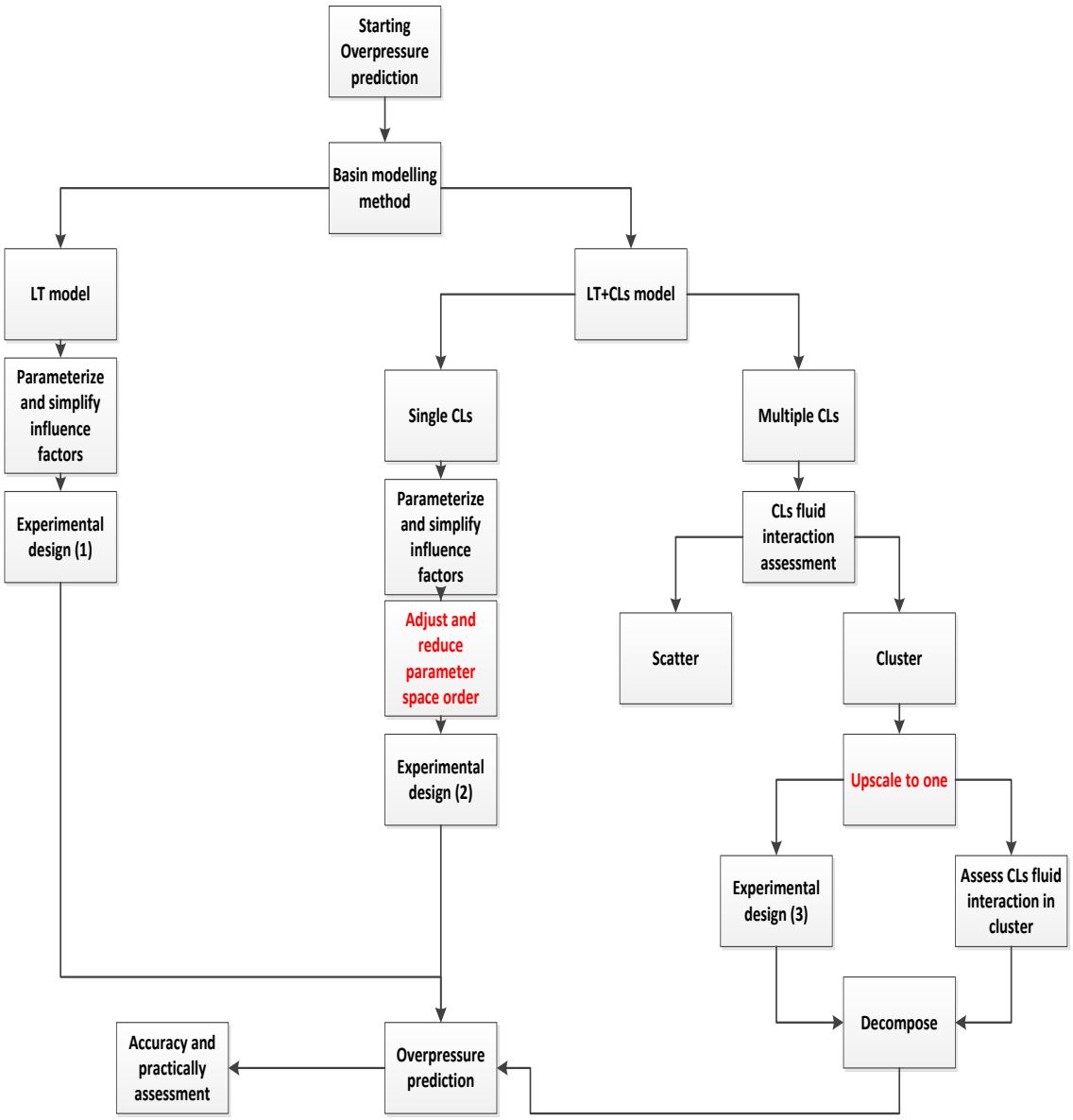

Figure 1-5 Researching technical processes in thesis.

Chapter 2. LITERATURE REVIEW

2.1 Introduction

In this chapter, important references relating to the field of thesis are reviewed. It contains the geological background, knowledge related to the main approach, methodology and tools. The chapter is divided into five parts.

Section 2.2 covers the literature concerning the geology of the main types of genetic units, the properties of multiple channel-levee systems and their structure and geological origin. Section 2.3 introduces the theory of disequilibrium compaction that could lead to aquifer dip and its fluid properties. The references which researched fluid properties of unconventional hydraulic systems in a dipping aquifer due to disequilibrium compaction is considered in two ways. Section 2.4 introduces concept of overpressure and its importance in lateral transfer cases. The literature on using LT model to analyse overpressure characteristics in an aquifer crest and the controlling factors on overpressure are identified. In section 2.5, the main tool for modelling basin evolution on overpressure of LTs is introduced, while Section 2.6 reviews several experimental design methodologies and the methodology I have chosen (D-Optimal) in this thesis.

2.2 Dipping sand bodies and multiple channel-levee systems in sedimentary basin

2.2.1 Introduction to the geology of typical genetic units

The main focus in thesis is the tilted sand body (the aquifer) which is related to fluid lateral transfer and thus the redistribution of overpressure compared to a similar situation without the connected aquifer unit. Fault-related tilting of blocks rotation which was introduced in Chapter 1, salt diapirs, tilting due to differential compaction and differential geological subsidence are the main reasons which could cause a dipping sand body in a basin.

Salt diapir is the process of salt movement by nature and mechanism which caused over-burden reservoirs of Cretaceous chalk, and Tertiary sandstones and shales to penetrate through such horizons. It will lift a dip on an over-burden sand aquifer and reservoir, which could form a dipping sand body. All the diapirs are interpreted to have grown by down-building from the Triassic through to Palaeocene times, and were probably triggered by extensional faulting, during the Triassic times [21-23]. A case of

a dipping sandstone body caused by salt diapir was investigated in the Central Graben field of the North Sea (Figure 2.2).

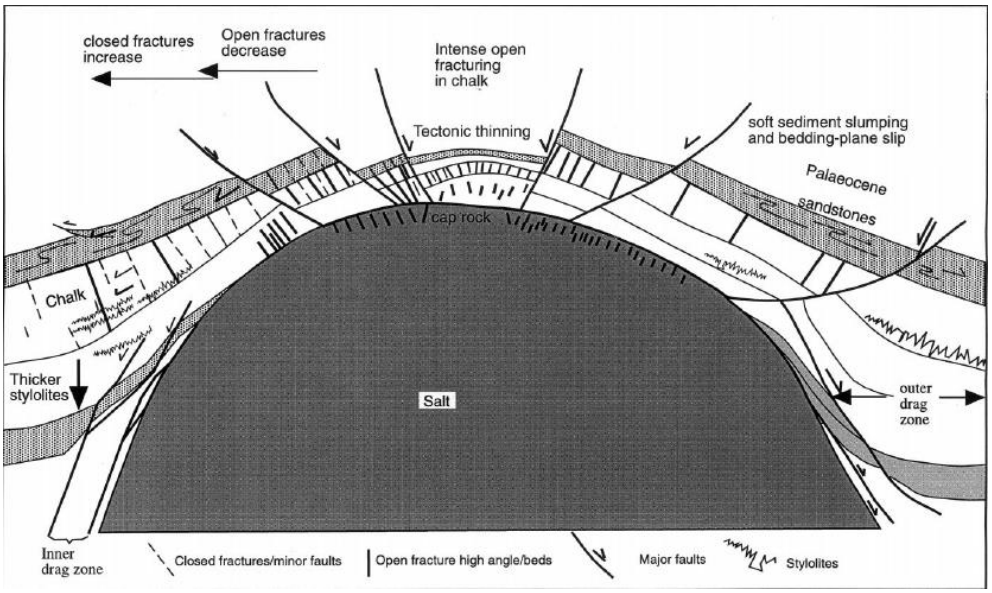

Figure 2-1 A case of a salt diapir which has lifted the overlying sandstone and created tilting blocks at the edges in Central Graben in the North Sea. Dark colour of over-burden zones property is sandstone.

Tilting differential compaction is the cause of dipping sandstone bodies in thesis. This is because previously deposited substrate is vary in thickness, and the thicker parts compact more than thinner which lead to a tilting sand body. Cases of this have been found in the Judy Field in the Central North Sea (Figure 2-2). In this case, the burial over the last 3 Ma has been so rapid that almost all the extra overburden load forms a dipping sandstone reservoir. The reservoir is chiefly capped by shales; however, over the structural crests, the reservoir is capped by chalks [24].

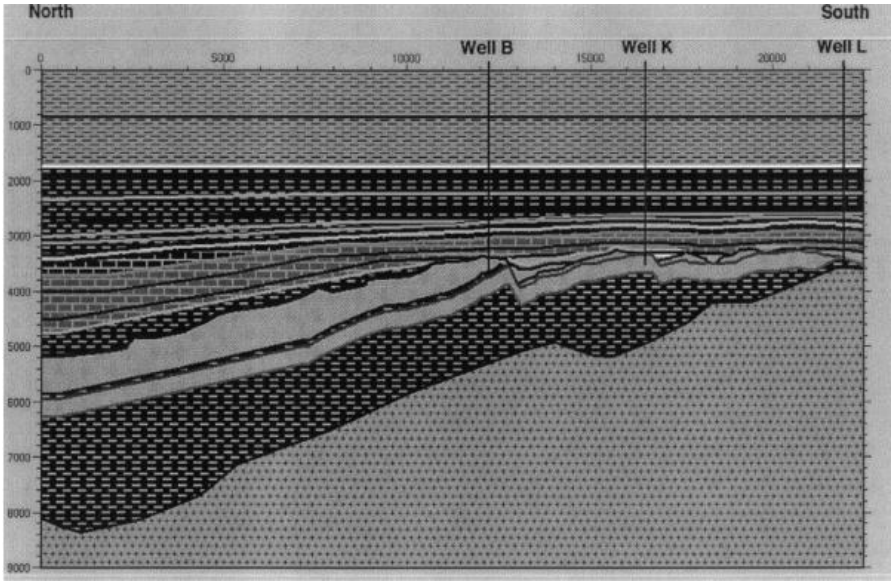

Figure 2-2 A case of disequilibrium compaction forming a dipping sandstone aquifer; the graphic is a NNW–SSE cross-section through the Judy field. The reservoir is chiefly capped by shales; however, over the structural crests the reservoir is capped by chalks.

The reasons for the formation of the dipping sandstone body above could be disequilibrium compaction in the aquifer bottom, driving fluid flow into the aquifer at the bottom and from below to the crest, as lateral transfer.

A case of this was found in Palaeocene strata of the Central North Sea (Figure 2-4)[4]. In the graphic, fluid flows from the bottom to the crest of the aquifer due to disequilibrium compaction. However, the dipping sandstone bodies are not only formed by disequilibrium compaction but also formed by salt diapir in some regions. This situation could form high overpressure on the aquifer crest; the case is main research objective and will be discussed in detail in this thesis.

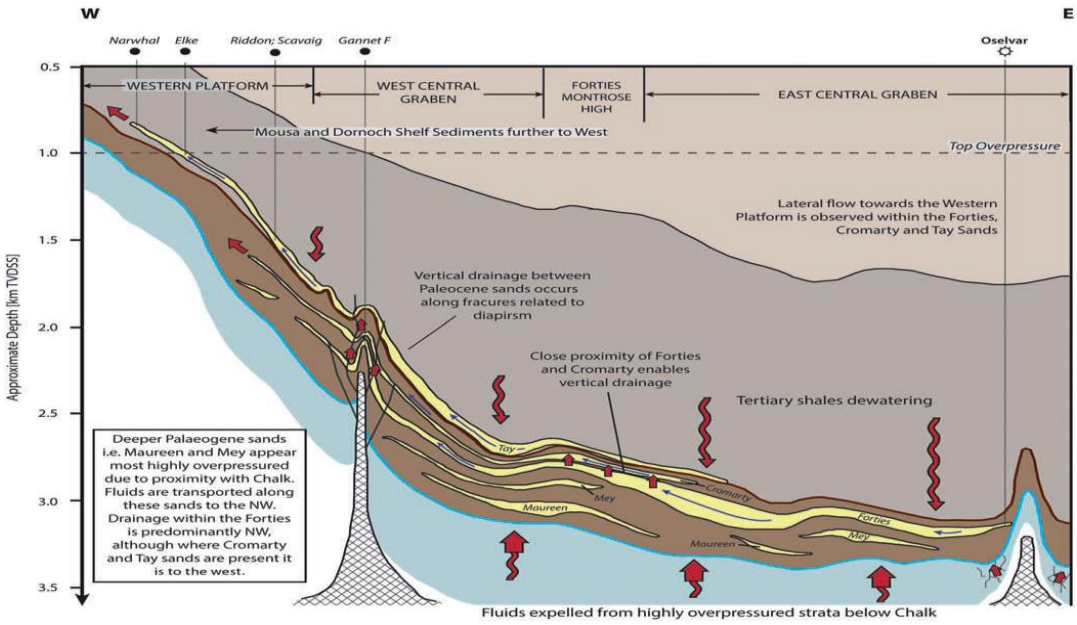

Figure 2-3 In the graphic, several dipping sand bodies are distributed in the bottom, some of which were formed by disequilibrium compaction and some were caused by salt diapir. The fluid flow which was presented by black arrow from bottom of sand body to crest was caused by disequilibrium compaction.

2.2.2 Multiple channel-levee systems in deposited basin

Multiple channel-levee sediments are very common in well-known deep-water fields in world, such as those in the Gulf of Mexico, East Kalimantan, West Africa and Indus basin. These channels are usually distributed in different spatial arrangement, so they were hard to get integral data and they have great influence on basin migration and pressure formation [2, 25, 26]. A case of channel-levee systems deposited above a dipping sandstone body was found in the Indus basin (Figure 2-4).

The offshore Indus Basin is a rift and passive margin basin which developed following the separation of the Indian plate from Africa in the late Jurassic. The Miocene and Plio-Pleistocene intervals over the Indus Fan are characterized by spectacular, large-scale channel-levee systems. Channel-levees are high relief features (200–900 m thick) with widths of 10–40 km, confining submarine channel flow.

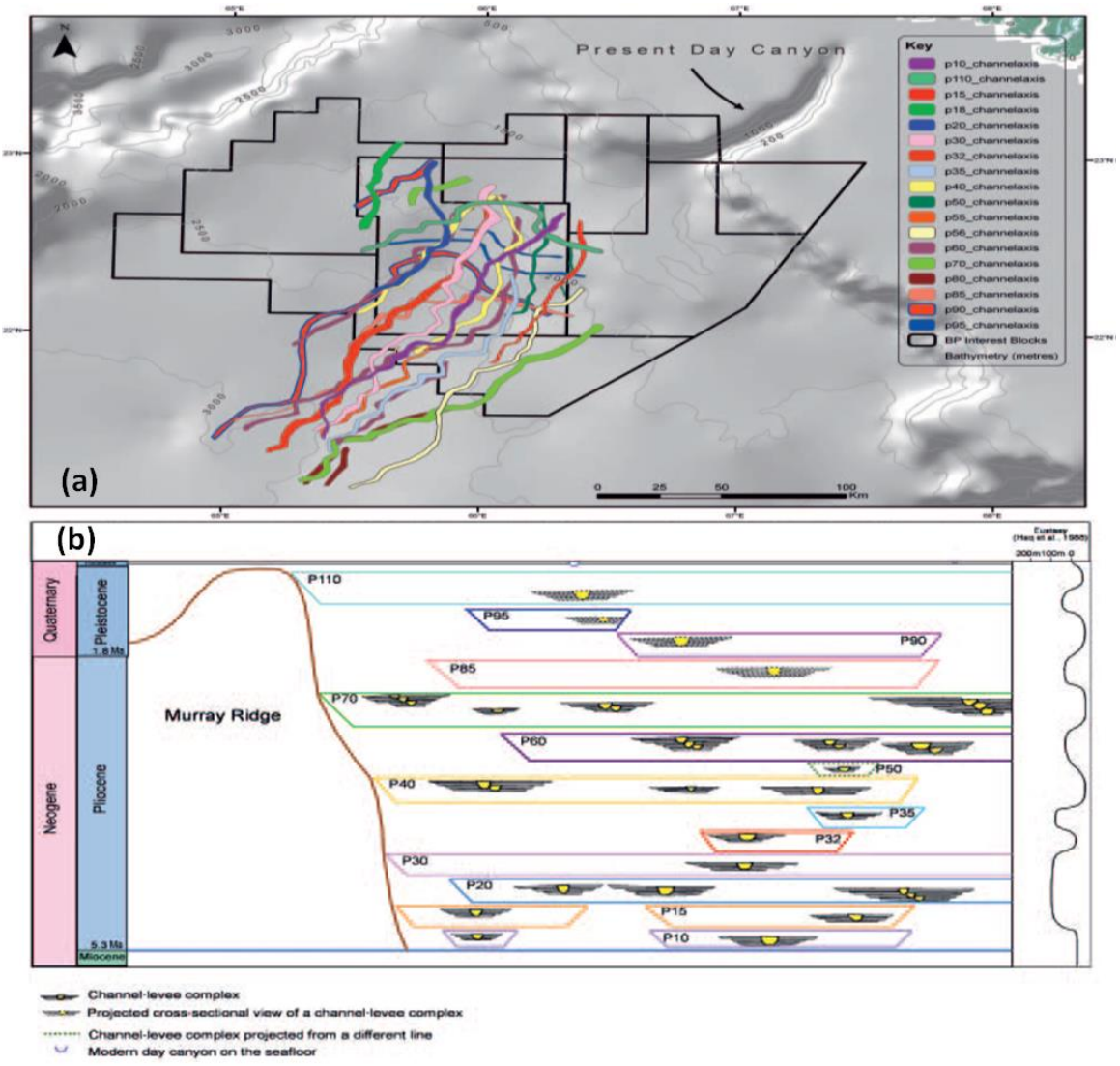

Figure 2-4 (a) Plio-Pleistocene channel trends in the proximal part of the Indus fan. (b)Dip seismic line and chrono stratigraphy of the Plio-Pleistocene channel-levee sequences. We can see on the graphic that many channel-levee systems are distributed irregularly; two or three of them form a cluster, but most of them are scattered. The constituents of channel-levee are sandstone and low clay content mud. [19]

Figure 2-4, (a) shows how multiple canyon systems form on a marine slope. The multiple channels were formed by one large canyon: the canyon deposits are defined by medium- to high amplitude reflectors that are laterally discontinuous with flat to erosional. In the geological background, this canyon developed into multiple, large channel-levee systems after the sedimentation process; the leveed-channels are interpreted to be sand prone, which has higher permeability than the surrounding around mud in a deep-water sedimentary basin area. Furthermore, dipping sandstone aquifers are very common on deep marine slopes, so these channels are very likely to have an impact on overpressure on the crest of an aquifer.

Figure 2-4 (b) shows divers distribution of such CLs: they can be distributed in clusters of two or three or singly. An accurate description of this area was proved by Fowler and Guritno in 2004 [27]. In Chapter 4, the different CLS spatial arrangement will be setting by basin modelling and analyse their fluid interaction impact on overpressure.

A similar type of multiple CL distribution can be found in other deep-water or off-shore basins around the world. Similar cases have been found in the EI 330 field in the Gulf of Mexico, as described by Sawyer in 2007 [28], and West Africa and the southern Brazil Basin also have these large parent canyon systems which have formed channel-levee systems in the sedimentary process[20].

2.2.3 The influence of CLs on aquifer overpressure

Channel-levee systems may form (partly-) connected paths for fluids to move from the muddy sediments and even from the aquifer to the surface [26, 29-32]; they can provide an alternate pathway for fluid motion, thus allowing the fluid energy to dissipate more easily, and therefore reducing the overpressure at the crest. This section focuses on studies which investigate how channel-levee systems can influence fluid flow and overpressure distribution in a deep-water basin.

The fact that CLS could actually impact fluid flow and overpressure distribution in deep-water basin has been given good support [1]. The example described here comes from seismic data, which was used to investigate overpressure distribution on the continental slope in offshore Louisiana in Gulf of Mexico. The sediment geology has a big canyon (CLS) and sandstone aquifer at the bottom.

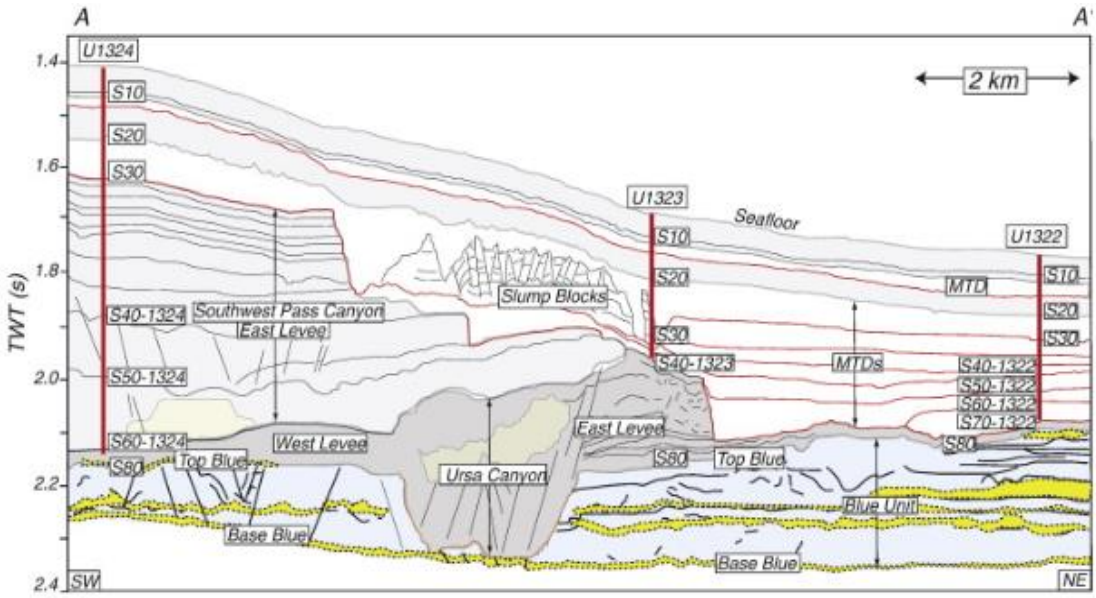

Figure 2-5 Cross-section of leg 308 region. Sand stone aquifers were deposited in Ursa Canyon. Light and dark grey represent mud-rich levee, rotated channel-margin slides, and hemipelagic drape; yellow represents sand-rich channel fill. The Blue Unit (light blue) is composed of sand (yellow) and mud (blue). Mass transport deposits (MTDs) have occurred in the mud-rich levee deposits above the Blue Unit.[1]

Binnh [1] has researched physical properties and overpressure distribution in such a region. The case could give a good example about how CLS could influence fluid flow and compaction in basin process. The research modelling results explained CLS could give rise to high overpressure in a channel and influence fluid flow. The modelling results suggest that the Ursa canyon controlled the fluid flow directions in the upper Pleistocene sediments of the Ursa Basin. Sedimentation in the Ursa channel caused fluid flow in the blue sand towards both east and west because of the development of larger overpressures in the channel.

Binnh used seismic data from published source and field, and used software to create very detailed basin modelling which describe overpressure distribution and fluid migration (Figure 2-6). It shows fluid flow from the left of the blue sand to right, which proved the geology genetic units could influence fluid flow direction and overpressure distribution in sedimentary basin.

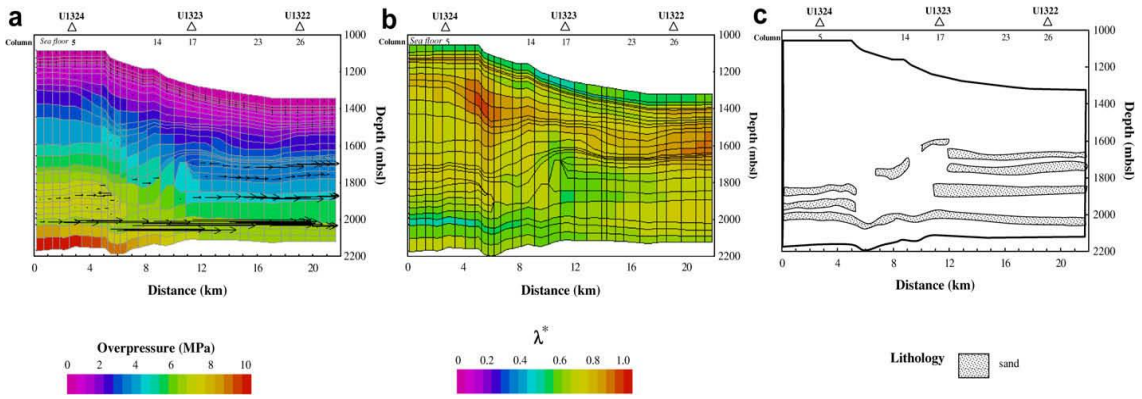

Figure 2-6 (a) Overpressures and fluid flow patterns and (b) pore pressure ratio "λ" at the present day for closed boundary condition. (c) Distribution of sands. [1]

From the results, CLS could actually influence overpressure distribution and fluid flow in basin process. In order to prove these conclusions, numerical basin modelling case was created to view overpressure distribution and migration in chapter 4. Fluid flow velocity will also be showed.

2.3 Interplay between mechanical compaction and fluid flow in tilting sand

Mechanical compaction is the basis of disequilibrium compaction that leads to overpressure generation in this research, and it is an inevitable consequence of burial and basin evolution. As such, a significant effort has been made to quantify the process and to incorporate a mathematical description within computer-based basin models by a number of researchers [33] [34] [35] [36] [37] [38] [39] [40] [41] [42] [43]. This section only talks about simple cases.

Terzaghi and Gibson [44] described the mathematical models of fluid and pressure characteristics in the mechanical compaction process in sediments which were used by most people. Modelling of sediment compaction using consolidation theory was well performed by Gibson [44] assuming constant sedimentation rate, a single lithology and constant sediment properties (compressibility, permeability and density). Gibson's original formulation was successfully applied by geologists to model overpressure [45] [46].

At a given depth in a sedimentary basin, the vertical load due to the overlying sediments is known as the overburden stress, $\boldsymbol{\sigma}$, given by

$$\sigma = W * bgh \qquad 2\text{-}1$$

Where W is the vertical thickness of the overlying sediments, b is the average bulk density, and g is the gravitational force, h is depth of reference point. Some of the weight of the overburden is borne by the fluid in the pore spaces; the remainder of the weight is borne by the matrix (effective stress).

The relationship between effective stress and overburden is given by Terzaghi's equation [47]:

$$\sigma' = \sigma - P \qquad 2\text{-}2$$

Where "**σ**′"" is the effective stress and P is the fluid pressure. Because rocks and soils can be compressed, their porosity depends on effective stress. If effective stress is small (high pore pressure), values of porosity will also remain high[48, 49]. If effective stress increases, porosity will decrease and the rock will compact.

Furthermore, fluid pressure could be interpreted as energy associated with specific pore fluid volume strain change. And the potential energy of the fluid is described as head. The head is defined as a concept: if you were able to insert a tube into a certain location, and fill the tube with fresh water, the head is the water level in that tube when the energy in the fluids is balanced at the bottom of the tube. Fluids do not flow because of pressure difference, even though it has different pressures at fluid column top and bottom, but head could drive fluid motion. So, fluid on overpressured location can flow towards to normal pressure location depend on the existence path.

In tilting sand (research focus in thesis), according the energy mechanism, overpressure which generated by disequilibrium compaction can be enhanced at structural crests by the tilting sand and fluids from deep. Because the sandstone supports a good fluid flow pathway, and overpressure in sand body bottom is higher than the crest (associated with the sediment loading). Potential fluid energy and head in the sand body bottom is also higher than crest, which drives fluid flow toward to crest. Then fluid pressure at the bottom is reduced, which lead more compaction (effective stress) in there. So overpressure and head in around mudstone is higher than sandstone, and fluid is drive into sandstone. In a sand body crest, fluid pressure is increased because of fluid flow from down-dip, and more fluid energy gathered here. And the overpressure and head in there is higher than around mudstone, fluid is drive into mudstone. So, fluid flows from mudstone to sandstone in a tilted sand bottom location and flows from sandstone to mudstone in crest location. This situation is very common in famous basin fields. For

example, in the Jurassic reservoirs of the Central North Sea, the crest pore pressures below about 4000 m (13,000 ft.) are close to the fracture pressure [50]. And Fleming [5] used two extreme methods to focus on fluid flow in tilted sand and produced the same results, which will be introduced in this section.

Because fluid could flow into an aquifer at the bottom and out of the crest under such conditions, it must have a point which has no fluid flow in aquifer; this point is termed the central point. This concept states that the pore pressure in the aquifer and the adjacent mud are only equal at one depth (approximately, at the mid height of the aquifer).

The Centroid Concept is an empirical method for predicting overpressures at the crests of inclined aquifers [51, 52]. It is assumed that the shale excess pressure increases uniformly with depth in a given study area and is caused by disequilibrium compaction. Away from this point, the pore pressure in the shales is assumed to vary with depth along a lithostatic parallel gradient (1 psi/ft, 22.62 MPa/km) [15]

Flemings, et al [5] demonstrated that appearance of disequilibrium compaction can lead lateral transfer hydraulic system and studied fluid flow pattern and central point in permeable sandstone body. They used numerical methodology and combining theoretical foundation on two ways (Rapid load and Steady flow) to explain fluid flow characteristics in sand bed and mudstone around system in sedimentary basin.
They used two extreme methods (mudstone burial characteristic) to gain insight into fluid flow in dipping sandstone; the first is undrained behaviour: if mudstone is undrained, the equation could be expressed as:

$$\mathrm{DP_{ms}} = B_P \mathrm{DS_v}$$

2-3

Where $\mathrm{P_{ms}}$ is mudstone pressure, B_P is pore pressure build-up coefficient, $\mathrm{S_v}$ is overburden stress. The change in mudstone pressure ($\mathrm{DP_{ms}}$) is proportional to the change in the overburden stress ($\mathrm{DS_v} = \rho_b \mathrm{g d_z}$).

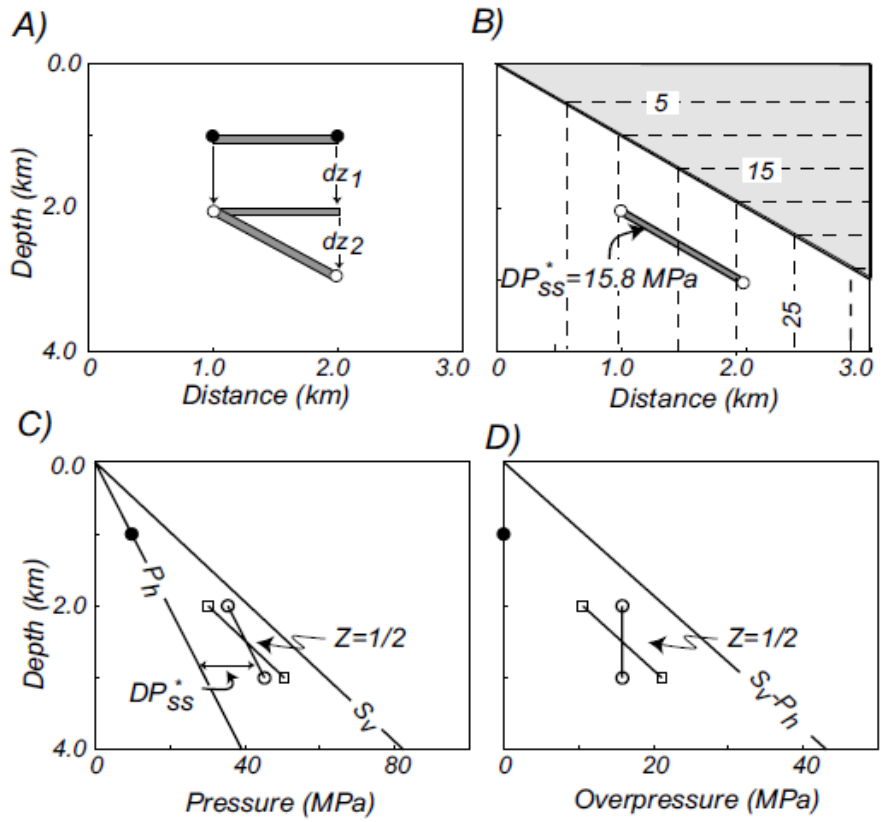

Figure 2-7 Undrained model. (A) A hydrostatically pressured sandstone body (grey-shaded lens) is initially encased in mudstone at 1 km depth. Its left edge is buried to 2 km and its right edge is buried to 3 km. (B) Sediment loading (shaded area) increases the sandstone overpressure (*DP* **ss*) to 15.8 MPa. Contours (dashed lines) are mudstone overpressure. (C) Sandstone pressure (circles) parallels the hydrostatic pressure gradient ($\boldsymbol{P_h}$) and is elevated above hydrostatic by *DP* **ss*. Mudstone pressure follows the lithostatic pressure gradient ($\boldsymbol{S_v}$). Sandstone pressure before burial is hydrostatic. *Z* is equal point position in sand and mud boundary which is ½ because the sandstone pressure equals the mudstone pressure at one half of the sandstone relief. [5]

They considered the pressure distribution that result from rapid burial of sandstone. A horizontal, hydrostatically-pressured, sandstone body of constant thickness is buried a depth *dz*1 and then rotated such that one edge is buried a further increment *dz*2 (Figure 2-7 a). The results proved that there is an equal point of pressure in boundary of sandstone and mudstone, that means flow direction is opposite in two side of the point, that because fluid is flow into sandstone in down dip of aquifer and flow out in crest.

Furthermore, Flemings, et al [5] also proved anticline parabolic shape of sandstone which equal point is in Z= $\frac{l}{3}$. That because that when sandstone is parabolic shape, it will have less loading than the normal shape, and there is less loading rate and compaction on sandstone, and this causes a different centroid point. This also proved there is an inseparable link between mechanical compaction and fluid flow. Then they

used a steady state flow model to prove the conclusion.

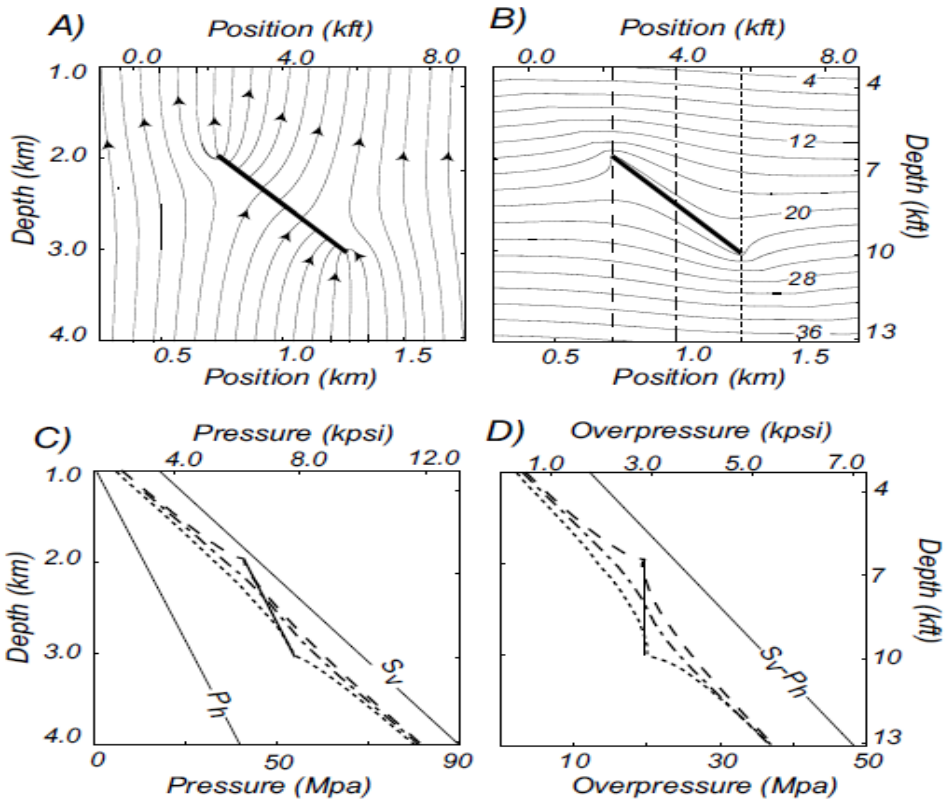

Figure 2-8 Steady-flow model. (A) Streamlines record primarily vertical flow, with enhanced flow into the base of the sandstone and out of its crest. (B) Mudstone overpressure contours (MPa) are elevated at the Sandstone's crest and are depressed near its base. Vertical lines locate pressure profiles shown in C and D. (C) Mudstone pressures converge onto the sandstone pressure at the crest (long dashes), centre (dash-dots) and base (dots) of the sandstone body. In which $\boldsymbol{P_h}$ is hydrostatic pressure gradient and $\boldsymbol{S_v}$ is lithostatic pressure gradient. (D) Overpressure in sandstone is constant, overpressure in mudstone rises to meet the pressure at the crest of the sandstone. [5]

In the model, flow is focused into the sandstone at the base and out of the sandstone at the crest (Figure 2-8 a). At the base of the sandstone, overpressure contours are depressed and at crest they are elevated (Figure 2-8 b). This is because fluid was derived by head from down dip of sandstone to crest, and pressure and overpressure is decreased in down dip, which lead more compaction (higher effective stress) occurring there and pore pressure gradient decrease. And in crest, there is more fluid energy and excess pressure were transferred from base and retard the compaction in overburden mudstone, which lead pore pressure gradient increase. (Figure 2-8 c).

When dipping permeable sandstone is encased in overpressured, low permeability mudstone, the pressure gradient within it is hydrostatic, whereas the pressure gradient in

the mudstone is greater. This drives a flow system where fluids are drawn in at the base of the sandstone and expelled at the crest. This process in an unconventional hydraulic system is termed fluid lateral transfer. Overpressure which is generated by disequilibrium compaction in dipping permeable aquifer structure high is research objective and much significant in many aspects.

2.4 Overpressure in lateral transfer case

2.4.1 Overpressure concept

Subsurface pore pressure generally increases as the depth increases below the surface. The pressure increase is a measure of the greater confinement (i.e. volumetric strain) of the slightly-compressible pore fluid at depth; thus, the pressure can be interpreted as the measure of the energy associated with the volumetric strain of the pore fluid. The subsurface pore system is generally thought to be fully connected, but the existence of very low permeability rocks means that a pressure (confinement) disturbance in one location can be separated, for a period of time, from the remainder of the pore system, while the (slow) flow seeks to return the fluid mass to an equilibrium state that is termed hydrostatic. A pore fluid is said to be overpressured if its pressure exceeds the reference hydrostatic pressure, and the difference in pressure is termed the excess pressure [4, 42, 50, 53-55] (Figure 2-10), which shows these types of pressure, in which the overpressure magnitude is expressed as a red line, with the value calculated by:

$$P^*(overpressure) = P(pore) - P(hydrostatic) \qquad 2\text{-}4$$

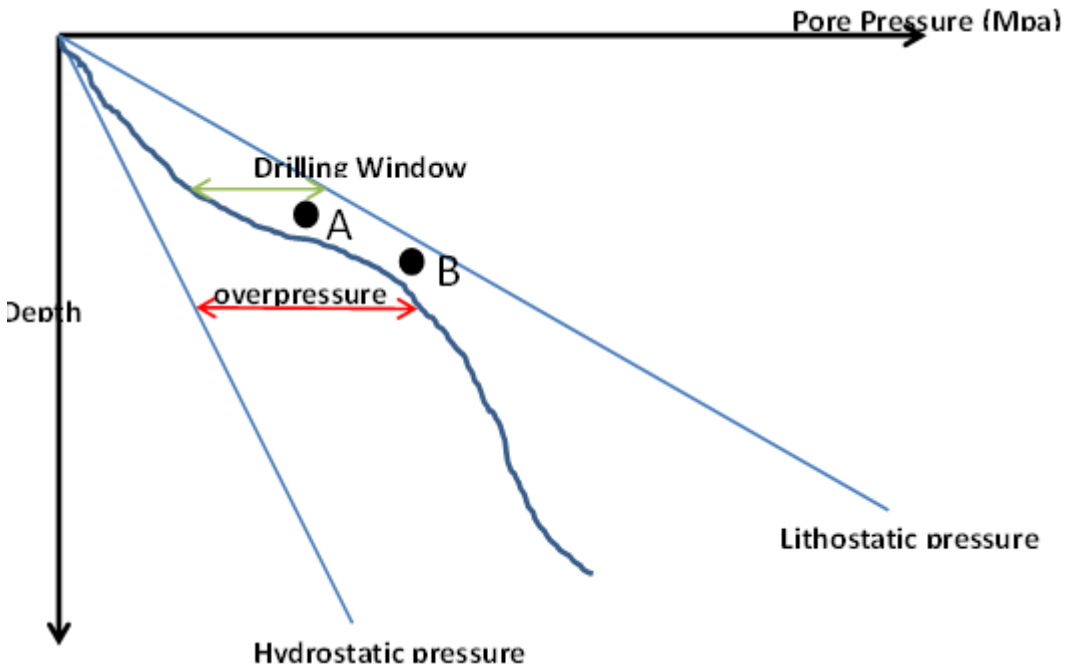

Figure 2-9 Overpressure concept and relationship with pore pressure and hydrostatic pressure.

2.4.2 Lateral transfer model

The lateral transfer model was introduced in the first chapter, and in this section, real cases will be shown which reveal the physical interactions and character of the overpressure evolution. These examples motivate the effort to generalize the model for a reference research purpose.

High overpressure in structural highs of a reservoir needs to be assessed for exploration, drilling and seal risk assessment. Figure 2-10 shows 2 cases of drilling on geological structural highs in the Central North Sea, and EI 330 field in the Gulf of Mexico, both of which shown overpressure, higher than normal, at the aquifer crest. This means that overpressure in geological structural highs is actually important to recognize in practice.

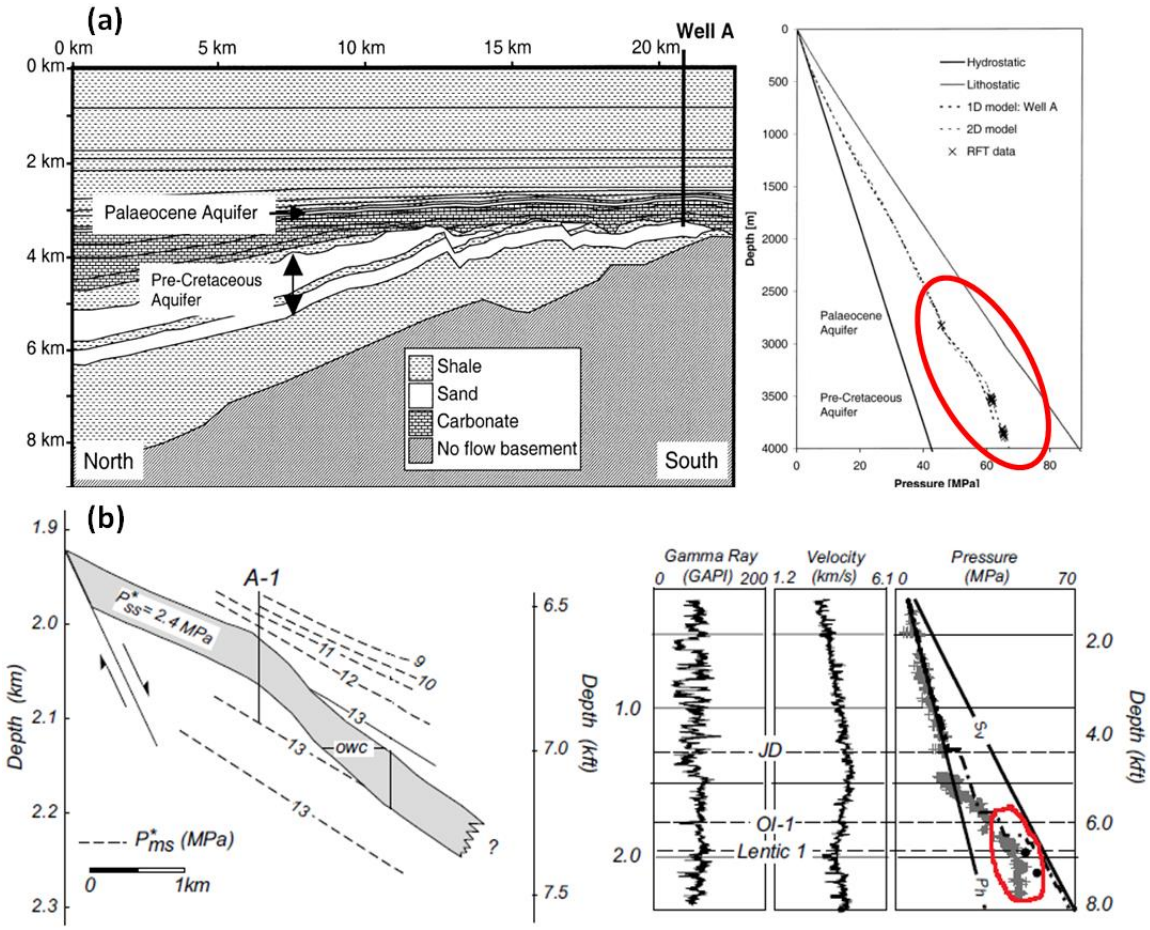

Figure 2-10 A 2D cross section through the Central North Sea case study, with a simplified stratigraphy. Pressure calculated for a 1D model of Well A and from a 2D model of the entire case study .In the Pre-Cretaceous aquifer the 2D model generates 1.6 MPa excess pressure above that in the 1D model [15]; (b) Above the reservoir, mudstone overpressure (P *ms) contours parallel the reservoir and converge toward the crest. On the graphic, overpressure close to 2 km depth (A1 well location) is higher than in other places and approaching to lithostatic pressure[5].

Here I use basin modelling as the main tool to develop understanding of comprehensive physical process and the system interactions in the lateral transfer case. Firstly, the factors controlling overpressure in such conditions and their geological meaning should be identified.

Yardley and Swarbrick [15] have investigated and researched fluid lateral transfer in such conditions through a theoretical approach and numerical analysis. They created a simple 2D model of lateral transfer and used the "PetroMod" software package to calculate the resulting overpressure at the crest of the model. A sensitivity analysis was then performed by individually varying the model parameters to determine the key controlling parameters governing the magnitude of overpressure redistribution by lateral transfer. A 1D model was also generated at the aquifer crest, and in the down-dip region,

for comparing with the outcomes of the 2D model (Figure 2-11). The outcomes showed that a multi-dimensional approach was crucial to be able to calculate the additional pressure contribution from lateral transfer over that created from 1D disequilibrium compaction.

The modelling undertaken by Yardley and Swarbrick, and also herein, assumes that overpressure generation is caused by disequilibrium compaction, and that sediment porosity loss is controlled solely by effective stress. This appears to be a satisfactory way of modelling sediment compaction [56] and yields good matches to observed pressures, especially in young basins where temperature-activated processes are not significant at the depths considered (e.g. [57]).

In a 1D model of disequilibrium compaction, the flow of fluid is only vertical, and thus there is a monotonic gradient (perhaps with variations) in the pressure-depth relationship. In the 2D lateral transfer situation, the aquifer provides a pathway for fluid flow. Excess fluid energy there (associated with the sediment loading) promotes fluid flow towards the crest, allowing the down-dip pressures to be reduced, and thus enabling additional sediment compaction to occur there. Indeed, the "drain" effect allows the fluid pressures in the overlying mudstones to be lowered, so that the fluid flow there is downwards into the aquifer, and the pressure-depth plot is no longer monotonic. The updip region experiences an increase in fluid pressure, above that which would occur there due to the overlying sediments. This excess overpressure retards compaction of the overburden mudstones, and there is a reverse gradient in the pressure-depth relationship below the aquifer. The lateral transfer case provides a powerful demonstration of the operating physical processes, and the way that they may differ over spatial and temporal coordinates.

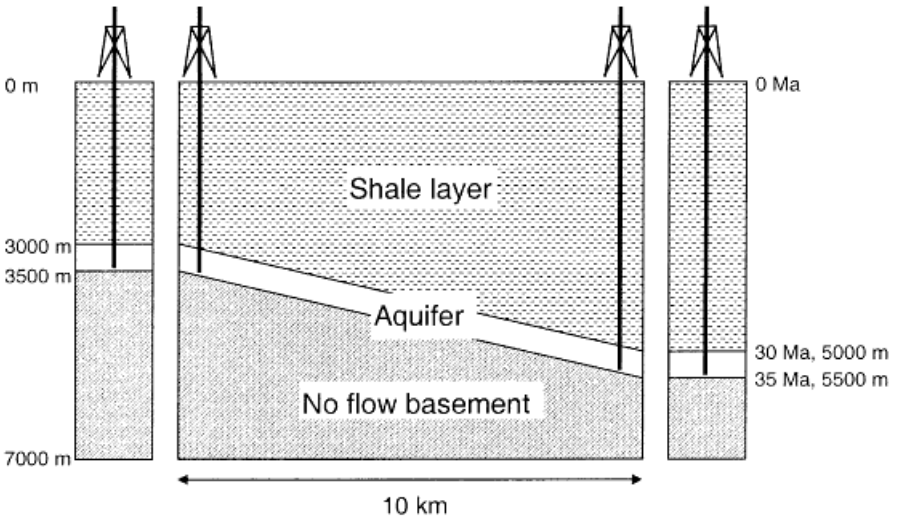

Figure 2-11 The 2D base case model used to examine the lateral transfer process together with 1D crestal and down dip models which were calculated for comparative purposes. The aquifer was initially horizontal but has become inclined due to the differential burial of the overlying shale over the last 30 Ma. The aquifer has a uniform present day thickness of 500 m. The base and sides of the model are no flow boundaries. [15]

Yardley and Swarbrick defined effective of lateral transfer which is

$$\frac{2D\,model\,aquifer\,XSP - 1D\,model\,crestal\,XSP}{1D\,model\,crestal\,XSP} * 100\% \qquad 2\text{-}5$$

where XSP is the excess pressure. This expression gives an indication of the additional contribution to crestal excess pressures from lateral transfer compared to the contribution from simple 1D compaction. Normalizing the pressure response in this way allows the impact of lateral transfer to be compared in the sensitivity analysis of models that have different burial rates, aquifer relief and burial history [10].

They also used numerical modelling methodology to find the influence of controlling factors which could impact lateral transfer effectiveness. However, they did not analyse each factor's degree of influence in detail. In this study, all the important factors which influence overpressure distribution and lateral transfer effectiveness will be analysed in terms of their importance and degree of influence to lay the groundwork for prediction of overpressure distribution.

The influential parameters mainly mentioned in Yardley and Swarbrick's [15]research are sedimentation rate, the properties of the over-burden mud, and the aquifer depth and relief. The details of the theory and geographical range of the five key influential parameters will be discussed in Chapter 3.

Sedimentation rate is the main controlling factor which can influence overpressure distribution in such conditions. If the sedimentation rate frequently exceeds the ability of previously-deposited sediments to drain in rapidly forming basins, pore fluid will be over-pressured, because it supports the overlying material and the sediment is under-consolidated [58, 59].

Rock properties play an important role in overpressure distribution and fluid migration in basin evolution. They can control fluid flow velocity in the pores of the rock and how quickly pressures dissipate. Gordon and Fleming [17] [60]have shown an equation for flow through a volume element composed of a constant number of solid grains, where only Darcy flow and sediment loading are considered, which express rock permeability which could change pore pressure distribution.

In equation 2-6, the pressure change is represented/ included along with permeability and porosity change. Gordon and Fleming [17] [60] used this to work out fluid flow in the complex pressure and porosity of EI 330 field in Gulf of Mexico, and produced a fluid flow model in the sedimentary basin. Pressure (P) in a compacting medium is described by:

$$\frac{\delta P}{\delta t}=\left[\frac{K\left(1-\Phi_{\eta}\right)^{2}}{S_{t}\rho_{f}g}\right]\frac{\delta^{2}P^{*}}{\delta\eta^{2}}+\left[\frac{\Phi_{\eta}}{S_{t}\left(1-\Phi_{\eta}\right)}\beta\right]\frac{\delta\sigma_{L}}{\delta t}+\frac{\alpha_{m}}{S_{t}}\frac{\delta T}{\delta t}+\frac{\delta P_{clay}}{\delta t} \qquad 2\text{-}6$$

This equation describes evolution of pressure for a deforming element that tracks the solid grains[60]. The symbol meanings were detailed in nomenclature. The change in fluid pressure through time comprises four components (from left to right): (1) fluid flow (the Darcy term), (2) sediment loading, (3) thermal loading and (4) clay dehydration. Overpressure develops when the flux from the Darcy flow term cannot balance pore pressure generated by the combined effects of the three source elements: sediment loading, aqua thermal pressuring and clay dehydration [60]. In research of thesis, we ignored the effect of aquathermal pressuring and clay dehydration, so the pressure change just related to parts 1 and 2, and thus rock permeability and porosity are the main components of the Darcy term, so the shale properties are the important influencing parameters on pressure and overpressure changes in the basin fluid flow system.

The relationship developed in soil mechanics between the void ratio and vertical effective stress in the one-dimensional, mechanical compaction of fine-grained, clastic

mudstones was researched by Yang and Aplin [62]. This account will be mainly used in this thesis to describe mud properties and further details will be given in Chapter 3.

The relief of the aquifer in a LT model in the conditions is also an influence which could impact overpressure at the reference point, which is shown by Yardley [15]. With increasing aquifer relief, the burial rate and depth to which sediments are buried at the down dip end of the aquifer increases, leading to the generation of more energy in the deepest muds, and fluid is retarded there, which leads more overpressure. The increased pressure generation in the deep muds leads to greater pressure dissipation into the down dip end of the aquifer and greater pressure enhancement at the crest of the structure. Yardley also used numerical methods to elaborate this effect; details will be given in Chapter 3.

2.5 Modelling basin evolution on overpressure of LTs using Basin Modelling (PetroMod 2012)

The overpressure in a LT setting can best be understood by considering the evolution of the basin. So, for predicting overpressure in the structural crest in LT and added CL models, basin modelling software is needed which is capable of expressing overpressure distribution by the parameters influential in basin evolution.

"Petroleum systems modelling" (PetroMod) is the main tool in these studies used for basin modelling, calculating the overpressure distribution and geological genetic units fluid interaction. PetroMod petroleum systems modelling software, developed by IES and now part of the Schlumberger Company, combine seismic information, well data and geological knowledge to model the evolution of a sedimentary basin. PetroMod software will simulate if and how a reservoir has been charged with hydrocarbons, including the source and timing of hydrocarbon generation, migration routes, quantities, and the type of hydrocarbon in the subsurface or at surface conditions [63].

Petroleum systems models are 1D, 2D, or 3D large-scale geologic models. From a single charge area for a prospect to regional studies of entire basins to resource assessments on a mega-regional scale covering multiple basins, these models cover all the above areas. The models provide a complete record of the petroleum system evolution, including pressure and temperature history, which contain relate the structural evolution of a basin to generation, migration, accumulation, and loss of oil and gas in a petroleum system through geologic time. Properties such as gas/oil ratios

and API gravities can also be analysed, understood, and predicted. A petroleum systems model provides the only means to integrate all physical aspects (source, trap, seal, and reservoir) and time (charge) to quantify and analyse processes and reduce the risks of exploration.

The main formats and model geometry used in "PetroMod" are: Dynamic, Layers, Facies, Boundary conditions, Special sub models and Local grid refinement. Except for Tec link, all of these formats will be used in this thesis to create a LT+CL model to predict overpressure distribution[63].

In the rock properties module (facies module), the lithological properties of different rocks will be considered. Each rock compaction and permeability curve is the theoretical basis of the deposition process and the pressure distribution. A compaction model relates porosity to effective stress, (hydrostatic) depth, or bulk compressibility [17, 64, 65]. In this study, two compaction models are mainly used, which are Athy's Law and the Mudstone Model.

A simple exponential dependency on effective stress can also be used, equivalent to the above Athy's law[48]. (Symbols meaning were detailed in the nomenclature)

$$\Phi(\sigma) = \Phi_1 + (\Phi_0 - \Phi_1)e^{-k\sigma} \qquad 2\text{-}8$$

The Mudstone Model which needs to be used for the mudstone which surrounds the aquifer is below. The following law from soil mechanics is especially applicable for clastic rocks:

$$e = \frac{\Phi}{1-\Phi} = e_{100} - \beta \ln\left(\frac{\sigma}{0.1\ \mathrm{MPa}}\right) \qquad 2\text{-}9$$

The related material parameters e_{100} (initial void ratio) and β, compressibility, can be related to clay content with the following relationships proposed by Yang and Aplin [62], which will be used on the mudstone clay content setting in the modelling process, where r is fractional clay content [62] [61]:

$$e_{100} = 0.3024 + 1.6867r + 1.9505r^2 \qquad 2\text{-}10$$

$$\beta = 0.0407 + 0.2479r + 0.3684r^2 \qquad 2\text{-}11$$

The models for permeabilities in this study were chosen Multipoint Model (Default) in the PetroMod package, and each data point is obtained from the relative reference. Any (multipoint) curves can be used for the vertical "h", and specimen permeability, "K_{vh}", depending on porosity. The corresponding horizontal, h and specimen permeabilities "K_{hh}" are calculated from the vertical values multiplied by the anisotropy factor a:

$$K_{hh} = a * K_{vh} \qquad 2\text{-}12$$

2.6 Response Surface Methodology

For predicting overpressure distribution on an aquifer crest using "PetroMod", a large number of attempted models and regularly unified simulation were constructed and simulated, for screening controlling parameters, obtaining a response and understanding fluid interaction between multiple CLSs on overpressure performance, which will be discussed in detail in later chapters. The next section will introduce the experimental design methodology chosen for obtaining the response relationship between overpressure and the controlling physical factors, which will be employed three times in this thesis.

In order to determine the relationships between the controlling factors identified in the previous section, and those identified in a following section, where other CLS are considered and also influence overpressure at the crest, response surface methodology (RSM) is an effective approach which is used to determine the relationship between the different factors (input variables or independent variables) affecting a process and the output (response) of that process.

RSM is a method of gathering of statistical and mathematical techniques used to develop, improve, and optimize a process which is first introduced by Box and Wilson [66]. It involves using a sequence of well-designed experiments to obtain an optimal response in which the influence on the responses of each factor, and their interactions, up to certain orders, is taken into account. RSM has evolved into one of the most widely used approaches in science and engineering disciplines for screening the influential factors on certain outputs or responses of concern [67-69] which may be hidden in certain processes, and for developing relationship models for making predictions.

In this thesis, in order to establish the relationship between controlling factors and overpressure, RSM can be used to define the minimal number of simulations need to be

carried out in this research. It can thus achieve the goal of overpressure prediction without building extra modelling that wastes so much time and cost.

2.6.1 Empirical Models

The theory of RSM can be generated based on the mathematical model. This model is an empirical model built from a multiple regression process and obtained from the observed data of the system. Multiple regression is a combination of statistical techniques that allows the simultaneous testing and modelling of multiple independent variables. A first-order response surface model for a multiple regression takes the form [70]:

$$y = \beta_0 + \beta_1 x_1 + \beta_2 x_2 + \ldots + \beta_k x_k + \varepsilon \qquad 2\text{-}13$$

This equation is called a multiple linear regression model. The parameters β_j (j=0, 1, 2.., k) are the regression coefficients. These coefficients are typically determined by the method of least squares.

In the case where interaction terms are added to first-order model, the equation can be written as follows [70]:

$$y = \beta_0 + \beta_1 x_1 + \beta_2 x_2 + \ldots + \beta_k x_k + \sum_{i<j}^{k} \sum_{=2} \beta_{ij} x_i x_j + \varepsilon \qquad 2\text{-}14$$

The model can be represented as a second-order model, with interaction terms that add the second-order part in above equation [70]:

$$y = \beta_0 + \beta_1 x_1 + \beta_2 x_2 + \ldots + \beta_k x_k + \sum_{i<j}^{k} \sum_{=2} \beta_{ij} x_i x_j + \sum_{i=1}^{k} \beta_{ii} x_i^2 + \varepsilon \qquad 2\text{-}15$$

This model can also be represented as a cubic, quartic and fifth order model.

2.6.2 Design involved and methodology chosen

2.6.2.1 Two factorial designs

If the target function is represented as a linear relationship, factorial designs are widely used to investigate both the main effects and their interactions. This design is useful at the early stage of a response surface study. Box and Wilson suggest using a second-degree polynomial model to do this, for which the designs fall into two broad categories: Box-Wilson central composite designs and Box-Behnken designs. This model is used to

screen how much each factor affects the response and its prominence. Two-level factorial design is a special case, where each of the k factors has only two levels, minimum and maximum. The design exactly generates 2^k experimental runs for k factors; it is therefore called 2^kfactorial design [70]. In Chapter 3 of this thesis, Box-Wilson central composite design is used to investigate the prominence of each controlling factor.

A Box-Wilson Central Composite Design, commonly called a "central composite design", contains an embedded factorial or fractional factorial design with central points which are augmented with a group of 'star points' that allow estimation of curvature. If the distance from the centre of the design space to a factorial point is ±1 unit for each factor, the distance from the centre of the design space to a star point is $|\alpha| > 1$. The precise value of "α" depends on certain properties desired for the design and on the number of factors involved.

Similarly, the number of centre point runs the design will contain also depends on certain properties required for the design.

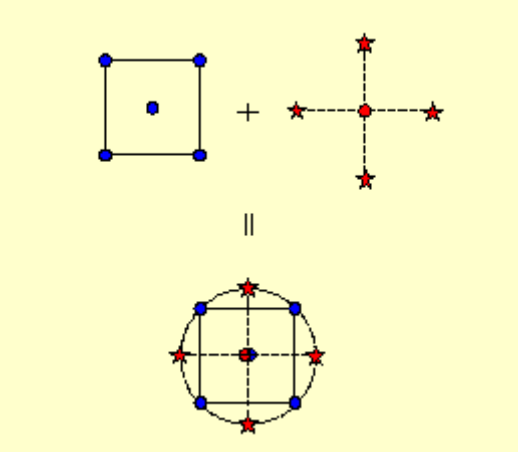

Figure 2-12 Generation of a Central Composite Design for Two Factors [71]

In general, the appropriate value of "α" is $[2^k]^{1/4}$ [72]. The number of central runs should be between three to five runs [73].

The Box-Behnken design is an independent quadratic design, it does not contain an embedded factorial or fractional factorial design in it. These designs are rotatable (or near rotatable) and require 3 levels for each factor. Compared to the central composite designs, the designs have limited capability for orthogonal blocking,

2.6.2.2 Computer-aided Designs – D-Optimal Design

In some situations, however, second-degree polynomial models (standard designs) are not appropriate or are impractical. In thesis study, most of the parameter spaces in research are constrained. The overpressure presented in research will not be a linear trend, represented by a set of incomplete accurate parameters for factors and not all combinations of factors are available in the parameter space. Because of the simplifying process which will be carried out and the limitations of the basin modelling tool, so that the experimental region in this thesis is not regular in shape. In this situation, normal designs are not adaptable, and computer-aided designs are a useful option [67] in this thesis. Computer-aided designs are experimental designs that are generated based on a particular optimality criterion and are generally 'optimal' only for a specified model as in thesis. The design treatment runs that are generated by the algorithms are chosen from an overall candidate set of possible treatment combinations.

One popular optimality criterion of computer-aided designs is D-optimality, which has been chosen in this research. It seeks to maximize |X'X|, the determinant of the information matrix X'X of the design. This criterion results in minimizing the generalized variance of the parameter estimates, based on a pre-specified model.

The main questions for D-optimal design are how to select a reduced set of points and how many points are needed at minimum. The first question is explained clearly in the reference referred to as the D-optimal Designs Tutorial [74]. However, for the second question there are no rules to define the exact number of experiments one should perform: the minimum number depends on the model proposed and the algorithm. Several algorithms have been developed in order to perform a D-optimal design efficiently. A comprehensive review of these algorithms and methods is beyond this thesis and the reader is referred to the following articles by Cook [75], St. John [76], Fedorov [77], Carlson [78] and Mitchell [79].

In this study, Design Expert [67], an experimental design software package, was utilised to perform the D-optimal response surface experiments in order to find relationships between each influencing factor and overpressure at the aquifer crest. This software package has been widely used to perform D-optimal response surface experiments for factor screening and response predictions in a wide context, including examples of optimisation of chemical flooding [69].

2.6.3 Multiple Response Optimizations

For choosing the best response models, multiple response optimizations will be used via the Design Expert package. The optimization method starts by building an appropriate response surface model, and then finding an optimum condition. An approach for optimization, used in the Design Expert software, is the desirability function. Derringer and Suich developed this method in 1980. They considered converting each response, Yi, into an individual desirability function, di, which is in the range of 0 and 1; the next step is to maximize the overall desirability shown in the function below:

$$D = \left(d_1 d_2 \ldots d_k\right)^{1/k} \qquad 2\text{-}16$$

where *k* means number of responses.

The individual desirability function di is equal to unity if the response Yi is equal to its goal. On the other hand, di is equal to zero if the response is outside an acceptable range. The goal of the response could be maximum, minimum, target, or within the range. The value of di can be calculated differently based on its goal, lower limit, upper limit, and the weight indicating the degree of importance of the target, respectively [70].

Chapter 3. CHARACTERISATION OF LATERAL TRANSFER REFERENCE CASE FOR ASSESSING USE OF UPSCALED GENETIC UNIT PROPERTIES IN BASIN MODELLING

3.1 Introduction

This chapter is concerned with overpressure characterisation in the basis reference case – the "classic" LT model with a dipping aquifer. The analysis is based on choosing a single reference point at the crest of the aquifer, but could, in principle, be extended to a larger set of comparison points. The analysis enables the potentially high-number parameter space in "F(Y)" to be reduced to a smaller parameter space, "X", which significantly influence overpressure, and has only 5 key parameters. The work then uses response surface methodology to define the minimal combination of simulations needed for determining a relationship between overpressure at the reference point (f(X)) and the 5 parameters. The outcome is an analytical model which can accurately represent the relationship between the overpressure value in the reference location, and the 5 key influencing parameters. The work also assesses the sensitivity of each factor relative to the predicted overpressure. The error analysis and application process will be discussed in a later chapter. This work was necessitated in order to create the reference framework for the research reported in later chapters. It is, nevertheless, a significant contribution in its own right, and the outcomes provide significant new clarity in understanding the way that crestal overpressures depend on combinations of driving processes, which are captured by the small set of controlling parameters "X".

The choice of the Yardley and Swarbrick LT model as a basis for the later stages of research demanded that this model be examined in some detail to understand its sensitivities. The Yardley and Swarbrick LT model (described previously in Figure 2-11) consists of an aquifer that dips from a crest on the left, to a deep region on the right side. Both left and right edges of the model are no-flow boundaries, as is the base. The no-flow lateral boundaries can be thought of as planes of symmetry, or equally as places where there are totally-sealing faults. Neither of these is totally realistic, but they suit the purpose of this study, which is to demonstrate the feasibility of determining a simple predictive method that could avoid the requirement for numerical simulation to calculate overpressure.

Previous forward modelling (i.e. Yardley and Swarbrick, 2000), which used the same geological and hydrodynamic settings, is re-created to discover the geological influencing factors that impact the overpressure value on the structural crest in this reference setting. These factors consist of the over-burden sedimentation rate, clay content of the overburden sediments, the inclined-aquifer reference point depth, the aquifer relief, and (in acknowledgement of Flemings, et al [5] , who examined this factor), the bending degree. Other factors, which might have been thought of as important, were excluded by the numerical modelling method and the resulting analysis of influences. The values in the resulting parameter space are defined in the literature review and experimental design methodology for creating an approximate relationship. I chose the D-optimal methodology to process the simulation outputs and derived the most appropriate mathematical model which could represent relationships between reference point overpressure value and the influencing factors.

Section 3.2.1 discusses Yardley and Swarbrick's classic LT model, and my current numerical model with the same parameters that follow theirs. The need for this replication is due to the fact that the software systems (i.e, commercial basin modelling tools) evolved since the time of their study, and also to the fact that they did not examine the whole range of sensitivities covered in this work. Section 3.2.2 then establishes the main LT model configuration adopted in this thesis and defines the overpressure prediction reference point for the research. In section 3.3, influencing factors on overpressure are identified, and each factor's common range and influence sensitivity is also defined in this section. Section 3.3.2 excludes extreme models from the factors' parameter space according to the limitations of "PetroMod" (mainly, the inability to properly simulate cases with very low effective stresses, which can arise when extreme overpressure energy is transferred to the crest, for example). Section 3.3.3 focuses on using the response surface D-optimal methodology to obtain the relationship between overpressure and the influencing factors.

3.2 Parameterized Lateral Transfer Model

Lateral transfer cases are widely distributed around the world, and block-faulted dipping aquifers are very common in off-shore and deep-water basins. Such cases have been found in the Gulf of Mexico and the Central North Sea. Some of these have been generalised by previous studies, which focused on the system interaction, physical process and overpressure distribution characteristics [15][5]. They were shown to have

big impacts on overpressure characteristics, and focusing on both fluid flow and mechanical compaction in the basin formation process. For this reason LT has been chosen to be the ideal reference base case to develop understanding of GU interactions with overpressure.

However, these publications have not sufficiently considered the interactions of the system, nor have they really expressed the physical processes in a fully linked way. Therefore, a new LT model needs to be created which focuses on and generalises the system interaction and leads to a physical understanding based on more comprehensively. This will allow the well estimated overpressure at the chosen reference point to be extended to every reference point by parameters of the key aspects of the system, to assess the system behaviour without doing a full simulation, thus laying the groundwork for the next step. If the predicted overpressure is of concern, simulations can then be undertaken to better understand the issues in a particular case.

3.2.1 Review original LT model

This section mainly discusses my current numerical model which is compared with Yardley and Swarbrick's classic LT model according to the same parameters. The purpose is to allow for the fact that the commercial basin modelling tools have evolved[63], and establish the limitations of their model in consideration of the physical process and the system interactions.

The fluid flow by lateral transfer and overpressure focused in such basin systems were researched by Yardley and Swarbrick [15], using the basin simulation software "Petro Mod" as the main tool. They used a classic model which has a simple and easily understood geological configuration and investigated fluid migration and overpressure pattern in the basin system which shown in Figure 3-1.

In this classic model, the modelling presented assumes that overpressure generation is caused by disequilibrium compaction and that sediment porosity loss is controlled solely by effective stress (i.e. the difference between the overburden load and the pore pressure). The model has an inclined aquifer, which was created by the deposition of a fine grained shale layer, with no flow basement at the bottom of it. In this thesis, however, I consider the aquifer as being surrounded by a shale layer, and both sides of the model are closed, which could express reality more accurately; additionally, more influencing factors than in the classic model are discussed in terms of their relative

importance). The aquifer in the present model was initially horizontal, and was deposited above a shale layer that had previously experienced much of its compaction potential, but the aquifer becomes inclined due to the differential subsidence and the consequent laterally-variable deposition of the overlying shale sequence over the last 30 Ma. The crest of the aquifer is at 3.0 km depth and there is 2 km of structural relief along the length of the aquifer. This appears to be a satisfactory way of modelling sediment compaction [56] and yields good matches to observed pressures, especially in young basins (e.g. [57]). For a given sediment type and burial rate, the key equations governing the amount of pressure build-up in compacting sediments are those that control how porosity is reduced with increasing effective stress and how permeability declines as porosity declines.

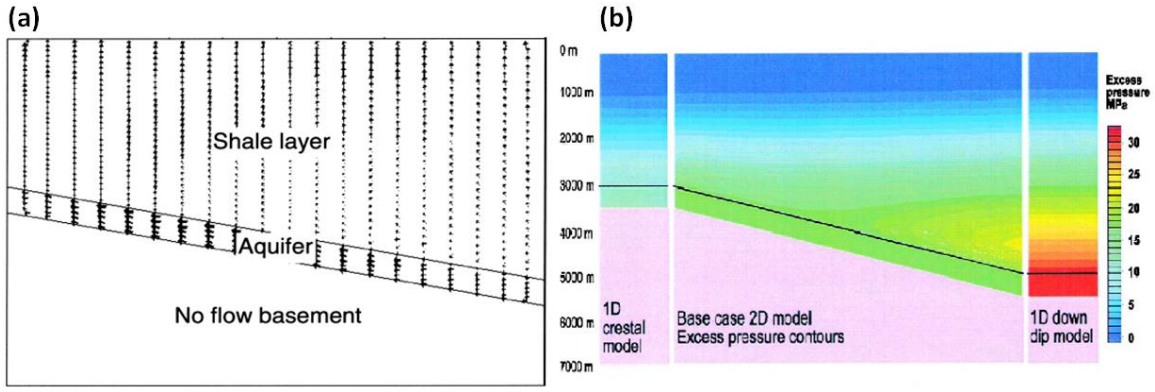

Figure 3-1(a) Water flow vectors at the present day in the base case model. The size of the arrow indicates the relative magnitude of water flow. In the 2D model, the deepest shales de-water downwards into the aquifer. This leads to water flow along the aquifer and pressure enhancement at the structural crest. (b) Excess pressure contours for the base case 1D and 2D models. Fluid flow along the aquifer decreases the pressure at the down dip end of the model and increases it at the crest, relative to the 1D model. [15]

The model assumes solid grains are incompressible. There are no thermal effects on compaction and no flow boundary on both sides of the boundaries, which could provide a better view and understanding of the overpressure distribution generated by disequilibrium compaction and LT. This model uses the compaction curve, in which the corresponding effective stress and porosity equation are also shown, as also used in PetroMod software.

In the model, only shales and sands are modelled in the following sensitivity study, although the term “shale” is used broadly to include any fine-grained lithology that has a low permeability. For typical shales (PetroMod) the reference void ratio and the compaction coefficient are 1.695 and 0.43, respectively [57]. The model’s horizontal shale permeabilities are always a factor of 10 higher than the vertical permeability,

Shale permeabilities evolve with porosity loss during the burial process; however, a typical shale vertical permeability in these models at 3 km is about $3*10^{-6}$ mDarcy, which is similar to shale permeabilities measured in the laboratory [80]. Modelled sand permeabilities are less important than shale permeabilities. The sand permeability (approximately 300 mDarcy) is many orders of magnitude bigger than the shale permeability and fluid flow through the sand is effectively instantaneous compared to fluid flow through the shales.

In Yardley and Swarbrick's research, their model gives only the general interaction between the mud properties, the aquifer relief, the over-burden burial rate and overpressure distribution in the aquifer crest, showing a simple trend defined by very few points. For considering more comprehensively physical process, I further examined more factors such as aquifer depth, bending and even thickness, and I tried to use more point to define their relationships with overpressure.

For starting my research, one similar model (Figure 3-2a) which has same assumptions with Yardleys' in geology (sedimentation rate),geometry (aquifer depth, relief) aspect and other settings needed to be created to examine the degree of similarity of results, and to define whether PetroMod 2012 can be used in my research. The model detail and overpressure pattern are shown in Figure 3-2.

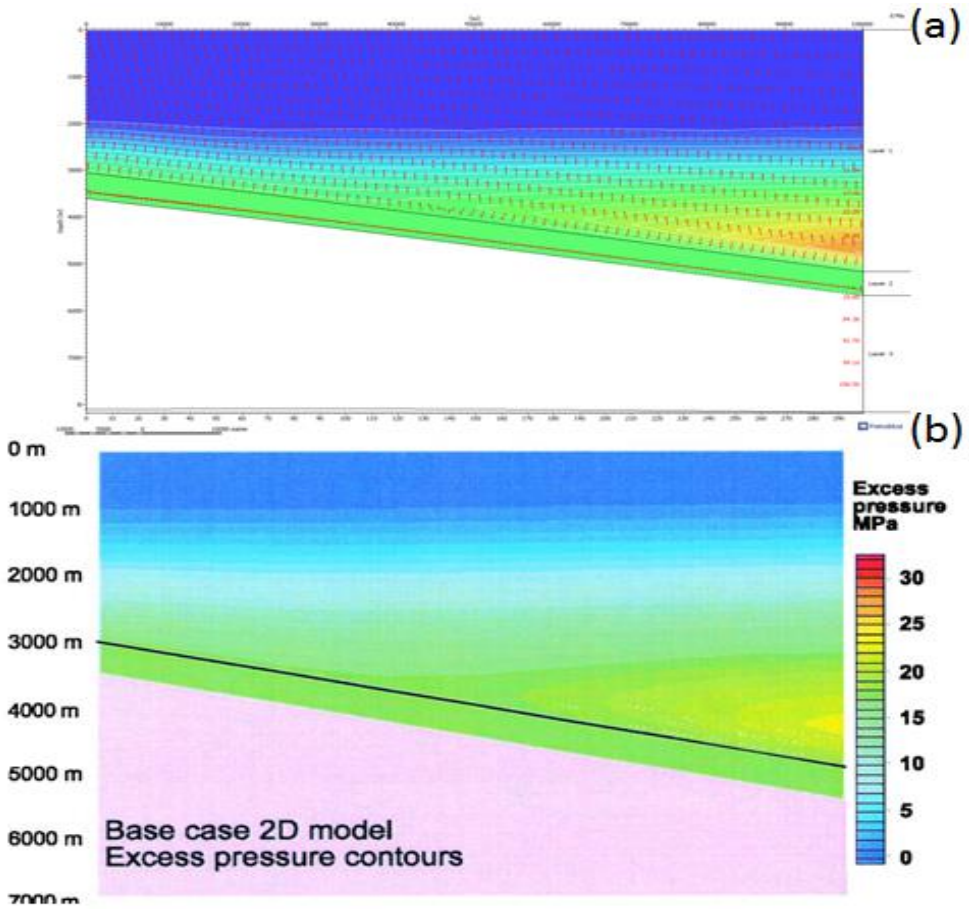

Figure 3-2 (a): Water velocity and overpressure distribution contours. Water flow into sandstone in aquifer base and out at crest .The flow along the aquifer from base to crest enhances pore pressure in crest. Overpressure in base could reach the highest value, which is almost 27 MPa. (b) Overpressure distribution contour of Yardley's model, for which the value could reach 26 MPa near the aquifer base. [15]

In terms of the water flow vectors and overpressure formation both models are nearly the same as each other: the fluid flows into the base of the aquifer and flows out of crest. Overpressure characteristics and values in surrounding mud are also similar. In aquifer crest, overpressure in sand is higher than surrounding mud, and the opposite in sandstone base. The value in aquifer crest is also similar (less than 1 MPa). This result provides the experimental and theoretical foundation to carry out a future study regarding the prediction of overpressure distribution in an aquifer crest by the influence of LT and disequilibrium compaction, and fluid interaction between GUs in such a sedimentary basin. In the next section, the basic model configuration of this thesis will be created, and a strong dependence of the specific parameters on Lateral Transfer will be demonstrated.

3.2.2 Simulation setup

3.2.2.1 Main model configuration and prediction reference point

In this section, an updated model is developed to serve as a basis for the remainder of the research described in this thesis. The updated model replaces the basement material of Yardley and Swarbrick's model with another, deeper interval of shale below the aquifer sand, which is identical to the shale of the overburden. The spatial configuration of the updated reference model (hereafter simply the reference model) is defined by a set of parameters whose values are assigned in such a way as to enable the sensitivities to be quantified.

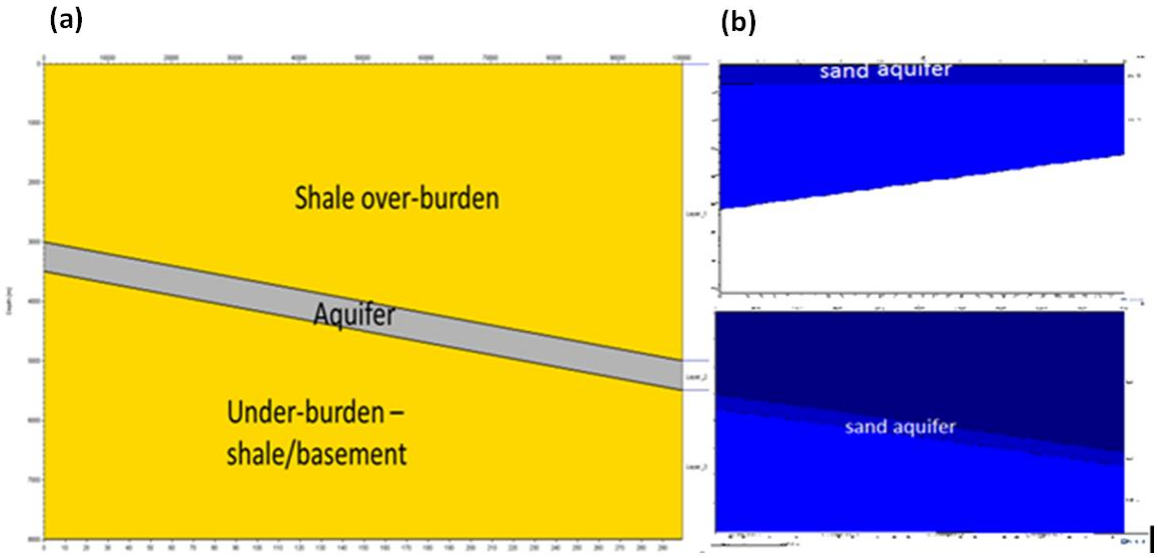

Figure 3-3 (a): The model configuration, which has two fine grain shale layers and a sandstone aquifer, and same properties between under and over-burden shale represented by yellow colour, the aquifer property is sandstone represented by grey. The length of the model is 10 kilometers and depth is 8000 kilometers. (b): The sandstone aquifer was initially horizontal, and became inclined due to the different depostional rates in crest and base. The crest of the aquifer is now at 3 km and there is 2 km of structure relief. The sandstone aquifer burial history showed the aquifer was level on top before over-burden shale deposit, then the sand subsided differentially and was rapidly buried to homoclinal.

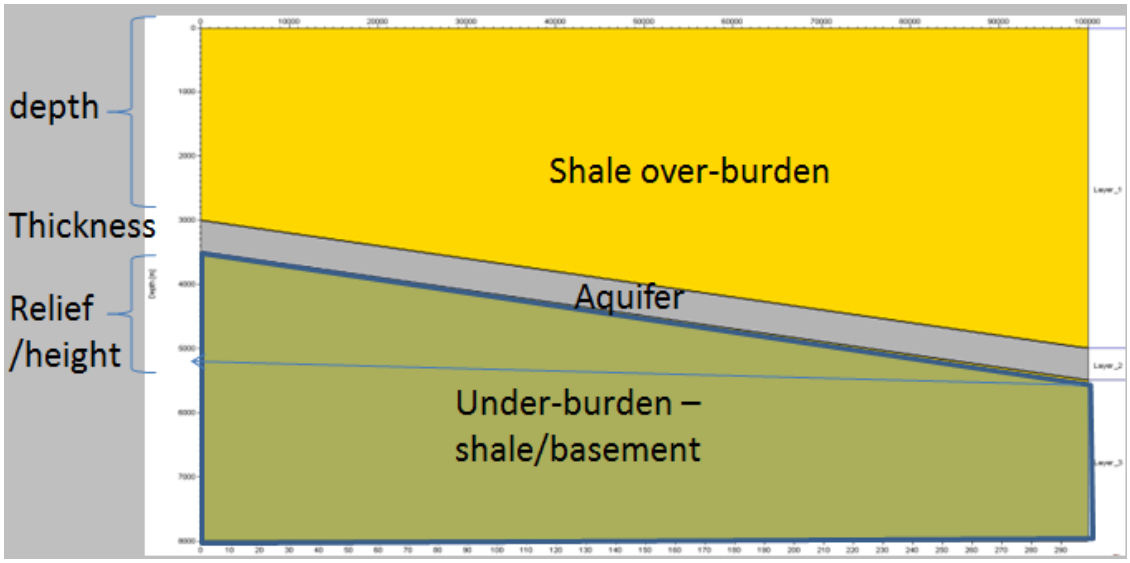

Figure 3-4 Main model configuration including the geology and geometry possible overpressure influencing parameters. The aquifer crest is fixed at 3000 m depth and the base at 5000 m. Relief is 2000 m; over-burden and under-burden properties of the aquifer are shale.

Figure 3-4 shows the generic configuration of the models. The geological parameters of the configuration model have been chosen according to Yardley's reference model, and the actual range in a well-known field. The range adopted in this simulation will be discussed in section 3.3 The model includes the over-burden shale sedimentation rate, the aquifer depth, relief and shale property, and also the aquifer thickness (which is the new parameter not mentioned in previous work; its influence and importance together with other new parameters will be discussed in later sections). The crest of the aquifer is now at 3.0 km and there is 2.0 km of structural relief along the length of the aquifer, because of the different sedimentation rate on each side of the aquifer associated with the differential subsidence from left to right. The shales above the aquifer crest were buried at an average rate of 100 m/Ma, whereas the shales over the down dip end of the aquifer were buried at a faster rate of 166 m/Ma. As shown in **Error! Reference source not found.**(b), the aquifer was initially horizontal but became inclined due to the differential deposition of the overlying shale sequence over the last 30 Ma, as the model region tilted towards the right.

For better understanding in future research about fluid migration and interaction between GUs in a basin, the boundary condition in this basin model was assumed according to main reference by Yardley and Swarbrick: (1) Strain is uniaxial (y axis); (2) Solid grains are incompressible; (3) Fluid and matrix are linearly compressible; (4) There are no thermal effects on compaction (consideration of this factor could make the

research more applicable in other settings); (5) There is a no-flow boundary condition on both sides of the model, and along the base of model.

In order to better interpret the characteristics of the overpressure distribution resulting from fluid lateral transfer and disequilibrium compaction in basin evolution, a reference point has been chosen at which the predicted overpressure is compared in this work. From previous research [5, 15], it has been established that an aquifer crest is a local structural high at which hydrocarbon might accumulate, and would therefore be a likely site for the drilling and development process. Laterally transferred fluid from the base to the crest generates a locally higher overpressure that could cause the mudstone cap of the crest to fracture or otherwise respond in some way, and so the estimation of overpressure at this location is important. In this research, reference point is selected, although the methods could be applied to multiple reference points in future work.

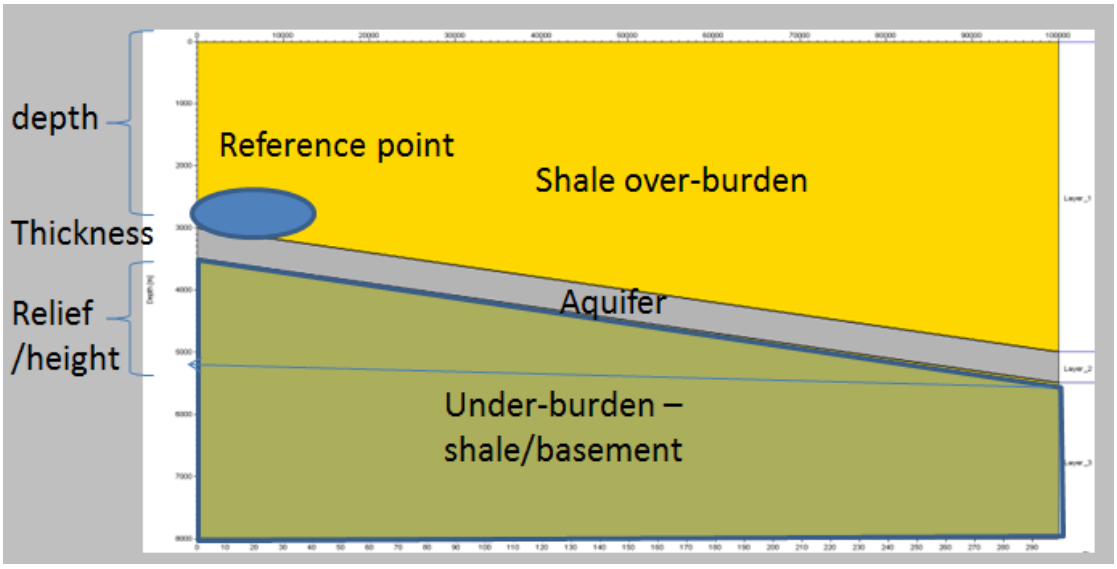

Figure 3-5 Main model configuration with geometry, reference point location and other variable parameters, which will be discussed on later sections.

In summary, I have chosen the reference point located on the crest of the sandstone aquifer in the configuration of the model (Figure 3-5), together with other multiple variable parameters. These include aquifer depth, relief, thickness, bending, and shale and sand properties. However, the extent to which each parameter may actually affect the over-pressure value at the reference point needs to be considered to predict overpressure distribution in the basin modelling of the test-bed base case.

3.2.2.2 Mathematical assumptions about the influence of LT

In this section, a mathematical function is created which expresses the relationship between overpressure at the aquifer reference point and the influential factors. It consists of three parts: the overpressure value in the model's output (real value), overpressure from the function prediction (which should be worked out by response surface methodology), and estimation error. The overpressure value at the aquifer crest (reference point) is mainly affected by the mudstone clay content, over-burden sediment rate, aquifer depth, aquifer relief and bending degree. (Figure 3-6) It is assumed that the overpressure function at the reference point (crest of aquifer) for influencing parameters is "F(Y)", and the estimated overpressure value predicted by a set of the key system parameters is "f(X), where "X" may include sedimentation rate (R), over-burden clay content (C), aquifer depth (D), aquifer relief (H) and bending (B). These will be defined in the next section.

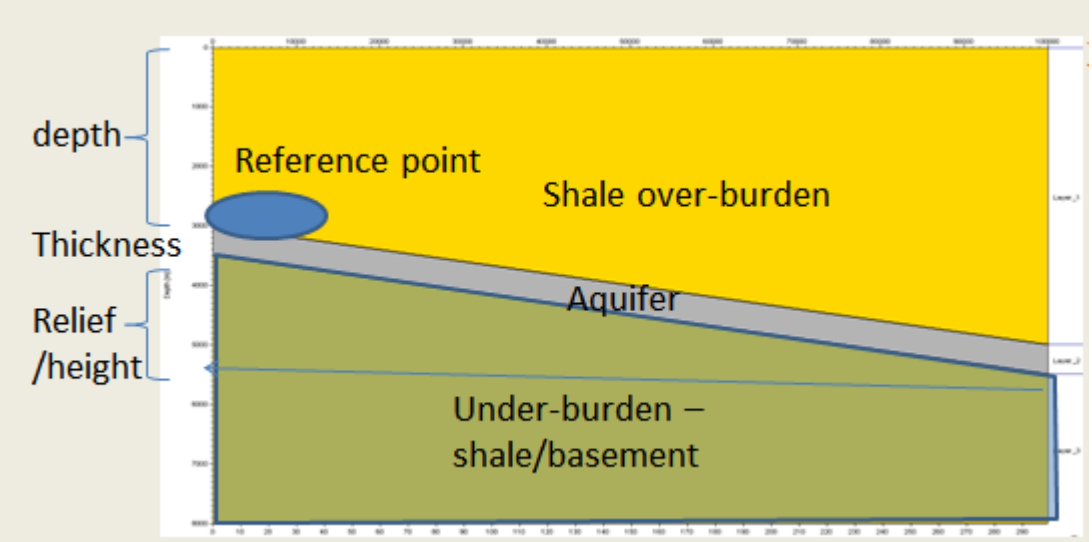

Figure 3-6 Model configuration without effects of channel-levee systems Showing five parameters influencing the value of the overpressure are. F(Y) is assumed to be unknown and true overpressure function, f(X) is the estimated element previously defined by Response Surface method, and Ɛ(Y) represents other unimportant factors and systems error after regression.

It is now possible to find suitable parameter space and 'best' f(X) so that Ɛ(Y) (other parameters and system error) is minimised:

Assume:

$$\mathbf{F(Y)} = \mathbf{f(X)} + \boldsymbol{\varepsilon}\mathbf{(Y)};\ \mathbf{X} = (\mathbf{D},\ \mathbf{H},\ \mathbf{C},\ \mathbf{R},\ \mathbf{B}),\ \mathbf{Y} = (\mathbf{X},\ \mathbf{others}) \qquad 3\text{-}1$$

The relationship can be obtained through a high number of simulations and the response surface methodology. These processes will be described in detail in the next sections. This relationship and the method also will be used in chapter 4 for developing an understanding of GU interaction relative to prediction of overpressure on LT and CLs models.

3.3 Impact from the five main factors

In order to describe the overpressure distribution at the reference point in the lateral transfer test-bed, many simulations are needed to work out the relationships between the influencing parameters and the overpressure value. First of all, it is necessary to define the parameters influencing the overpressure at the reference point and to establish their range, which is significant and important for connecting the future simulation.

In this section, influential geological and geometrical factors will be studied by numerical modelling, with value ranges drawn from the previous literature. Their sensitivities will also be studied by numerical methods. The sedimentation rate and clay content of over-burden deposits could influence pressure distribution in basin evolution, as mentioned in much previous research. [5, 15, 17]. These factors will be discussed in sections 3.3.1.1 and 3.3.1.2. Also to be discussed is how inclined aquifer relief can influence overpressure distribution and LT effects in basin sediments. Furthermore, the depth and relief of an aquifer could also influence overpressure distribution at the aquifer crest, which will also be discussed in sections 3.3.1.3 and 3.3.1.4, while section 3.3.1.5 will discuss the impact of aquifer bending which could also influence overpressure distribution at the reference point. In section 3.3.1.6, the factors which do not obviously appear to influence overpressure distribution will also be studied by a numerical method; these factors include the basin depth, basin scale, and aquifer thickness. The influential factors will be considered as parameter space and an experimental design will be constructed to predict overpressure value at the aquifer crest. Those factors which are less important will be excluded in this study.

This section also presents and defines the parameters' ranges by using information from the literature review, and also basin modelling method to obtain a more realistic range. I use some studies of well-known deep water or offshore basins around the world, and focus on their depositional rate, lateral sandstone reservoir relief, crest depth and summarize these results to establish the over-burden burial rate, sandstone aquifer relief and crest depth range in this study. The mudstone porosity-effective stress relationships

worked out by Yang and Aplin, in 2004 [62], are also used for this simulation. Finally, the value and range of the degree of aquifer bending are defined for this study through an assumption of parabolic sandstone aquifer geometry. The non-planarity of the aquifer in these cases extends the simulation outcomes to situations that would not easily be termed block faulting.

In the configuration model, aquifer depth is between 3000m and 5000m, and the model does not have cementation and does not adopt organic maturation, so there is no need to take amount of the temperature effect on the basin system. Therefore I ignore the influence of temperature on basin evolution, and under such condition, chemical reaction effects can also be ignored. As compaction disequilibrium is the most extensively studied mechanism of overpressure generation, this was the only effect considered to generate overpressure formation in my basin modelling. Some factors which could influence compaction disequilibrium and the effect of lateral transfer thereby altering the pattern of overpressure formation and value at the reference point will be discussed below.

3.3.1 Examination of Key influential parameters and their adopted range on lateral transfer

This section mainly focuses on possible key parameters which have a relationship with overpressure at the reference point in the LT case model, in order to consider fully how the systems interact and how physical processes are linked. Five key parameters were identified, and the value range of each key parameter in a well-known field will be reviewed to enable the research to cover the whole significant parameters range and be more comprehensive than previous studies. The first two key parameters have an important relationship with overpressure are over-burden clay content (permeability) and the sedimentation rate at the reference point; these will be examined in sections 3.3.1.1 and 3.3.1.2. And previous publishing also gave much support to the parameters physical interaction on overpressure in 1D and LT models. Aquifer depth also has a strong relationship with overpressure in the LT case model; section 3.3.1.3 will focus on the physical process of this parameter and the sensitivity will be analysed. Aquifer relief is also a key parameter in relation to overpressure at the chosen reference point in the LT model, which was proposed by Yardley and Swarbrick[15]. In 3.3.1.4, this parameter and its value range will be examined more comprehensively in numerical simulations. Aquifer bending is also a key parameter which could influence overpressure distribution in the LT model. The parameter's sensitivity and reason for

influencing overpressure will be examined and a simple definition of the range will be given in section 3.3.1.5.

3.3.1.1 Clay content of over-burden mud

The clay content of the aquifer over-burden mud plays an important role in overpressure distribution around the aquifer and at the reference point in the LT system. Any change in the clay content means a change in the mud compaction curve, and, thus, the porosity and permeability will be changed. Permeability is important factor that can influence pressure distribution. In basin evolution, lower permeability could block the motion of fluid from the pore space and generate more overpressure as previously was supported by previous work [5, 15, 17]. This mechanism is also effective in a 2D LT system. This section will examine the sensitivity of the overpressure to the clay content in the system by using a set of common complete compaction curves[62].

Yardley and Swarbrick's 2D Lateral Transfer model also uses a basin modelling methodology to establish that permeability and porosity are essential factors able to influence both overpressure distribution in basin evolution and lateral transfer.

Mechanical compaction is an inevitable consequence of burial and basin evolution. As a result, a significant effort has been made to quantify the process and to incorporate a mathematical description within computer-based basin models. This study focuses on the mechanical compaction of fine-grained, clastic sediments: muds and mudstones (hereafter referred to collectively as mudstones). Yang and Aplin, in 2004, have defined mudstone effective stress – porosity relationships and permeability – porosity relationships from natural mudstones and well log data from the North Sea and Gulf of Mexico, plus published experimental results. The relationship developed in soil mechanics between void ratio and vertical effective stress is a simple but practical way of describing the one-dimensional mechanical compaction of fine-grained clastic mudstones. The compression coefficients (e_{100} and β) that define this relationship are strongly influenced by grain size, which can be simply described by the sediment's clay content. The one-dimensional mechanical compaction of mudstones in sedimentary basins is adequately described by the simple relationship, developed in soil mechanics, between void ratio and vertical effective stress. The compression coefficients e_{100} and β are strongly dependent on clay content. Yang and Aplin generated the following relationships between clay content and compression coefficients by experiments[62].

$$e100 = 0.3024 + 1.6867\,clay + 1.9505\,clay^2 \qquad 3\text{-}2$$

$$\beta = 0.0407 + 0.2479\,clay + 0.3684\,clay^2 \qquad 3\text{-}3$$

And they defined effective stress – porosity relationships and permeability – porosity relationships, as shown in Figure 3-7.

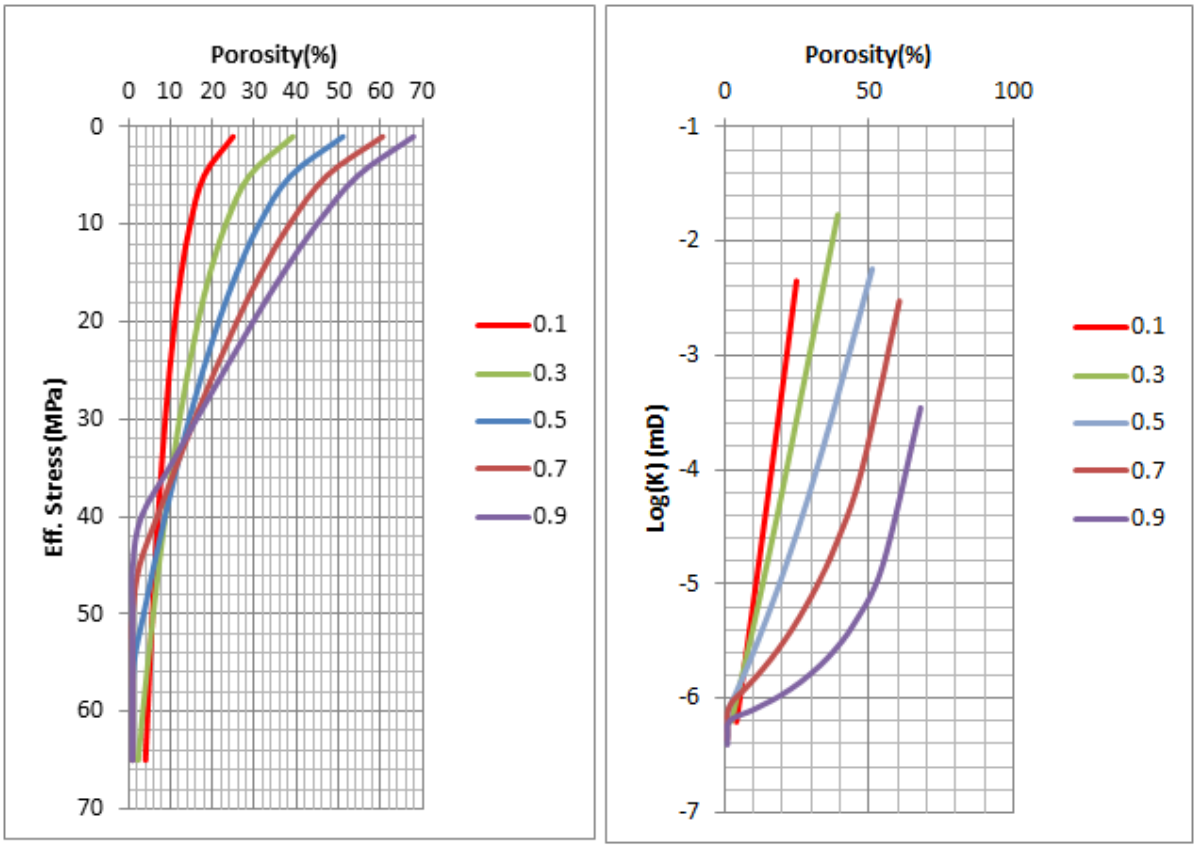

Figure 3-7 Mudstone effective stress & porosity and porosity & premeability relationships calculated by Yang and Aplin for natural mudstone from the North Sea and Gulf of Mexico. The different colour means different clay content value[62]

From this study, five values of mudstone clay content have been defined for the present simulation designed to obtain the relationships of the overpressure values at the reference point and the five influencing factors by response surface methodology. These values are 0.1, 0.3, 0.5, 0.7 and 0.9.

Before that, to examine the influence of clay content on overpressure, three sets of shale properties with different clay content which were calculated by Yang and Aplin (stress vs porosity and porosity vs permeability functions) were adopted in basin simulation for a view of the sensitivity of overpressure distribution to clay content; other conditions are the same as the configuration model. A summary of the curves, shale properties parameters and overpressure value are shown in Table 1:

Table 1 Compaction curve (stress vs porosity and porosity vs permeability) of lithology in which clay contents are 0.3, 0.5, 0.7 [62] and the overpressure value at the reference point. According to the curve and results, the overpressure value increase as shale clay content increases.

Clay content	Overpressure on crest(reference point)
0.3	10.34 MPa
0.5	12.57 MPa
0.7	16.11 MPa

From the results shown in Table 1, it can be seen that overpressure value on the crest increases from 10.34 MPa to 16.11 MPa when the shale clay content increases from 0.3 to 0.7. At the reference point location, the porosity of the three cases is different (Figure 3-7). The mudstone with the clay content of 0.7 has the highest porosity, and that with a clay content of 0.3 has the smallest porosity of the three. Comparing this to the same value on the permeability - porosity curve, the mudstone with the clay content of 0.3 has the highest permeability, and clay content of 0.7 has the smallest permeability of the three. This can explain why the clay content of 0.7 could generate the highest overpressure at the reference point in this case. Clay content can be used to calculate stress vs porosity and porosity vs permeability functions, but this does not mean that the permeability and porosity value for each property will vary by increment or decrement along with the clay content verified at the same location.

3.3.1.2 Over-burden sedimentation rate

The burial rate of the over-burden can be varied in the model by changing the time over which the mud was deposited. This parameter also influences the overpressure in the LT model. As the burial rate of the over-burden layer changes, the excess pressure at the reference point changes. For example, if the burial rate increases, the loading rate is increased. For those sediments which have already compacted to a point where their permeability is low, the ability to de-water becomes a controlling factor in responding to the higher loading rate[81], so more of the new loads become expressed as higher pore pressures. Consequently, at high burial rates more overpressure is generated. Changing the burial rate will change the absolute amount of overpressure generated in both the 1D and 2D models, as found by previous work [15] [17].

Yardley and Swarbrick [15] studied the influence of burial rate on overpressure in their 2D LT model. Figure 3-8 taken from Yardley and Swarbrick, illustrates the build-up of

pore pressure as a function of depth. As the burial rate increases, the amount of overpressure increases, and also overpressure develops at shallower depths.

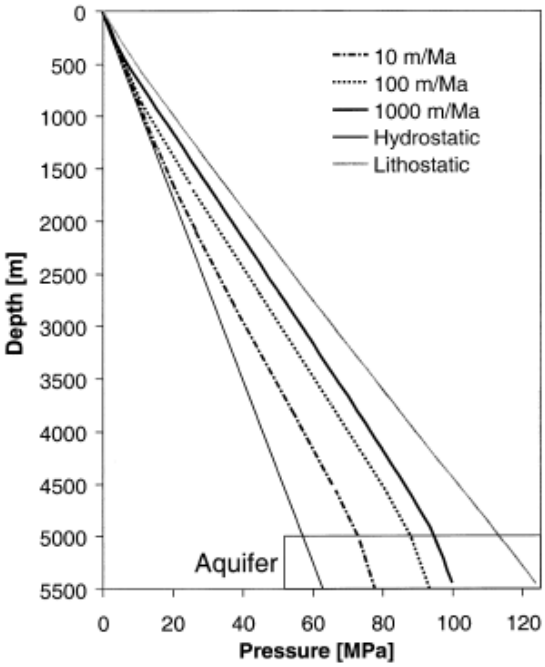

Figure 3-8 Pore pressures generated by disequilibrium compaction in the down dip 1D model for a range of burial rates of the shale layer. As the burial rate increases the pressure in the aquifer also increases. [15]

Yardley and Swarbrick's work only adopted certain values of burial rate and demonstrated the variation of overpressure and influence on overpressure on the lateral transfer model, with a small parameter range (from 10 m/Ma to 1000 m/Ma), and also did not establish a relationship between over-pressure on dipping sandstone crest and over-burden burial rate in 2D lateral transfer case model. This is the work that will be undertaken in this thesis by using Response Surface Methodology to work out a Mathematical model for overpressure variation at a reference point under the effect of such influencing parameters.

In this section, the parameter sensitivity will be examined more comprehensively in a 2D LT system, and the range of the parameters in the real world is reviewed. Sedimentation rates vary by 11 orders of magnitude and are strongly dependent on the time scale and spatial scale of measurement [82]. At the metre scale, average sedimentation rates can reach values of many metres per hour, for instance during turbidity deposition, but these rates are representative only for very short periods of time. Sedimentation rate at geological time-scales are, obviously, significantly lower.

Hardson presented an overview of sedimentation rates in relation to the Phanerozoic time-scale in 1964 [59]and using thickness data from Holmes [83] and radiometric date from Kulp [84] was able to work out a cumulative curve of maximum thickness of sediment for each system as shown in Figure 3-9.

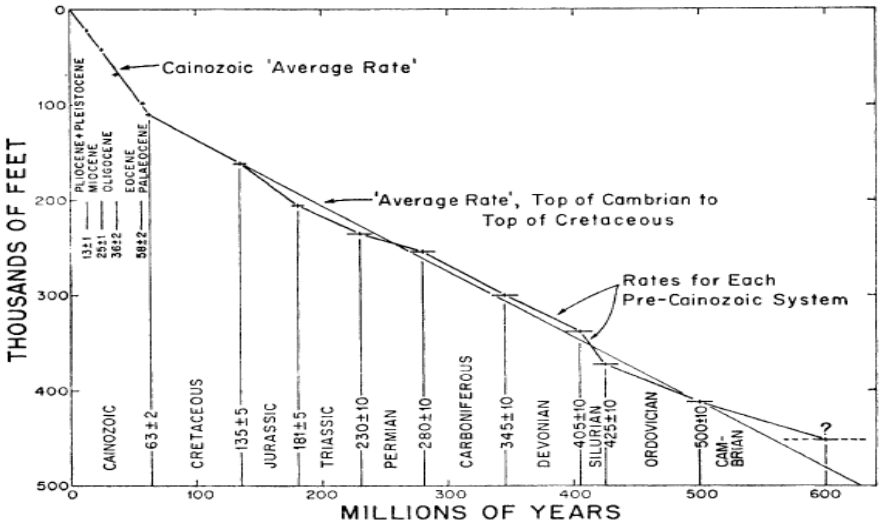

Figure 3-9 Cumulative curve of maximum thickness of sediment for each system against the radiometric time-scale: from Hardson [59].

The average sedimentation rate in each system can be calculated: the maximum sedimentation rate is 800m/Ma and the local area can achieve over 1000m/Ma (SILURIAN).

In the Baltic Sea, rapidly accumulating [66 to 140 cm $(1000\ y)^{-1}$] (660m/Ma to 1400m/Ma) hemiplegic sediments off southwest America (Peru) while in the Gulf of Mexico, the fastest average depositional rates in some local areas could have been as high as 4 thousand meters per million years.

This thesis considers overpressure generation by both fluid flow and mechanical compaction in the basin formation process. If the sedimentation rate is very low (less than 100 m/Ma), overpressure at the chosen reference point will not be obvious in numerical simulations. Thus, for more effective research into this parameter, I have chosen the range of the sedimentation rate at the reference point in the configuration model as 100 m per million years to 4000 m per million years. In addition, from the previous literature review, a few representative values of sedimentation rates according to the field data situation have been defined: these are 100 m/Ma, 300 m/Ma, 500 m/ Ma, 1000 m/Ma, 2000 m/Ma and 4000 m/Ma.

In this section, the six different values of the over-burden burial rate were picked from previous studies reviewed as explained above in order to check and view the influence of sedimentation rate on overpressure and the trend of this relationship. These were set in the simulation, other conditions were the same as in the configuration model, and the adopted shale property used a mudstone model in which clay content is 0.3 (stress vs porosity and porosity vs permeability functions as shown in Fig 3-6). A summary of the over-burden burial rates and overpressure values is shown in Table 2.

Table 2 Overpressure variation with over-burden burial rate changes in basin evolution. Overpressure is increased by an increase in the over-burden burial rate, amplitude can get 16.55 MPa where sedimentation rate is 100m/Ma to 4000m/Ma, and Changes in amplitude at a low sedimentation rate are more obvious than at high sedimentation rates. Where sedimentation is 100 Ma to 300 Ma, the alteration in value of overpressure is 6.91 MPa, between 2000m/Ma and 4000m/Ma ,alteration in value is only 1.73 MPa.

Over-burden sedimentation rate (m/Ma)	Overpressure at reference point (MPa)
100	13.26
300	20.17
500	22.83
1000	25.8
2000	28.08
4000	29.81

The value for overpressure variation at six different burial rates is listed in Table 2. Overpressure value at the reference point is increase with an increase in the over-burden sedimentation rate. This is mainly because, when the sedimentation rate is rapid, the fluid has less time to and is hard to dissipate from pore and stays in the pore to increase pore pressure, which is thus is more close to the over-burden lithostatic pressure. This effect may be because, when the sedimentation rate is high, the available rock deformation is smaller than when the sedimentation rate is low; thus less fluid, which cannot dissipate with the high burial rate, is locked in the pore. The results in this section showed the same patterns and phenomena as those from previous studies.

3.3.1.3 Aquifer depth

This section will examine aquifer depth, which is also a key parameter of system. Aquifer depth is the reference point depth in this study. Greater depth means lower permeability, where other conditions are constant, which could mean that fluid cannot easily dissipate, and hence more overpressure.

This section will use numerical simulations with different aquifer depths to examine the interaction between the sensitivity of overpressure to aquifer depth. At first, the range of the parameter in a real case needs to be reviewed, to make the work more comprehensive and more realistic when considering the range.

Sandstone aquifer depth has been proved to be one of the factors which could influence overpressure with reference in configuration model. Actually, the factors values are dependent largely on geological and sedimentation conditions, and vary in different basins and fields around the world. I intend to perform a scoping exercise and take a few representative values to apply in a simulation. The EI330 field seismic and Central North Sea seismic have been used by Fleming and Swarbrick [5][15] for different studies. A well correlation panel for Paleocene strata of the Central North Sea is also used, as shown in detail in Figure 3-10:

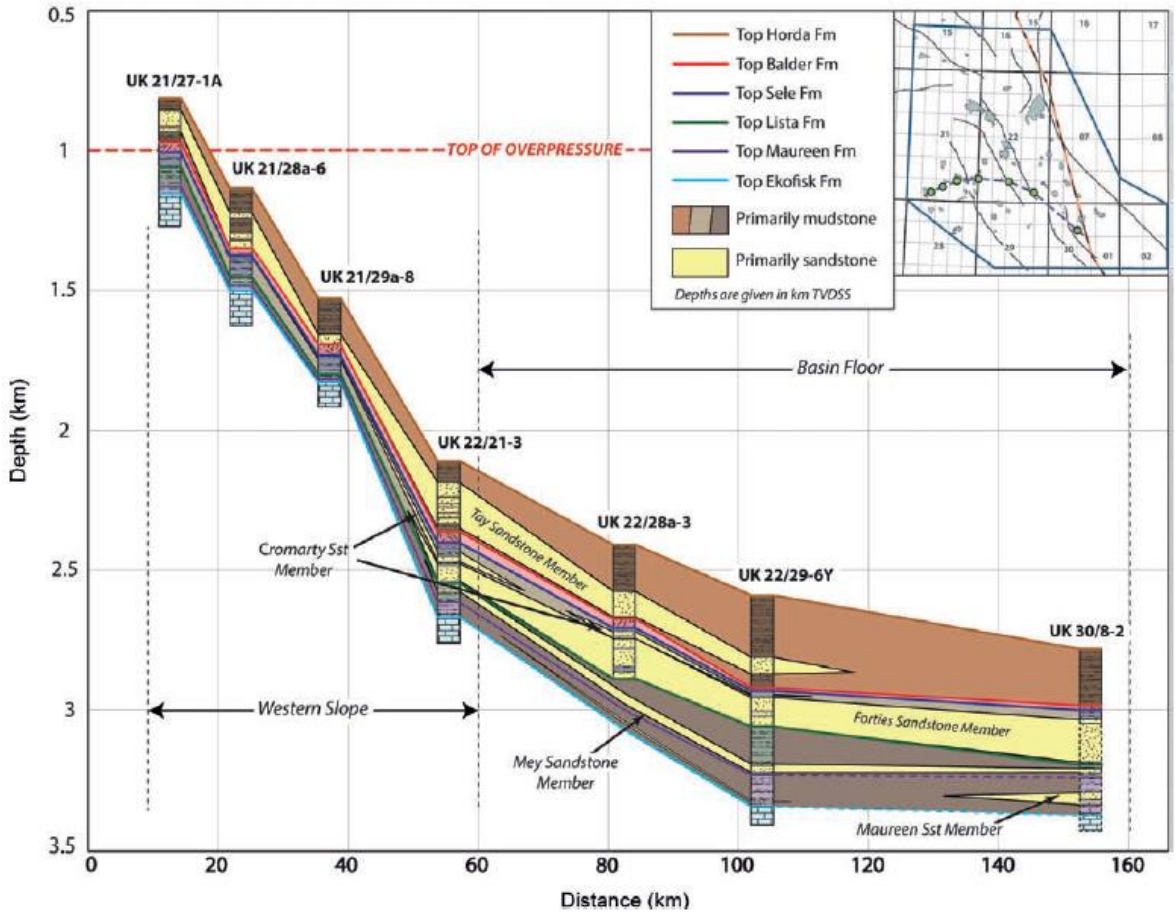

Figure3-10 Well correlation panel for Paleocene strata of the Central North Sea. In this graphic, at least four dipping sandstone layers are shown, each of which has different sandstone layer depths and relief. Probably the range of depth is between 1000 meters and 3000 meters; the relief values range between 1000 meters to 2500 meters. [85]

From Figure 3-10, it is clear that the dipping sandstone aquifer depth of the sandstone aquifer is nearly 4 km. In the seismic for the EI 300 field of the Gulf of Mexico, the dipping sandstone aquifer depth is nearly 1.9 km. In Figure 3-10, showing the seismic for the multiple sandstone aquifers, the sandstone aquifer dips from 1 km to nearly 2.5 km. In summary, the range of the dipping sandstone aquifer depth has been defined from 1 km to 4 km. Thus the representative values for sandstone aquifer depth chosen in this study are 2000 meters and 3000 meters.

From the main model configuration, the other Geometrical and petro physical parameters are kept constant and only the depth of the reference (the sandstone aquifer) is altered. According to the Central North Sea seismic, depth values of 1000m, 2000m and 3000m were adopted in this section and the results showed big gap on the overpressure on reference point. (Figure 3-11)

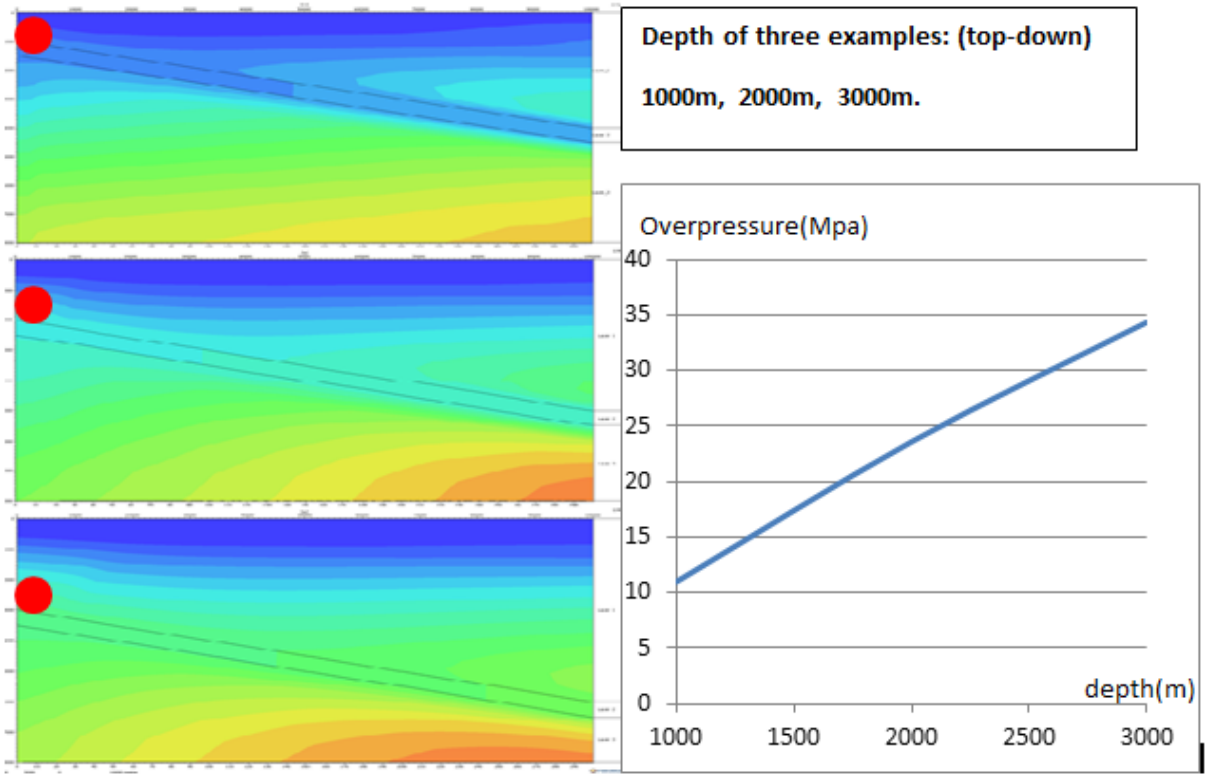

Figure 3-11 Examples of basin modelling have three different aquifer depths. From the top down, these are 1000m, 2000m and 3000m.The plots represents how overpressure value at the reference is changed by depth. According to the equation $P_L = \rho_b gh$, pressure and overpressure values increase with increasing aquifer depth of the plot. The results which are 10.99 MPa, 23.61 MPa and 34.39 MPa, followed this relationship and the plot shows a linear relationships between overpressure value and depth.

In the mechanical compaction curve, the plots shows strong relationships between depth and shale porosity and permeability, and the plots show almost linear correlations.

Knowledge of the relationships between overpressure values and reference point depth in different shale properties is also necessary for defining such parameter weights and ranges of experimental design in future work. Five groups of designs were set to represent how overpressure values are altered by the by the change in different shale properties for different depths of the reference point. Summary and plots are shown in Figure 3-12.

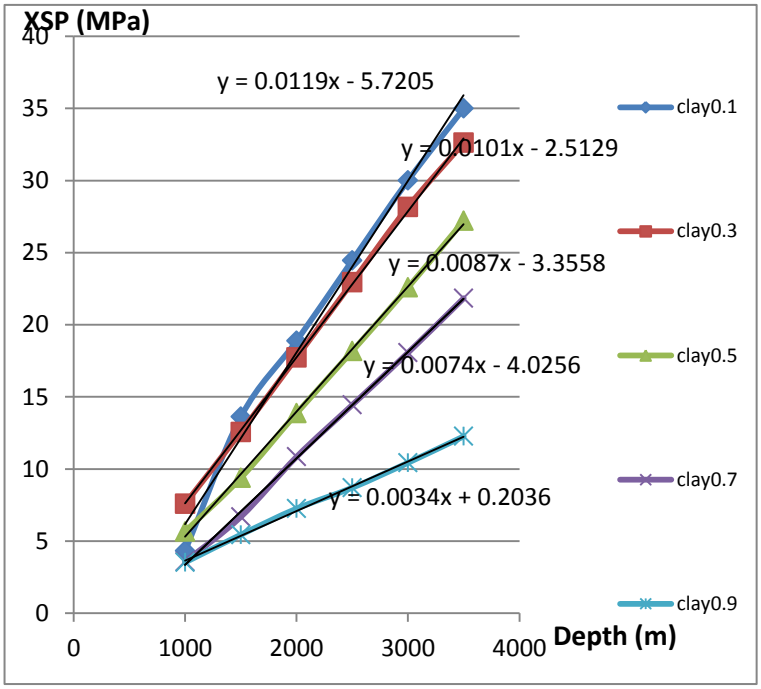

Figure 3-12 Plots of the relationships between aquifer depth and overpressure with others factor constant. Overpressure increases with increased aquifer depth, depending on clay content. They are all expressed as a linear relationship. This means that only two points need to be adopted in simulation design in later work.

The plots show a linear relationship for each of the shale properties except at 1000m to 1500m in 10% clay content. This is probably because, in a shallow water basin, composition and structure are more complex than in other places; furthermore, the properties of 10% clay content are nearly approaching those of sandstone. Thus, it is

hard to clearly and accurately describe relationships between effective stress and porosity from the compaction curve in these cases. Such conditions can be seen as a linear relation as with other shale properties shown in the plots. In the future work on the experimental design, the response surface methodology will be used; the range of aquifer depth could adopt a region which is defined by two different values which are common in real situations.

3.3.1.4 Aquifer Relief

Change in aquifer relief can also alter overpressure distribution in basin evolution which has a lateral transfer aquifer system. In this study, aquifer relief was varied by changing the amount of sediments deposited over the down dip end of the model. With increasing aquifer relief, the burial rate, and thus the depth to which sediments are buried at the down dip end of the model, increases, leading to more overpressure generation in the deepest over-burden mud. The increased pressure generation in the deep mud leads to greater water influx potential into the down dip end of the aquifer, and a greater pressure enhancement at the crest of the structure (Figure 3-13). In previous research Yardley and Swarbrick used a LT model to examine aquifer relief interaction with overpressure character in several cases. They found the same interaction through numerical simulations and found that the excess pressure generated in a dipping aquifer crest partly depends on the effectiveness of lateral transfer, and the lateral transfer effectiveness is approximately proportional to the aquifer relief. However, their study only used a few default compaction curves (Petro Mod software package) in the over-burden mud and no flow basement in the under-burden mud, which is not close to reality. In this section, the parameter of aquifer relief interaction with overpressure will be examined by numerical modelling in a more realistic parameter range and by using a common compaction curve in both over-burden and under-burden mud, which makes the work more realistic and systematic.

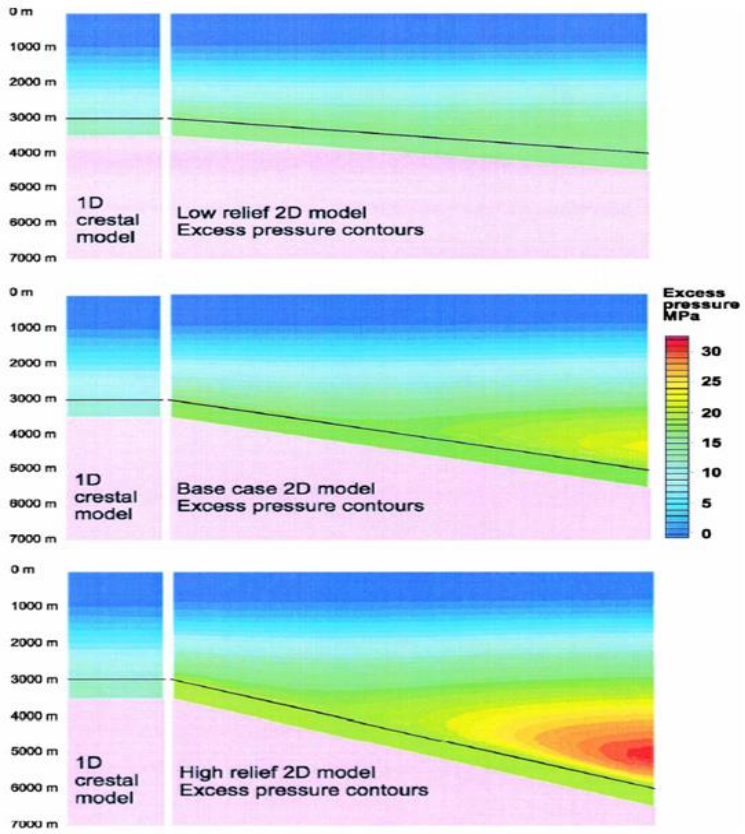

Figure 3-13 Excess pressure contours, showing the increasing pressure generation in the deepest shale for increasing aquifer relief. This also leads to increased pressure in the 2D aquifer relative to the 1D crestal model. [15]

Sandstone aquifer relief has been proved to be one of the factors which could influence overpressure at the reference in the configuration model. In reality, the factor's values are also dependent largely on geological and sedimentation conditions, and vary in different basin fields around the world. I intend to take a few representative values to apply in this simulation. The EI330 field seismic and Central North Sea seismic have been used for different studies, and detailed geological section was shown in Figure 3-14. I have also cited the well correlation panel for the Paleocene strata of the Central North Sea. From the graphic shown above, it can be seen that the dipping sandstone aquifer relief in Central North Sea is nearly 2300 metres and the depth of the sandstone aquifer is nearly 4 km. In Figure 3-14, which shows multiple sandstone aquifer section, the dipping sandstone aquifer relief value is between 1000 metres and 2500 metres. From the reviewed above, I defined the range in sandstone aquifer relief value in as 1km to 3km. The representative values for sandstone aquifer relief chosen for the later simulation Response Surface are 1000 metres, 2000 metres and 3000 metres.

Increasing the aquifer relief increases the volume of shales that can de-water into the down dip end of the aquifer. However, it also increases the surface area over which pressure dissipation can occur at the crest of the structure and the net change to the crestal pressure is therefore minimal [15]. Yardley and Swarbrick's model showed overpressure contours altered by changes in aquifer relief with no flow basement in basin evolution. I using the same theory and methods this research has simulated another group of models which have same shale properties as Yardley's model in the under-burden sediment. Three values of aquifer relief, ranging from 1000m to 3000m, were used in this section, and the model configuration and results plot are shown in Figure 3-14.

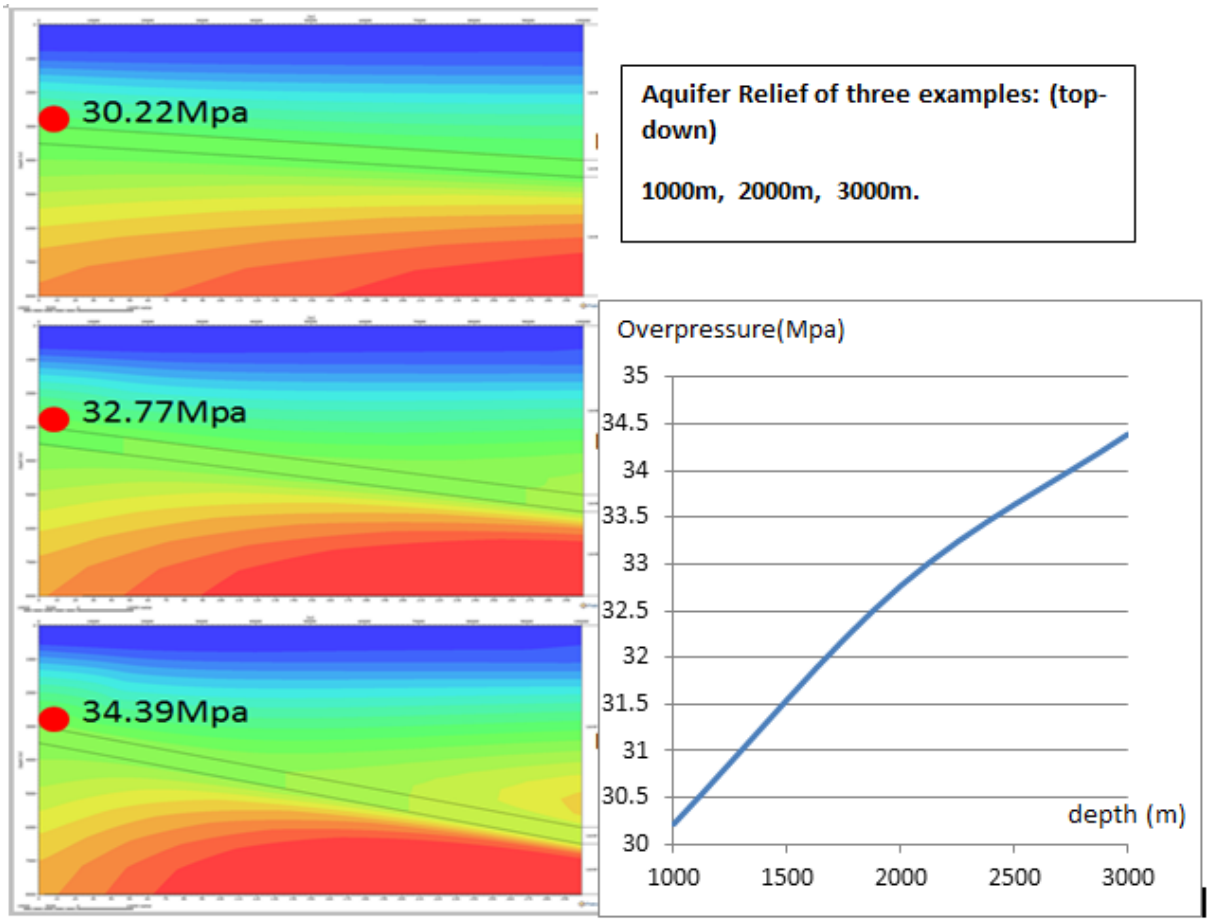

Figure 3-14 A group of models which have three different aquifer relief values: their overpressure appears as a regular ascending scale as aquifer relief is increased. The difference between these is less than 4.17 MPa from a relief of 1000m to 3000m. At the base of the aquifer, the under-burden shale has a great deal of overpressure, but it does not have a noticeable influence on overpressure value at the reference point or the effect of lateral transfer. Thus, under-burden shale burial rate is not a necessary parameter in this section as will be proved by basin modelling methodology in this chapter.

According to the results, the aquifer crest overpressure in the system will be increased by increasing aquifer relief. When aquifer relief is increased from 1000m to 3000m;

overpressure value at the chosen reference (aquifer crest) is also increased from 30.22 MPa to 34.39 MPa. The fluctuation range is obviously smaller than of the sedimentation rate and over-burden clay content in the defined parameter's range. However, it is clear that aquifer relief does interact with the overpressure characteristics in a LT system, and they showed a positive relationship. This is because, as burial rate increases in down dip part, sediments have less time to de-water and the pore fluids support more of the additional overburden load. Consequently, more overpressure is generated and pressure retention starts at a shallower depth (aquifer crest), inhibiting compaction at this location (and thus preserving higher porosity and permeability) .The plot shows overpressure changes with alterations in the aquifer relief, as in Yardley and Swarbrick's LT model. However, they focused only on the differences in overpressure values between the 2D and 1D models and the regular pattern shown by changing three values of aquifer relief, but did not address how the difference in elevation (relief) influences overpressure value in a 2D model nor the clear relationship (guideline) between overpressure value at the reference point and changed aquifer relief in the range commonly found in realistic situations. That is work which will be addressed by the response surface methodology in this chapter.

3.3.1.5 Aquifer Bending

Aquifer bending (Aquifer geometry) in a LT model can also influence overpressure distribution around the aquifer, as demonstrated by Stump [86] and Flemings, et al [5]. They used analytical forward modelling to examine pressure difference between synclinal, no bending and anticlinal aquifers and found that a synclinal shape could create more crestal overpressure than the anticlinal case in modelling an LT setting.

In this section, the parameter will be examined by numerical simulations to develop its interaction with the overpressure character in LT systems.

Aquifer geometry is caused by the tectonic evolution. The classic LT case was imagined as being caused by the tilting of a rigid faulted block. However, there are many ways that an aquifer layer can be deformed into a similar arrangement, especially if the planarity assumed for the original case is not the main characteristic of interest. So, any type of large-scale folding is an alternate means of deforming an aquifer layer into an arrangement where a crestal region is connected to a down-dip region. Here, I investigate the extent to which the non-planarity impacts on the crestal overpressure in such cases. In Stump's thesis, [86], she mentions that sandstone aquifer geometry

(anticline and syncline) could change the equal pressure point (the point where pressure is equal in sandstone and mudstone) position, which means this could change overpressure formation in sandstone and around mudstone. The model assumption and details are shown in Figure 3-15.

The work of Stump considered a sand layer which is buried at a rate that allows it to completely dissipate fluids and remain hydrostatically pressured to a depth of 2042 m (6700 ft). The sand then subsides differentially and is rapidly buried to form three different structures: a) anticlinal, b) homoclinal, c) synclinal. If burial rate then increases significantly as the sand subsides differentially, the sand and mud become overpressured. (Figure 3-15)

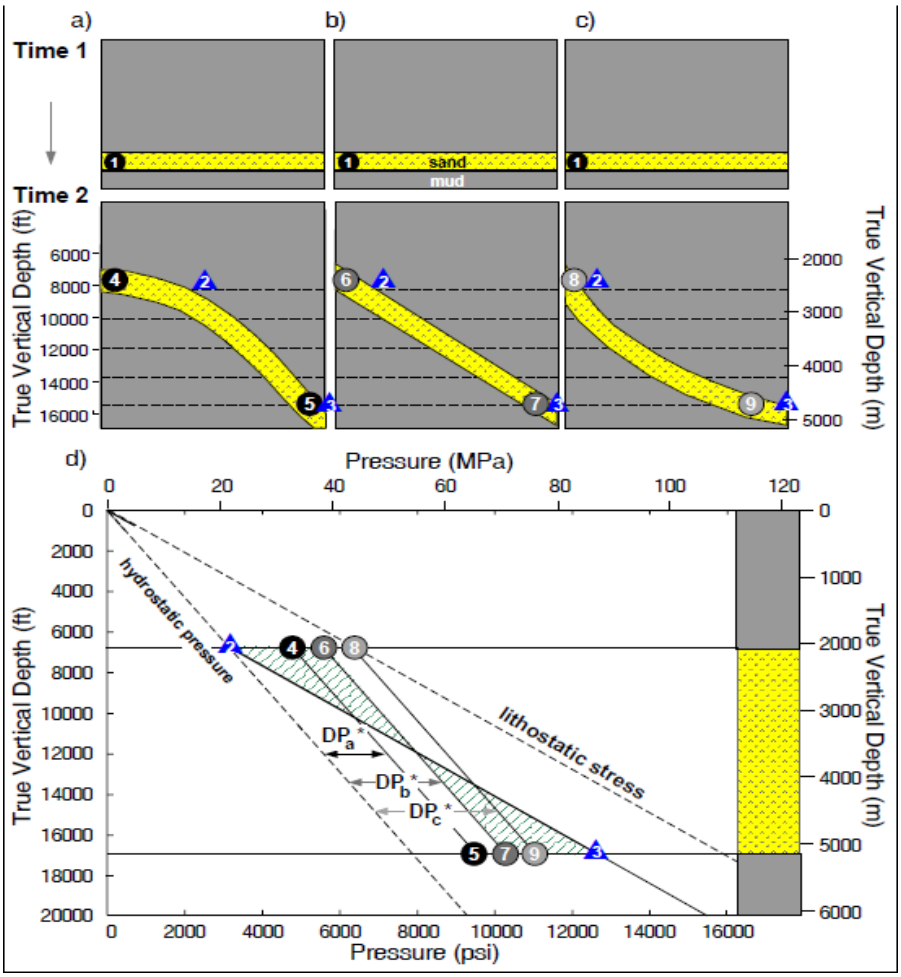

Figure 3-15 A sand is buried at a rate that allows it to completely dissipate fluids and remain hydrostatically pressured to a depth of 2042 m (6700 ft). The sand then subsides differentially and is rapidly buried to form three different structures: a) anticlinal, b) homoclinal, c) synclinal. Overpressure in mud is a linear function of depth, therefore overpressure contours (dashed lines) in the mud are horizontal. d) Fluid pressure from the surface to 2042 m is hydrostatic in both the sand and mud. Upon differential burial, fluid pressures in the sand diverge from pressures in the adjacent mud. Overpressure in the sand (DP*) is dependent on the overburden load (Equation 3-5b). Dashed lines

represent hydrostatic pressure (10.5 MPa/km; 0.465 psi/ft) and lithostatic stress (21 MPa/km; 0.94 psi/ft). Circles 4, 6,8 represent pressures in the sand at the structural highs; points 5,7,9 represent pressures in the sand at the structural lows. Triangles 2 and 3 represent fluid pressure in the mud at the structural high and low, respectively. Fluid pressure gradient in the mud is parallel to the lithostatic stress gradient; the pressure gradient in the sands is hydrostatic. [86]

The magnitude of overpressure within the sand and the depth at which the fluid pressures in the sand and mud are equal are affected by the geometry of the overlying load (Figure 3-15 d). A synclinal sand (Figure 3-15 c) sustains more overpressure than an anticlinal sand (Figure 3-15 a), because the synclinal sand supports a greater sediment load between both sides. As a result, the depth at which the sand and mud pressures are equal (termed the centroid depth by Traugott and Heppard [54]) varies with the structural geometry. The pressure difference between sand and mud changes with position in the structure. From Stump's results, it appears that aquifer geometry could influence overpressure distribution in sand and mud. However, in that work, she only demonstrated that aquifer shape could change the position of the central point on aquifer, but did not give a clear relationship between aquifer bending and overpressure in the LT system, and adopted only one value of each bending style. In this section, the parameter's interaction with and sensitivity to the overpressure character will be examined by assigning different values of bending degree which are given by a simple assumption.

Bending degree is a parameter that can influence overpressure value at the reference point in the configuration model, which has been confirmed in previous work. In addition, aquifer geometry has many types of presentation; the more common types of bending are anticline and syncline which involve different bending directions. Thus, I have only considered the anticline type in this section, and the same method can be used to calculate syncline cases in future work.

In order to more systematically and comprehensively define the parameter range of the degree of bending of a sandstone aquifer, realistic data that are available about this are of little use. A mathematical assumption of the shape of bending of the aquifer is necessary. We assume this parameter is "B", and establish a coordinate system on the configuration system which assumes a no bending aquifer is the "X" axis, a vertical line which across the midpoint of aquifer is the "Y" axis; the details are shown below (Figure 3-16):

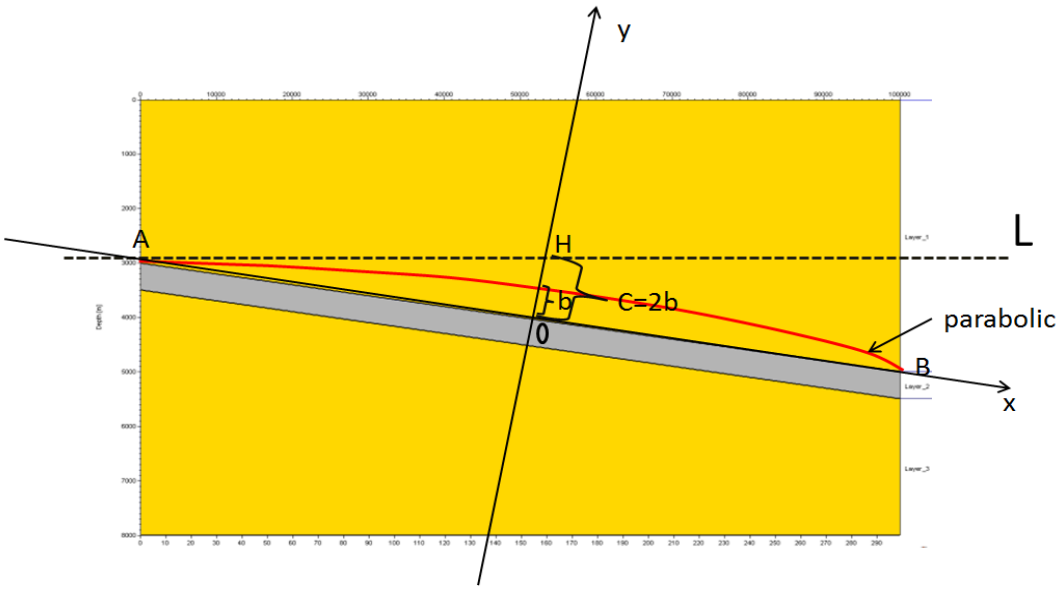

Figure 3-16 Assumption model of bending degree: a parabola which crosses the aquifer crest and base is assumed, and distance between the intersection point of parabola and the Y axis and origin O is “b”. The other line which crosses the aquifer crest is horizontal; the distance between intersection point of the line and Y axis and origin O is “C”. The maximum value of B is C/2. The process of proof will be shown in this section.

The Figure 3-16 shows the assumption of the anticline model and defines two important distances “C” and “b” which are the distance between the intersection point of the line and Y axis and origin, and the distance between the intersection point of the parabolic and Y axis and origin. If the parabolic support crosses the aquifer crest and base, and the highest geometrical point is on the reference point, the parabolic parameter “b” has the limitation that the maximum value is half “C”. The process of proof is shown below:

Assume a parabolic line which crosses point A and B: y=-ax^2+b

Assume length of aquifer AB is “d”, and distance value of “OH” is C.

If the parabola supports that the highest geometrical point on it is “A” (meaning distance b is the highest value of the range), the tangent of this point is line “L”, and the gradient of “L” is $\frac{C}{d/2}$.

The parabolic tangent gradient at point “A” also could be presented as Y’=-2ax.

Apply the coordinate of point “A”, which is (-d/2, 0), and gradient of “L” in this, to get a=2C/d^2

Substitute coordinate of point “A” and value “a” into the parabolic equation, to get b=C/2

Thus, the value is the highest bending degree in this study.

When this condition is satisfied, assume the bending degree parameter value “B” is 1. When the aquifer is not bending, “B” is 0.

We define the range of “B” as 0 to 1 and allow a random bending degree value variation in this region. Considering the accuracy of the simulation and the appropriate number of models in this study, five values from the range, are adopted: these are “0, 0.33, 0.5, 0.67, and 1”, respectively, and the corresponding model of different aquifer bending is established according the range required to carry out the simulation.

In this section, the three basin models have different geometry of the sandstone aquifer and the configuration models were set accordingly. The other conditions of setting are the same as configuration model; the details are shown in Figure 3-17.

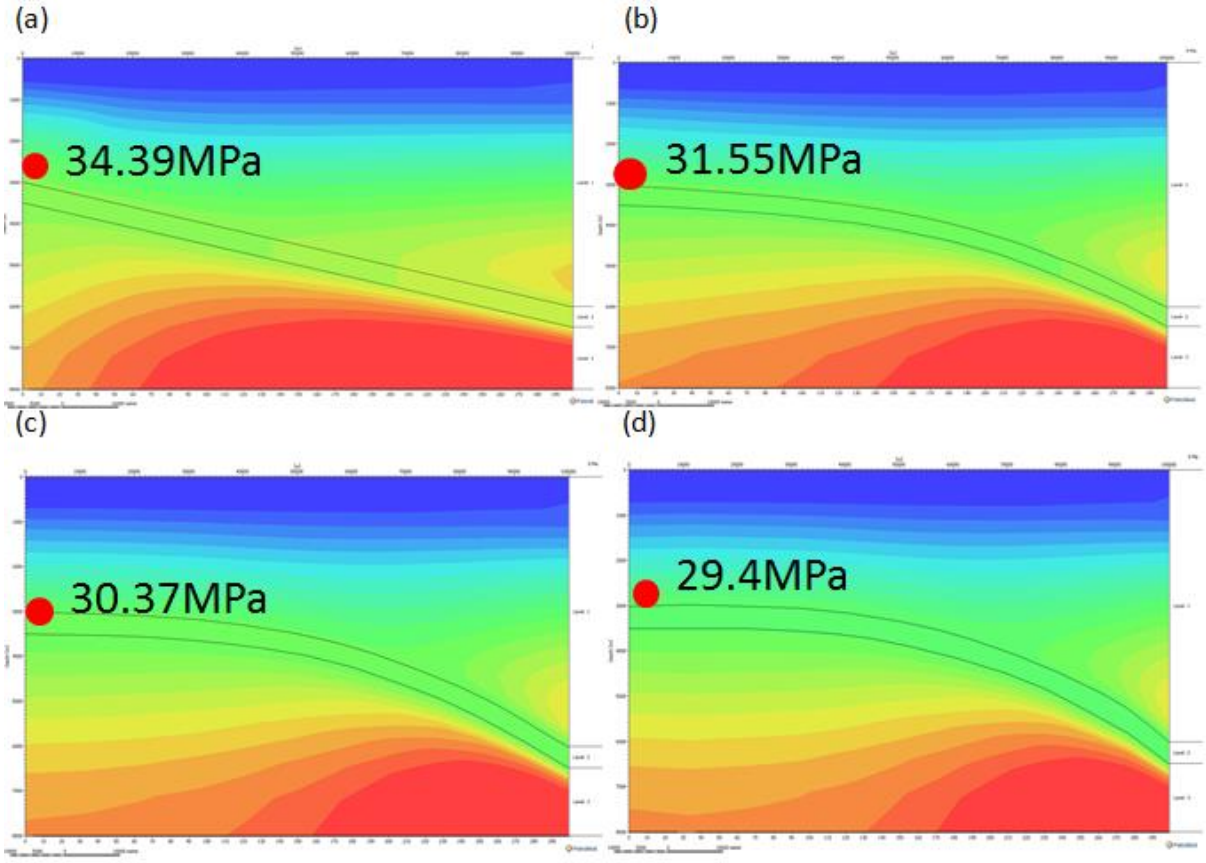

Figure 3-17 Overpressure contours of the base model, based on the configuration model:the three cases have differing degrees of sandstone aquifer bending, from weak to strong. (a) Base case model, in which overpressure value at the reference point is 34.39 MPa. (b) Case where aquifer has minor degree bending, in which overpressure value at the reference point is 31.55 MPa. (c) Case where aquifer has medium degree bending in which overpressure value at the reference point is 30.37 MPa. (d) Case where aquifer has relatively large degree of bending, in which overpressure value at the reference point is 29.4 MPa. The results do not showed a large difference between the three cases, but there appears to be a descending trend from case b to d.

From Figure 3-17, it is clear that the bending degree of the sandstone aquifer influences overpressure value at the reference point, and follows a descending trend with an increase in the aquifer bending degree (i.e. when the aquifer has an anticlinal shape). Since a change in the degree of aquifer bending means a change on over-burden mud sedimentation quantity and the sedimentation load of the unit, a higher bending degree means the aquifer affords a larger amount of sedimentation and sedimentation load of the unit than at a lower bending degree, resulting in a higher sedimentation rate and permeability in the mud, except at the two extreme points which lead different overpressure distribution with normal shape. However, the impact degree of the aquifer bending is obviously smaller than that of the over-burden shale burial rate, shale properties and reference point depth, which were studied above.

So far, five parameters have been determined that can influence overpressure value at the reference point: these are over-burden shale burial rate, shale properties, reference point depth, aquifer relief and aquifer bending. Other geometric and geo-physical factors that may also affect overpressure distribution at and around the aquifer crest, such as basin scale and sandstone aquifer thickness, will also be considered in the next section.

3.3.1.6 Unimportant Factors

In order to systematically and completely define the influence of the parameters of overpressure on the reference point, in addition to the factors already considered above (over-burden shale properties, burial rate, and depth of the sandstone aquifer (reference point), sandstone aquifer relief and aquifer bending), several other independently varying factors (the aquifer thickness, basin scale and depth) also need to be considered by the basin modelling methodology in this section.

In this section, the central equal point concept will be cited. If the depositional basin has an inclined aquifer which is surrounded by mudstone, there is a point on the boundary of the overlying mudstone and the high permeability aquifer where fluid will not flow in or out of the aquifer, and pressure will equal at this point. So in the main reference model, the fluid will flow out of the aquifer between the aquifer crest and the equal point, and will flow into the aquifer between the aquifer base and the equal point. Clearly, changing the position of the central equal point may change the pressure and overpressure distribution at the boundary of the aquifer and mudstone.

The thickness of the aquifer represents the volume of sandstone, and a gradual change of sandstone thickness could alter the equal pressure point between the sandstone and mudstone, as demonstrated by Fleming in 2000. In his study, he introduces the parameter *Z*, (Figure 3-18), the dimensionless depth along the structure where the sandstone and mudstone pressure are equal. This is calculated by dividing the vertical distance from the crest to where the sandstone and mudstone pressures are equal according to the total relief of the sandstone. Above *Z*, the sandstone pressure exceeds the mudstone pressure; below *Z*, the sandstone pressure is less than the mudstone pressure.

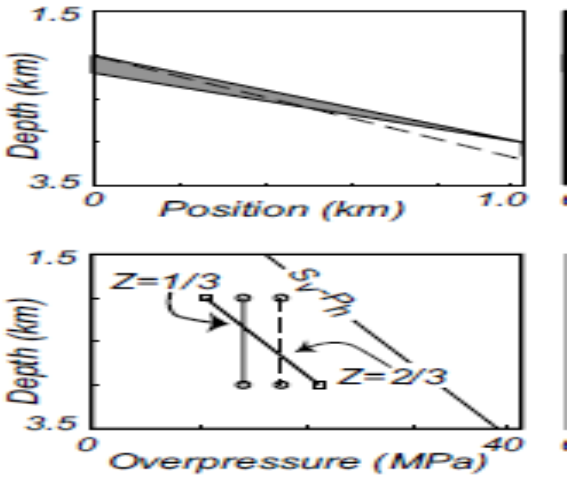

Figure 3-18 Overpressure for different sandstone geometries in undrained model. When sandstone thickens down-dip (dashed line), overpressures are elevated relative to when sandstone thickens up-dip (solid line). [5]

According to Flemings, et al [5], variable thickness of the aquifer could change the equal point between the aquifer and the over-burden mudstone; thus, the thickness of the aquifer can affect the overpressure distribution around the aquifer, and therefore may influence the overpressure at the reference point. To demonstrate this, two models with different aquifer thicknesses were simulated keeping all parameters the same as before but with different gradual changes of aquifer thickness.

Figure 3-19 shows the configurations at the end of the simulations for these two models, with respect to the main reference model.

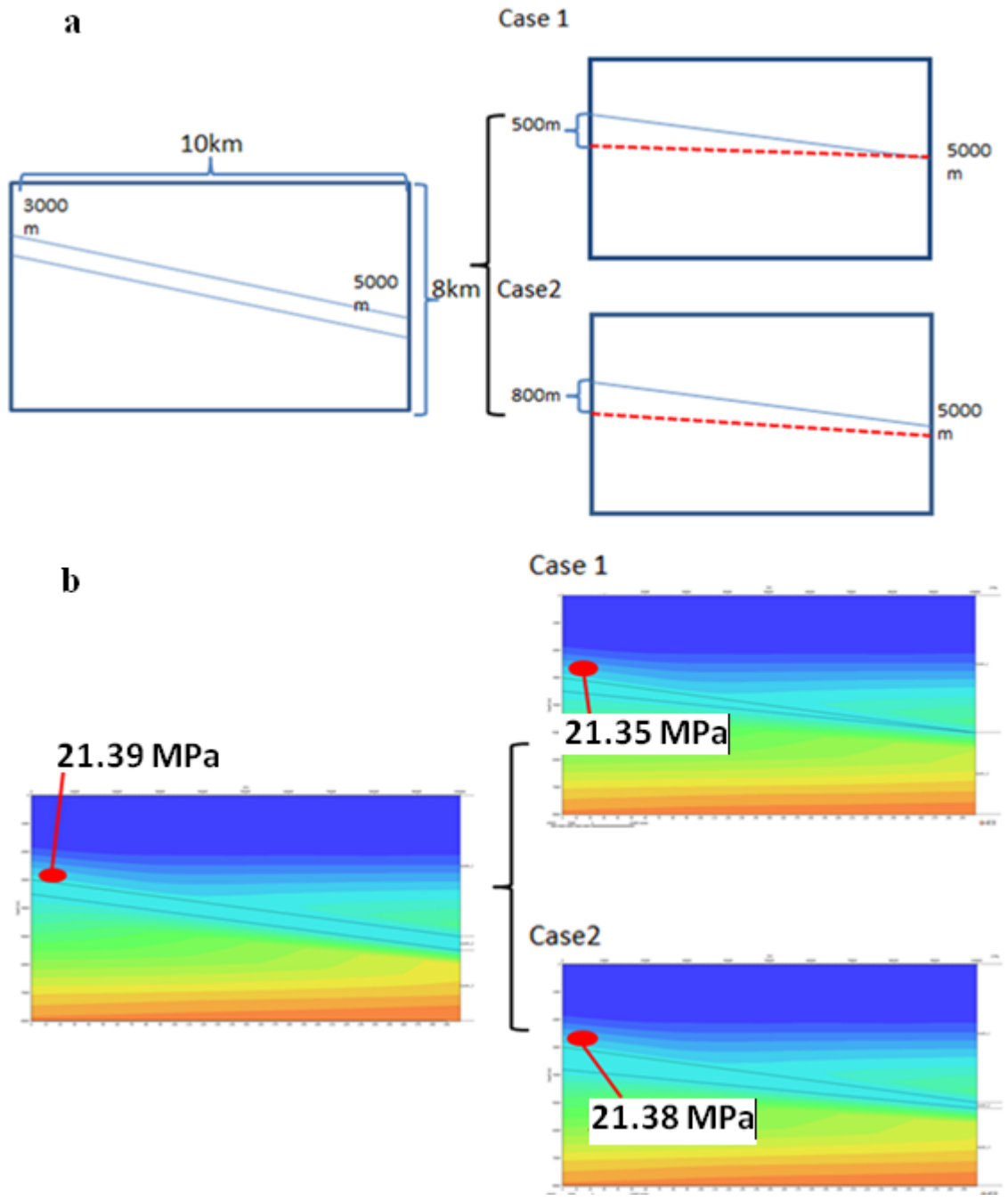

Figure 3-19 (a) The main reference model (left) and two additional models (right) with different sandstone thicknesses at the end of corresponding simulations. Model on left is main configuration model in which scale in length is 10 km and the depth is 8 km; thickness of sandstone aquifer is 500m. In the two additional models, the maximum thicknesses of the aquifers are 500m and 800m respectively, and both are gradually thinning towards the deeper basin. (b) Simulated overpressure values for these 3 models at the reference of the three models are nearly 21.35MPa; the results have little obvious change.

From figure 3-19, the base model and the two cases appear to have almost the same contours and value of overpressure at the reference point on the viewer. It can be understood that as the thickness of the sandstone has changed, this did not change the conditions of sedimentation and over-burden load, and that overpressure distribution

will not be noticeably altered by changes in the aquifer thickness. Thus, although changing the thickness of the sandstone aquifer could alter the equal pressure point in a sedimentary basin, it cannot noticeably influence overpressure character at the chosen reference point in a LT system.

The under-burden shale burial rate is a parameter which should also be considered in basin evolution. The burial rate in the under-burden shale could change the overpressure pattern at the base of the aquifer. Maybe these conditions could transfer more fluid energy along the sandstone aquifer and enhance the pressure on the crest. In order to prove the assumption correct or not, two cases, which have different under-burden shale burial thickness from the configuration model were adopted. The modelling geometry and result is shown below (Figure 3-19).

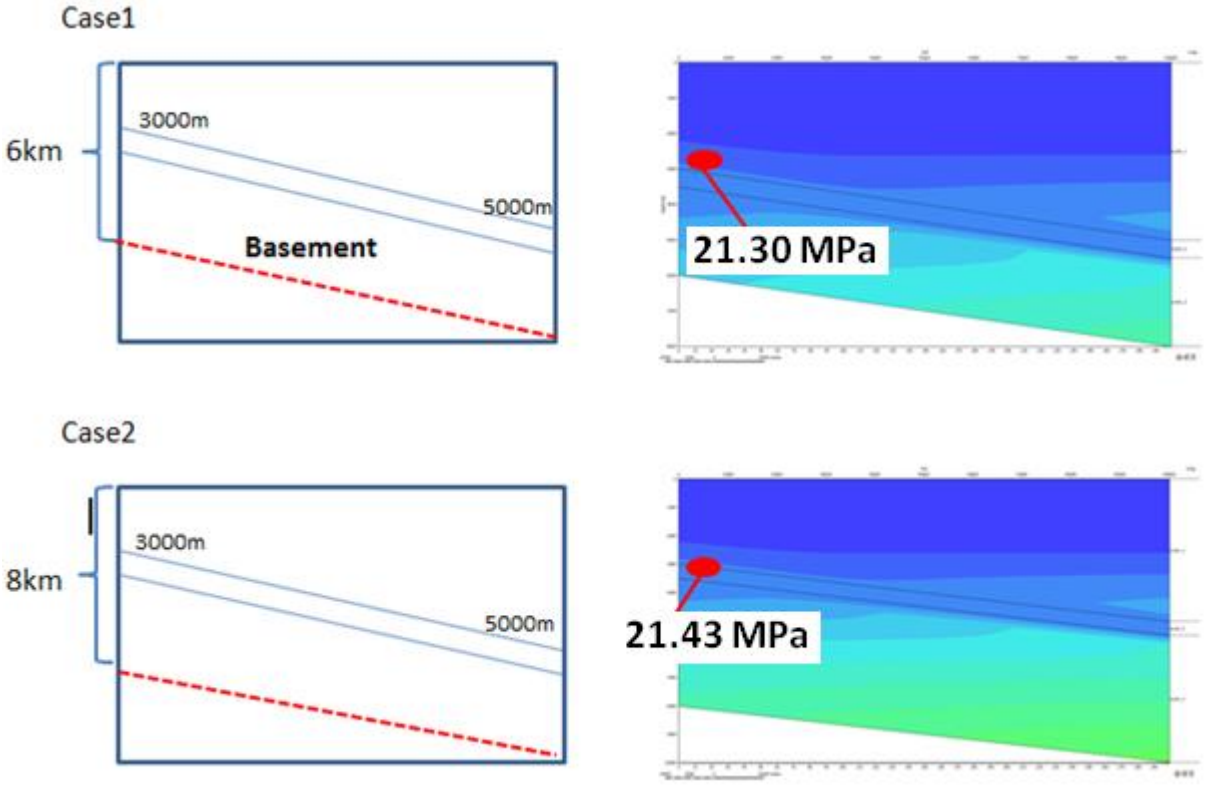

Figure 3-19 Modelling Geometry which changes the under-burden burial rate and configuration (depth of under-burden shale was changed and deposit time was kept constant. In case 1, under-burden burial rate was increased and the bottom of the base was changed. In case 2, the under-burden burial rate was slowed down, compared with the burial rate in case 1. The results show overpressure contours at the reference of each case: in case 1 it is 21.33 MPa and in case 2 it is 21.43 MPa, respectively. Both overpressure values are nearly 21.4 MPa, and each of them shows little change.

The results shows that the parameters have no obvious interaction with the overpressure character in the LT system and the overpressure value at the chosen reference point are

nearly same as each other. Overpressure distribution will not be noticeably altered by changing the under-burden burial rate.

Basin scale is the last parameter that will be considered in this section. Basin scale comprises basin length and under-burden shale depth, converting this in the basin modelling means changing the model dimensions. Four cases which have different basin scales (2 in length and 2 in depth) were developed in this part. Details of the model configuration and results for the overpressure value at the reference point are shown below (Figure 3-20):

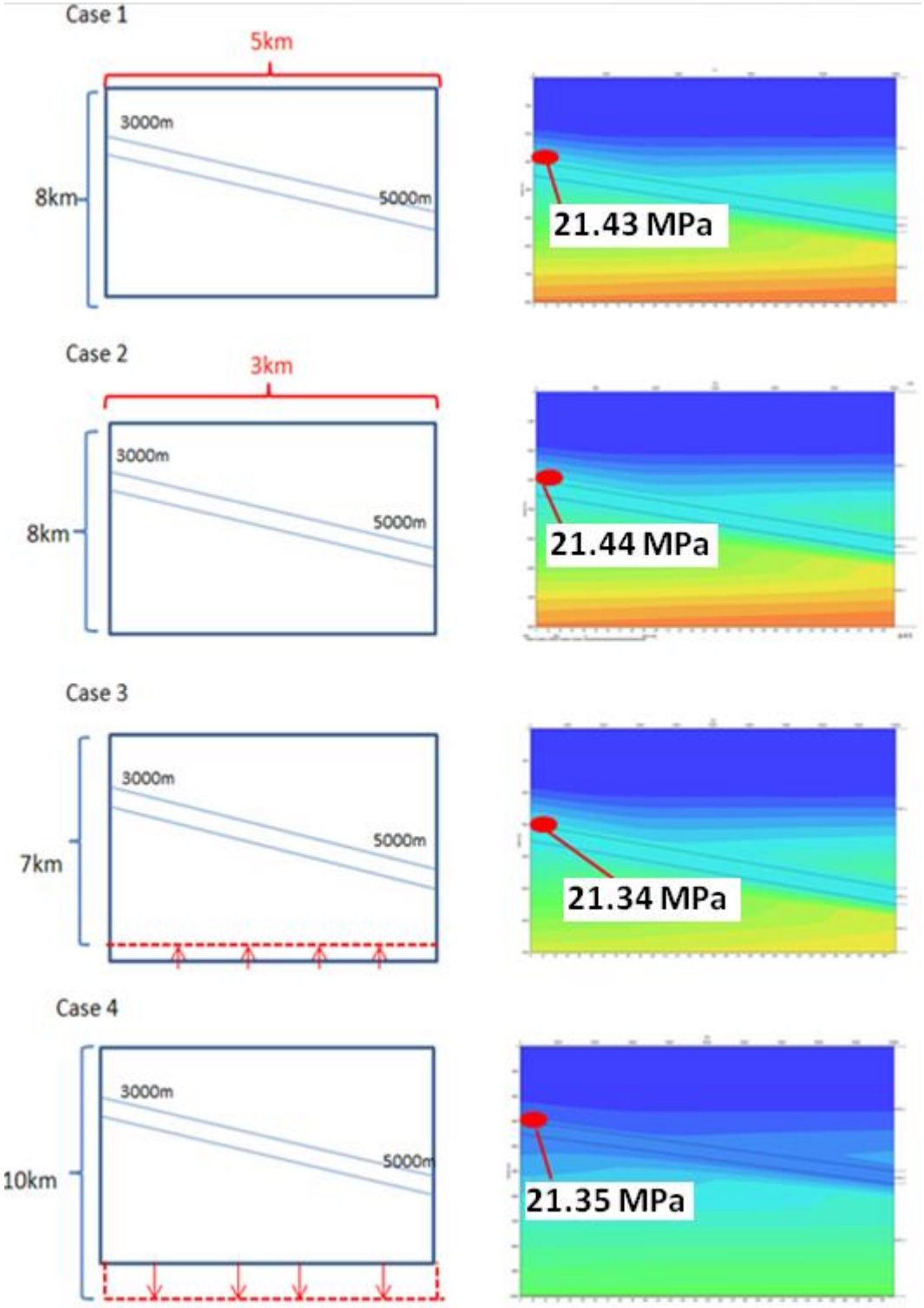

Figure 3-20 Modelling geometry which changes basin scale and over-burden and under-burden depth. In case 1, the basin length was decreased from 10 km to 5 km; in case 2, it has decreased by two kilometres more than in case 1, compared with the base case; in case 3, under-burden depth was changed from 8 km to 7 km.; in case 4, under-burden shale depth was increased to 10 km. The results show overpressure contours at the reference point of each of the four cases: overpressure values at the reference point of these four cases are 21.43 MPa, 21.44MPa, 21.34MPa and 21.35 MPa, respectively. For all of the cases, overpressure values are nearly 21.4 MPa, and each of them shows little change compared with each other and with the base case.

The results in Figure 3-20 for the overpressure contours of the four cases with different basin scales show little difference, and the values are nearly same as the base case. Changes in basin length could increase the sandstone aquifer length and overall over-burden load, but did not proportionally alter the pressure contours and average load in each unit.

Changing the under-burden depth put another way, means transforming the under-burden burial rate, so this cannot produce any obvious change in overpressure value at the reference. In summary, it has been shown that other physical and geometrical factors, such as sandstone aquifer thickness, under-burden shale burial rate and basin scale are less important in influencing overpressure value at the reference. Thus five factors, namely, over-burden shale properties, over-burden shale burial rate, aquifer depth, aquifer relief and aquifer bending will be used in further analysis of the relationship with overpressure value at the reference point in the Lateral Transfer base case condition by the Response Surface methodology in this chapter.

3.3.2 Retaining only plausible models in the simulation

This section will remove the non-compliance cases, such as effective stress reaching nearly zero, for more realistic results. When some parameters take values beyond certain thresholds, the simulated pore pressure at the reference point may lead to hydraulic fracturing pressure; the pore fluids no longer behave as they normally do in the pore space, nor do the mechanics. At this critical point, the basin simulator must be able to respond by simulating suitable flow and mechanical processes. Unfortunately neither PetroMod at the present time, nor other basin simulators the author was aware of at the time, is capable of doing that. For this reason, we exclude from the parameter space models which have zero effective stress (i.e. pore pressure reaches lithostatic pressure) at the reference point, for accurate prediction of the overpressure value at the reference with the capacity of PetroMod. The details will be provided in this section.

Parameters which can influence the overpressure value at the reference point relating to their impact have been confirmed in this study; these state that the overpressure value at the reference point will increase with over-burden burial rate, sandstone aquifer depth and relief increase. It is possible that overpressure value may reach fracture or lithostatic pressure when the factors reach a threshold value. In a real situation, this case could lead to a fracture occurring, fluids dissipating along the fracture and pore pressure would drastically unload at the reference point. In the numerical simulation, pressure

and geometry appear to show a discontinuous pattern in the output, so the credibility and authenticity of the results is unknown.

In this section, a case model with relatively high values for such factors has been simulated, the overpressure contours output showing a discontinuity on the crest of sandstone aquifer. In the 1D model, the overpressure value is very near to the over-burden mudstone lithostatic pressure and the effect is nearly “zero” at the aquifer crest. Some of the loading rates lead to very high overpressure at the crest, for the high clay-fraction overburden. In a real basin modelling study, these extreme cases would need to be dealt with (via increasing the permeability or allowing fractures to open) – but for this reference study, I exclude them. In this study, models with different combinations of parameters were simulated to identify models which do not meet the criteria (i.e., the effect is nearly “0” at the crest of the aquifer); details are shown in Figure 3-21. In Figure 3-21, we consider some representative influencing factors and analyse the effective stress at the aquifer crest with different combinations of such factors. We retained only the plausible models which have significant effective stress in the sandstone aquifer crest.

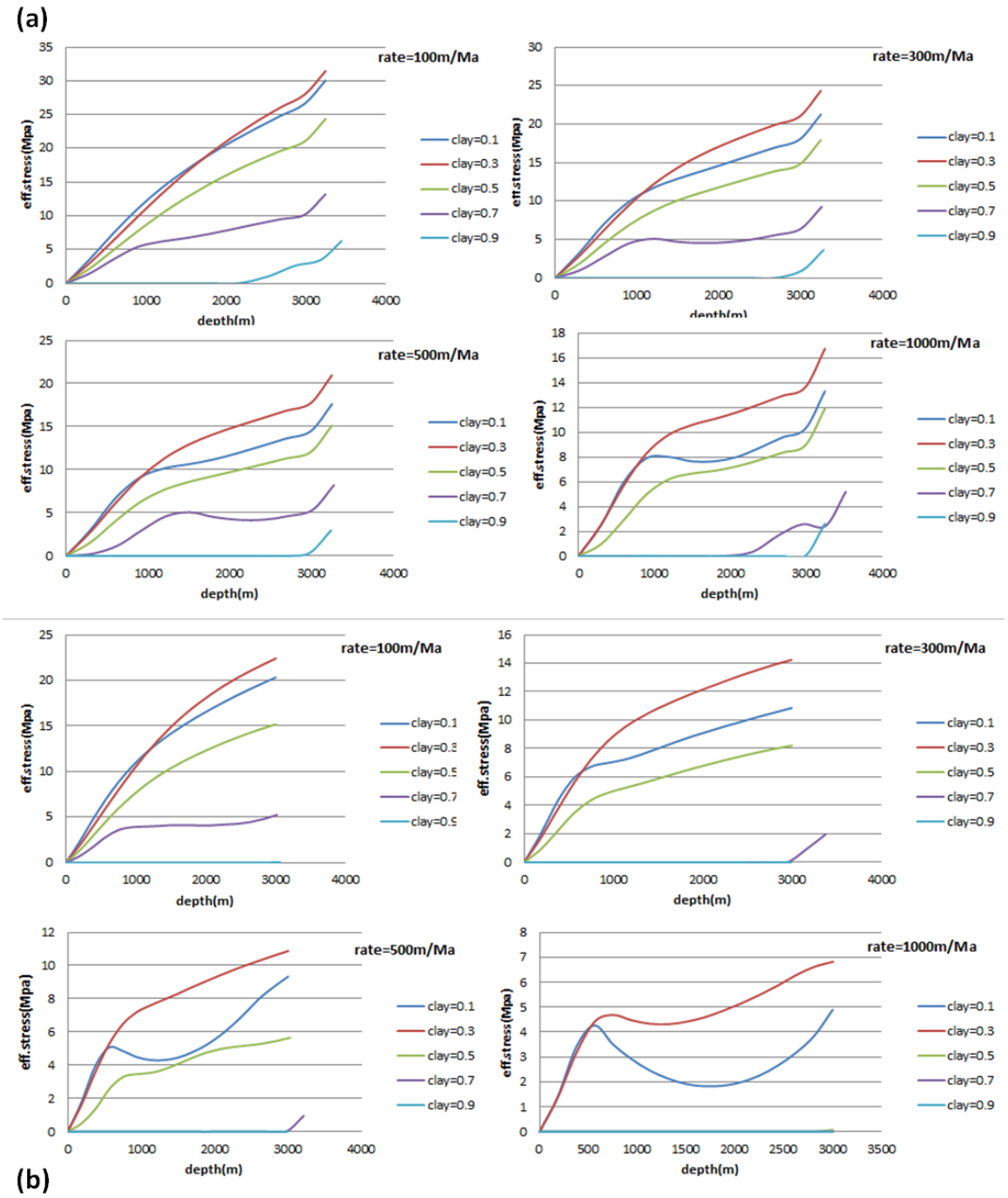

Figure 3-21 Effects of change with different over-burden burial rate, clay content, aquifer relief and aquifer depth value. (a) Sandstone relief is 1000 metres, effective stress is always near to "0" when mudstone clay content is 0.9, and clay content is 0.7 while burial rate over 1000 m/Ma. (b) Sandstone Relief is 3000 metres, effective stress is always near to "0" when mudstone clay content is 0.9, clay content is 0.7 while burial rate over 300 m/Ma, and clay content is 0.5 while burial rate over 1000m/Ma.Clearly, models where sandstone relief is 3000m have less effective stress at the aquifer crest than models where the aquifer dips by 1000m.

In Figure 3-21, effective stresses at the aquifer crest changes to close to "0" in the parameters that have specific values. Over-burden mudstone clay content and burial rate

play a more important role than the other two factors in this section, and also become the paramount standard measure of a model's plausibility. I then eliminated models where the effective stress at the aquifer crest is nearly "0" from all the factor combination models in this study. The following combination of parameters produced models with effective stress close to 0: all models with 0.9 clay content, models that the sedimentation rate over 300m/Ma while clay content is 0.7, and models that the sedimentation rate is over 1000m/Ma, aquifer relief is over 3000m while clay content is 0.5, respectively.

3.3.3 Prediction

After analysing of the LT system character and physical processes between each key factor and overpressure, a synthesized prediction of overpressure at the chosen reference point needs to be carried out to assess the system and lay the foundation for the next stage (developing an understanding of GU interaction). The response surface methodology was used to calculate the relationship between overpressure at the reference point and each of the five key parameters, which will be shown in this section. Given the identified key parameters, i.e. sedimentation rate, over-burden clay content, aquifer depth, relief and bending, and their ranges, LT basin simulations can be carried out to assess the relative importance of each parameter and the effect of each one on overpressure at the reference point. For this purpose, a full fractional factorial design was used, which requires 32 runs to capture the influence of each individual factor and pair-wise two-factor interaction. Using Design Expert [ref], 32 designs were generated, and then they were simulated with "PetroMod 2012". PetroMod software provided the overall results for overpressure distribution in the output. The results from this process are shown in Table 3.

Table 3 Full fractional factorial design results

Run	Factor 1 A:Burial rate m/Ma	Factor 2 B:Clay content	Factor 3 C:Depth m	Factor 4 D:Height m	Factor 5 E:Bending	Response 1 XSP Mpa
1	4000.00	0.50	3000.00	1000.00	0.00	18.16
2	100.00	0.10	2000.00	3000.00	0.00	14.36
3	100.00	0.50	3000.00	1000.00	0.00	12.57
4	100.00	0.50	2000.00	3000.00	0.00	10.1
5	100.00	0.10	2000.00	3000.00	1.00	8.9
6	4000.00	0.10	2000.00	3000.00	1.00	21.14
7	100.00	0.50	3000.00	1000.00	1.00	10.9
8	100.00	0.50	2000.00	1000.00	0.00	6.21
9	100.00	0.50	2000.00	1000.00	1.00	5.07
10	4000.00	0.50	2000.00	1000.00	1.00	10.44
11	100.00	0.10	2000.00	1000.00	0.00	9.05
12	100.00	0.10	3000.00	1000.00	0.00	15.37
13	4000.00	0.10	3000.00	1000.00	0.00	32
14	4000.00	0.10	2000.00	1000.00	0.00	21.85
15	4000.00	0.50	3000.00	3000.00	0.00	30.32
16	100.00	0.10	3000.00	3000.00	0.00	21.51
17	100.00	0.50	3000.00	3000.00	0.00	17.29
18	4000.00	0.10	3000.00	3000.00	1.00	32.97
19	4000.00	0.50	2000.00	3000.00	0.00	19.86
20	100.00	0.50	2000.00	3000.00	1.00	6.03
21	100.00	0.10	2000.00	1000.00	1.00	7.49
22	4000.00	0.50	3000.00	1000.00	1.00	17.37
23	4000.00	0.50	2000.00	1000.00	0.00	11.34
24	4000.00	0.10	2000.00	3000.00	0.00	21.84
25	4000.00	0.10	3000.00	1000.00	1.00	31.46
26	100.00	0.10	3000.00	1000.00	1.00	13.72
27	4000.00	0.10	3000.00	3000.00	0.00	32.53
28	4000.00	0.50	2000.00	3000.00	1.00	11.03
29	100.00	0.50	3000.00	3000.00	1.00	12.16
30	4000.00	0.10	2000.00	1000.00	1.00	19.72
31	4000.00	0.50	3000.00	3000.00	1.00	18
32	100.00	0.10	3000.00	3000.00	1.00	15.61

Table 3 shows the full fractional factorial design results, which contain 5 input parameters for 32 simulations (2^{nd} to 6^{th} column) and the simulated overpressures at the crest are shown in the last column.

In order to assess the influence of the 5 input parameters on the overpressures, a half-normal plot was constructed of the overpressures. The significant degree depends on how much they deviate from the straight line. The plot is presented in Figure 3-22,

which indicates that all of the five factors could have a significant influence on overpressure at the aquifer crest. Consequently, it is reasonable to retain all of the five factors in the response surface of the study. The plot also implies that burial rate is the most significant model term, while the effect of aquifer bending only is less significant. The second most significant factor is aquifer depth and the third and fourth is over-burden clay content and aquifer relief. The half-normal plot illustrates the degree of significance of other model items.

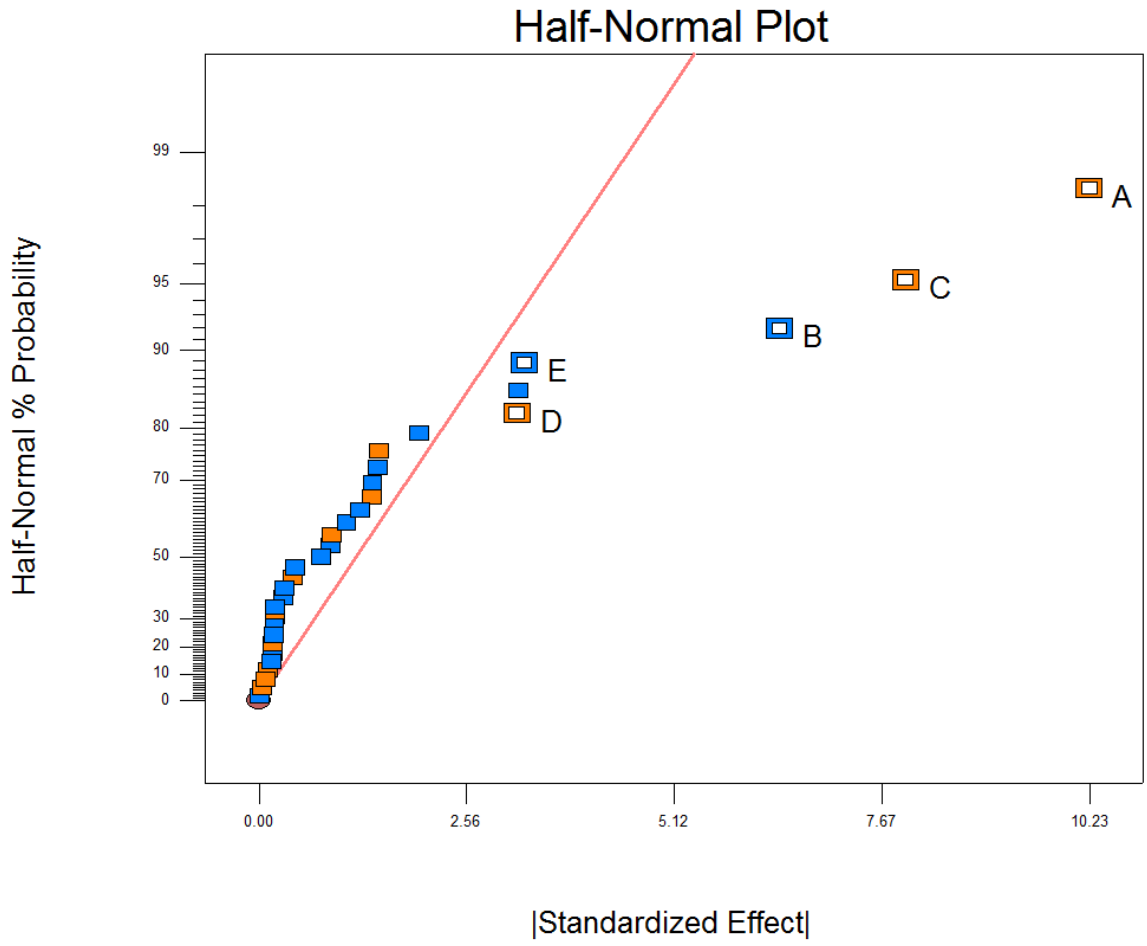

Figure 3-22 Half-normal plot of half fractional factorial design from design expert software, which used to define whether the 5 factors have significant influence on overpressure. In the graphic, A represents sedimentation rate, B represents around mud clay content, C means aquifer depth, D and E represents aquifer relief and bending, respectively. Points in the red line mean that the factor could have a significant influence on the overpressure at the reference point, and the greater the distance between the red line and the point the greater the importance of the overpressure. The orange coloured points represent positive effects and the blue represent negative effects on overpressure.

More details of the analysis are provided in the ANOVA table (Table 4), where it is confirmed that aquifer relief and bending have a less important role in overpressure

distribution at the aquifer crest. However, all of the 5 remaining parameters should be used in the study.

Table 4 ANOVA table from the half-fractional factorial design

Analysis of variance table [Partial sum of squares - Type III]

Source	Sum of Squares	df	Mean Square	F Value	p-value Prob > F	
Model	1841.52	5	368.30	42.33	< 0.0001	significant
A-Burial rate	*837.33*	*1*	*837.33*	*96.24*	*< 0.0001*	
B-Clay conte	*329.41*	*1*	*329.41*	*37.86*	*< 0.0001*	
C-Depth	*508.09*	*1*	*508.09*	*58.40*	*< 0.0001*	
D-Height	*81.06*	*1*	*81.06*	*9.32*	*0.0052*	
E-Bending	*85.64*	*1*	*85.64*	*9.84*	*0.0042*	
Residual	226.21	26	8.70			
Cor Total	2067.73	31				

After retaining all of the five factors from the design variables, the next step is to build the response surface for overpressure on these 5 parameters using the D-optimal design of the Design Expert software. As the default, a quadratic model was chosen. D-optimal design required 31 cases based on 5 factors. According to the previous analysis and parameter space defined in this chapter, 364 models in the range were simulated. This number is totally sufficient, as quadratic models are used in D-optimal design, and the even satisfies the quartic model, which needs 136 cases based on 5 factors. I used all of the 364 models' results and input to D-optimal design, in order to get more accurate model determination and response surface results from the D-optimal design. The overpressures corresponding to those 364 models were obtained by using PetroMod and an Excel spreadsheet, as shown in Appendix A.

Next, it is required to select the appropriate model to fit the overpressure response surface. Table 5 shows the statistical approach.

Table 5 Fit summary table

Summary (detailed tables shown below)

Source	Sequential p-value	Lack of Fit p-value	Adjusted R-Squared	Predicted R-Squared	
Linear	< 0.0001		0.7433	0.7375	
2FI	< 0.0001		0.8450	0.8383	Suggested
Quadratic	< 0.0001		0.9275	0.9232	Aliased

Sequential Model Sum of Squares [Type I]

Source	Sum of Squares	df	Mean Square	F Value	p-value Prob > F	
Mean vs Total	91466.27	1	91466.27			
Linear vs Mean	11460.52	5	2292.10	208.87	< 0.0001	
2FI vs Linear	1605.30	10	160.53	24.23	< 0.0001	Suggested
Quadratic vs 2	1226.22	4	306.55	98.97	< 0.0001	Aliased
Residual	1053.17	340	3.10			
Total	1.068E+005	360	296.70			

Model Summary Statistics

Source	Std. Dev.	R-Squared	Adjusted R-Squared	Predicted R-Squared	PRESS	
Linear	3.31	0.7468	0.7433	0.7375	4027.36	
2FI	2.57	0.8515	0.8450	0.8383	2481.04	Suggested
Quadratic	1.76	0.9314	0.9275	0.9232	1179.24	Aliased

From the fit summary in Table 5, a linear and two-factor interaction (2FI) model is suggested by D-optimal design, and a quadratic model is aliased. Thus, it is statistically suggested that the 2FI model is the appropriate model.

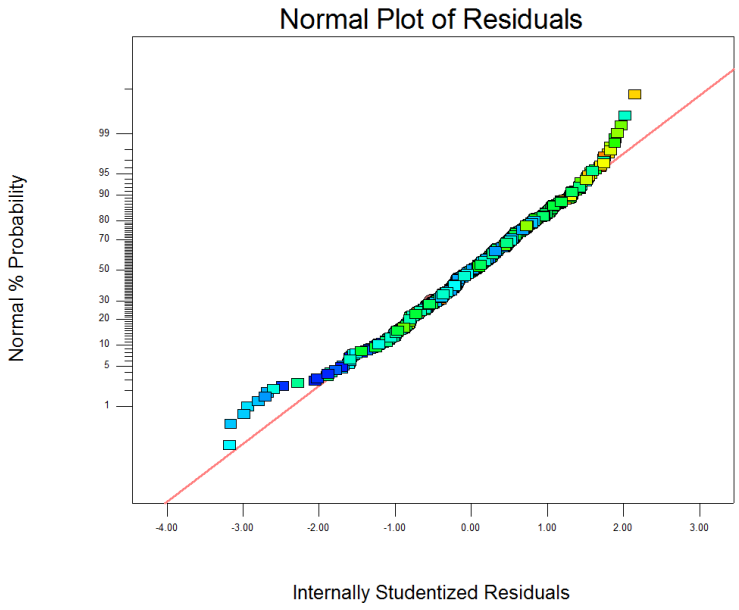

Figure 3-23 Predicted overpressure vs. Actual overpressure value after D-optimal design.(2FI)

As can be seen from Figure 3-23, the overpressure response surface provides reliable predicted values of overpressure, compared with the actual value of overpressure. From the graph, the fitting situation is ideal in most of cases: on both "ends" of the parameter space, the difference between the predicted and actual overpressure value is bigger. The detail and reasons for this will be analysed in Chapter 5. The final equation is shown below. The final equation includes the linear and the effect of each parameters interaction between the factors.

Final Equation in Terms of Actual Factors:

Overpressure =

-11.66753
+2.05271E-003 * Relief
-3.39398 * Aquifer Bending
+6.37681E-003 * Depositional Rate
+12.08524 * Clay content
+9.76759E-003 * Aquifer Depth
-8.05017E-004 * Relief * Aquifer Bending
-2.34950E-007 * Relief * Depositional Rate
-2.01278E-003 * Relief * Clay content
+6.27000E-008 * Relief * Aquifer Depth
+4.43886E-004 * Aquifer Bending * Depositional Rate
+5.67589 * Aquifer Bending * Clay content
-4.05000E-005 * Aquifer Bending * Aquifer Depth
-0.012263 * Depositional Rate * Clay content
+7.82561E-007 * Depositional Rate * Aquifer Depth
-5.69933E-003 * Clay content * Aquifer Depth

This equation represents the fitted equation of the overpressure surface for 2FI model.

As can be seen in the equation, the 2FI model includes the interaction terms. Therefore, this model can provide a good fit for the true overpressure response surface from the Design Expert report. The values of overpressure generated from the model were compared with the actual values from the simulation, as presented in the D-optimal final report. This comparison showed that the percentage difference between both overpressure values is in the acceptable range. The results and analysis will be shown in detail in Chapter 5, which presents the simulation data and analysis of the results.

The result outcomes show that the response of such a system is very well characterised, such that the overpressure at a reference point can be estimated with high accuracy, based on the five key parameters that express the key aspects of the system. However, the prediction value may be not used to predict overpressure in a real case, because there can be more complex situations and the simulation tools are only partly adequate, and cannot handle this very well. Nevertheless, such systems can be assessed on overpressure character and without repeating full simulation again, which could lay the foundation for the next stage.

3.4 Summary

In this chapter, the classic lateral transfer model was reviewed and a new LT model has been created, which sufficiently considers the interactions of the system and expresses the physical process more comprehensively than previous research and publications. According to an analysis of the physical understanding and sensitivity of possible parameters in this chapter, five parameters were defined to express the key aspects of the overpressure character of the system, and the resulting outcomes showed that the response of such a system is very well characterised, such that the overpressure at a reference point can be estimated with high accuracy based on the five key parameters. This method can assess the system quickly in terms of overpressure character, without the need for repeated full simulation, which could lay the foundation for the next chapter work. A summary of the work and findings reported in this chapter is as follows: The detail about the chapter work as below:

1. Established numerical models according previous research and obtained the same results for fluid and overpressure distribution. I also expressed the case of

block rotation causing disequilibrium compaction and LT forming overpressure by using basin modelling method.

2. Parameterized the overpressure influence on a dipping aquifer crest. Summarized and obtained influential factors on overpressure and its sensitivity to their influence: these are over-burden mud sedimentation rate, clay content, aquifer depth and aquifer relief, which are proportional to overpressure at the aquifer crest. Aquifer bending was also found to have an inverse influence on overpressure.
3. It was found that aquifer thickness, basin scale and basin depth does not have any obvious interaction with overpressure in the LT system.
4. A relationship was obtained between overpressure and the influence factors by using response surface D-optimal methodology (equation in section 3.7). The error analysis will be discussed in Chapter 5.
5. The result could accurately predict overpressure at the aquifer crest in a wide range of parameter space when basin has only a dipping aquifer. This also provided the grounds for the next research phase, concerning GU interaction in relation to overpressure prediction in cases of basins with multiple CL deposition in the over-burden.

Chapter 4. MULTI-GENETIC UNIT FLOW PROPERTIES IN BASIN MODELLING – DEVELOPMENT OF METHODS FOR ASSESSMENT

4.1 Introduction

In Chapter 3, the overpressure at the reference point of the reference case i.e. the crest of a tilted aquifer in a LT model, was studied to determine a response surface with respect to 5 key parameters that have strong influences on the formation of overpressure. The models are of the classic LT type, and are simplified in the sense of not considering the heterogeneity in the over-burden. In this Chapter, that basic model is used as a reference case to examine the role of higher-permeability Genetic Units (GUs) in the over-burden on overpressure at the same reference point. This investigation has two main motivations: (1) to assess whether, or at least, under which sets of circumstances, the existence of a non-uniform overburden can still be addressed by the simple predictive approach developed in Chapter 3; and, if this is the case, (2) to use this model configuration to develop an initial understanding of the potential for capturing the effects of multiple GUs in the overburden via simple estimations like those developed in Chapter 3.

In this Chapter, channel-levee systems (CLSs) are the GU type considered as "additions" within the over-burden of the LT model. CLSs introduce coarser materials into the dominant mud-rich overburden succession, and there is an expectation that CLSs will alter the way that compaction and overpressure (OP) evolve in a system with CLSs compared to one with a uniform muddy overburden. In this Chapter, I will show, firstly, that a single CLS can be accommodated via the predictive approach as developed in Chapter 3. I then examine the situation where multiple CLSs exist, with the need to consider their interactions in the flow + compaction process, and again, seek to determine if multiple CLSs can still be accommodated via the approach developed.

When analysing overpressure at the chosen reference point where multiple CLSs exist, it is necessary to focus on the interaction between the aquifer and the CLs, and between different CLSs, to predict overpressure at the reference point. For LT basins with CLS, the number of parameters in the parameter space X will increase dramatically in order to characterise them simultaneously by following the same approach applied to LT only in the previous chapter. This makes this approach impractical. Since those interactions are likely to have marginal effects on reducing overpressure at the reference point, and if

this is the case, the overpressure could well be characterised by the estimated effect of LT and the effect of CLSs additively; that is F(Y) = f(X) + G(XCLS) + E(Y), where G(XCLS) is the effect due to the interactions and XCLS is a parameter space concerning the interactions, E(Y) is the error term. The chapter will model and predict the term of G(XCLS) and estimate E(Y) .

The spatial arrangements of multiple CLSs could mainly influence interaction between the GUs which relate to G(XCLS) in this research. For the cases where CLSs are scattered in terms of relative distance from each other and the aquifer, one could imagine that G(XCLS) may be sufficiently approximated by the summation of the contributions of individual CLS($G_i(XCLS_i)$), where $G_i(XCLS_i)$ is the contribution of the single CLS on overpressure. Note that $XCLS_i$ is subspace of XCLS. For the cases where CLSs are clustered and close to the aquifer, the linear decomposition of $\Sigma G_i(XCLS_i)$ is unlikely to work, given the expected stronger interactions among them. However, if each cluster is further apart from another cluster and each cluster could be treated as an upscaled super CLS, the linear decomposition of G (XCLSs) can be applied on the clusters; in this case, one would imagine that the contribution of each cluster may be estimated by a weighted linear decomposition of the contribution of each CLS in that cluster. This suggests a hierarchy of linear and weighted linear decompositions. Thus, interaction between each CLS and the aquifer in LT need to be predicted.

For the analysis of the LT model with one CLS, screening and response surface methods via a large number of simulations were used to derive a function, g(XCLS) that approximates G(XCLS); The definition of the parameter space XCLS will be given. This analysis will be discussed firstly in section 4.2 and further in sections 4.3 and 4.4.1. The physical criteria to define whether CLSs are scattered or clustered will be discussed in 4.4.2. The weighting factors will be determined for each cluster in 4.4.2 – 4.4.4, in which response surface methodology will be used. The parameter space will be divided into two parts, to answer the question whether this approach would work over the whole parameter space or not, in section 4.4.1. Finally, a summary of the GUs' interaction relative to prediction of overpressure will be given in 4.5.

In section 4.2, the importance of GU interaction was examined through the literature and numerical methods. A mathematic assumption to predict overpressure at the aquifer crest is developed out, which consists of include two elements: the (main) influence of a

dipping sandstone aquifer and the (additional) influence of channel-levee systems (CLS) on reference overpressure. The main problem of this thesis, regarding parameter space increasing and the CLS flow effect on overpressure upscaling methods and their solution in this research will be discussed in this section. In section 4.3, the configuration of one CLS and two CLSs which are above the aquifer will be defined for screening and simulation analysis. The key parameters for the influence of single CLS are examined, which include over-burden rock sedimentation rate, mud property, aquifer depth and relief, location, depth and area of the CLS, the sensitivity of overpressure distribution to these parameters is also examined in each section. The parameter dimension of the factors was seven which is too high, so in section 4.4.1, a systematic numerical and mathematic analysis method is adopted to reduce parameter space and dimensions from 7 to 4, on the basis of the factors' importance. In section 4.4.1.3, a clear response of overpressure at the reference and the parameters is worked out when the basin has single CLS, by using D-optimal methodology. Sections 4.4.2, 4.4.3 and 4.4.4 examine basins that have two or more CLS cluster cases. The effect of correlation (fluid interaction) between CLS on overpressure behaviour becomes an important factor in this section, and a clear response where two CLS have significant interaction (close to each other) is worked out (response surface between the each effect of two single CLS on overpressure and the overall influence on overpressure at the aquifer crest) in section 4.4.2.3). The results show that the impact of the multiple CLS on overpressure at the aquifer crest can be expressed as the overall impact of each of two CLS with significant interaction and closest to aquifer crest and to each other in one CLS cluster, added to the effect of each other single CLS. Then, an approach of the multiple channel-levee systems fluid effect upscaling on predicted overpressure was developed out. Fluid interaction between each CLS and aquifer relative to the predicted overpressure also has been understood in the research, the target function (applied understanding of fluid interaction and upscaling method) of overpressure prediction at the reference point will be demonstrated.

4.2 Main problem

4.2.1 The importance of channel-levee systems in influencing fluid and overpressure distribution in a deep water basin

If the "anomalous" Genetic Unit sediment is above a dipping sandstone aquifer, it is likely to change overpressure distribution, when compared to the case where a dipping sandstone exists alone. The channel-levee systems may form partly- or mostly-

connected paths to withdraw fluids from the muddy sediments and the aquifer, allowing the fluids to reach the surface via an alternate pathway (compared to leakage through the caprock above the crestal location). Fluid could flow from the aquifer to these CLSs and thus change the motion of fluids and thus the overpressure distribution on a dipping aquifer crest. There would also be an impact on compaction state (perhaps a small effect) in many parts of the model region. The influence of these CLSs on overpressure is very important in drilling projects and seal risk assessment. As highlighted earlier, seismic images commonly reveal that the overburden is complex, with multiple identifiable rock units, so there is a need to extend the ideal LT model to cases where the overburden is not uniform. Detecting overpressure change caused by these CLSs and fluid interaction between them is also significant in both development and exploration contexts. In this section, I use numerical methods to establish the importance of CLSs in overpressure distribution, and the main model configuration, to which CLSs are added from the previous, is defined.

On the basis of the conceptual model described in Chapter 3, the main purpose in the configuration models created here is to add new properties above the dipping aquifer. I also use the point at the crest of the aquifer as a reference point in the complex CLS model. This is because, according to previous work, that point could better express pressure and overpressure distribution and fluid migration in the deposition process and around the sandstone body.

In the geological setting, for a better view of the interaction of the channel levee and to increase the flexibility of the model, each CLS is designed as a homogeneous rectangular sandstone body (Figure 4-1). Different clay content will be used in the surrounding mudstone from 0.1 to 0.9. And in low clay content, the property (permeability) will closer to CLS (sand stone). But in their mechanical compaction curve, at the same depth, their permeability differences still at least have three order magnitudes, that means in this study considered depth (lower than 5000 meters), CLS and background mudstone have so much difference on their property, despite the back ground mud clay content is low which is more close to property of CLS. Under the premise that CLSs have effects on migration and overpressure distribution, this can more clearly express the reasons for changes in the overpressure and also be more flexible and convenient in setting up multiple CLSs.

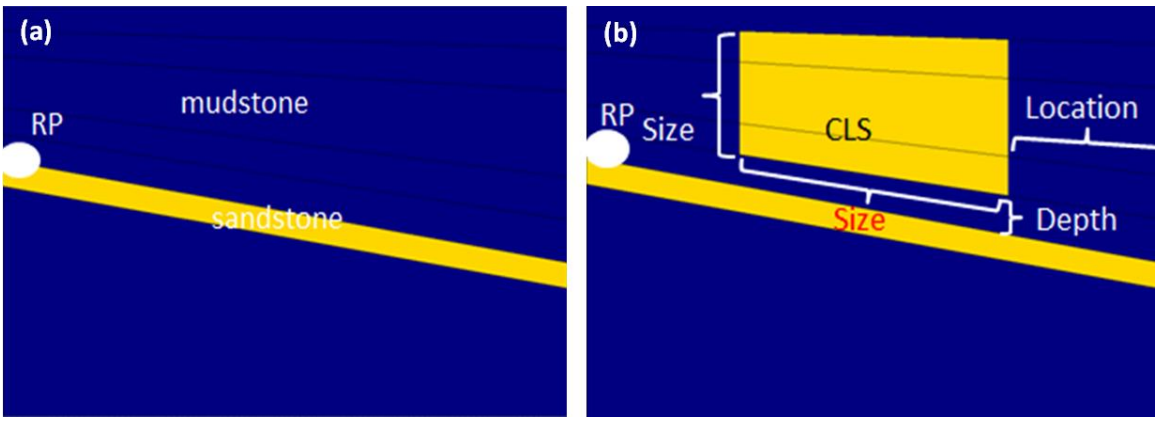

Figure 4-1 Conceptual model configuration of channel-levee effects. (a) Dipping sandstone body surrounded by mudstone; RP is still on aquifer crest, (b) one channel-levee system deposited above the dipping sandstone body. The overpressure at the RP may be changed by CLS effects.

In the conceptual model, channel-levee systems appear as a homogeneous trapezoidal sandstone body, because of different sedimentation rates, the CLS showing little inclination. Each CLS also has its own size, deposit depth and location, which could be important factors impacting overpressure at the crest of the aquifer. The size setting of each channel will be set according to information from the literature review and clearly affects the degree of overpressure. Mathematic assumptions regarding the effects of CLSs on overpressure will be given in next section, which will be the core of the analysis of fluid interaction between CLSs and the basis for later study.

In this section, a mathematical assumption is created to express the overpressure value at the aquifer crest (reference point) and the influence of CLSs on overpressure. It is to be established below that the influence of CLSs is an additional term of overpressure at the reference point; the influence of LT is dominating. The result is also the basis for some of later methods and computing procedures.

Firstly, I created the group of models to investigate the limits of the effect of CLS(s) on overpressure. That could define which term in the function is more important (between estimated function f(X) and channel effects) and which part is additional, to lay the foundation for the definition of the mathematical assumption function, and creation of future models, data processing and system error analysis. In this group, models which have a sufficiently large size of channel-levee systems were created. The largest size of CLS occupied 20% of the over-burden sediment, which is much bigger than those in canyon data from the Gulf of Mexico and West Africa.

The effects of every CLS model were consistently less than 30% of the results from the corresponding LT models. This suggests that CLSs do have just additional influences on overpressure on LT models. In other words, Eq. 4-1 gives a suitable model expressing the orderly importance of the influences of the aquifer and CLSs where G(XCLSs) represents negative influence on overpressure. According to Section 3.3, we should find a suitable sub-parameter space in XCLSs, denoted as Z and a 'best' function g (Z) for G(XCLSs) so that E(Y) is minimised. Since f(X) has been defined in Chapter 3, determining g(Z) will enable the prediction of F(Y).

$$F(Y) = f(X) + G(XCLSs) + E(Y); \qquad X = (D, H, C, R, B) \tag{4-1}$$

The sub-parameter space Z of XCLSs may include the factors of LT which were examined before and other geological factors such as channel size. In the next section, a numerical simulation method will be used to define in detail the influence of these factors.

In this section, three groups of numerical models were created for establishing the importance of CLSs' effects. Pseudo-rectangular sand bodies of variable sizes were added in the overburden above the dipping aquifer to mimic CLSs. The effects of CLSs depend on their size. When sizes are relatively small, there is no obvious overpressure change at the aquifer crest (Figure 4-2). In this group, the base LT model is constructed using the following parameters: aquifer depth is 3000 metres, and the relief adopted is 2000 metres; there is no bending, and over-burden mud clay content is 0.1 (which is more conducive to fluid flow into and out of the channel than a high clay content), 0.3 and 0.5. Sedimentation rates adopted were 100, 1000 and 2000 m/Ma.

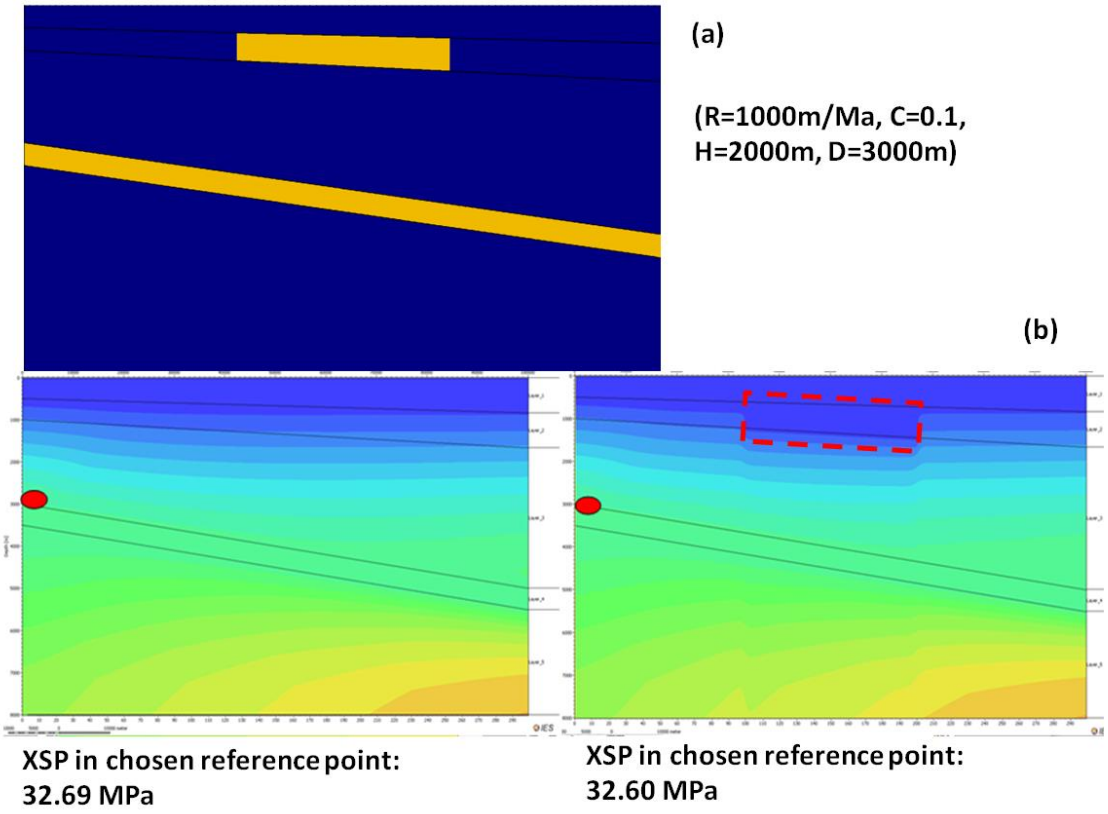

Figure 4-2(a) Model configuration of this group: one channel with sandstone has been added above the aquifer, the size is relatively small. (b) Results for overpressure value and contour of models; rate is 1000m/Ma, over-burden clay content is 0.1, relief and depth of sandstone aquifer are 2000, 3000 metres, respectively. In left graphic, the aquifer exists alone, and in right graphic, there is a CLS which is expressed red dotted line. From the results, no obvious overpressure change can be seen from the presence of the channel, the difference between basic and test models are 0.09 MPa.

Table 6 Others models which have different clay content and sedimentation rate were created for viewing channel effects, the parameter setting is: R=1000m/Ma, C=0.1, H=2000m, D=3000m. From the results, it appears that overpressure shows little change in each model, the biggest change is only 0.11Mpa.

Rate(clay=0.1)	Overpressure (without channel)	Overpressure (with channel)
100	18.76	18.65
1000	32.69	32.60
2000	35.30	35.26

Clay(rate=1000)	Overpressure (without channel)	Overpressure (with channel)
0.1	32.69	32.60

0.3	25.80	25.69
0.5	22.35	22.27

From Figure 4-2 and Table 6, it can be seen that there is little reduction in overpressure in every case; the biggest change between the basic model and test model is 0.11 MPa. That means the channel did not cause significant effects on overpressure distribution in the aquifer for such a small size. So in the next step, the size of the channel-levee systems was amplified many times (Uniform expand the area in width and thickness) to view their effects on overpressure distribution (Figure 4-3). In this group, aquifer depth is 3000 metres, and the relief adopted is 2000 metres; there is no bending, and over-burden mud clay content is 0.1, and the sedimentation rate adopted is 100 m/Ma.

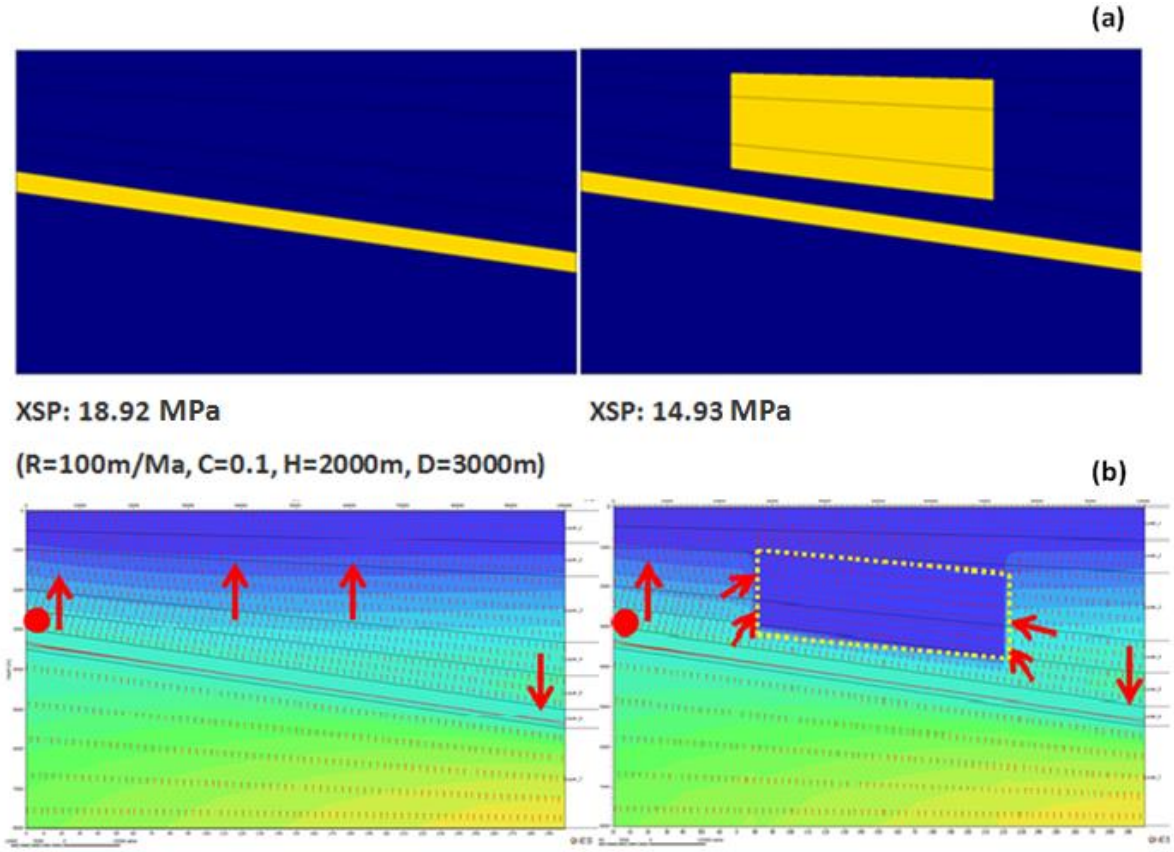

Figure 4-3 (a) Model configuration and overpressure value results after amplifying channel size many times. Overpressure changed by almost 4 MPa after channel deposits; it changed 21% from the basic model. (b) Water-vector in simulation results. When LT affect alone is considered, fluid flows from mud to sand in the aquifer base and flows out of sand at the crest, In the over-burden mud, fluid flows along the pressure gradient to the surface. With the presence of channel-levee systems, fluid flows into the channel from the over-burden mud, and overpasses the channel to the surface.

From Figure 4-2, it can be seen that fluid can flow into CLS in the over-burden mud and the flow path of the channel-levee systems to the surface causes a reduction of the pore

pressure and overpressure at the crest of the aquifer; the value in this case fell to 4 MPa. The channel changed the time-dependent pattern of fluid flow, and thus compaction and overpressure development was also changed by channel. The degree of the channel-levee effect depends much on its body area. When the GU is deposited in basin, the fluid energy and overpressure in the GU sand is lower than tilted sand which is associated with the sediment loading and the head can drive fluid toward the GU from more excess fluid energy region – sand body crest, and try to balance head in GU and aquifer, so the GU size influences fluid and energy transfer from the sand body crest. But there is no good fluid pathway (mudstone) between them, so the energy and fluid transfer (amount of overpressure decrease) will be influenced by distance between sand body crest and GU.

In summary, CLS can actually impact fluid direction and overpressure distribution at the aquifer crest and reduce overpressure noticeably at the aquifer crest when they are of large size; in this condition the degree of influence could be high.

4.2.2 Increasing the parameter space

So far we have established that CLSs influence overpressure in the dipping aquifer crest. If we want to approximate G(XCLSs) (see Equation. 4.1) by g(Z), we will need to identify influential parameters in XCLSs to form a sub-parameter space Z. The parameters in space z may contain the factors in space "X" which was studied in chapter 3, and also may contain factors like CLS size and position. So the number of considered parameters in "Z" wills maybe than "X", which is a big challenge in this study.

4.2.3 Influence of interaction of multiple CLSs - upscale

In realistic data from sedimentary basins around the world, it is not common to find only one channel-levee system sediment above an aquifer in an enclosed space; for example, in the Indus basin, there are many channel-levee systems above the aquifer each with its own different features. If we use a single channel-levee consideration method to consider more than one CLS environment, this is obviously not feasible, because the effect of several channel-levee systems on fluid and overpressure distribution will differ from that of a single one. So it is necessary to try to find an effective workflow to express the effect of multiple CLSs on overpressure distribution, which could make the research and study results closer to reality and can solve practical problems under the appropriate conditions.

Finding the overpressure change at the aquifer crest when two or more channel-levee systems act jointly is still the core in this study. After the effect of a single CLS effect on overpressure has been studied, this assumption could be proposed here: Can the impacts of multiple 'decentralised' channel-levels be decomposed 'additively', as a sequence of those of each single channel-levee? (Figure 4-4 (a)):

$$F(Y) = f(X) + \Sigma\, g_i(Z_i) + e(Y)$$
$$G(XCLSs) \approx g(Z) = \Sigma\, g_i(Z_i) \qquad 4\text{-}2$$

Here $\{Z_i\}$ is a partition of Z corresponding to individual CLSi, and g(Zi) is an estimate of G(Zi) in absence of all other CLSs.

However, if several CLSs are close together, considering fluid correlation and the interaction of CLSs, can the impact of a cluster of spatially-proximate channel-levees systems (two, three or four CLS) be modelled via upscaling into an equivalent single channel-levee iteratively? (Figure 4-4(b)).

$$F(Y) = f(X) + gg(Z) + e(Y) \qquad 4\text{-}3$$

where (gg(Z) is the function representing the upscaling of several closed CLS to the effect of a synthesized CLS, considering the effect of multiple CLSs as one.

If the hypothesis is true, we can use the effect of a single CLS or upscaled CLS to calculate the influence on overpressure distribution at the aquifer crest in different actual conditions.

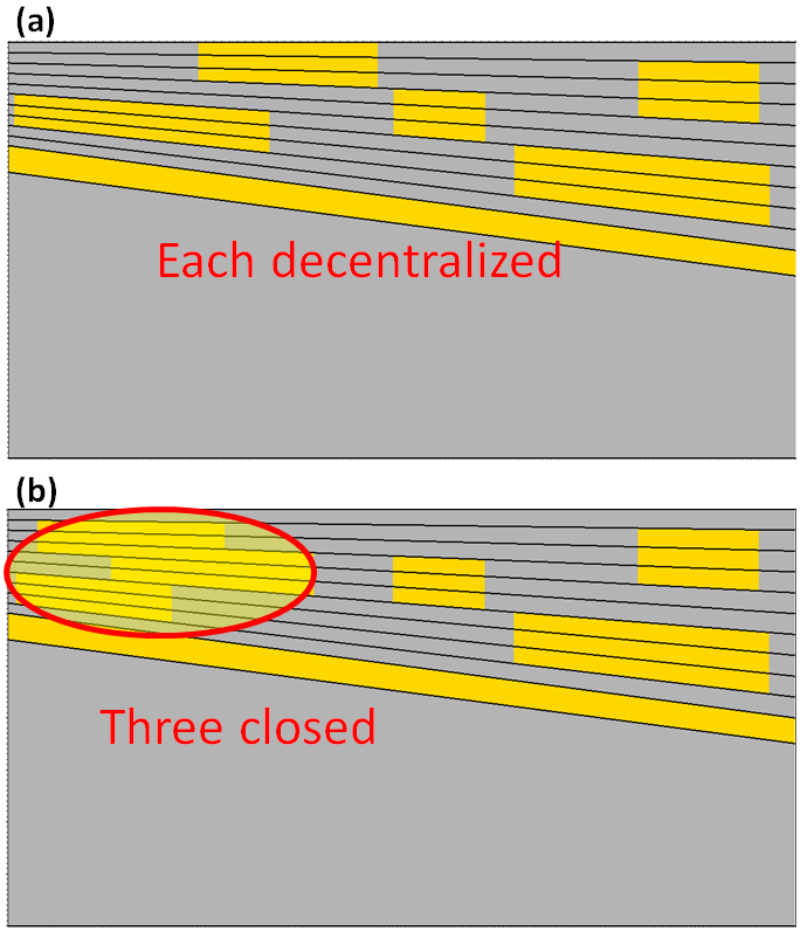

Figure 4-4 (a) If there are many CLSs deposited in a basin, and each CLS is decentralized, the overall impact on overpressure at the aquifer could be decomposed into the effect of each CLS. (b) If several CLSs are close, the overall impact of these CLS could be upscaled to that of a synthesized single CLS, and the function for the situation after upscaling the single CLS effect is "gg(zi)", which needs to be defined by a large amount of simulation, data analysis and statistical methods

To test this, firstly, models with two CLSs were investigated for all possible combinations in a parameter space, to see at which conditions the CLSs can be treated as decentralised or as a super-CLS by upscaling. If the two CLSs are close, they form a cluster, which needs to be upscaled; response surface D-optimal methodology will be used here in later section.

If three or more CLs form a cluster, an upscaling method also needs to be used here. I propose to show that for every configuration, there is an upscaling scheme to reduce each CL 'iteratively', and if all these upscaling schemes share a common feature, a generic one can then be applied.

A study of the effect of multiple CLSs on the overpressure distribution will also make a contribution to the understanding of the fluid interaction between each geological Genetic Unit in a sedimentary basin. First of all, cases where the sedimentary basin has

two channel-levee systems which lie physically above a sandstone aquifer need to be considered to view the interaction of the different features of the CLSs. A conceptual model configuration of the two channel-levee systems also needs to be defined.

4.3 Design of simulations

In this section, the CLS depositional basin configuration will be defined for this research and their impact on overpressure and interaction investigated. Section 4.3.1 will focus on a basin that has a single CLS deposition case; the configuration and the process of screening the influencing parameters are also discussed in section 4.3.2. The influencing parameters identified after screening are: over-burden rock sedimentation rate, mud properties, aquifer depth and relief, location of CLS, depth and area, their sensitivity in relation to overpressure distribution were also studied in each section. The number of influential factors is 7, which is too high to make accurate predictions, so in the next section; the parameter space will be discussed and justified to simplify the complexity of the factors and prediction. Section 4.3.2 focuses on a basin with multiple CLSs deposition. To confirm the hypothesis proposed in section 4.2, the effect of the interaction of two CLs on overpressure needs to be first studied, to identify in which conditions the interaction needs to be considered and in which conditions it could be ignored. Section 4.3.2.2 reports how group simulations were created in to view these effects, and the detailed analysis will be shown in section 4.4.

4.3.1 Configuration where the basin has one CLS

The configuration of a basin which has one CLS is shown in Figure 4-5; the CL configuration is shown as a homogeneous rectangular sandstone body for a better view and analysis. A reference point was also chosen at the aquifer crest. The CLS has its own features: factors such as size, location and depth, which will be discussed in detail in the next section.

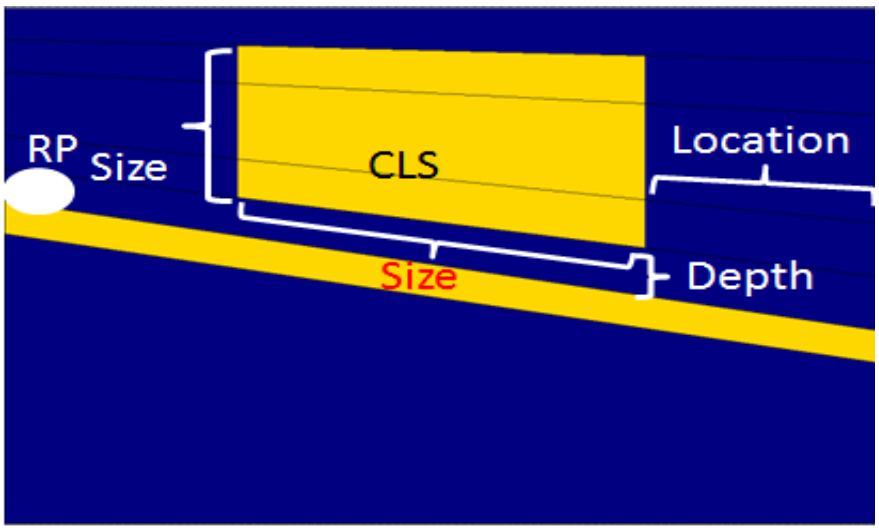

Figure 4-5 Configuration of a single CL deposit. The CL body is chosen as a homogenous rectangular sandstone body; a reference point is also located at the aquifer crest. The others parameters setting is the same as model in Chapter 3.The features of a CLS which may influence its impact on overpressure at the reference point are size, location and depth.

4.3.2 Basin with one CLS - screening

In this section, several factors associated with the presence of one CLS which influence overpressure ("G(XCLS)") at the aquifer crest are considered. Here I consider a sub-parameter space Z containing four of 5 parameters in X, which are sedimentation rate, mud clay content, aquifer depth and relief, and three CLS parameters: CLS location relative to the crest, depth to the aquifer and area. Their range and sensitivity are defined and discussed in this section. The less important factors will be discussed in section 4.3.2.6.

In this section, I set up simulation models to consider the ratio of the effect in the presence of a CLS to that in absence of any CLS for distinguishing the importance of the effect of CLS. Later in this study, this type of method will also be used in error analysis.

The change in value of overpressure at the reference point due to the presence of a channel-levee system will be impacted by one or several petro physical and geophysical factors. Firstly, the features of the channel-levee system, such as channel size, depth and location should be considered. In order to identify the importance of these factors, a numerical simulation method was used for comparison of the models and analyse the results. In this section, a comparison of the models' results is the main measure, by adjusting the target parameter when others are constant, then viewing the change in the

value of overpressure and its degree to define the important factors which impact the additional part of the function: "G(Z)".

Important factors will be adopted in this section and unimportant factors ignored. These important factors are defined for the future experimental design and large number of simulations, then regression and response surface methodology are used to define the channel-levee effects (G(Z)) which combine with LT effects (f(X), as previously defined) to express overpressure value at the sandstone aquifer crest (F(Y)) after multiple channel-levee system deposits.

4.3.2.1 Over - Under burden Depositional Rate and Mud Clay Content

Over-burden sedimentation rate and shale properties are important factors in overpressure distribution through the LT effect alone, which was previously established. These factors could affect rock permeability and porosity, which could alter the fluid pathway from aquifer and CLS, and the speed and efficiency of fluid flow into or out of the pore, and control fluid energy and fluid generation and dissipation, thus influencing overpressure distribution in basin evolution. (Equation 4-4) [17]

$$\lambda = \frac{k_0 g\left(\rho_{gr} - \rho_{fl}\right)}{\mu v_0} \qquad 4\text{-}4$$

In this equation, v_0 is sedimentation rate for surface conditions, k_0 is rock permeability. λ is essentially the ratio of hydraulic conductivity to surface conditions, which means fluid dissipation capacity. This is controlled by the permeability of rock and sedimentation rate. When λ is small, that means permeability k_0 is small (clay content is big) or sedimentation rate v_0 is big, the fluid dissipation capacity is low, and less fluid will flow into the CLS and more fluid will be held in the pores. This may impact the fluid status around the channel-levee system and thus influence the overpressure effects generated by a CLS.

In this section, two groups of models were created for viewing the impact of sedimentation rate and shale clay content on overpressure. The models used the same channel size as before; aquifer depth and relief are 3000 metres and 2000 metres, respectively. There is no bending and other factors are variable. (Figure 4-6)

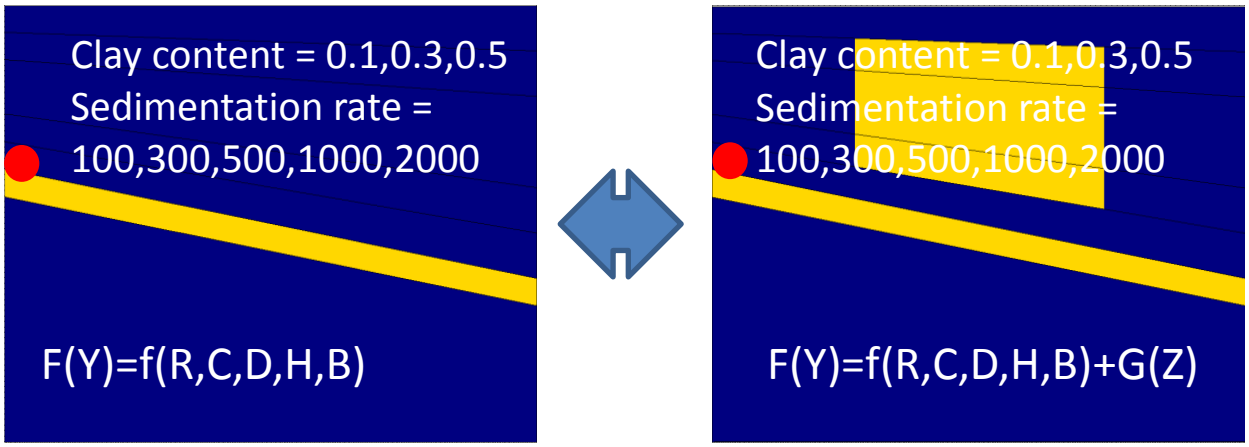

Figure 4-6 Model configuration for deposition rate and clay content test. In these models, CLS property is same as aquifer, other factors are held constant and the sedimentation rate vary from 100~2000 (m/Ma) (the range adopted in the previous LT study), and the clay contents are 0.1,0.3,0.5. Channel-levee effects on overpressure were obtained after calculation, and viewing the two factors' influence on G(y).

30 models were simulated in this part for analysing overpressure changes due to channel-levee effects, with the sedimentation rate and clay content adjusted. The results are shown in Table 7 (overpressure value at RP without CLS effects) and

Table **8** (overpressure value at RP without CLS effects).

Table 7 Overpressure value at reference point due to LT effects.

Sedimentation Rate/Clay content	0.1	0.3	0.5
100m/Ma	18.92MPa	14.15 MPa	16.26 MPa
300m/Ma	27.25 MPa	21.04 MPa	21.07 MPa
500m/Ma	30.29 MPa	23.8 MPa	22.58 MPa
1000m/Ma	32.84 MPa	26.77 MPa	-
2000m/Ma	34.93 MPa	28.81 MPa	-

Table 8 Overpressure value at reference point due to the combined effects of LT and channel-levee systems.

Sedimentation Rate /Clay content	0.1	0.3	0.5
100m/Ma	15.43 MPa	12.02 MPa	15.37 MPa
300m/Ma	24.01 MPa	19.28 MPa	20.73 MPa
500m/Ma	27.74 MPa	22.43 MPa	22.41 MPa
1000m/Ma	31.39 MPa	25.98 MPa	-
2000m/Ma	33.82 MPa	28.37 MPa	-

From Table 7 and

Table **8**, after removing cases which could cause fracturing which were examined in chapter 3(C=0.5, R=1000, 2000), the change overpressure is seen to be regular and the two tables are similar, and differences between them are much smaller than in the comparable data in Table 7. This provides further evidence that the CLS effect is an additional element, and that the LT effect is the main influence on overpressure distribution at the aquifer crest. However, it appears that sedimentation rate and shale clay content do have an influence on the effect of channel levees, and the relationship is analysed in Table 9.

Table 9 Different between overpressure with/without CLS. (CLS fluid interaction on overpressure in different value of sedimentation rate and clay content).

Clay content /Sedimentation rate	100 m/Ma	300 m/Ma	500 m/Ma	1000 m/Ma	2000 m/Ma
0.1	3.49 MPa	3.26 MPa	2.55 MPa	1.45 MPa	1.11 MPa
0.3	2.13 MPa	1.76 MPa	1.37 MPa	0.79 MPa	0.44 MPa
0.5	0.89 MPa	0.34 MPa	0.17 MPa		

According Table 9, we find that “R” and “C” could influence the effect of channel-levee systems on overpressure and when sedimentation rate and the surrounding shale clay content is increased, the channel’s effect on overpressure will be decreased. The degree of influence of the 2 factors decreases as the values increase? When the deposition rate and clay content reach a certain value, the effect of the CLS on overpressure is not obvious; thus, in later analysis, in models which have a low CLS effect (G(Z)), the CLS effect will be ignored.

In summary, this section has shown that the over-burden sedimentation rate and clay content could influence the effect of channel-levee systems on overpressure. The effect of the CLS will decrease as the two factors increase; this is because a high sedimentation rate and clay content could retard fluid flow in and around channel-levee systems, making less fluid flow into or out of the channel, thus decreasing the change in overpressure at the reference point and aquifer. In the next step, the impact of aquifer depth on CLS effects will be analyzed by the same method.

4.3.2.2 Influence of depth of high permeability Aquifer

Aquifer depth is the main factor which influences the value of overpressure at the crest in the LT condition. In this study, others parameters need to be constant in order to examine aquifer depth sensitivity on CLS fluid interaction in sand body crest. And if the depth increases, the sedimentation rate in sand body crest is constant, but average sedimentation rate between crest and base is decreased. That means permeability at the same point which have compacted is higher in sediment process. So the pathway of fluid energy and fluid between sand body crest and CLS will have an influence. The amount of the overpressure change due to the effect of CLS and whether it is related to the aquifer depth is the main target of this section. Three groups with different aquifer depth were created for this study. In these groups, channel size is constant at 20% of the over-burden sediments at the same depth and location; aquifer relief is 2000 metres, and sedimentation rate and clay content are 100 m /Ma, 1000 m/Ma and 0.1, respectively. (Figure 4-7)

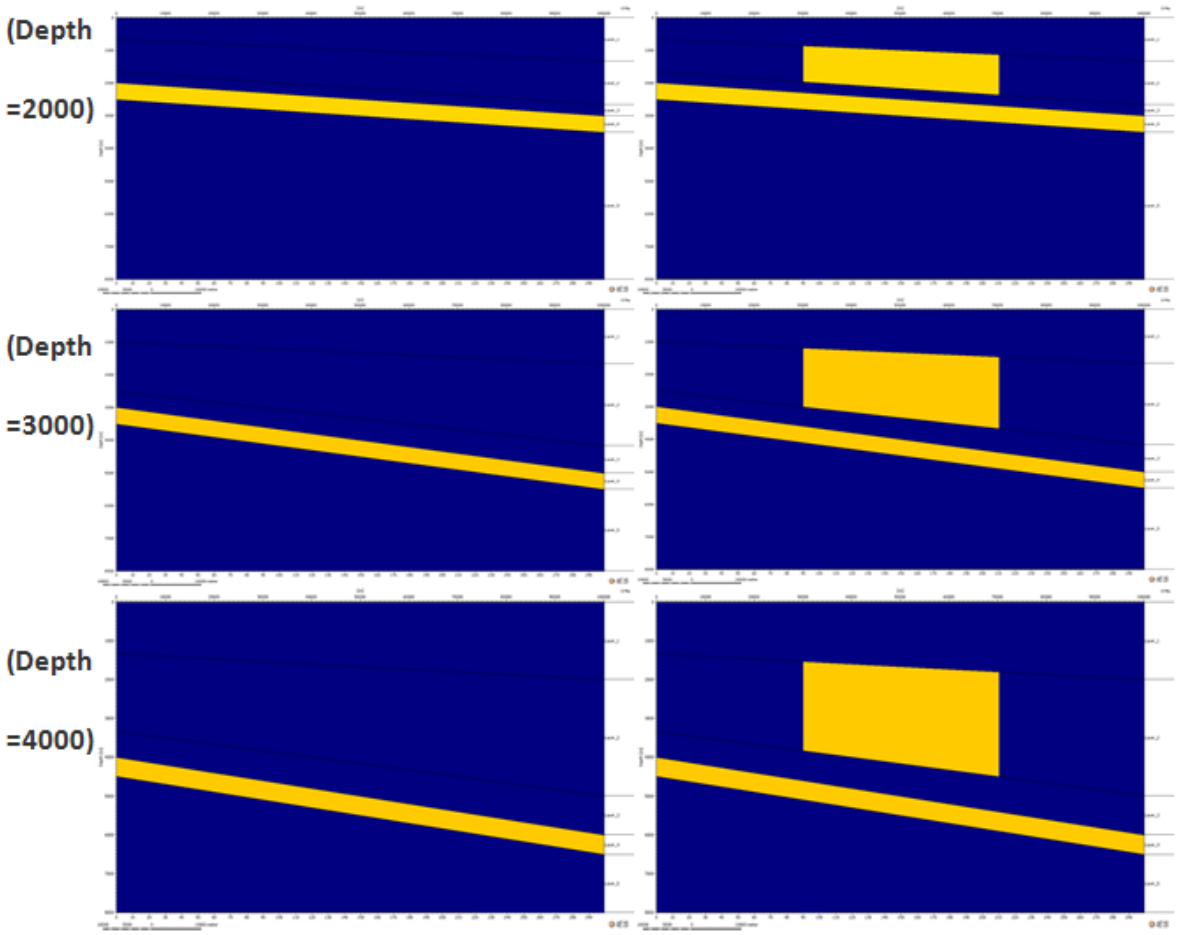

Figure 4-7Model configuration in this section: yellow areas are sandstone, blue areas are over-burden mud. The three groups of models have different aquifer depths and other factors are held constant.

12 numerical models were simulated to view overpressure at the crest of the aquifer. The results in Table 10 show same trends: overpressure increases with depth of aquifer and is increased by channel effects. The effects of the channel on overpressure also change with aquifer depth and the difference in value can reach 1.21MPa. The effect of CLS on overpressure at the aquifer crest will increase with aquifer depth. However, in conditions where there is a high depositional rate, the effects of depth on the influence of CLS are less obvious than at low depositional rates.

Table 10 Model results for overpressure at the aquifer crest in LT and CLS conditions. It can be seen that aquifer depth can influence the channel's effect on overpressure, and when the depth increases, the CLS effect will also increase. This is more obvious at low over-burden sedimentation rates as shown in the previous section.

Rate/ Depth (LT)	2000m	3000m	4000m
100m/Ma	12.05 MPa	19.05 MPa	25.56 MPa
1000m/Ma	22.15 MPa	32.96 MPa	43.26 MPa
Rate/ Depth (CLS)	2000m	3000m	4000m
100m/Ma	9.81 MPa	16.05 MPa	22.11 MPa
1000m/Ma	21.35 MPa	31.95 MPa	42.14 MPa

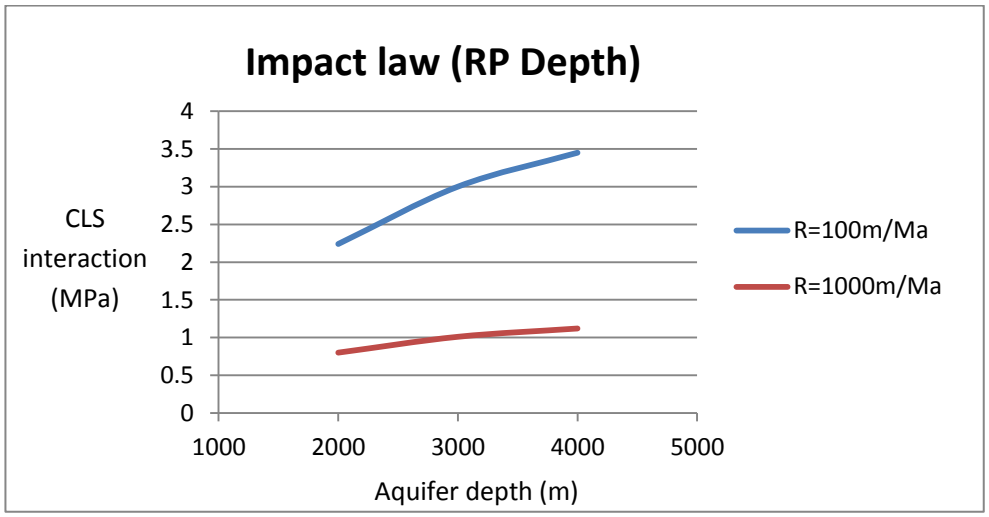

Figure 4-8 Influence trend of aquifer depth on channel-levee system interaction. The different colour line represent in different sedimentation rate condition.

From the table 10, it can be seen that depth could actually influence the channel-levee system's effect on overpressure at the reference point and that when the depth of the aquifer increases, the effect of the CLS will also increase. This because that change in depth means change average sedimentation rate (in crest is constant, but in average is lower) between sand body crest and base, so the permeability is higher, fluid path between aquifer crest and CLS become better which allow fluid energy and head derived more fluid from crest to CLS. That is explaining why overpressure can reduce more by CLS effect when sand body depth is higher with other parameters constant. In the next section, aquifer relief will also be considered; the method and justifications are similar to those used for the depth effect.

4.3.2.3 Influence of relief of high permeability Aquifer

Aquifer relief is also a major factor which could influence overpressure at the aquifer crest because it could alter the effects of Lateral Transfer Furthermore, it could also change the aquifer base sedimentation rate, causing more fluid energy to transfer from

the aquifer base to the crest, and increase the overpressure on the crest. When multiple channel-levee systems are deposited above the aquifer, the effects of the channel on the overpressure may be influenced by adjusting the aquifer relief, because of the change in sedimentation rate (the reference point sedimentation rate is constant; changing the aquifer relief means changing both the base and average sedimentation rate). In this section, three groups of models were created for viewing the channel's effects on overpressure distribution. In these models, the over-burden reference point sedimentation rate is 100 m/Ma, mud clay content is 0.1, and aquifer depth is 300 metres. Others factors, like the channel-levee system's size, depth and location are all constant, and the aquifer relief is changed from 2000 to 3000 metres. The main model's configuration is showed in Figure 4-9, and the results shown in Table 11.

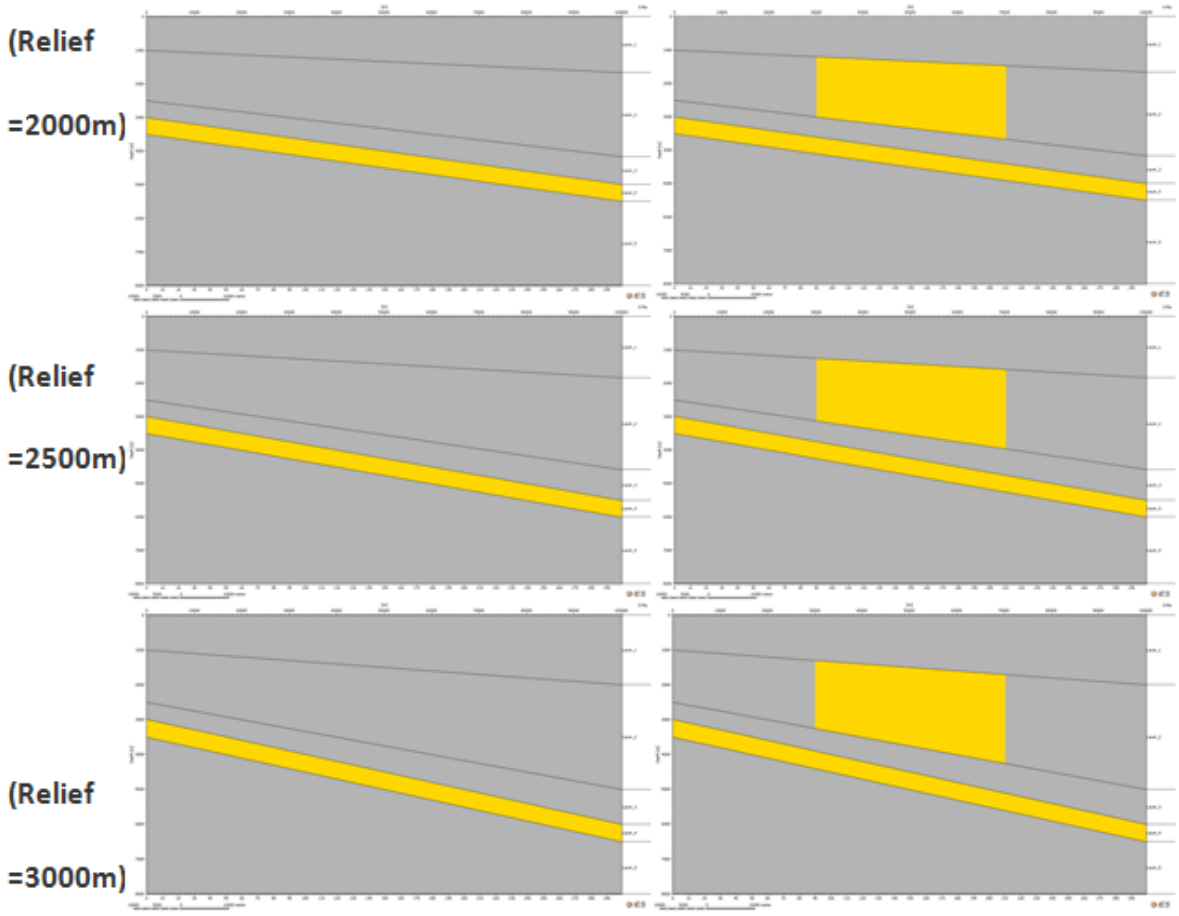

Figure 4-9 Model's configuration of influence of relief on the channel's effect. In this study, other defined and possible factors are kept constant and relief is changed from 2000m to 3000m. Real size of channel has a small change, but percentage of over-burden is kept constant. In a later study, channel area percentage of the over-burden mud is a factor which can influence the effect of CLS on overpressure but not math area of CLS.

Table 11 Overpressure value at reference point in different models. The graph shows the channel-levee system's effect on overpressure. From the results, it appears that aquifer relief could influence the channel effect: when the aquifer relief increases, the channel effect on overpressure will decrease. The magnitude of impact is nearly 0.5 MPa, which smaller than the effect of depth, sedimentation rate or clay content.

Relief / CLS condition	Without CLS	With CLS
2000m	32.88 MPa	31.86 MPa
2500m	33.76 MPa	33.06 MPa
3000m	34.51 MPa	33.93 MPa

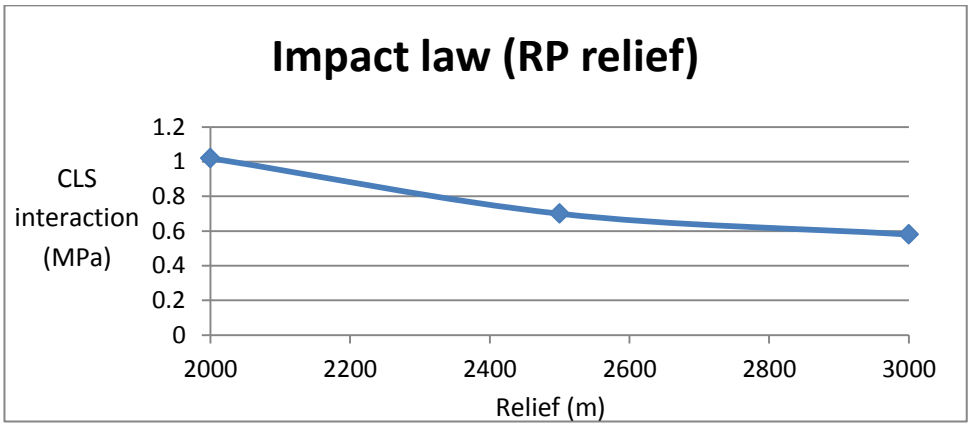

Figure 4-10 Influence trend of aquifer relief on channel-levee system interaction.

From Table 11, it can be seen that the models have same "H" factor value: the effects of "without CLS" and "with CLS" on overpressure formation are different: channel-levee systems interaction on overpressure will decrease when aquifer relief increases, but the magnitude of impact is smaller than the interaction of depth, sedimentation rate and clay content. Increase in the relief means that the aquifer base and average over-burden rock depositional rate increase, and permeability in the region between sand body crest and CLS is decreased, so the pathway of fluid energy and fluid transfer from sand body crest to CLS become worse and less fluid will be derived from the sand body crest to CLS, in a similar way to the interaction of sedimentation rates which were studied before.

In the mathematical assumption, the function "f()" has influencing factors "X" which include RP sedimentation rate R, over-burden clay content C, aquifer depth D, relief R

and Bending B. Four of these have been proved to have influence on channel-levee systems. In the next section, the features of channel-levee factors will be discussed; they include channel size (real size and over-burden percentage), channel depth and channel location. In the study, different methods and definitions of the factors will be adopted to analyzing their influence on the effect of channel-levee systems.

4.3.2.4 Channel-Levee systems: depth and location

Head drive fluid flow potency will depend on their fluid pathway. In this study, CLS distance from sand body crest will influence fluid pathway so that the fluid energy and fluid transfer will also be influenced (sand body crest overpressure reduce amount). The depth of a channel-levee system is the vertical distance between sand body crest and the CLS. It means the depositional time after the aquifer deposit in this thesis. This could make the channel closer in distance to the sandstone aquifer, and head will drive fluid more easily to flow into the channel from more fluid energy region - sand body crest. In this section, the influence of the channel-levee system's depth on the way CLS affects overpressure will be considered. First of all, the depth of the CLS in the model configuration was defined, it was assumed that the vertical distance between the channel bottom and aquifer is "h", and aquifer average depth is "H", the depth of channel-levee systems is then defined as "h/H" (Figure 4-11). Then a group of models with different channel depths and the same other factors (RP depositional rate is 100m/Ma, clay content is 0.1, aquifer depth is 3000 meters, relief is 2000 meters and size of CLS is 0.1) were created to examine the influence of the depth of the CLS on the effect of the channel . The results for overpressure at the RP for different channel depths are shown in Figure 4-12.

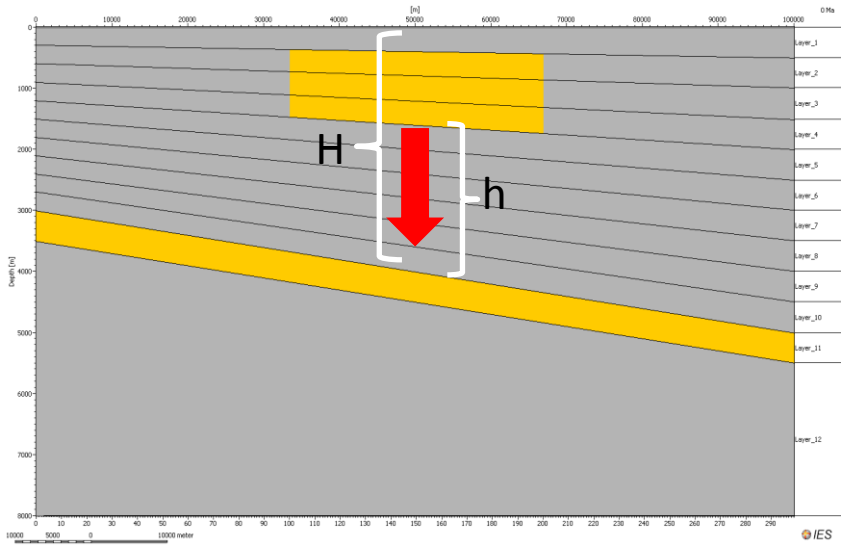

Figure 4-11 Model configuration for definition of channel-levee system's depth: vertical distance between channel bottom and aquifer is assumed to be "h", and aquifer average depth is "H", defining the depth of the channel-levee system as "h/H". Red arrow means the configuration of the group of models, which changes CLS depth from large to small by the arrow direction; the values of CLS depth are 0.033, 0.1, 0.2, 0.3, 0.4, 0.5, and 0.6, respectively.

Using channel-levee locations and positions in a well-known deep-water basin (as previously shown in the literature review), the procedure combines the setting the limit of numerical basin modelling, defining channel-levee depth lowest boundary in this study is 0.1, which means channel-levee systems were deposited 0.2 to 3 million years after the sandstone aquifer deposit.

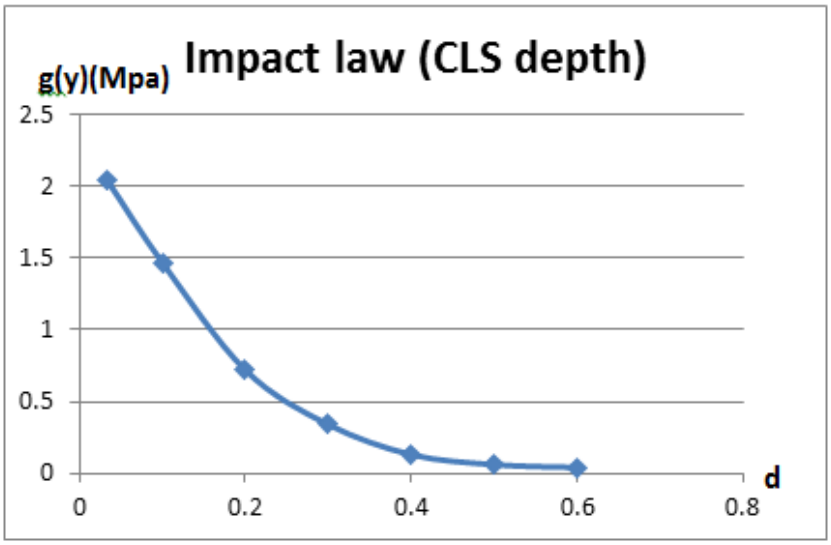

"d"	CLS eff.
0.6	0.04
0.5	0.06
0.4	0.13
0.3	0.34
0.2	0.72
0.1	1.47
0.033	2.05

Figure 4-12 Effect of channel on overpressure change for different CLS depths. From the results, channel depth could change the channel's effect on overpressure distribution: when the channel is closer to the sandstone aquifer, its effect on overpressure will greater; the difference in this group could reach 2 MPa.

From Figure 4-12, it can be seen that the depth of the channel-levee systems could influence their effect on overpressure: when the channel depth increases, the effect on overpressure will decrease. As the CLS approaches the aquifer, its effect will be more obvious. When the sandstone layer is deeper, the pressure value in the formation around the sandstone is higher than for a shallow layer, and if a new CLS is then added, more pressure could dissipate from the overpressure region and aquifer, and more fluid could flow into the channel.

As well as the depth, the location of channel-levee systems is horizontal distance between sand body crest and CLS, which also needs to be considered. Changing the horizontal position of the channel means changing the fluid pathway from sand body crest and CLS. Furthermore, this also changes the depositional rate in and around the channel in simulation setting in this study. This is also very likely to influence the effect on overpressure. To establish the role of the CLS's location in affecting overpressure, definitions of CLS location were assumed in numerical models:, horizontal distance between reference point and central of channel is assumed to be "l", basin length is "L", and location of channel-levee systems is "l/L" (Figure 4-13). Defining the influencing factors will assist in the future data analysis and parameter space design.

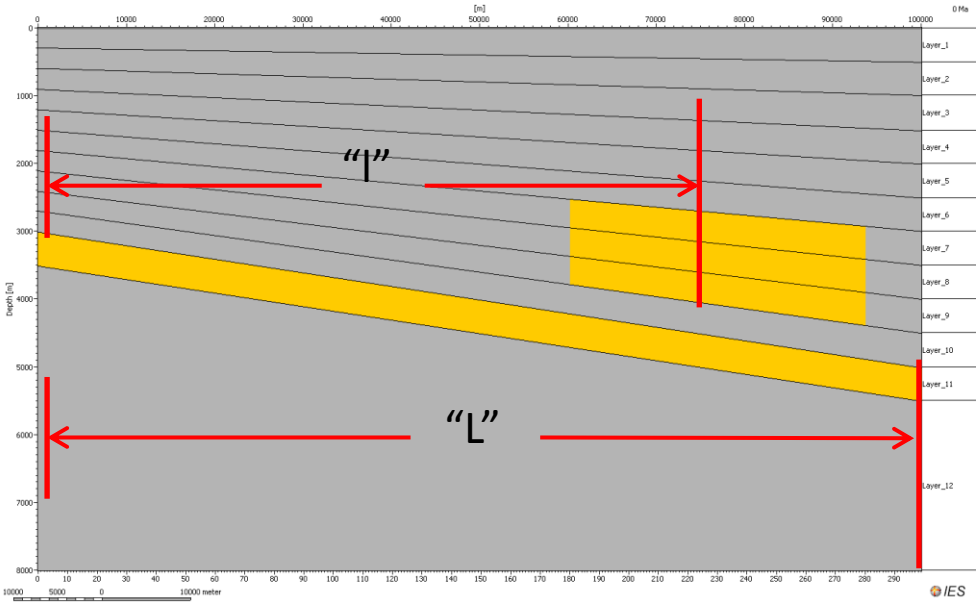

Figure 4-13 Assumption of channel-levee system's location in numerical models: horizontal distance between reference point and central of channel is assume as "l", basin length is "L", location of channel-levee systems is "l/L".

According to the literature reviewed above and combining this with setting the limits of numerical basin modelling, the defined CLS's location range was selected as 0.2 to 0.7; these are displayed in the numerical modelling on the left side and right side of the basin boundary (Figure 4-14).

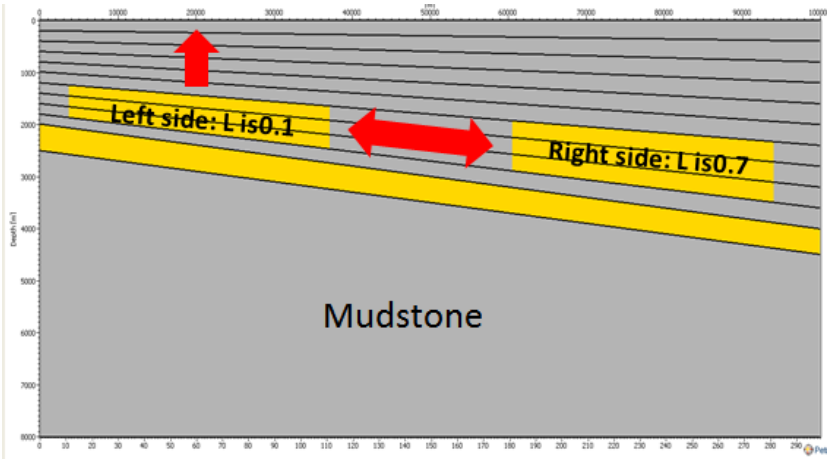

Figure 4-14 Model configuration of boundary of channel-levee depth and location. The depth chosen for the lowest value boundary is 0.1, meaning this was deposited 0.2 to 3 million years after the sandstone aquifer. The location of the low value boundary is 0.1 (left side) and high value boundary is 0.7 (right side) which is because of the numerical setting. The CLS could move in this parameter space by size value between 0.1 and 0.2.

For investigating the importance of factor location, a group models with different channel locations and the same values for other factors were created. In this study, RP depositional rate is 100m/Ma, clay content is 0.3, aquifer depth is 3000 meters, relief is 2000 meters, size of CLS is 0.1 and CLS depth is 0.1, the channel location adopted is 0.23, 0.5, and 0.77 (Figure 4-15). The results for the effect of the CLS location are shown in Figure 4-16.

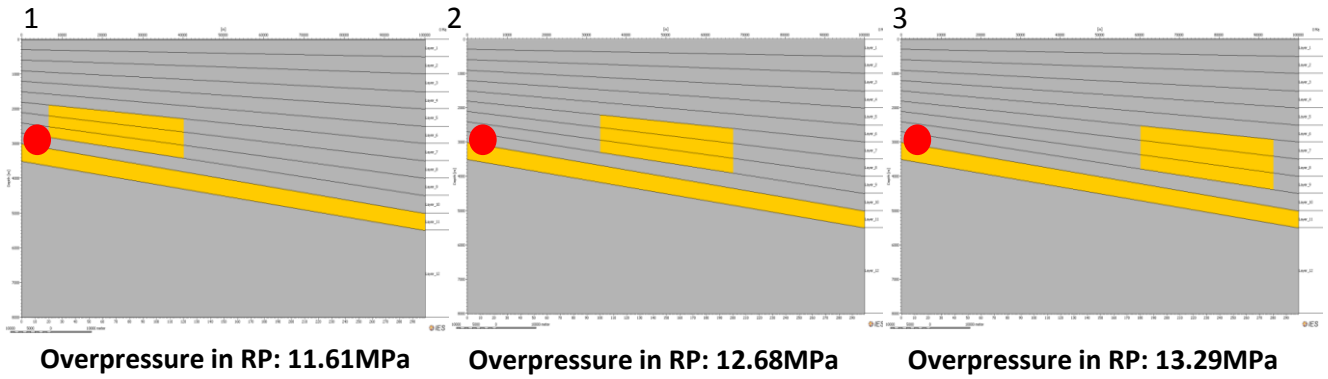

Figure 4-15 Models' configuration for different channel locations, in this study, adopted channel location is 0.23, 0.5, and 0.77 (dimensionless) to view the change of overpressure at the RP.

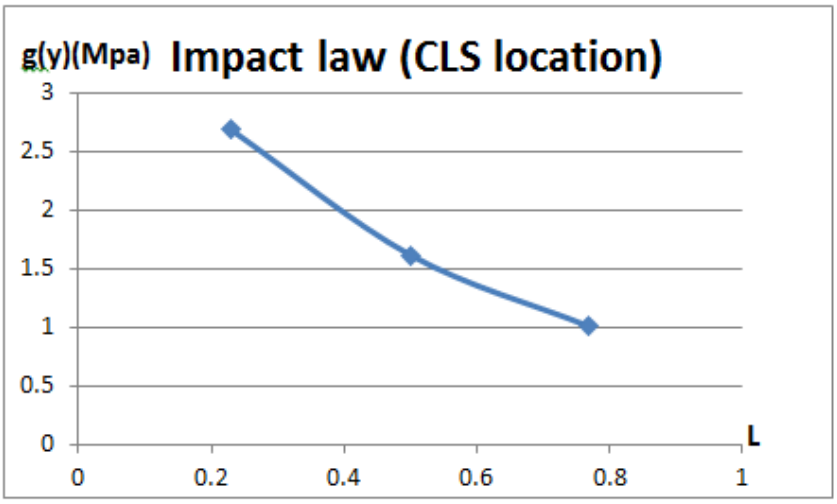

L	CLSeff
0.23	2.69
0.5	1.62
0.77	1.01

Figure 4-16 Channel-levee system's effect on overpressure according to different channel locations, from the result, channel effect will decrease by channel location value increase, the difference in overpressure in this study could reach 1.6 Mpa.From results in Figure 4-16, it can be seen that the location of channel-levee systems could influence their effect on overpressure, and that this effect will increase as location value decreases.

In the LT model, depositional rates in the over-burden rock are different, so the Lateral Transfer effect and uneven burial rate in the over-burden rock are the reasons that the location and depth of a CLS could influence its effect on overpressure distribution. When the location of the CLS increases, the depositional rate in and around channel will also increase in the case, which will retard the fluid flow and decrease the channel's effect on overpressure at the aquifer crest.

4.3.2.5 Size (area) of the channel-levee system

In the previous stages of this study, the factors involved in Lateral Transfer have also been proved to influence the effect of channel levee systems on overpressure: these are RP over-burden sedimentation rate, over-burden mud clay content, aquifer depth and relief.

When the GU sediment is deposited in basin, the fluid energy and overpressure in CLS is lower than tilting sand which associated with the sediment loading and the head can drive fluid toward the GU from more excess fluid energy region in the sand body crest, and try to balance the head in CLS and sand body crest, so CLS size influence fluid and energy transfer amount from sand body crest. As well as depth and location, it is clear

that, the size of a channel-levee system is an important factor that could change the channeled sand-filled area and make more fluid dissipate in the surrounding mud, increase the system's effect on overpressure and this has been partially proved in the previous study. In this section, the channel's mathematics area, relative size on over-burden (the percentage of over-burden) and geometry will be considered and the key factors of the channel's effects will be defined.

Groups of numerical models which have same mathematics area and different percentages of over-burden were created to view the overpressure value at the reference point and define the key factors. The model's configuration is shown in Figure 4-17. The results have observable differences in terms of overpressure value; however these differences reach only 3 MPa, meaning that the intuitional size of the channel-levee system is not a key factor in influencing the effect of the channel. Models with the same percentage but different intuitional size were also created. The results can be predicted which have little difference. However, the ratio of the CLS to basin scale (percentage of over-burden) is an important factor which can influence channel-levee systems effect on overpressure.

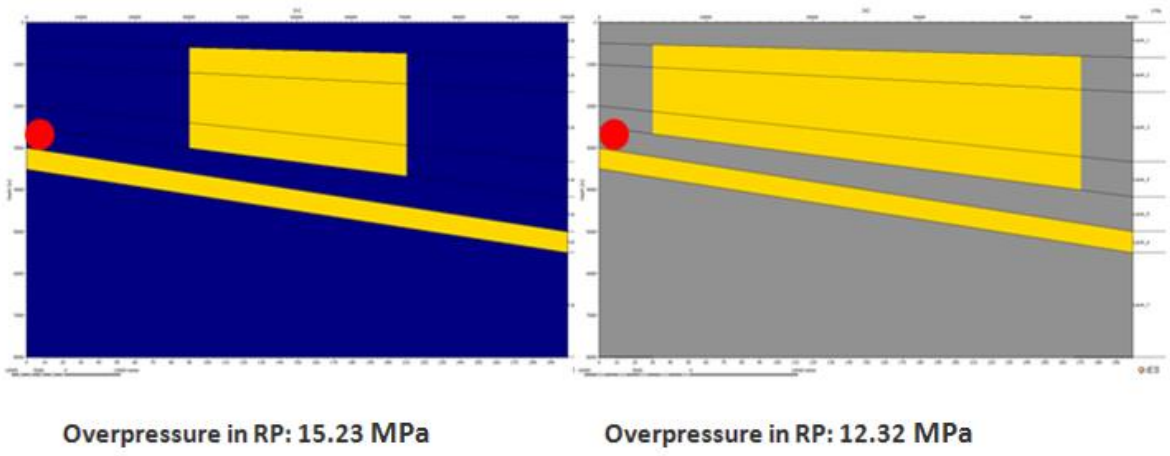

Figure 4-17 Configuration of models with the same channel mathematics area and different percentage of over-burden. The intuitional size of them is 5000 metres in length and 2000 metres depth. Channel percentages of over-burden are 20% and 50%, respectively. From the results, it can be seen that the channel with the a higher percentage of the over-burden has more influence on on overpressure; the difference could reach 3 Mpa in this group.

Based on these models, new models which have different channel geometry were created which to investigate the importance of the shape of the channel-levee systems. The model configurations are shown in Figure 4-18. The two models have different shapes of channel-levee system; the second has a relatively flatter channel than the first.

The results of overpressure value at the RP show little difference between them, only 0.06 MPa, which means the geometry of the channel has little impact con its effect on overpressure; thus, it is not a key factor.

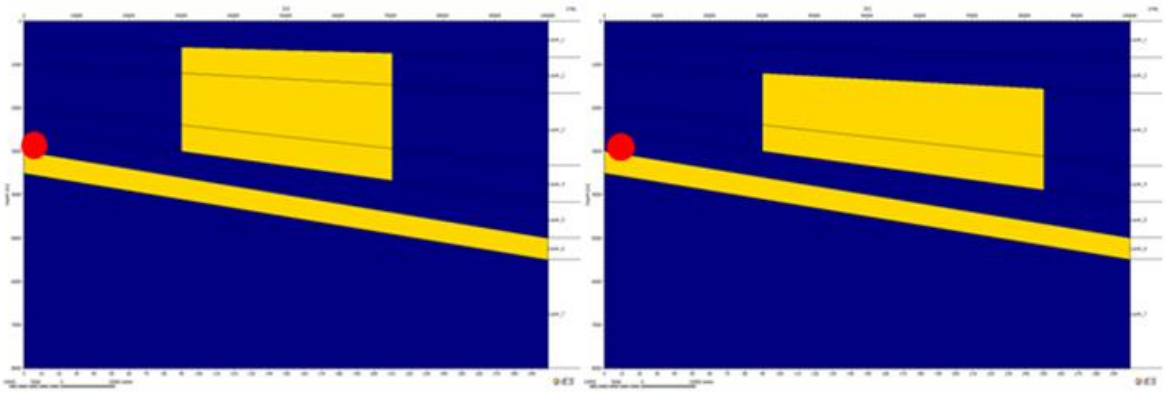

Figure 4-18 Model configurations to test importance of factor channel geometry. The second test model has a relatively flatter shape than the first. The overpressure result shows little difference in value, 0.06 MPa.

Although the over-burden percentage of a CLS can change its effect on overpressure formation, real size and channel geometry are not found to be key factors influencing channel effect. I defined the important factor (over-burden percentage of CLS) as the ratio of the CLS area and basin scale: [(CLS length/basin length) *CLS height/basin height]], [(l*h)/ (L*H)] (Figure 4-19, a). To view impact relationship of channel-levee size, a group of models with different channel over-burden percentages were created: 10%, 15%, and 20%, respectively (Figure 4-19, b), in this group, others factors were kept constant.

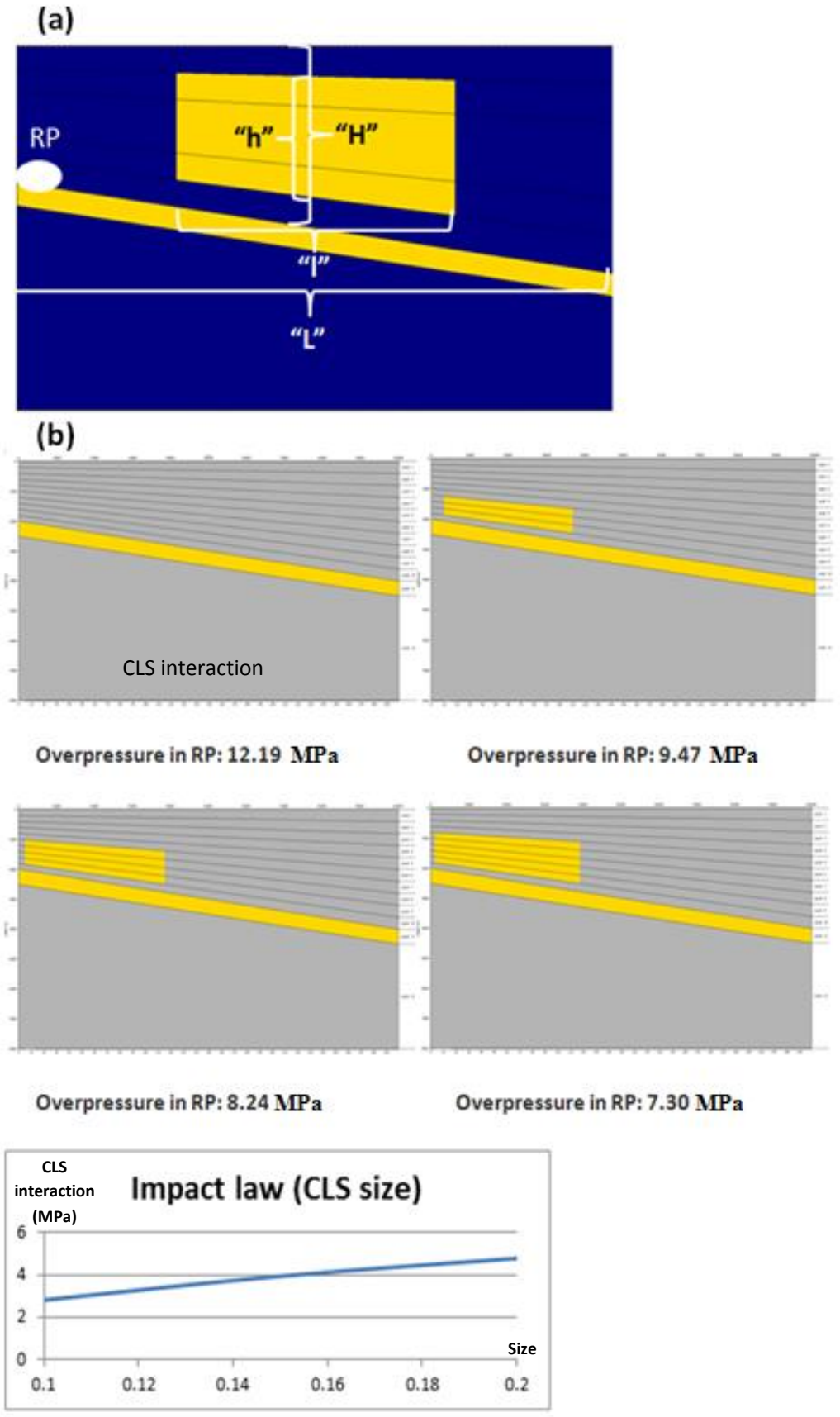

Figure 4-19 a) Definition of channel-levee systems in numerical modelling: the important factor was defined (over-burden percentage of CLS) as a ratio of CLS area and basin scale: [(CLS length/basin length) *CLS height/basin height]], [(l*h)/ (L*H)].

Fig 4-17 b) 4 models were created with different CLS size value, 0.1, 0.15, 0.2. According to the overpressure value at the aquifer crest, the CLS effect of these models can be seen from the graph, where we can see that a channel-levee system's effect increases as CLS size increases, giving a difference of up to 2.2 MPa, which is greater than for previous LT parameters (R, P, D, H).

Channel-levee size is the relative CLS area on overburden mudstone, defined above as: [(CLS length/basin length) *CLS height/height above aquifer]], [(l*h)/ (L*H)]. In this study, the factor minimum boundary is defined as 0.1, because according to the impact law of other influencing factors, sedimentation rate is held at 100m/Ma, clay content is 0.1, and aquifer depth is chosen as 2000 meters (because the LT effect will be smaller than for a greater depth in the parameter range; lesser depth could make the CLS effect smaller, but because of the low LT effect, considering the size of the base, the ratio of CLS effect and LT effect will be larger) and relief is 2000 meters. The CLS position shown in Figure 4-20, in that position, the CLS could have the biggest influence on overpressure of all cases where size value is 0.1 in the parameter space. In this condition, the importance of the effect of a CLS (the ratio of the CLS effect and the LT effect) is less than 10%. In a mathematic function this could be expressed as: $G(Zi)/f(Xi) < 0.1$, defining the CLS effect as not important in the system in this condition. According to the previous impact law, the CLS effect on the LT effect will much lower than 10% in the condition where CLS size is lower than 0.1 and other CLS position (L & d become larger). In later analysis, it will be assumed that the CLS effect is insignificant ($G(Zi) \approx 0$) in this condition, so at least most cases are insignificant when CLS size below 0.1. In this section, the lower limit of CLS size in parameter space is defined as 0.1.

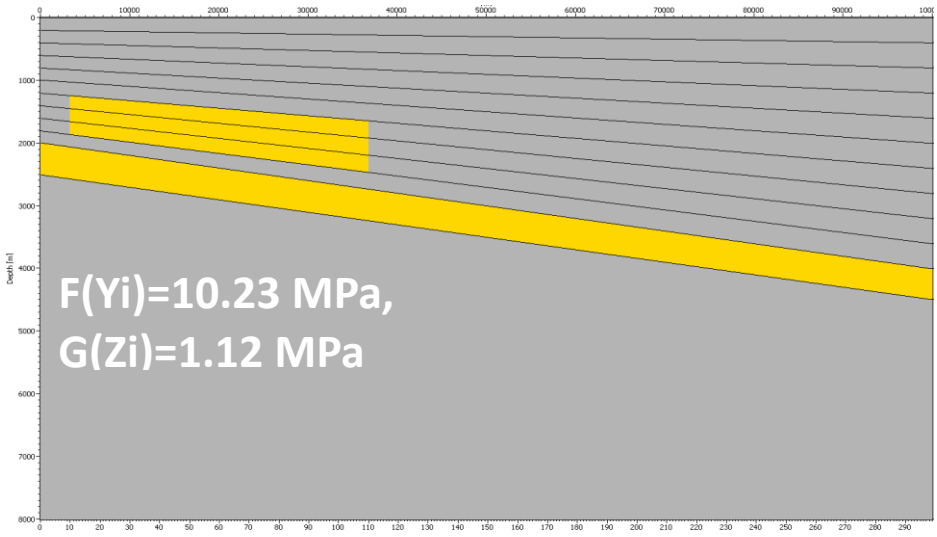

Figure 4-20 Model configuration of CLS size is 0.1; other factors adopted that could lead to CLS affecting overpressure is biggest of all combinations in chosen parameter space. From the results, the CLS effect could only represent 9.87% of the LT effect,

which is not important, according to the assumption. Moreover, in other parameter space, the CLS effect on the LT effect will be much lower than in this case where CLS size is 0.1 or below 0.1. Thus the lower limit of CLS size in parameter space is defined as 0.1 in this study and future work.

From the literature review concerning deep-water basins, it was observed that huge sized channel-levee systems in deep-water fields are not common. Thus, in considering the setting of the numerical simulation and the intention to study a combination of multiple channel-levee systems in future work, the upper limit of CLS size in this study is defined: 0.2.

From the results, the size of a channel-levee system is an important factor which could have considerable influence on channel effect on overpressure. When channel size increases, its effect on overpressure will also increase, causing a difference of nearly 2.2 MPa, in this group. This is because a bigger channel size has more channeled fill area and fluid dissipates on the surrounding mud, and in the aquifer crest. The degree of influence is larger than for the factors studied previously.

4.3.2.6 Less important factors

Aquifer bending is also among the geometrical factor like relief, which have the smallest influence on the parameters of Lateral Transfer (sedimentation rate, clay content, aquifer depth, aquifer relief, bending). Changes in aquifer bending mean that the effects of LT and the over-burden sediment's average sedimentation rate also change, so this factor influences overpressure distribution at the aquifer crest in LT models. In the multiple channels condition, changing aquifer bending could also change the depth of channels, which could strengthen the flow interaction between the aquifer and channel (Figure 4-21). However, in this study, due to the low importance of aquifer bending and its numerical modeling complexity, the factor is ignored in the future analysis.

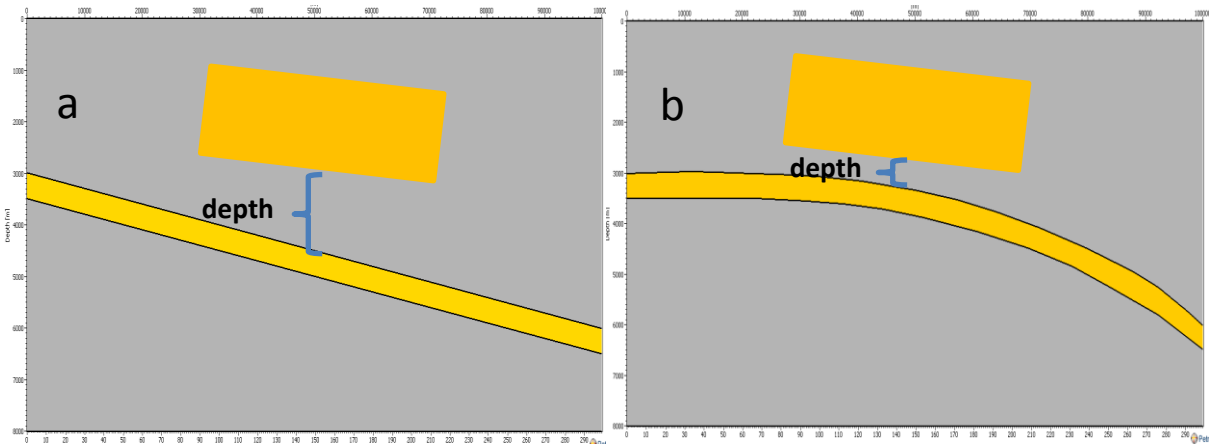

Figure 4-21 The GU's depth is different between two kinds of aquifer bending. Fluid will more easily flow between sand and channel in "b", so F(Yb) will differ from F(Ya). The two cases also have different aquifer average sedimentation rates, which could also influence channel effect on overpressure.

Although aquifer bending could also influence overpressure distribution when channel-levee systems are deposited, the degree of influence is less than that of other parameters in the LT condition (Influence ranges of the parameters are in the order: Clay content(C) (54.45%)> Depth (D) (27.32%)> Rate(R) (8.86%)> Relief (H) (5.97%) > Bending (B) (3.39%).

Other limitations in considering this factor are: (1) Models created have great complexity, (2) aquifers with no bending or no obvious bending are the main structures in basins worldwide. Thus, based on this section, parameter "B" is removed in the analysis of the condition of multiple channel-levee systems. In the mathematical assumptions, the LT element adopts four importance parameters and the CLS effect includes seven key influential parameters.

In summary, the factors influencing the channel effect on overpressure were studied and the key factors identified in these section above: these are RP over-burden depositional rate (R), over-burden mud clay content (C), aquifer relief (H), aquifer depth (D), and feature factors of channel-levee systems: channel size (S), channel depth (d) and channel location (L). In the mathematical assumption, the channel-levee system's effect element G(Z) has seven parameters, which are a larger number of parameters than in the element representing the LT effect. For better working out the relationship between them and possible simplifying the complexity of the parameter space, only the optimal parameters in "G(Z)" parameter space, according to the importance of the channel's effect on LT effects need to be considered. This enables a more accurate data analysis and reduces unnecessary simulation in future studies, and also allows a more meaningful and intuitive way to analyses the effects of multiple channel-levee systems.

4.3.3 Basin with multiple CLSs

In basin numerical modelling, a conceptual model is created for two channel-levee systems above a dipping aquifer for viewing the importance of the interaction of CLSs and prove the hypothesis prosed above is first to be considered. If the values of size, location and depth are defined, the modelling configuration for two channel-levee systems is shown in Figure 4-22.

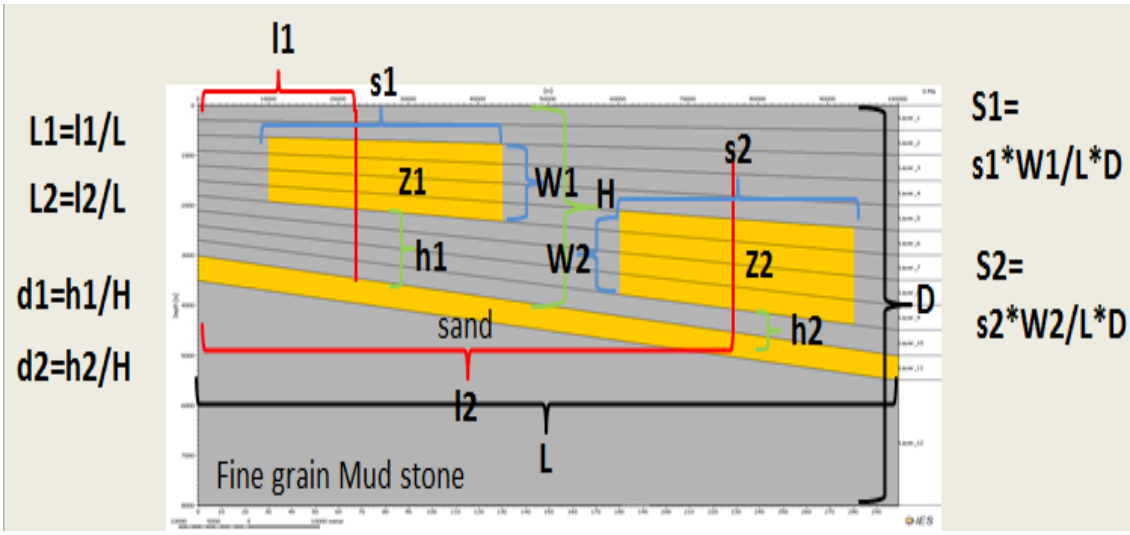

Figure 4-22 Model configuration for two channel-levee systems (z1, z2), expressing their own feature parameters. RP over-burden sedimentation rate is 100 m/Ma, clay content is 0.1, aquifer depth is 2000 m and relief is 2000 m.

According to the modelling configuration, a random sampling scheme was developed to generate the arrangement of the CLSs; a group of models were created for viewing the fluid interaction between the two CLSs and their effect on overpressure behaviour. In the group, sampling details of the two CLSs parameters (S, L, d) are shown in Table 12, in which some of the previous settings are adopted to perform a simulation for examining the relationships of each GU. 576 models were created in this section, and the details and a sample of results are shown in Appendix D.

Table 12 Value cases of two CLS in this section. There are 24 cases for each channel-levee system and 576 combined, in total. In this group, values adopted are CLS size 0.1 and 0.15, location values 0.2, 0.35, 0.6 and 0.7, and depth values 0.1, 0.4 and 0.6, respectively.

Area(S1)	Length(L1)	Depth(d1)
0.1	0.2	0.1
0.15	0.35	0.4
	0.6	0.6
	0.7	

From the results in Table 12, the two CLS' overall impact on overpressure at the aquifer crest was calculated using: G(Zi) = F(Yi) – F(Xi) (which is the LT effect from

simulation, is equal to F(Y) in Chapter 3), and decomposition of the single effect of each CLS was performed using: $\Sigma g(Zi) = g(Z1) + g(Z2)$, and their difference was calculated: $\varepsilon = G(Zi) - \Sigma g(Zi)$. The importance of "ε" was then analysed to define in which condition the overall impact of the two CLS could be expressed as a single effect decomposition, and in which condition the overall impact needed to be upscaled. If "ε" value is less than 10 % of the LT effect: $\varepsilon/f(Xi) < 0.1$; in these cases, errors are considered to be unimportant, meaning the results of the decomposition of the single effect of two CLS are nearly same as those of two CLS in terms of overall impact on overpressure on aquifer crest, so the overall impact on overpressure could be expressed by overlaying the effect of two single CLSs. Analysis of the modelling results tries to find whether or in which condition the overall impact could be expressed as a decomposition of the effect of two CLS and in which condition this does not work, thus verifying whether the hypothesis is correct or not, before performing the next step of the analysis. Details of the analysis will be shown in the next section.

After that, the upscaling process for two close CLSs will be analysed by response surface methodology, for the prediction of overpressure in a basin case with up to two CLSs which are close together. When the basin has up to three or more neighbouring CLSs, a combination of all the models in parameter space will also be used to analyse interaction in of each CLS with those in the cluster and their overall impact on overpressure, by upscaling.

4.4 Analysis

In this section, the main problem about the increase in parameter space and need to reduce it will be resolved in Section 4.4.1. The prediction of the impact of a single CLS on overpressure using response surface methodology on the factors, after simplification, is then discussed in Section 4.4.1.3. Section 4.4.2.1 mainly addresses analysis of CLSs' interaction through simulation discussed above in section 4.3.3, and highlights the main results which support the hypothesis. Section 4.4.2.2 explains how a new group of simulations which was created using all the combinations according to the CLS' relative distance from each other, to clearly understand under which conditions the interactions need to be considered. An upscaling method was used in these cases, using the response surface methodology, to predict the overall impact on overpressure, as reported in Section 4.4.2.3. In Section 4.4.3, cases are discussed in which the basin has three closely located CLSs whose interaction cannot be ignored, according to the results in

Section 4.4.2.2. The simulation design also chooses all possible combinations between the three CLSs in parameter space to analyses their interaction and upscale this to predict the overall impact on overpressure. In Section 4.4.4, cases of a basin with four neighboring CLSs will be discussed; because of the PhD time limit and according to results of 4.4.2 and 4.4.3, the methods in this section were chosen to work out guidelines from the study of several selected examples, and the accurate and complete method, which would be the same as that described in section 4.4.3 could be done in future work.

4.4.1 Influence of a single CLS - Simplification and reduction of parameter space

4.4.1.1 Retaining the significant range of parameter space in the CLS effect

It is the objective of this research to express G(Z) through simulations and non-linear Response Surface. Before doing this, the range of parameter space should first be considered and defined. In the previous section, the limit of CLSs effect on overpressure has been confirmed to be less than 30% of the LT effect. In that section, I adopted the parameter space of the Lateral Transfer effect and channel-levee systems features and the factors' range will be defined as before. In this section, the basic and treated parameter space (excluding the cases which have insignificant CLS influence on overpressure) will be defined. In this part of the work, the ratio of the CLS effect and LT effect is main foundation to define the importance of the CLSs' influence and separate parameter space.

The range adopted for each of the channel-levee system's main influencing factors which will be used in the parameter space and numerical simulations are performed to view overpressure output; Response Surface methodology is then used to work out an appropriate relationship between these factors and overpressure at the aquifer crest. The parameter space of the channel-levee effect is shown in Table 13. The values of the seven factors are adopted according previous parameter space and assumption and the total number of simulations needed to try to work out the relationship between the seven important factors and overpressure, and determine their weight is 1680.

Table 13 Parameter space for this section. For the LT effect parameters, I adopted settings from the previous study setting. For the CLS feature factors, minimum and maximum limits of the parameter range were adopted. The number of simulations of the parameter space could reach 1680 cases in this study.

Rate(R)	Clay(C)	Depth(D)	Relief(H)
100	0.1	2000	2000
300	0.3	3000	3000
500	0.5		
800	0.7		
1000	0.9		
2000			
4000			

Area(A)	Length(L)	Depth(d)
0.1	0.2	0.1
0.2	0.7	0.2
		0.4

Because of the huge number of simulations which need to be created, balanced simplification of the parameter space will be considered, which could make the results more concise and precise. In this study, if the importance of the CLS effect (ratio of CLS effect and LT effect) is less than 10% (i.e. G(Zi)/f(Xi) < 0.1), the CLS effect will be considered as non-important (G (Zi) $\approx$ 0), so the importance of the effect of the CLS becomes the basis for simplifying the parameter space. I adopted a numerical simulation method to define in which parameter space the CLS effect is not important.

Following this idea, the overpressure value on aquifer crest can be expressed as:

$$F(Y) = f(X) + G(Z) + \varepsilon(Y) \begin{cases} F(Y) = f(X) + \varepsilon(Y) & (X \in (\ldots) \\ F(Y) = f(X) + G(Z) + \varepsilon(Y) & (X \in (\ldots) \end{cases} \quad 4\text{-}5$$

Over-burden sedimentation rate and clay content are the most important factors in LT effect. These two factors could also largely affect the importance of the channel-levee systems' effect. Other factors which were studied are monotonic impact of the CLS effect from the simulation output, so the main idea of this section is to hold the factors constant that are at the extreme boundary of parameter space constant and change the

over-burden sedimentation rate and clay content to find target region (where the CLS effect is non-important). Aquifer depth is defined and relief is 2000 meters; the channel-levee system's size value is 0.2, depth value is 0.1 and location value is 0.2. The 5 factors with these values could make the biggest CLS effect of all the parameter space, with over-burden sedimentation rate and clay content constant; if the values of the CLS affect G(Z) are insignificant on these limitations, it will be insignificant in other parameter ranges.

Five groups of models which have different over-burden clay content and sedimentation rate were created to view the importance of the channel-levee effect on the LT affect. The results are shown in Figure 4-23. From the results, it can be seen that, if the sedimentation rate is greater than 1000m/Ma, no matter how much clay content is changed, the effect of the CLS will be less than 10%. Moreover, if the over-burden clay content is 0.3, the sedimentation rate is above 800m/Ma, and if over-burden clay content is 0.5, rate is above 300m/Ma, the CLS effect on LT will also be less than 10%. When the clay content is 0.7 or 0.9, in the defined parameter space, the effective stress on the aquifer crest will be "0" in the numerical output. This means that in a real basin modelling study, these extreme cases would need to be dealt with by increasing the permeability or allowing fractures to open, but for this study, I exclude such cases.

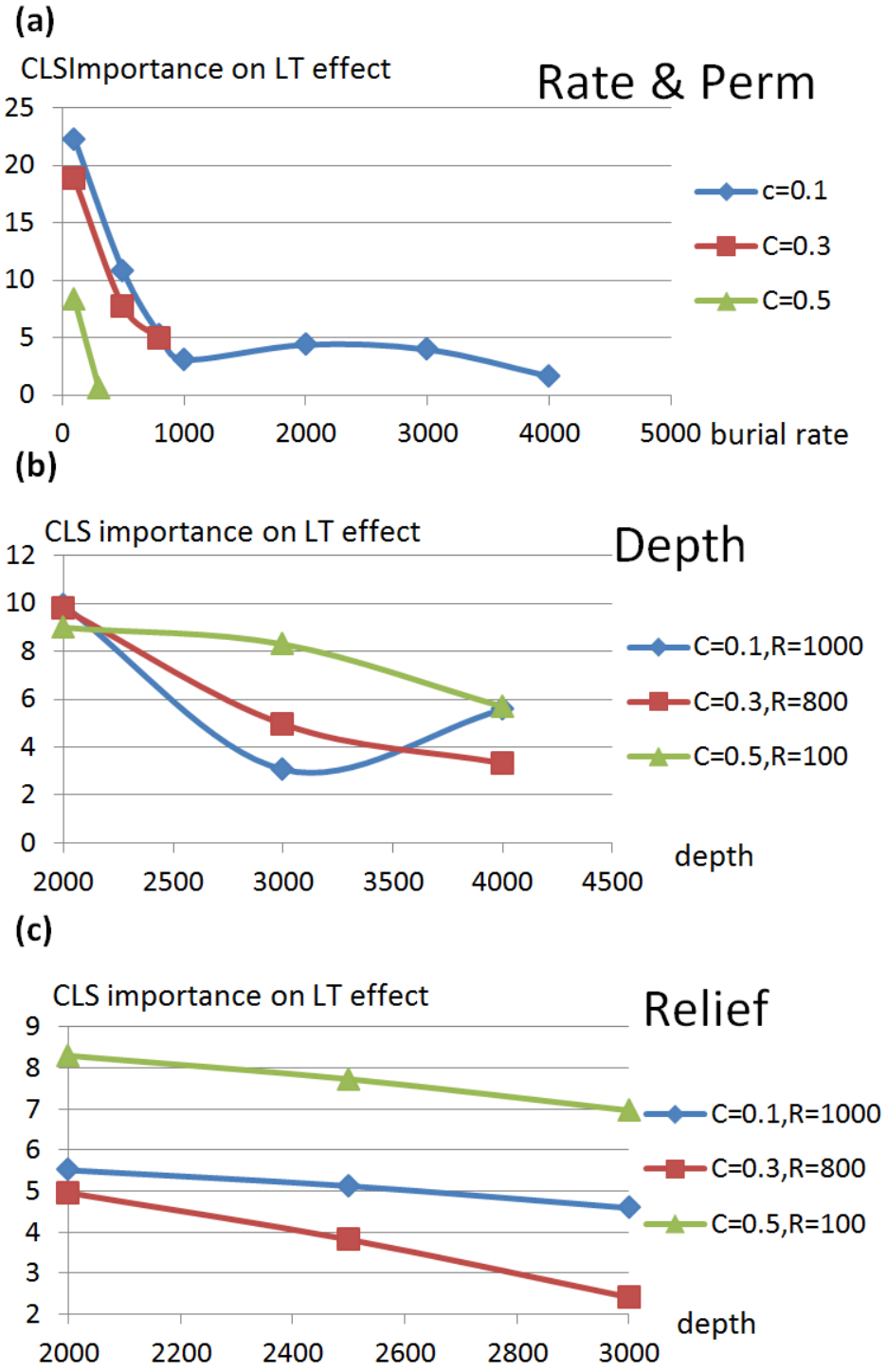

Figure 4-23 Channel-levee systems effect on overpressure at the aquifer crest in different LT parameters. A) Result: if R is bigger than 1000m/Ma, no matter how clay content is changed, the CLS effect will be less than 10%. If C= 0.3, the rate is greater than 800m/Ma; C=0.5,rate is greater than 300m/Ma, CLS effect will also less than 10%. B) At boundary of burial rate and clay content, depth of sand layer change could mean CLS has less than 10 % influences. C) At boundary of burial rate and clay content, change in relief of sand layer could also mean CLS has less than 10 % influence.

After simplifying the parameter space by holding clay content and sedimentation rate constant, it is not important to separate the region of the CLS effect, which achieves the purpose of narrowing down the parameter space (Table 14). In the red region of Table

14, the CLS effect is not important and the overpressure value at the aquifer crest will follow: F(Y) = f(X) +ε(Y), and in the other region, the overpressure value at the aquifer crest will follow: F(Y) = f(X) + G(Z) +ε(Y). The value of G(Z) need to be calculated, in which "Z" has seven important parameters. In such regions of parameter space, the importance of the CLS effect on the LT effect is between 0.1 and 0.3, where clay content and sedimentation rate are constant. In some cases of this region, the CLS effect could also be lower than "0.1 f(X)"; however in the process of analysis, considering its workload and complexity, I considered the region as one type for which the CLS effect is important and cannot be ignored.

Table 14 Simplified Parameter space: the CLS effect will be less than 10 % of the LT effect in the red region. This analysis achieves the purpose of narrowing down the parameter space

Clay/Rate	100	300	500	800	1000
0.1					
0.3					
0.5					

+ Other parameters

After simplifying the parameter space, the total number of cases which need to be created was reduced from 1680 to 480. This study was thus effective in reducing the work load, and could also make future modelling analyses more accurate after narrowing this space, and more easily employed by other researchers. In the next step, all of the 480 models were created. The next step is the consideration and analysis of the modelling results.

4.4.1.2 Reducing the high dimensions of the parameters

After separating the parameter space, seven dimensional functions in left hand region in Table 14 need to be analyzed in terms of the relationship with aquifer crest overpressure. The parameter space of this section is shown in Table 14. In the part relating to the assumption of parameter values, I adopt the range and value from previous study and systematic sampling. To find models in which CLS effect is not important, 480 plausible models were created for inspecting the relationships between the seven

important factors and overpressure on the aquifer crest. The models results are shown in Appendix B.

Because of the parameter's complex situations, seven parameters will make analysis much more difficult and lead to complex results: the results also cannot express ideal and straightforward relationships between the overpressure value and all seven parameters. I thus tried to find another simplifying method to reduce such a high dimension of parameter space and make the process of analysis and its results more precise and easily accepted. Among the seven parameters, sedimentation rate, clay content, aquifer depth and relief are also important factors in the LT effect, whereas the channel-levee system's size, depth and location are factors relating to its own characteristics.

From the modelling output, I calculated the channel-levee system's effect (G(Z)) by the subscript assumption: F (Yi) = F(xi) + G (Zi). The seven important factors in "Z" could be divided into two parts: LT effect factors and the CLS own feature factors, by analyzing the weight and importance of these two parts and defining which part could be expressed as an error and which part needed to be calculated. From the results (Appendix A), if four factors (sedimentation rate = 100m/Ma, clay content = 0.1, aquifer relief =2000m and depth=2000m) are held constant, the three factors CLS depth, location and size could lead the CLS effect to change from 0.57 to 4.16 MPa, and the greatest difference between all the cases could be over 5 MPa. However, if the three factors (CLS depth=0.1, location=0.3 and size=0.1) are held constant, the four factors sedimentation rate, clay content, aquifer relief and depth could change the effect only from 0.61 to 3.17 MPa, with less influence than the other three factors. From the whole set of cases, I chose 12 groups (Appendix B) which have the same values for the three factors, and found that the biggest difference in the CLS effect for all these cases is 2.5 MPa; in some groups, the difference is only below 0.5 MPa. Thus, from this analysis, it is clear that the four factors sedimentation rate, clay content, aquifer depth and relief produce less influence and have less weight in the CLS effect function than the three factors (CLS size, location and depth).

Thus, a good method to reduce the parameter order and function complexity is to hold the four factors at constant values, and express the channel-levee system effect by the three dimensional functions. That is: F(Y) = f(X) + G(Z) = f(X) + g(X*, z) + error (from G(X*,z) to G(Z) (where Z = X + z, X* is four parameters R,C,D,H have constant value).

From the 12 groups which have same the three factors, the values for the four constant factors are: RP over-burden sedimentation rate is 100m/Ma, over-burden clay content is 0.1, aquifer depth is 2000 meters and relief is 2000 meters. If the values of the four factors are changed, their influence values on "G(Z)" [G(Zi) - G(X*, zi)] are all less than 8% of LT effect (f(Xi)), and most of them are less than 5%: [G(Zi) – G(X*, zi)]/f(Xi) < 0.08 (the relative error is less than 10% which can be ignored in thesis analyze). So the function G(Z) is divided into two parts: g(X*, z) and an error, for which the value is less than 8% of the LT effect. g(X*, z) will be expressed as "g(z)" in later sections.(Analysis results are shown in Appendix B)

In three dimensional function g(X*, z), "z" has three importance influence factors, CLS location, depth and size. In next step, the response surface methodology will be used for working out the relationship between the three factors and the simplified function g(z). Let h(z) be a regression of g(z), the overpressure value at RP could be expressed as: F(Y) = f(X) + h(z) + error, and this error includes three parts: the regression error of the LT effect, the influence of the four factors in G(Z) and the regression error of the three dimensional function g(z).

4.4.1.3 Influence of single CLS – prediction

The impact law of the three factors (CLS size, location and depth) cannot directly determine their linear relationships, so D-optimal design will also be used in this study to determine relationships between decreased values of overpressure and the three factors. After defining the three influential parameters from the design variables, the next step is to build the response surface of overpressure on three parameters using D-optimal design of the Design Expert software. As the default, the quadratic model was chosen. D-optimal design required 20 cases, based on 3 factors. From the previous assumption and parameter space, as defined, 108 models (detail as in Section 4.4) in the range have been simulated in the previous work. This number is also totally sufficient as quadratic models which need 20 cases in D-optimal design. And they even satisfy a quartic model, which needs 45 cases based on 3 factors. I used all of the 108 models' results and input to D-optimal design, in order to get a more accurate model determination and response surface results from D-optimal design. By using PetroMod and Excel spreadsheet, the overpressures corresponding to those 108 models were obtained, as shown in Appendix C.

Next, it is required to select the appropriate model to fit the overpressure response surface. From the fit summary table, a linear relationship and interaction, the (2FI) model was suggested by D-optimal design, and the quadratic model was aliased. It was statistically suggested that the 2FI model is the appropriate model.

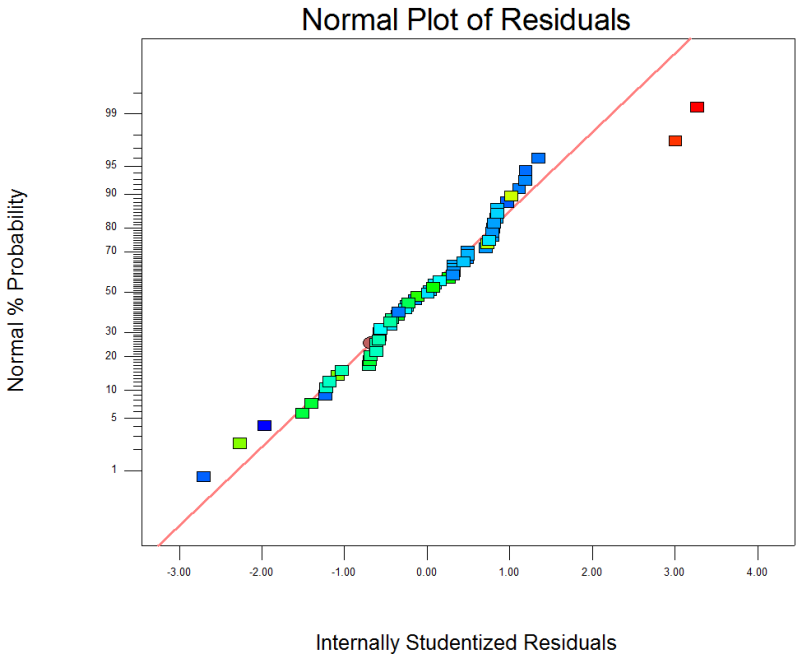

Figure 4-24 Predicted overpressure vs. actual overpressure value after D-optimal design. (2FI)

As can be seen from Figure 4-24, the overpressure response surface provides reliable predicted values of overpressure compared with the actual value of overpressure. From the graphic, it can be seen that the fitting situation is ideal in most of the cases. However, there is a similar situation as that in the previous response, that on the both sides of the parameter space, the difference between the predicted and actual overpressure value is greater. The details and reasons for this will be analysed in Chapter 5. The final equation is shown in the equation below; the equation includes the relationship and interaction of each of the influencing factors.

$$
\begin{aligned}
h(z) &= \\
&+1.95736 \\
&+17.23974 * S \\
&-4.81457 * L \\
&-1.31561 * d \\
&+2.73254 * S * L \\
&-42.48979 * S * d \\
&+7.55950 * L * d
\end{aligned}
$$

This equation represents the fitted equation of the overpressure surface for the 2FI model,

where: h(z): channel-levee effect on overpressure value on aquifer crest

S: Channel-levee system size

L: Channel-levee location

d: Channel-levee system depth

As can be seen in the equation, the 2FI model includes the interaction terms. Therefore, this model can provide a good fit for the true overpressure response surface from the Design Expert report. The values of overpressure generated from the model were compared with the actual values from the simulation, as presented in the D-optimal final report. It showed that the percentage difference between both overpressure values is within an acceptable range. The results and analysis will be presented in Chapter 5 which deals with the simulation data and analysis of the results.

4.4.2 Analysis of the interaction of two channel-levee systems - upscale

In this section, the influence of multiple CLSs is studied. First, the hypothesis of the influence of multiple CLSs is re-presented, as mentioned above – if the positions of CLSs in a basin are scattered, the overall impact on overpressure will be decomposed into each single system's influence on overpressure at the aquifer crest. However, if several of systems are close to each other, forming clusters, the fluid correlation between them cannot be ignored and thus needs to be considered. Then in a basin with two neighbouring CLSs, the two systems' interaction becomes the main factor which needs to be considered. The parameter space regarding the combined position of the two

CLSs was also separated, according the level of importance of the interaction. Then a clear response (for the importance of interaction in these cases) between the effect of each single CLS and their overall effect on overpressure was worked out.

After that, basins which have three and more CLS clusters were studied. The results regarding their influence on overpressure at the reference point revealed that, for most of the cases, the overall effect on overpressure could be expressed as simple superposition of a CLS single effect for each system. Moreover, if special cases are encountered in which two or more channels are collapsed together, the cluster's overall impact on overpressure can be expressed as the upscaled effect of two specific closest CLSs of the cluster and single effect decomposition that of other CLSs of the cluster. The conditions for the two CLSs which need to be upscaled will be detailed in section 4.4.2.3.

4.4.2.1 Numerical analysis: interaction of two CLS cases

After analysis of the modelling results as described in section 4.3.2, they can be roughly divided into two elements: the overall impact of two CLSs on overpressure can be expressed by two single CLS effect decompositions, (ε/f(Xi) < 0.1),

$$F(Y) - f(X) = G(\mathrm{Z}) \approx \sum_{0}^{i} g(z_j) \qquad 4\text{-}6$$

in which the two CLS are relatively distant, (Figure 4-25 a).

As the overall impact on overpressure distribution of two CLS cannot be expressed as the single effect overlay (ε /f(Xi) ⩾ 0.1),

$$F(Y) - f(\mathrm{X}) = G(\mathrm{Z}) \neq \sum_{0}^{i} g(\mathrm{z}_j) \qquad 4\text{-}7$$

then

$$G(Z) \approx gg(z) \qquad 4\text{-}8$$

Where (gg(zi) is a weight function which is composed from two g(zi) and means $\varepsilon_{g}(yi)$ is minimised; upscaling: g(zi) → gg(zi)),

in which the two systems are relatively close together (Figure 4-25 b).

The detailed results are shown in Appendix D. From the results, it can be seen that the difference between the effect of the two CLSs ("G(Zi)") and single effect decomposition ("Σg(zi)") will also change according to the relative distance between them: when their relative distance is greater, the value of "ε" is smaller (LT effect f(xi) is constant in this study); when their relative distance is smaller, the value of "ε" is higher. That means an interaction between fluid transfers or pressure of the two channel-levee systems really exists, and their interaction depends on the relative distance between them.

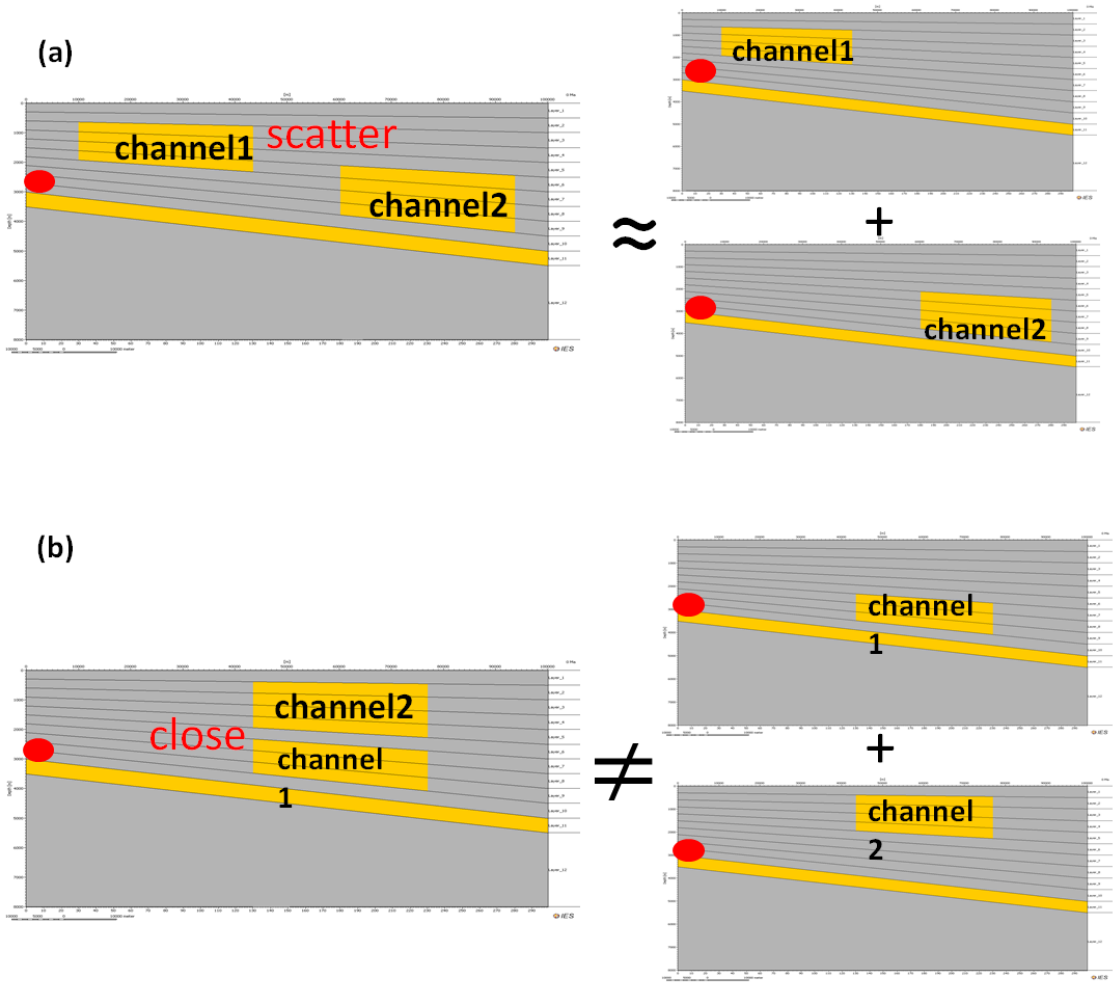

Figure 4-25 a) The two channel-levee systems' overall impact on overpressure at the aquifer crest can be expressed as a decomposition of two CLSs' single effects: F(Yi) ≈ f(Xi) + Σg(zi). In this condition, where the two CLSs' relative directions are scattered, the interaction between them is relatively small. b) the two channel-levee systems' overall impact on overpressure at the aquifer crest cannot be expressed as the two CLS single effect decomposition: F(Yi) ≠ f(Xi) + Σg(zi), in which the difference between Σg(zi) and G(Zi) is more than 10% of the LT effect f(Xi). In this condition, where the relative distance between the two CLS is small, interactions between them are relatively large/ significant.

From the results in Appendix D, the previous hypothesis has been proved to be correct; fluid interaction between the two CLS is a very important factor on overpressure distribution in a multiple CLS basin, and should be considered in the overall impact on overpressure distribution. Hence, to better express overpressure value at the aquifer crest in the presence of multiple channel-levee systems, a key method is to study the correlation of their importance in terms of their different relative distances.

Fluid will flow between two CLS in basin evolution; the amount of flow is correlated with their position and distance. In mathematical model's assumption, different interaction could be represented as different coefficients in front of each CLS effect, when these co-exist:

$$F(Yi) - f(Xi) = G(zi) = m1\, g(z1) + m2\, g(z2) \qquad 4\text{-}9$$

When their positions are scattered, the interaction between them are small, and coefficients m1, m2 could be seen as "1":

$$F(\mathrm{Y}\,i) - f(Xi) = G(Zi) = \sum_{1}^{2} g(z_j) + \varepsilon_g(Yi) \qquad 4\text{-}10$$

In the function " $\varepsilon_g(Yi^1, Yi^2)$" is the error from G(Zi) to $\sum_1^2 g(zi)$, which will be less than 10% of the LT effect f(Xi).

When their positions are enough close, or they even collapse, the interaction between them cannot be ignored:

$$F(Yi) - f(X\,\mathrm{i}) = G\,(Z\,\mathrm{i}) = m1\, g(z1) + m2\, g(z2) = gg(z1, z2) + \varepsilon_g(Yi) \qquad 4\text{-}11$$

where gg(z1,z2) is a function from the fitting method, which is close to m1 g(z1) + m2 g(z2). This step will be worked out by a large number of simulation and Response Surface methodologies in the next section.

Interaction between channel-levee systems is an important factor which needs to be considered in studying how overpressure distribution is affected multiple CLSs. For better analysis of the plausibility of the decomposition and upscaling, knowing the importance of the CLS interaction for different relative distances is the first consideration. If a parameter space is created regarding the relative distance of two channel-levee systems, it can be divided to two parts, according to the level of importance of the CLS interaction, and each part analysed to calculate the CLS's impact

on overpressure distribution at the aquifer crest by undertaking systematic simulation cases and statistical methodology.

4.4.2.2 Design of simulation cases – different combination of relative distance of two CLSs

In this section, in order to study the importance of CLS fluid interaction a group of models, a group of simulations was carried out with variable relative distance between two channel-levee systems. Consider the cases of two channels and use simulation methods (Random pick, Table 10) according to relative distance (ΔL, Δd).

For making the model's configuration more compact and more representative, I chose one of the CLSs located near to the reference point on the aquifer crest, with as large a size as possible (0.15) in the parameter space. This is because in this position and at this size, the CLS could cause the largest effect on overpressure at the aquifer crest of all the possible CLS positions in the parameter space, and when the other CLS are deposited near it, the interaction between them will higher than for any other position and size. From the previous modelling results (Appendix D), it was shown that when two CLS are together, in most relative positions, the area size is 0.1, the interaction error is nearly 10% (9+%, limit) of the LT effect f(Xi). When the CLSs size is 0.15 and follows the position, in the parameter space "interaction unimportant" means that it will also not be important in other parameter spaces (CLS effect smaller and LT effect is constant). However, in the "interaction important space", the interaction importance may be considered or not considered in other region of parameter space. I looked at this space as "dangerous space", meaning it would be needed to use a statistical regression method for these cases in this space: the difference between G(Zi) and Σg(zi) should still be less than the results without fitting, and the results are also more accurate.

So considering the cases of two channels according to relative distance (ΔL, Δd), simulation methods were used and the parameter space defined using "Random Pick"; the details are shown in Figure 4-26. The LT parameters were adopted as before, and a different sedimentation rate was used in each group to provide a better view of the results and give them more clarity. The basic channel-levee system's size value was defined as 0.15 with numerical software (PetroMod 2012), setting limits and reference point: the location value is 0.2; depth value is 0.1 which is near aquifer crest (reference point). The reason for choosing these values is that they can make the greatest effect from each CLS on overpressure distribution of the parameter space, and the greatest

interaction effect on the LT effect, with the LT effect constant. The other channel-levee was positioned according to the relative distance from the base, and the size value defined for this channel was also 0.15. The model configuration of this group is shown in Figure 4-26, and 240 models were created to assess the CLS interaction importance (G(Zi)- Σg(zi)) in influencing the LT effect (f(Xi)) at different relative distances.

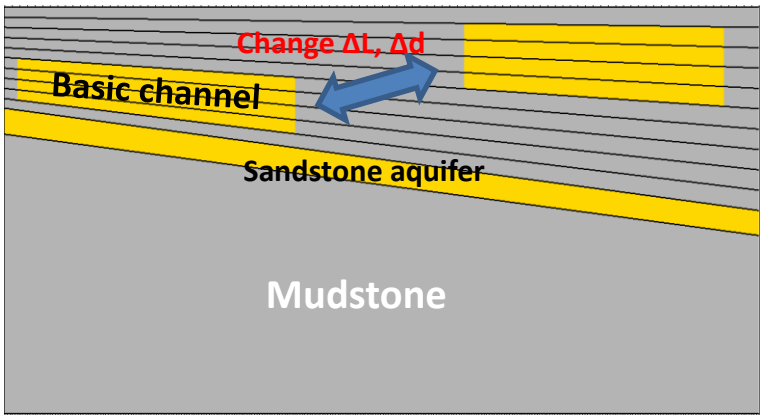

Figure 4-26 model configuration of CLS relative direction. In this section, the basic CLS position was chosen near the aquifer crest (S=0.15, L=0.2, d=0.1) because a CLS in this position could cause a bigger effect on overpressure than any other position in parameter space. The other CLS was varied according to relative distance with regard to depth and location. Details of the relative distance setting in this section are shown in Table 4-15.

Table 15 Setting two channel-levee systems' relative distance in the numerical simulation group.

ΔL	Δd
0	0
0.1	0.1
0.15	0.2
0.2	0.3
0.25	0.4
0.3	0.5
0.35	
0.4	
0.45	
0.5	

Four groups of models with different sedimentation rates (R) were generated (4*60=240) to calculate F(Yi) , and find the difference between the importance of "G(Zi) and "$\sum_o^i g(zi)$ " in its influence on the LT effect (f(Xi)), then the parameter space was divided into two parts, according to the results (Appendix D). From the results, it was found that the parameter space was divided into two parts. The first one is where the overall effect of two CLSs on overpressure could be expressed as the decomposition of the two systems' single effect: F(Yi)=f(Xi)+ $\sum_o^i g(zi)$; in this condition, the relative distance of the two CLS was generally large. The other one is where two CLS effects overlap and thus there is a need to regress with single effects which are near to their overall effect on overpressure distribution: F(Yi)=f(Xi)+gg(zi), in which gg(zi) is "m1g(z1)+m2g(z2)": in this condition, two CLS are generally collapsed together, or very close in vertical distance and have a vertical overlap area. The results also confirm previous assumptions: the relative distances of CLSs influence fluid flow within them.

In these simulations and the previous simulations (240+288 models), there are over 75% cases in which the two channels' effects (G(Zi)) can be expressed as g(z1)+g(z2) + ε(g) (ε(g)<=0.1$f(Xi)$). In the group where sedimentation is 100m/Ma, when one channel is close to the aquifer (d1=0.1, deposited nearly 2 Ma after the aquifer), or the other channel is just touching it or very close in the vertical direction, their relative distances in these group are satisfied by: 0<=ΔL<=0.35, 0.3<= Δd <=0.4, or 0<=ΔL<=0.15, 0.4<= Δd<=0.5. In these conditions, the two channels' effects cannot be expressed as Σg(zi), (ε(g)>0.1$f(Xi)$). This is because when two CLS are close in their relative distance and have a vertical overlap area, the vertical permeability of each CLS will lead to more fluid interaction between them, and the overall impact on the overpressure at the aquifer crest will not be equal to the decomposition of the effect of two single CLSs. If the two channels' position are very close, (0<=ΔL<=0.15, 0<=Δd<=0.2), the effect of the two channels could be expressed as that one of them, (gg(zi)=g(z1) or g(z2), and ε(g)<=0.1$f(Xi)$). But from previously studies of similar deposits around the world (GOM, Indus basin and West Africa), for each channel's relative distance to follow this condition (very close, such that the overall area could be expressed as that of one of them) is very rare, so the condition is uncommon in geology.

In the group where the sedimentation rate is 300m/Ma, 500m/Ma and 1000m/Ma, the trends of the CLS relationships' importance have not obviously changed but their absolute value were decreased, (Figure 4-27 b, c, d) because when the sedimentation rate increases and the LT effect will also increase, the CLS's effect on overpressure will

decrease, the two CLS's relationship of importance on the LT effect will thus also decrease.

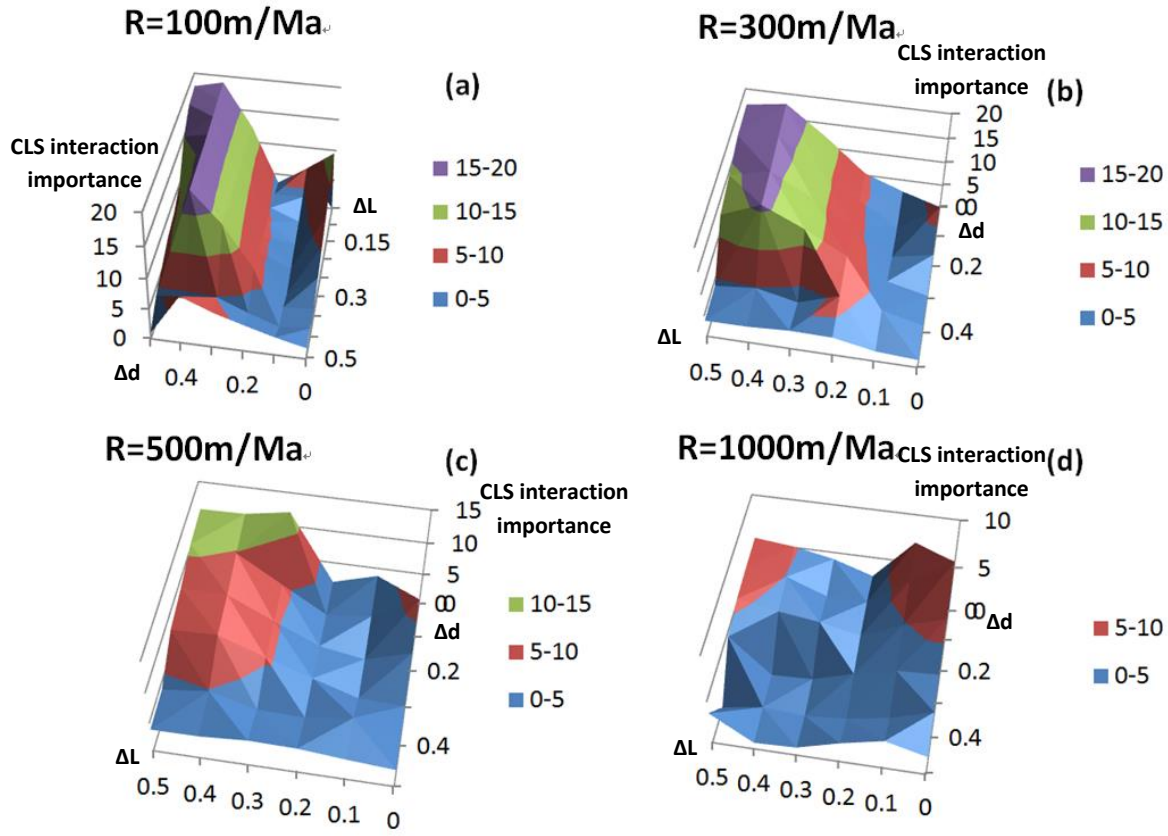

Figure 4-27 a) Interaction difference importance in the LT effect ("y" axis)' "x" axis is the relative distance between the two channel-levee systems. In the graphic, region in colour green and purple are means CLS interaction is important which could not be ignored and the value is more than 10% of LT effect f(Xi). When relative distances in these group satisfy: 0<=ΔL<=0.35, 0.3<= ΔD<=0.4, or 0<=ΔL<=0.15, 0.4<= ΔD<=0.5, the interaction could be over 10 % of the LT effect which is colour green and purple. b, c, d, The graphic shows importance of interaction on the LT effect when sedimentation rates are 300 m/Ma, 500 m/Ma and 1000 m/Ma, respectively. The trend of the importance of CLS relationships has not obviously changed but their absolute value has decreased. When the sedimentation rate is over 500 m/Ma, whichever other factors change in parameter space, there is no green or purple region in graphic and the interaction between the CLS importance will be always less than 10% of the LT effect.

From Figure 4-27, it can be seen that parameter space has been divided according to the importance of the CLS relationship. Interaction between two channels will be very small when the sedimentation rate is higher than 500m/Ma. This is because each channel's effect on overpressure is smaller compared with at a lower sedimentation rate. Fluid flow capacity relative to each other will also reduce.

When the over-burden rock sedimentation rate is less than 500m/Ma, 2 the channels satisfy the condition that the position is near the aquifer (near 2 Ma deposited after

aquifer, value in “d” is 0.1), regions just touch, or vertical distance is small (less than 0.4 in value) and overlapping area is large (“dangerous region”), fluid and pressure Interaction between them becomes a necessary factor to consider, the two CLSs’ overall impact on overpressure can be upscaled into a single equivalent, and the function form is:

$$F(Yi) = f(Xi) + m1g(z1) + m2g(z2) = f(Xi) + gg(zi) + \varepsilon(Yi) \qquad 4\text{-}12$$

in which “ε(Yi)” means difference between the two channel-levee systems’ overall effect (m1g(z1) + m2g(z2)) on overpressure distribution and the fitting function for each CLS effect.

In other conditions and parameter space where channel-levee systems are far from aquifer (larger than 3 Ma deposited after aquifer), do not collapse together, and vertical relative distance is large (bigger than 0.4 from the models results), the two CLS overall impact on overpressure distribution can then be expressed as a decomposition of two single CLS’s effects:

$$F(Yi) = f(Xi) + \Sigma g(zi) + \varepsilon(Yi) \qquad 4\text{-}13$$

in which “ε(Yi)” means the difference between two channel-levee systems’ overall effect and two single CLS’s effects overlaid. The value should less than 10% of LT effect (f(Xi)).

A fitting method needs to be considered for finding universal “m1” and “m2” which could make gg(zi) always approximates with the two channel-levee systems’ overall impact on overpressure at the aquifer crest (G(Zi)).

4.4.2.3 Prediction upscaling the influence of the two channel-levees

The impact of the two factors (effect of each CLS) cannot directly determine their linear relationships, and not all combinations are reasonable in this study, because it only considers cases where the relative distance of two CLSs is small, which can result in a high interaction with overpressure at the aquifer crest. Cases in which the relative distance of two CLSs is large, and the interaction between them is small are not considered in this study. So D-optimal design will also be used in this study to determine relationships between the overall effect on overpressure value from two CLSs and the effect of each of the two CLSs. After defining two influencing parameters (h(z1)

and h(z2)) from the design variables, the next step is to build the response surface of overpressure on 2 parameters using D-optimal design of the Design Expert software. As the default, the quadratic model was chosen. D-optimal design required 16 cases, based on 2 factors. According to the previous assumptions and parameter space as defined, 133 models in the range have been previously simulated. This number is also totally sufficient for a quadratic model as it needs 16 cases, and even for the quartic model which needs 25 cases only. I used all of the 133 results as the inputs to D-optimal design, to get a more accurate model determination and response surface results. The results of 108 models were obtained using PetroMod and listed in Appendix D.

Table 16 shows the cubic model suggested by D-optimal design, which suggested it to be the appropriate model. The values of "Prob>F" less than 0.05 indicate the model terms are significant. It is required to select the highest order polynomial where the additional terms are significant and the model is not aliased. In addition, the model must have an insignificant lack of fit, and maximum "Adjusted R-Squared and Predicted R-Squared". Therefore, the cubic model was suggested to fit the overpressure value Response Surface, as shown in Table 16.

Table 16 Fitting summary results of Response Surface.

Summary (detailed tables shown below)

Source	Sequential p-value	Lack of Fit p-value	Adjusted R-Squared	Predicted R-Squared	
Linear	< 0.0001		0.5612	0.5204	
2FI	< 0.0001		0.7631	0.7518	
Quadratic	0.0628		0.7741	0.7596	
Cubic	0.0208		0.7968	0.7748	Suggested
Quartic	0.6012		0.7929	0.7191	
Fifth	0.5075		0.7908	0.6679	
Sixth	0.8802		0.7759	-13.2969	

Sequential Model Sum of Squares [Type I]

Source	Sum of Squares	df	Mean Square	F Value	p-value Prob > F	
Mean vs Total	1603.47	1	1603.47			
Linear vs Mear	36.99	2	18.50	52.16	< 0.0001	
2FI vs Linear	12.91	1	12.91	67.46	< 0.0001	
Quadratic vs 2	1.05	2	0.52	2.87	0.0628	
Cubic vs Quad	2.03	4	0.51	3.10	0.0208	Suggested
Quartic vs Cub	0.61	5	0.12	0.73	0.6012	
Fifth vs Quartic	0.90	6	0.15	0.89	0.5075	
Sixth vs Fifth	0.54	7	0.078	0.43	0.8802	
Residual	9.60	53	0.18			
Total	1668.12	81	20.59			

Model Summary Statistics

Source	Std. Dev.	R-Squared	Adjusted R-Squared	Predicted R-Squared	PRESS	
Linear	0.60	0.5722	0.5612	0.5204	31.00	
2FI	0.44	0.7720	0.7631	0.7518	16.04	
Quadratic	0.43	0.7882	0.7741	0.7596	15.54	
Cubic	0.41	0.8197	0.7968	0.7748	14.56	Suggested
Quartic	0.41	0.8291	0.7929	0.7191	18.16	
Fifth	0.41	0.8431	0.7908	0.6679	21.47	
Sixth	0.43	0.8515	0.7759	-13.2969	924.25	

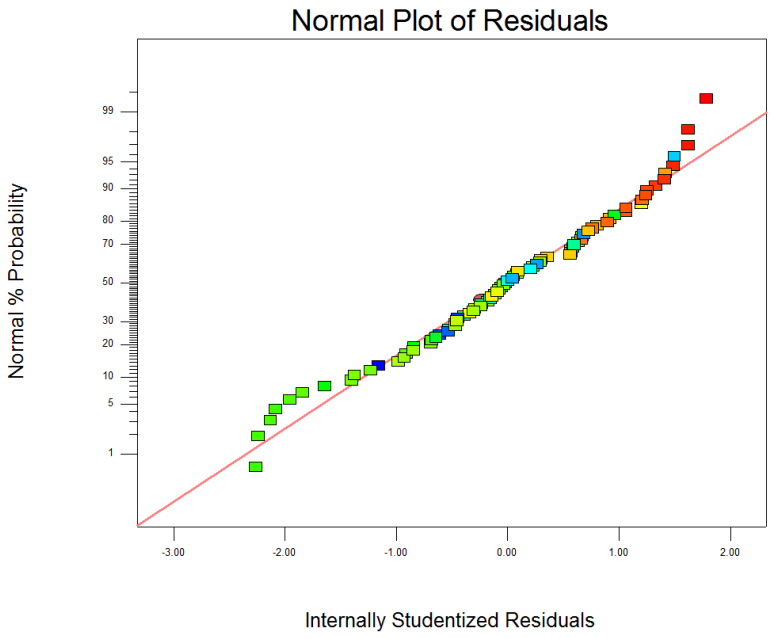

Figure 4-28 Residuals Normal Plot

As can be seen from Figure 4-28, the overpressure response surface provides reliable predicted values of overpressure compared with the actual value of the overpressure. From Figure 4-28, the fitting result is ideal, and error is in an acceptable range. The details and reasons for that will be analysed in Chapter 5. The final equation is showed in the equation below, which contains linear relationship and interaction of each influencing factor.

Final Equation in Terms of Actual Factors:

$$
\begin{aligned}
f(x)\text{-}F(Y) \;=\; & \\
& +3.24192 \\
& -2.69666 \;* h(z1) \\
& -0.14678 \;* h(z2) \\
& +2.53783 \;* h(z1) * h(z2) \\
& +1.70680 \;* h(z1)^2 \\
& -0.34120 \;* h(z2)^2 \\
& -0.72679 \;* h(z1)^2 * h(z2) \\
& -0.14617 \;* h(z1) * h(z2)^2 \\
& -0.21061 \;* h(z1)^3 \\
& +0.14782 \;* h(z2)^3
\end{aligned}
$$

In this equation: h(z1) h(z2) is a single CLS's effect on overpressure in a 2 CLS cluster

As can be seen in the equation, the cubic model includes third order polynomial terms. It also captures the three-factor interaction effect. Therefore, this model can provide a good fit for the true overpressure response surface from the Design Expert report. The values of overpressure generated from the model were compared with the actual values from the simulation, as presented in the D-optimal final report. This showed that the percentage difference between both overpressure values is in the acceptable range. In the next step, the models were verified by rerunning some optimized cases in PetroMod and calculating overpressure. The model details and analysis results will be presented in Chapter 5.

4.4.3 Interaction analysis of a three-channel cluster

In the previous study, the deposit basin had multiple channel-levee systems and up to two CLSs forming a cluster (the interaction between them cannot be ignored) for which the effect on overpressure at the aquifer crest has been proved. In real cases, clusters of CLSs with more than two CLSs can also be seen. The case of three CLSs which are connected to each other or have a high degree of fluid interaction between them is present in reality and the overall impact of the cluster on overpressure needs to be considered.

In this section, modelling of a cluster of 3 CLSs at possible configurations will be considered, with the purpose of showing that for every configuration there is an upscaling scheme to reduce CLSs by forming a super-CLS 'iteratively'. Here an interest is to see if all cases of an upscaling scheme share a common feature or not. If so, a generic method and workflow can then be applied to calculate effect of a cluster with 3 CLSs. Figure 4-29 shows, a model configuration with three CLSs collapsing together. The positions of CLSs are located near the aquifer crest because they could have the biggest effect on the overpressure. In the configuration model, CLS a and CLS b have a significant and unneglectable relationship, but according to results in section 4.x.x, despite the fact that they are connected together, the importance of the interaction between CLSs a and c and b and c is small, and could be ignored in these cases.

To investigate fluid flow directions and features in evolution of a basin which has three channel-levee systems clustered, a group of models with different numbers of CLSs from one to three was created Figure 4-29. In the model, over-burden sedimentation rate is 100 m/Ma, clay content is 0.1, aquifer depth and relief are 2000 meters. The size of CLSs is 0.1, which is the largest size in these conditions as previously defined (setting

limits and according to the literature review), and their positions are near the aquifer crest, for the same reasons as before (two CLSs are collapses). One channel was deposited into the basin, for which depositional time was 2 Ma after the aquifer formation, and overpressure values in the channel and aquifer crest are 5.64 MPa and 9.39 MPa, respectively. (Figure 4-29 a) Once the second channel was deposited, the first channel just collapsed in the vertical direction, and overpressure value in the channel is reduced from 5.64 MPa to 1.32 MPa, because fluid flowed from CLSs 1 to 2 for balance. Overpressure at the aquifer crest is 7.23 MPa, the overall impact of channel 1&2 (4.96 MPa) is greater than two single CLS effects' decomposition (3.82 MPa). When the other CLS collapses with the original channel, fluid in the base channel will flow into "channel 2" to equilibrate the overpressure in both. Thus, the overpressure in the cluster is now lower than before (only "channel 1" effect), and more fluid was allowed to flow into the cluster from the surrounding mudstone and aquifer, which was because of the CLS interaction effect. When the third channel was deposited which collapses the cluster and forms a new 3 CLS cluster, overpressure value on aquifer crest is 6.46 MPa, where the single effect of "channel 3" (g(z3)) is 0.62 MPa, which is smaller than the single effects of "channel 1" (2.8 MPa) and "channel 2" (1.02 MPa), respectively, because of the position. The overall impact of the cluster is 5.73 MPa, which shows little difference with effects of "channel 1&2" and "channel 3" (5.58 MPa). When "channel 3" is deposited into the system, the fluid in "channel 1&2" and the aquifer will also flow into "channel 3", for pressure balance and the interaction effect. But because the effect of "channel 3" is small, the fluid interaction effect between "channel 3" and other channels is also smaller, and compared with the LT effect; it can thus be ignored in this case. As fluid in the aquifer crest is already close to balance due to the channel 1&2 effect, less fluid will flow into the cluster when "channel 3" exists. The two reasons for the overall effect of three CLSs on overpressure can be expressed by the effect of two of them and decomposition of the effect of the other one.

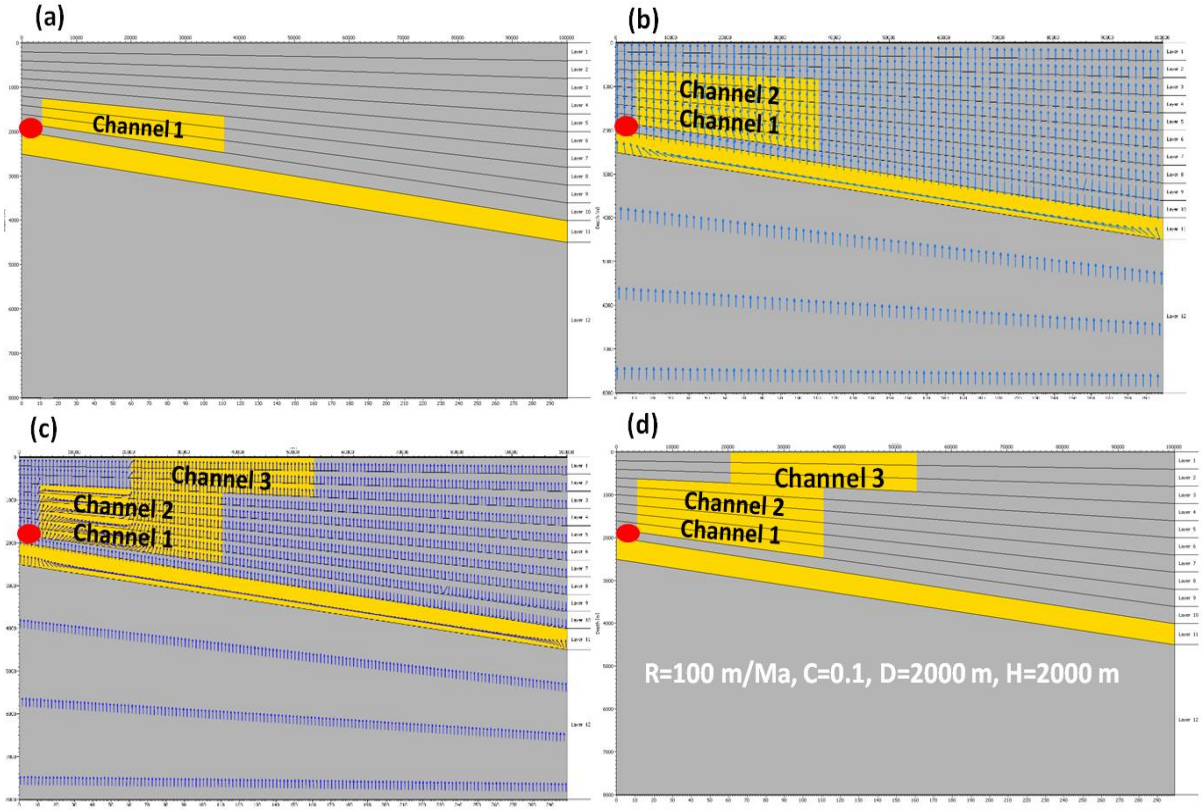

Figure 4-29 Model configuration of a group of models which have different CLS numbers from one to three. a) channel 1: deposited 2 Ma after aquifer, and effect of channel 1 is 2.8 MPa. b) when channel 2 is deposited, which collapses channel 1, fluid will balance in both channel, and a cluster is formed. More fluid in the aquifer will flow into the cluster for pressure balance, because of interaction of two CLS. C) when third channel is deposited which collapses the cluster, fluid will also flow from aquifer and cluster into channel 3 for pressure balance, but channel 3 has a small effect on overpressure on aquifer crest, so the interaction effect between channel 3 and other channels is also small, and fluid in aquifer crest is close to a balance from channel 1&2 effects, so less fluid will flow into the cluster when channel 3 exists. D) Possible and basic configuration of 3 channel-levee systems cluster: the 3 channels collapse together and fluid is in balance in the cluster. In this case, channel 1 just touches channel 2 and they have big vertical collapse area, channel 1 and channel 2 could be upscaled to one channel effect, according to previous results. However channel 1&3 and 2&3 have little interaction, which is considered separately, so group of models was created with 3 channel cluster for viewing interaction between the 3 channels and overall impact on overpressure.

Thus, in the condition of a cluster with 3 contact CLSs, the assumption is the three CLSs overall impact on overpressure could be expressed as the upscaled effect two of them and the other single effect as an overlay:

$$F(Yi) = f(Xi) + gg(z1\&z2) + g(z3) \qquad 4\text{-}14$$

In order to confirm this hypothesis preliminarily, a group of simulations which have clusters of three collapsed channels were created; they were all located around the basic

channel and collapsed together. The results were divided to two parts the first one showing the interaction importance between the three CLSs: importance of the difference between the cluster's overall impact and three single CLSs' effects as an overlay (G(Zi)-Σg(zi))/f(Xi). The other one is the interaction of the importance of two upscaled CLSs and the importance of the difference between the cluster overall impact and the two CLSs' overall impact, which is overlaid with the other single effect (G(Zi)-gg(z1&z2) - g(z3))/f(Xi). The two CLSs which could be considered together need to satisfy these conditions: they should be nearest to the sand layer and to each other. The setting details and results are shown in Figure 4-30, these combinations are all reflected on basin modelling setting. From the results, the overall impact of the three channel-levee systems on overpressure in all 5 cases could not be expressed as a decomposition of three single CLS's effect. However, the overall impact of the 3 CLSs has little difference from the results of 2 CLSs upscaled and the other single effect overlay (G(Zi)-(gg(z1&2)+g(z3))/f(Xi) < 0.1), in the previous study; if the error value is less than 10 percent of the LT effect, we regard this as an ideal result. So in these cases, the three-CLS cluster effect on overpressure could be expressed by upscaled results for 2 of them and the other one's effect as an overlay. That means the cluster in the yellow circle has little fluid interaction with the other channel, and the overall impact on overpressure at the aquifer crest could be seen as the decomposition of the effect of the two parts.

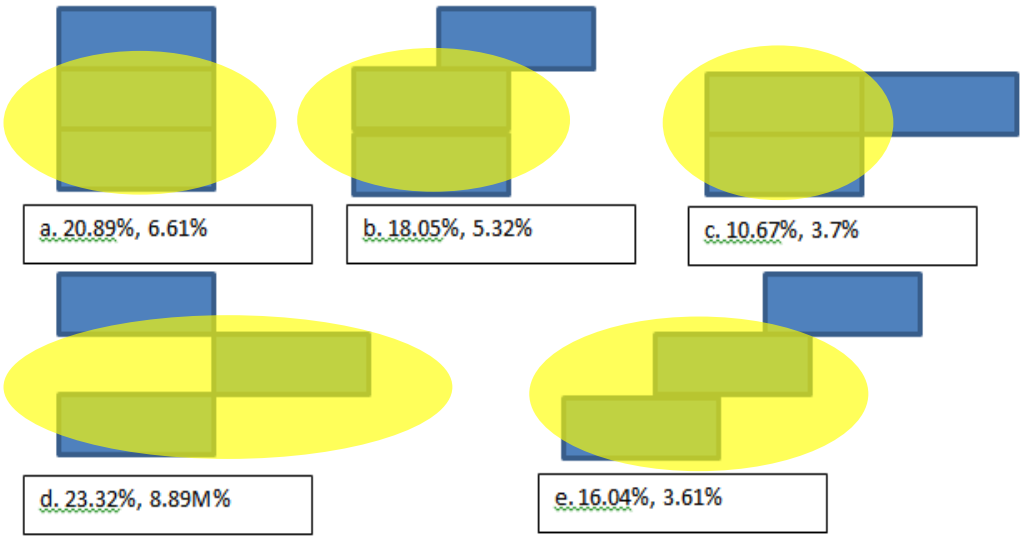

Figure 4-30 Five cases of three channel cluster combinations: the graphic just describes the combinations of the channels, and they were all adopted in numerical setting and overpressure output obtained. In each case, the first number is the importance of difference between G(Zi) and $\sum \mathbf{g(zi)}$ on the LT effect (f(Xi)). The difference is between the three single CLS effects' decomposition and the cluster's overall impact on

overpressure obtained from the output. The second value is is the importance of difference between G(Zi) and "$\mathbf{gg(z1, z2) + g(z3)}$" on the LT effect (f(Xi)), in which the difference between cluster's overall impact on overpressure obtained from output and two of them (in yellow circle) have upscaled impact and the other single CLS effect as overlay. From the results, the second values are much less than the first value; the cluster's overall impact cannot be described by three single CLS overlays , but may expressed by the upscaled impact of two of them and decomposition of the other single CLS's effect.

In Figure 4-30, the first number means the difference in importance of the influence on the LT effect between 3 CLSs' single effect decomposition and their overall effect: 100% * ((G(Zi)-Σg (zi))/f(Xi)). The second number means the difference in importance regarding the LT effect between 2 CLSs' (in yellow circle) upscaled effect and the other CLS single effect's decomposition and their overall effect: 100% * (G(Zi)-(g (z1&2) + g(z3)) /f(Xi)). From the results, the second values in all the five cases are less than 10 percent of the LT effect. This result means the interaction between two CLS upscaled clusters and the other one could be ignored in these cases, and the three CLS overall effects on overpressure at the aquifer crest could be expressed as the effect two of them and the decomposition of the effect of the other single CLS. The results further confirm the hypothesis. The parameter of the two channels which could be upscaled for calculating the overall impact should satisfy these conditions: (1) interaction between them could not be ignored; (2) Position nearest aquifer crest of the three; (3) Position nearest each other out of the three.

The purpose now is to further prove the hypothesis and carry out a systematic analysis of the overall impact of the 3 CLS cluster. To do this a group of simulations which tries to show every configuration of the three CLS cluster was created to view the expression of their overall impact on overpressure. In these cases, I set the three channels in square (Figure 4-31 a) which was near the aquifer; LT effect parameters (R, C, D, H) are the same as previously. This is because this group of models have the biggest fluid interaction of all parameters combination with CLSs in the position, if there is not obvious fluid interaction between the CLSs by this position and parameters combination, it should not obvious in others position and parameters combinations. Then one or two CLS are set in a transitional position (Figure 4-31 b) of the square in the condition of contact together to better simulate the combination of the 3 CLSs. (If the results share common features with the three CLS in the transition location and extreme positions in square, the results of CLSs are in other positions of the square should have the same

features). 44 cases were simulated in this section for viewing overall impact on overpressure expression; the parameter detail and results are shown in Appendix E.

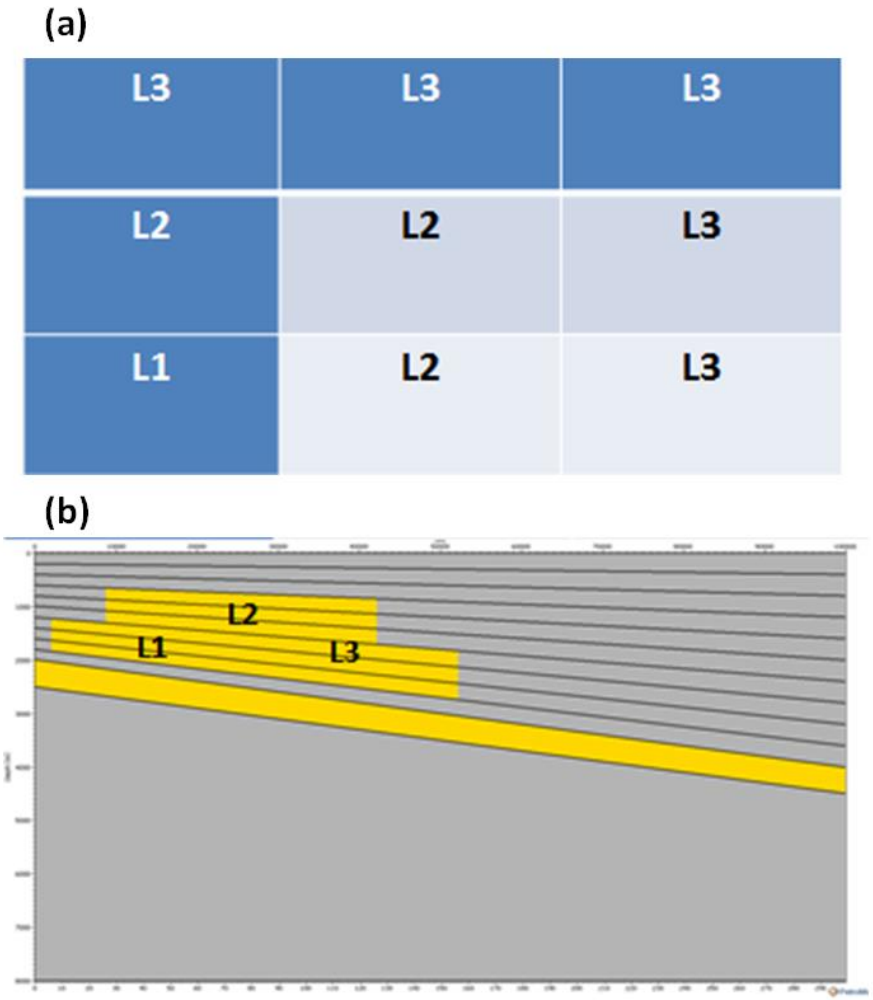

Figure 4-31 a) modelling setting details for three channels distributed in a square located near the aquifer crest where the position could make the greatest effect of all parameter space on overpressure, "L1~3" means each channel's position, which tries to describe every combination in the square. b) Transition position based on the square setting; if the channels are located at the extreme and transition positions and they all have small interaction which could be ignored, they will also have small interaction in other combinations. The setting is helping to expand simulation cases for trying to describe every possible combination effect, the number of cases in the two groups is 44.

After analysis, all of the 44 cases showed the same feature, which was that the 3 CLS cluster's overall impact on overpressure could be expressed as the upscaled impact of two of them and the decomposition of the impact of the other one. The hypothesis was proved correct and the simulation results showed the same features as predicted in the hypothesis and found in the previous cases:

$$F(Yi) = f(Xi) + g(z1\&2) + g(z3) + \varepsilon(Y) \left(which\ less\ than\ 10\%\ of\ LT\ effect\ f(Xi)\right) \quad 4\text{-}15$$

After analysis, the interaction between the upscaled effect of the two CLSs and the other single CLS effect is small, which can be ignored, and the interaction will be smaller in other positions in parameter space. So when 3 channels collapse together, the overall effects could be expressed as the resulting effect of the combination of one channel and its closest channel plus the third channel's effect, and the difference from the 3 CLS's overall effect will be less than 10 percent of the LT effect, f(Xi). The two CLSs which could be upscaled in this study should satisfy the conditions that the interaction between them could not be ignored; their position should nearest to the aquifer crest and nearest to each other of the three.

In summary, in this section, the impact of CLSs on overpressure at the aquifer crest has been studied, in a deposited basin which has multiple channel-levee systems where up to three channels are collapsed together. This impact can be expressed by upscaling the impact of two of them and decomposing the impact of the other one. This may be because the effect of "channel 3" is small on the overpressure of the aquifer crest, and the fluid interaction effect between "channel 3" and others channels is also smaller, compared with the LT effect, so it can be ignored. The fluid in the aquifer crest is close to balance when only the effect of channel 1&2 (which could be upscaled)exists, which means that less fluid will flow into the cluster when "channel 3" exists. The two CLS which could be upscaled from previous results should satisfy the following conditions:

(1) Interaction between them cannot be ignored;

(2) Position is nearest the aquifer crest, out of the three;

(3) Position is nearest each other, out of the three.

In geological reality, the cases where more than three channel-levee systems collapse together are not very common. In the next step, the impact of a cluster of more than three channels will be analyzed to provide a general method to express the overall impact.

4.4.4 General analysis method for other cases (basin has four or more channels in cluster)

The effect of CLSs on overpressure in cases where a basin has two or three channels in a cluster has been studied in the previous sections. Interaction between CLSs is an important factor which needs to be considered in cases of two or three channel clusters. In geological deposits, conditions where a basin has three or more channel-levee

systems which collapse together are very not common, furthermore cases of two channels connected together are still in the minority. In most of cases of well-known deposited basins, channel-levee systems are scattered and have little interaction, which can be ignored according previous studies. For example this is the pattern found in the Gulf of Mexico, West Africa, the Indus basin and Malaysia. (Figure 4-32)

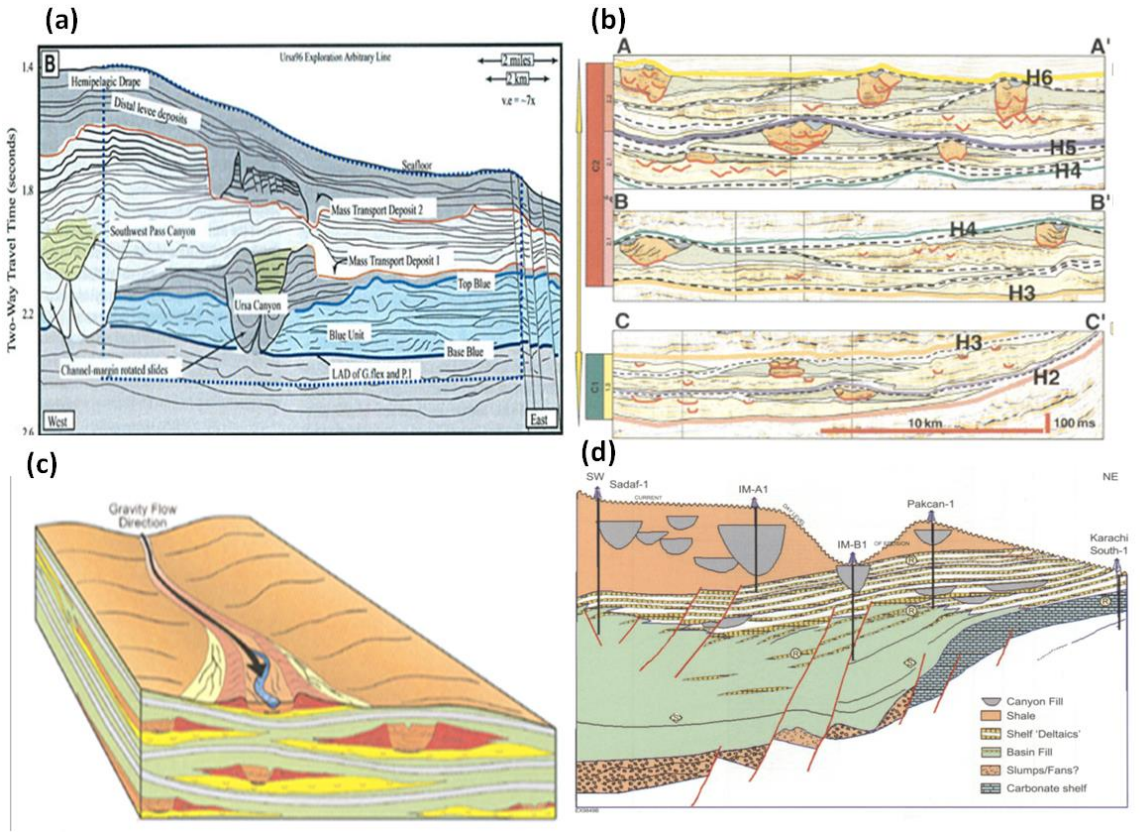

Figure 4-32 a) Geology of two canyons in the Gulf of Mexico, the two canyons are not touched together, but the relative distance between them is not very big. b) and c) channel geology of the West African basin: there are multiple channels distributed in the basin, and they are not collapsed together. d) stratigraphic geology of the Indus basin: multiple channels can be found above on a of shelf sand (yellow), which have three channels and two channels clustering which jointly impact overpressure distribution. [87] [20] [19]

For better research integrity, a general analysis about the effect of a cluster of more than three CLSs on overpressure needed to be considered, and thus a group of models which has four or more CLSs in a cluster were created for detecting fluid interaction between them and their effect on overpressure at the aquifer crest was calculated. The models' configurations have same Lateral Transfer effect factors as previous basic models, and have four and five CLS clusters which collapse together near the aquifer crest (Figure 4-33).In the previous study of three collapsed CLSs, the third CLS has little fluid interaction with the other pair of CLSs because of the small single CLS effect, and

because fluid in the aquifer crest is already close to balance when the two CLS (which could be upscaled) affect it, less fluid will flow into the cluster when the third channel is deposited. Then if one or more further CLSs are deposited on this configuration basis, the interaction between new CLS and the previous cluster should also small, as the fluid condition around the aquifer crest will be same as the explained for the previous situation.

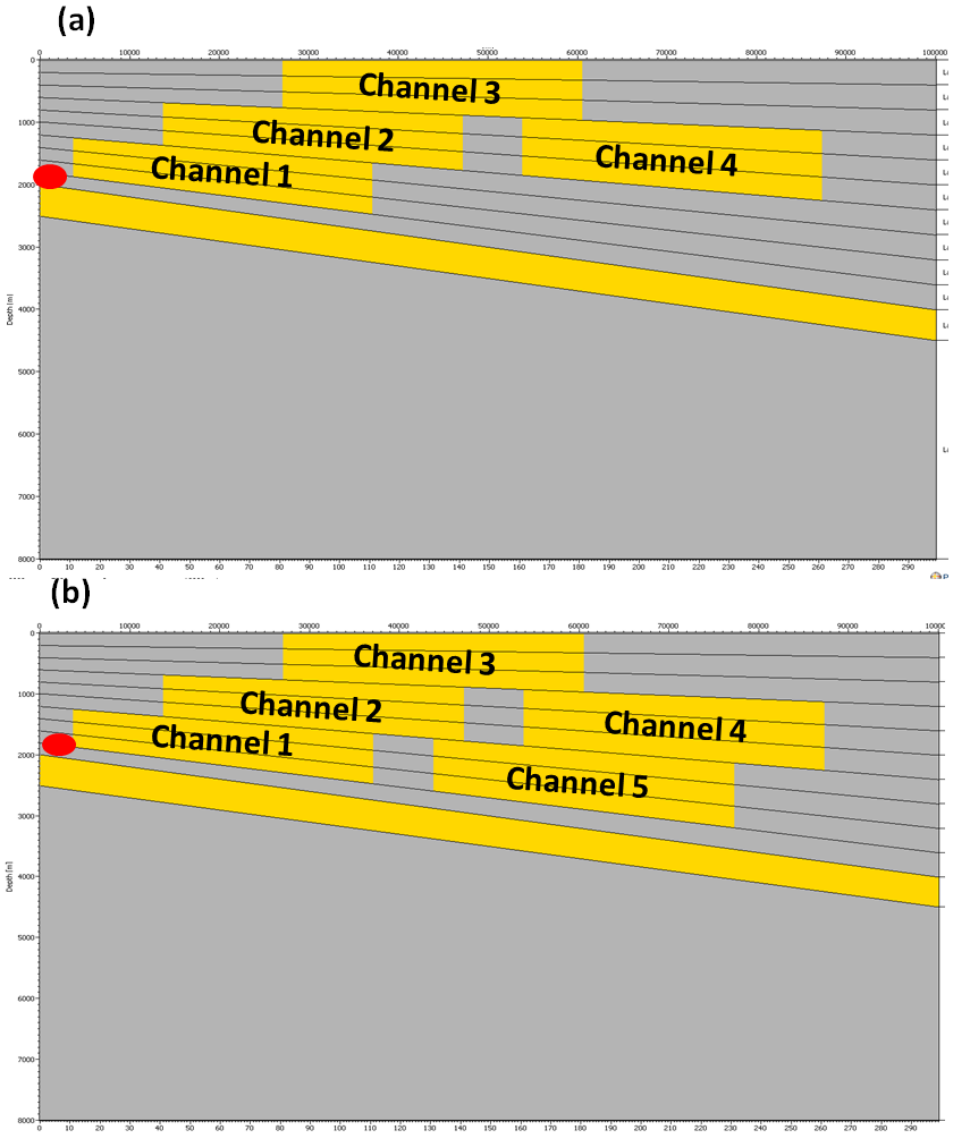

Figure 4-33 Model configuration has 4 Channel-levee systems clustered, in which the channels are located near the aquifer crest because this position could make the largest effect on overpressure in parameter space, and the interaction values also are largest. Channels 1~4 are collapsed together, the overall impact on overpressure is 5.82 MPa, which is nearly the same as the results of first two channels upscaled effect and decomposition of the single effects of the other two. b) The other model configuration has a 5 channel-levee system cluster, in which channel 5 has dcollapse with channel 4 and channel 2, to form a cluster with the other channels. Despite channel 5 having a bigger effect than channels 3 and 4, according to the fluid features and reason given in previous cases, the overall impact on overpressure (6.82 MPa) is also nearly the same as

the results of first two channels upscaled effect and decomposition of the other three's single effect (6.68 MPa).

In Figure 4-33 a, four channels which have collapsed together are near the aquifer crest. When channels 1&2 are deposited, the effect on overpressure is 4.75 MPa (gg(z1&z2)), after channel 3 is deposited, it have little interaction with channel 1&2, and the effect of the triple cluster (1&2&3) is the effect of channel 1&2 with the addition of the single effect of channel 3: the value is 5.35 MPa which shows only a small difference from the overall impact of the 3 CLSs: 5.82 MPa. If channel 4 joins this system, fluid will flow together in the cluster for balance. Channel 4 has a small effect on overpressure at the aquifer crest and small interaction with the other channels. According to the reason given in the previous study (where 3 channels have collapsed together), the overall impact of the 4 channels (5.82 MPa) should be expressed as the first two channels' upscaled effect and decomposition of single effect of the other two the result after calculation is 5.66 MPa, which has a 0.16 MPa difference from overall impact of the 4 CLS cluster, which just stand at 1.3% of the overall LT effect. In Figure 4-33 b, five channel-levee systems which have collapsed together are near the aquifer crest. According to the hypotheses and previous conclusion, as channel 5 has little fluid interaction with the first 4 channels, their effect on overpressure at the aquifer crest (6.82 MPa) could be expressed as first 4 channels' overall impact (5.66 MPa) and decomposition of channel 5's single effect (1.02 MPa), the value after calculation is 6.68 MPa, which is only 0.14 MPa lower than the 5 channels' overall impact, which just stands at 1.1% of the LT effect. From the results, a general conclusion regarding the overpressure effect of clusters of more than three CLS can be defined thus: if a basin has more than three CLS in a cluster, the overall impact on overpressure could be expressed as upscaled impact of two of the CLS and decomposition of the single effect of the others CLSs:

$$F(Yi) = f(Xi) + \Sigma gg(z1\&2),\ g(zi) + \varepsilon(Y) \qquad 4\text{-}16$$

in which the value of ε(Y) should be less than 10 percent of the LT effect (f(Xi)), and "i" cannot include"1" and "2".

In other words, if a basin has more than two channel-levee systems in a cluster, the fluid interaction of the first two CLS, which can be upscaled, should be considered, and interaction of the other CLSs with these are small compared with the LT effect, and can

be ignored. The cluster's overall impact on overpressure can be expressed as upscaled effect two CLS of them that and decomposition of the single effect of the other CLSs. The two CLSs which could be upscaled should satisfy these conditions:

(1) Interaction between them cannot be ignored;

(2) Position is nearest to the aquifer crest of all CLSs of the cluster;

(3) Position is nearest to each other of all CLSs of the cluster.

In this section, more cases which have four or more CLS clusters were created and showed the same features as those in the previous studies. The results and details will be shown in the later chapter of data analysis. In well-known basins around the world, deposited basins which has two or more channel-levee systems collapsed together are not common, and over 75% of simulations in the study showed that interaction between CLS could be ignored (relative distances are scattered). So in most of the cases overall effect on overpressure could be expressed as a CLS single effect simple superposition. If special cases are encountered that have two or more channel collapsed together, the cluster's overall impact on overpressure could be expressed as: upscaled effect of two CLS of the cluster and decomposition of other CLSs of the cluster's single effect. The results confirm the importance of fluid interaction between geological Genetic Units and also the authenticity of the hypothesis. In the next chapter, the data analysis of the results of simulation and Response Surface regression will be undertaken.

4.5 Summary

In this chapter, higher-perm GUs were introduced into the reference case that was examined in Chapter 3, to consider their interaction and role on overpressure character in the system. Channel-levee systems were considered to be the type of GU, since they are spatially delimited in both thickness and width terms, and thus act like "point" anomalies instead of layers. The thickness and width of CLS was considered as integrated nature – size in this study. And with CLS's depth and location, the CLSs like many anomalies points in spatial space, and each point have their coordinate values – s, L, d, according define their significance and value to use the functions after response surface can predict their fluid interaction effect on overpressure in specific simulation cases. The idea could much reduce analysis complexity and support thinking on research GUs fluid interaction in such cases. It is not examined and detail summarized

here, but the expectation is that other GU types could be examined in a similar way, since they would mostly be of simpler geometric characteristics.

Firstly, it was demonstrated that a single CLS can be accommodated via the predictive approach developed in Chapter 3. Then the situation was examined where multiple CLs exist, and their interactions in the flow + compaction process were considered, and these were divided into two situations on the basis of their spatial relationship: scattered or close. For each situation the aim was to predict overpressure at the chosen reference point via the approach developed. The results showed high accuracy in prediction of the overpressure at the chosen reference point, which means the understanding of the interaction and effects on overpressure character of multiple GUs in the overburden is successful in this reference case. Moreover, the approach and process created a novel workflow which could be extended to other reference cases to consider the effects of their GU interaction on overpressure character. The details of the results and conclusions are shown as follows:

1. Channel-levee systems could influence fluid migration from the aquifer crest to CLs and reduce overpressure on a dipping aquifer crest in the basin process. The degree of influence is only an additional part of the basic LT process(less than 30% of LT).
2. The area of a CLS needs to be first considered, if it accounts for a small proportion (less than 0.1) of the over-burden sediments, the interaction between the aquifer and the CLSs or clusters can be ignored in affecting overpressure distribution.
3. T are seven important controlling factors of single CLSs relative to their effect on overpressure distribution, which are over-burden sedimentation rate, over-burden mud clay-content, aquifer relief, CLS location and CLS depth, which inversely impacts the CLSs' influence, and also aquifer depth, and the area of the CLS, which could proportionally impact the CLS's influence.
4. In a sedimentary basin which has a dipping aquifer and single CLS deposition, if the aquifer over-burden mud sedimentation rate is greater than 1000 m/Ma, clay content is greater than 0.1, sedimentation rate is over800 m/Ma, clay content is over 0.3, and sedimentation rate is over 500 m/Ma, clay content is over 0.5, then interaction between CLSs and the aquifer can be ignored, because in these conditions the CLSs have not any obvious influence on overpressure at the aquifer crest. If the sedimentation rate is less than 1000 m/Ma, clay content is

0.1, sedimentation rate is less than 800 m/Ma, clay content is less than 0.3, or sedimentation rate is less than 500 m/Ma, clay content is less than 0.5, interaction between CLSs and the aquifer need to be considered, because in these conditions the CLSs can obviously influence overpressure at the aquifer crest. The degree of influence can be calculated by the equation given in section 4.4.

5. When a basin has two or more CLSs deposited, the interaction between them which could influence overpressure in aquifer crest needs to be considered the importance of this interaction between CLSs is mainly influenced by their spatial arrangement. When the positions of each of them are scattered or far in the vertical direction, the fluid interaction between them is not obvious and can be ignored in terms of its influence on overpressure behaviour, and the CLSs' overall interaction on overpressure can be seen as a decomposition each one's single influence on overpressure (calculated by the equation in section 4.6).
6. When a basin has two or more CLs deposited, and at least two of them form a cluster (collapsed with each other, or vertical distance is small, close to aquifer and has overlapping area in vertical), the cluster can be seen as a whole, and overall interaction within such a cluster relative to prediction of overpressure at the aquifer crest could be expressed as its influence after upscaling (calculated by the weight function given in section 4.4.5) which follow conditions about being closest to each other, closest to the aquifer and having an overlapping area in vertical distance in the cluster; then the single influence of the other CLSs is added (calculated by the equation in section 4.4) to predicting overpressure in the aquifer crest. The interaction between the other CLSs in such a cluster relative to predicting overpressure in the aquifer crest can be ignored.

Chapter 5. RESPONSE SURFACE RESULTS ANALYSIS AND ERROR EVALUATION

5.1 Introduction

In this chapter, the function of overpressure prediction on the chosen reference point which includes experience and the results from the simplified parameters will be focused. The accuracy of the findings regarding the interaction between CLSs and the aquifer, and between each CL and the others will be demonstrated by examples. There is further explanation of how the complex heterogeneity of the CLSs' spatial arrangement could be simplified relative to overpressure prediction and in which conditions.. The chapter will also summarize the work flow which could be extended to other fields and reference cases to develop understanding of the role of GUs to help to simplify their heterogeneity.

The results of every response surface will be used to analyse each simulation step by step, to test the accuracy of the previous conclusions. The error analysis in each part will also be examined and additional test examples will be used to illustrate to what extent overpressure can be predicted by these results and the workflow. Section 5.1, focuses on the results of the response surface regarding the relationship between overpressure and five influencing factors in Lateral Transfer cases. In this section, all the simulations in the response surface process and 80 additional cases are used to verify the accuracy of the results and error analysis. In section 5.2, the response surface results for the function describing the channel-levee systems' effect (h(z)) is brought into the function for calculating overpressure value and the relative error analysed compared with the LT effect, then used together with LT effect (f(x)) into the function which predicting overpressure on chosen reference point for analysing and evaluating the total error in all cases where only one channel exists. In section 5.3, the response surface results of the two channels upscale (hh(z)) is examined and analysis of the relative error compared with LT effect is analysed in cases which have 2 collapsed channels, then used together with the LT effect (f(x)) into the function which predicting overpressure on chosen reference point for analysing and evaluating the total error in all cases which have two collapsed channels. Section 5.4, present a summary of the workflow for developing GU interaction relative to predicting overpressure on the aquifer crest. A workflow summary is given for an application where a real case has multiple CLS deposition, to investigate in which conditions the CLS complexity could

be simplified in terms of spatial heterogeneity, and how. The target functions relative to predicting overpressure at the aquifer crest are developed by simplifying the parameters and the GUs interaction results, which also prove the accuracy of the representation of GU interaction. In addition, more random simulation cases are presented with different conditions for testing. In the examples examined it is found that this workflow results in exact predictions. .

5.2 Results and error analysis in test-bed Lateral Transfer Model

In Chapter Three regarding the calculation of the overpressure distribution at the aquifer crest, five main influencing factors were considered and they are: reference point over-burden sedimentation rate (R), mudstone clay content (C), reference point depth (D), aquifer relief (H) and bending (A). A function for the relationship between overpressure value at the reference point and the influencing factors was expressed notionally as:

$$F(Y) = f(R, C, D, H, A) + \varepsilon(f) \qquad 5\text{-}1$$

ε(f) is an error term the difference between the predicted value from the response surface, f(X), and the value from a simulation case F(Y). The calculation of f(X) has been detailed in Section 3.5. The error analysis and assessment will be shown in this part by analysis of previous simulation modelling data and data from additional simulations which not appeared in response surface methodology.

Figure 5-1 shows f(X) constructed from response surface methodology. It is clear that most of the points (the points are simulation data used in response surface) can be well fitted to the function and the relative error appears to be in the acceptable range (Figure 5.2).

Overpressure =

-11.66753

+2.05271E-003 * Relief

-3.39398 * Aquifer Bending

+6.37681E-003 * Depositional Rate

+12.08524 * Clay content

+9.76759E-003 * Aquifer Depth

-8.05017E-004 * Relief * Aquifer Bending

-2.34950E-007 * Relief * Depositional Rate

-2.01278E-003 * Relief * Clay content

+6.27000E-008 * Relief * Aquifer Depth

+4.43886E-004 * Aquifer Bending * Depositional Rate

+5.67589 * Aquifer Bending * Clay content

-4.05000E-005 * Aquifer Bending * Aquifer Depth

-0.012263 * Depositional Rate * Clay content

+7.82561E-007 * Depositional Rate * Aquifer Depth

-5.69933E-003 * Clay content * Aquifer Depth

Figure 5-1 Function representing relationship between five influence factors and overpressure value on aquifer crest. The function is a linear equation, which was adopted rather than a square or cube, because it could ensure the accuracy and guarantee the applicability. Each part of the equation has a regression coefficient which was worked out from the response surface methodology, and single arguments or a product of two of them.

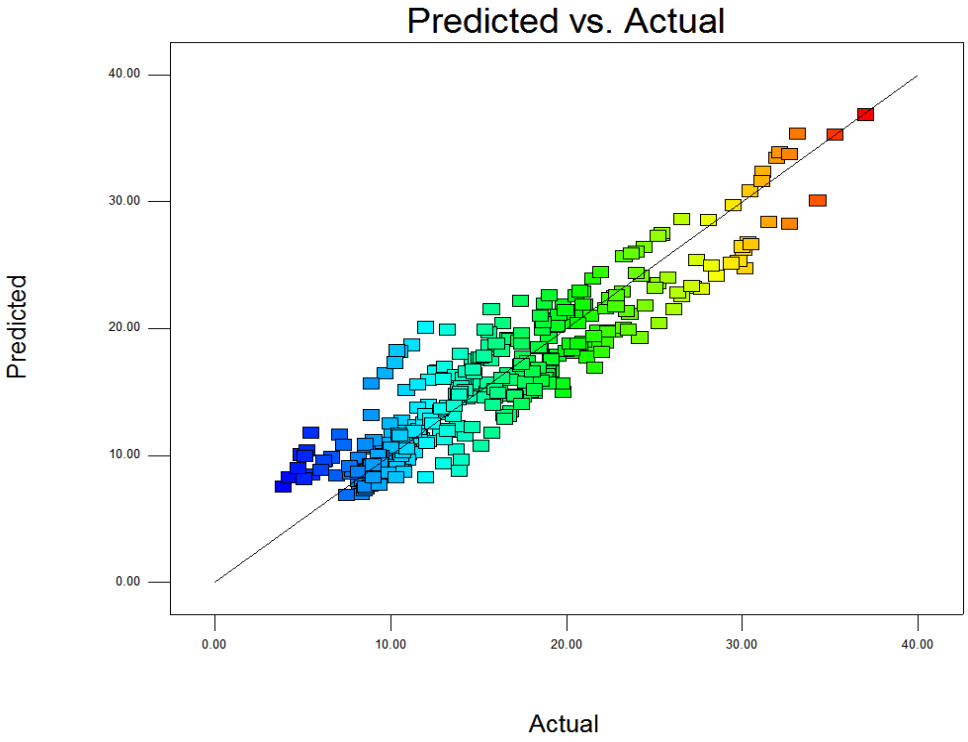

Figure 5-2 Predicted vs actual overpressure analysis results from response surface of Design Expert. In the graphic, the y axis represents the predicted overpressure value, derived from the function in Fig 5.1, while the x axis represents the actual value from

simulations. Each of the pairs matches each other well if their point is close to the black line. From the results, the coloured points are mostly concentrated in the vicinity of the black line, the some of them have large distance from the line.

The results of Equation 5.1 were applied to all of the 360 initial models which were involved in response surface fitting process and analysis of relative error of "f(X)". The detail is shown in Appendix A. The results show that "f(X)"fits satisfactory to most of the cases; in over 85% of cases, the relative errors (ε(Y)/f(X)) were found to be less than 20%, and in over 66% cases, the relative errors were less than 15% (Figure 5.3). Figure 5.3 plots the relative errors for all the simulations for fitting f(X). We can see that the relative errors are mostly less than 20%. For cases where the relative errors are above 20%, they share some common features: their clay contents are 0.3 or 0.5, sedimentation rates are small and most of their bending degree values are "1". After analysis, it is suggested that there are two main reasons which cause this situation:

1. The overpressure value with a clay content of 0.1, 0.3, 0.5 is not monotonically increasing or decreasing with others factors (see details in Appendix A), because the rock permeability for each of these is not monotonically increasing or decreasing in same conditions.
2. The low value of sedimentation rate could lead to a small value of overpressure, as shown in Chapter Three, equivalent to reducing the denominator in the process of calculating relative error.

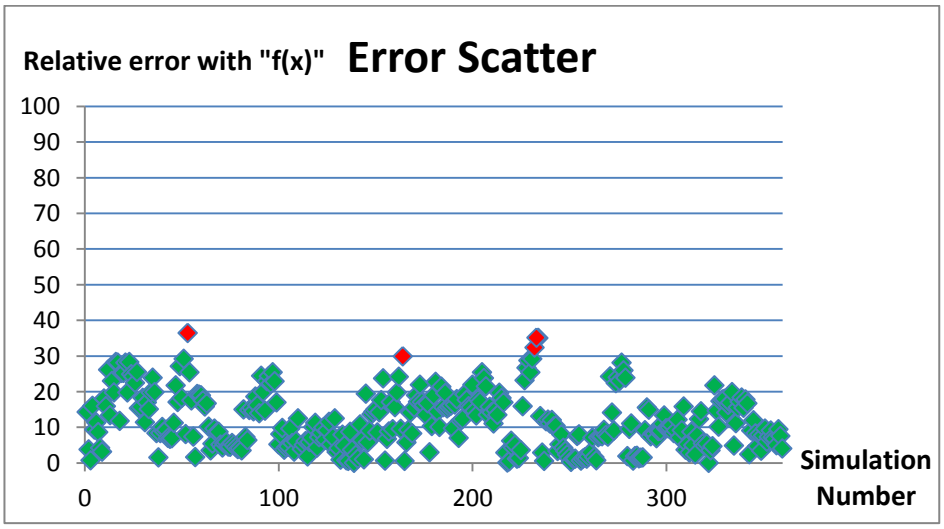

Figure 5-3 the plot of relative error scatter; y axis represents relative error of LT effect (f(x)), and x axis represents the simulations. Over 85% cases have relative error below20%, and over 66% cases relative error less than 15%; in almost all cases relative error was less than 30%. Only 1% cases have relative error above 30%. Green points have relative errors less than 30%, while the extreme ones over 30% are in red.

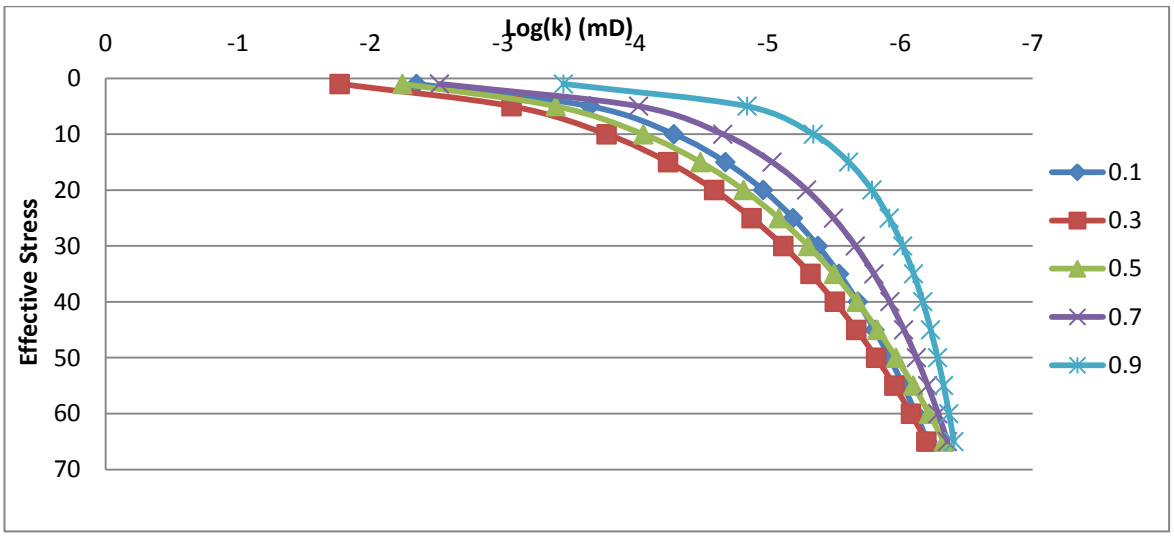

Figure 5-4 A plot of rock permeability and effective stress for different clay contents. Under the same effective stress, the permeability of clay 0.1 is smaller than both clay 0.3 and most area with clay 0.5. However, if effective stress is over 38 MPa, the permeability relationship of clay 0.1 and 0.5 will change. Permeability in clay content from 0.1 to 0.9 is not monotonically increasing or decreasing under the same conditions.

There are only 4 cases whose relative errors are greater than 30%. These four cases have the greatest degree of aquifer bending, for which the value is "1", and clay content is 0.3, sedimentation rate and aquifer depth are small, which could lead to a low value of overpressure and greater relative error compared with "f(X)". In reality, a dipping aquifer could appear bent when encountering a particular geological phenomenon but it is rare to meet such a large bending degree. So the cases which have a high relative error are not common in reality, and the relative errors are all less than 30% in reasonable cases. A set of additional 70 verifications were run at the random chosen conditions in parameter space and they showed the same results as cases used to fit the function.

In summary, the function derived by response surface analysis can model the overpressure in the aquifer crest well. Models with very low sedimentation rates (100, 300, 500m/Ma), a high degree of aquifer bending and clay content of 0.3 or 0.5 showed larger relative errors, but for all other simulations the resulted (calculated by the function in Figure 5.1) relative errors are less than 30%.

In the next step, the same process and methods were used to analyses and assess the relative errors by using response surface results in the condition of single channel-levee systems deposited above the aquifer.

5.3 Results and error analysis in model with single channel-levee system

In this section, results concerning the effect of channel-levee systems on overpressure distribution will be applied to all of the relevant previous simulations. In the previous studies, it was shown that overpressure value at the aquifer crest with a single channel-levee systems effect could be expressed as:

$$F(Y) = f(X) + h(Z) + \varepsilon(Y) \qquad 5\text{-}2$$

In which "F(Y)" is the overpressure value at the reference point, "f(X)" is the regression function for the overpressure value without the effect of the channels; "h(z)" is a regression result obtained from "g(z)", which represents the channel-levee system's effect on overpressure; "ε(Y)" represents total relative error, it includes "ε(f)" in function 5.1, for which the importance is less than 30% percent of LT effect (f(X)); and ε(h), difference between G(Z) and h(z) which was analysis in chapter 4. Every part of the error has been studied previously in Chapter 4 and Section 5.2, and the value is in the acceptable range which can be ignored in this study. In this section the main consideration will be to apply "h(z)" to Equation 5.2 and view whether the influence of "ε(Y)" is within an acceptable range.

From the results of the response surface methodology, expressions of "h(z)" are shown in Figure 5.4. From 5.4 a, it can be seen that the function is a linear equation, which is more convenient to apply and could also maintain a relatively high accuracy. The comparison the between predicted value and the simulation data for response surface is shown in Fig. 5.4 b. The fitting result and the relative error seem to be maintained within an acceptable range, and the accurate result will be defined after error analysis. Then the function is applied to the simulated data used previously for analysing, the effect of a single CLS. There are 384 simulation cases used for investigating the impacts, performing response surface analysis, and calculating the error ε(h) = G(Z) -h(z)) relative to f(X); The data and details of the calculation are shown in Appendix C. The results show that, in all 384 cases, ε(h) is less than 10% of the LT effect f(X), and in over 80% of cases it is less than 5% of the LT effect. That means the difference between the regression function "h(z)" and the objective function "g(z)" is in an acceptable range and thus not important in this study.

(a)

h(z) =

+1.95736

+17.23974 * S

-4.81457 * L

-1.31561 * d

+2.73254 * S * L

-42.48979 * S * d

+7.55950 * L * d

(b)

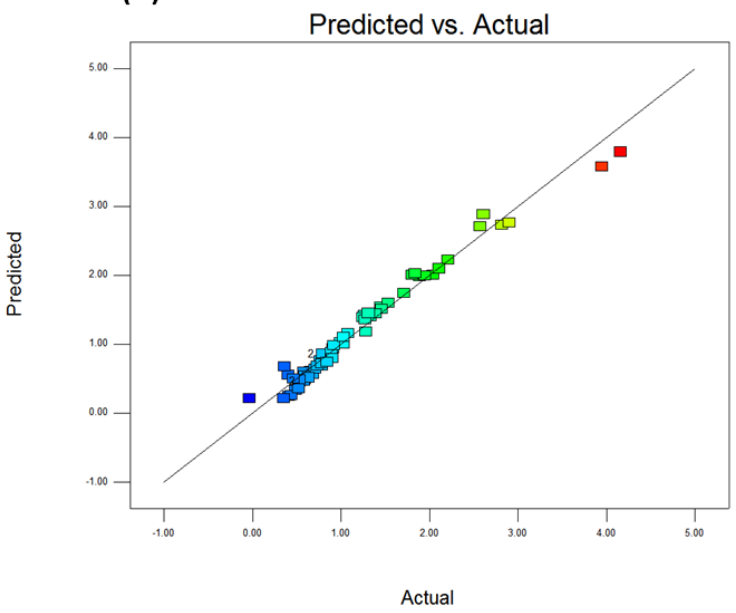

Figure 5-5 a) Function from response results for effect of single channel-levee system on overpressure at the aquifer crest. It has three arguments and presents a one-dimensional equation. b) Comparison between predicted value and simulation result. The greatest difference between predicted and actual overpressure value is nearly 1 MPa, but when the relative error of LT effect is viewed, the fitting results seems to be maintained within an acceptable range.

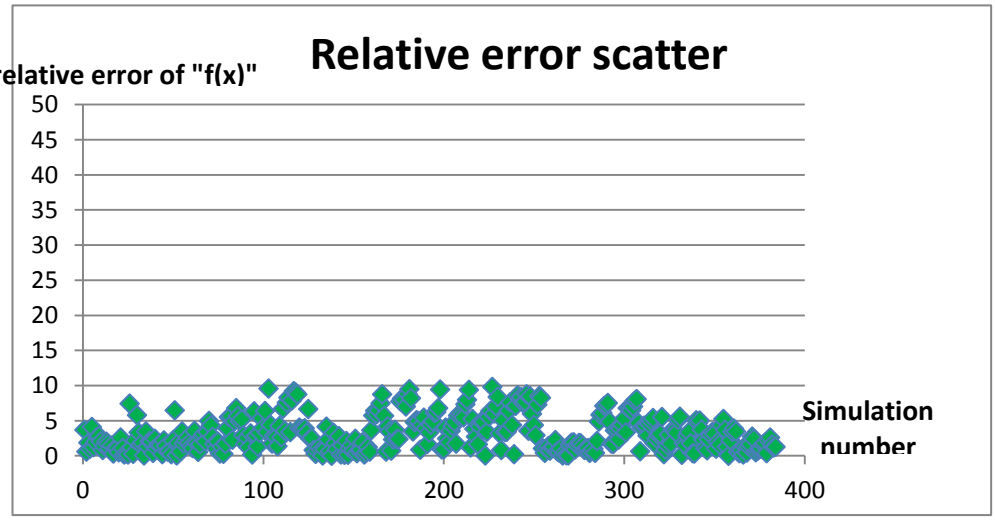

Figure 5-6 Relative error scatter graph for this study. From the results of all the simulations it can be seen that relative error is less than 10% of the LT effect, and in over 80% of cases, less than 5% of the LT effect. That means the importance of "ε(f)" can be ignored in this study because it is less than 10% of LT effect (the error limit was studied in previous sections), and the difference between the regression function "h(z)" and the objective function "g(z)" is in an acceptable range and not important in this study.

If the difference between the regression function "h(z)" and the objective function "g(z)" is in an acceptable range after analysis, then the importance of the total error "ε(Y)" will

also be considered. In section 5.1, the importance of relative error "ε(f)" was assessed, which is less than 30 percent of the LT effect ("f(X)"), and the regression error "ε(h)" is less than 10 percent of LT effect ("f(X)"), taking into account their value vectors, the total relative error of the LT effect will definitely be less than 40% of the LT effect. Then the regression results for the LT effect "f(X)" and single channel effect "h(z)" are used to see the importance of the total relative error. The scatter of results is shown in Figure 5-7. From the graph, all of the simulations involved have a single channel-levee system affect for which total relative error remains within 30% of the LT affect which is because of their vectors (not superimposed with symbols). In 43 cases the relative error is over 25%. These cases have common features: their sedimentation rate is in a small part of the defined parameter space and clay content is 0.3 or 0.5: such parameter range could produce a large relative error for the LT effect, as studied in Chapter 5.1, so the total error is relatively larger than in other cases.

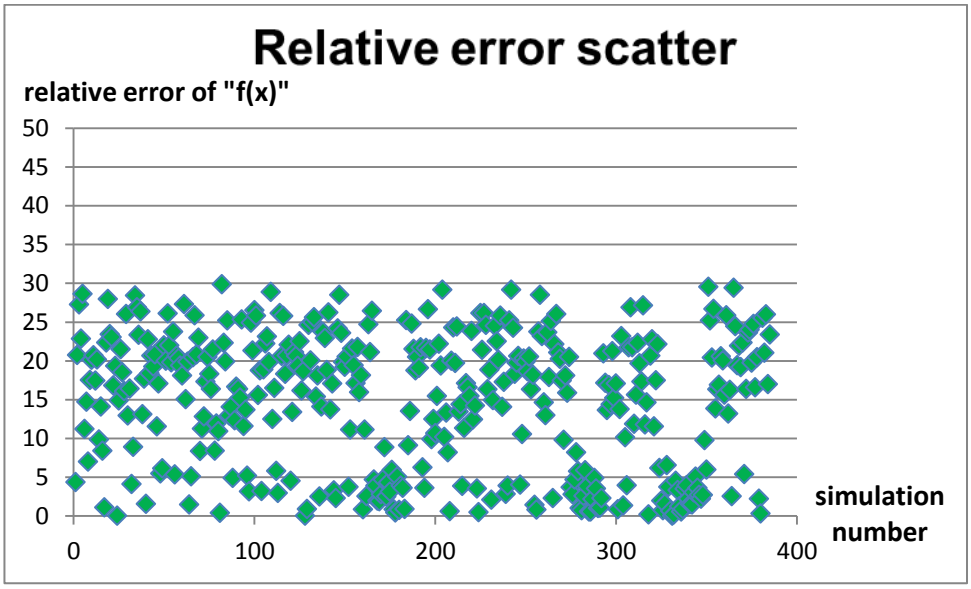

Figure 5-7 error scatter graph of total error for all involved cases. From the results, totally relative error in all of the cases is less than 30% of the LT effect, and in most of the cases the error remain 25%, and the 43 cases where relative error is more than 25% have common the feature that their sedimentation rate is small (less than 300 m/Ma) and clay content is 0.3 or 0.5. All the involved models could be accurately fitted in this study.

In summary, response surface regression results for the effect of a single channel-levee system effect could be well fitted and applied in the simulations involved; the relative error of this process could be less than 10 percent of the LT effect. Moreover, when the results of both the LT effect ("f(X)") and single channel-levee system effect ("h(z)") are applied in the function for calculating overpressure value at the aquifer crest, the total

relative error of all cases that have a single channel effect could be less than 30 percent of the LT effect. This conclusion shows that the response surface regression results could be well fitted and applied to all of the simulations involved. In the next section, the response surface regression result for the upscale for two collapsed channels will be analyzed in terms of their relative errors, accuracy and adaptability.

5.4 Results and error analysis in models with a two-channel-levee systems cluster

In this section, response surface results regarding effect of two collapsed channel-levee systems upscaled to a single channel effect will be used to check applicability and accuracy in the involved simulations. In the previous research, the importance of interaction between the channels was studied and it was found that the distance between each channel is a very important factor as it influences their fluid interaction. The importance of interaction between two channels with different relative distances between them was also investigated in Chapter 4. In Chapter 4, the function of upscaling two collapsed channel-levee systems ("gg(z)") was worked out by response surface methodology, and the overpressure value at the reference point (in the condition where a basin has two collapsed channels in a cluster) was found to be able to be expressed as:

$$F(Y) = f(X) + \Sigma h(zj) + gg(zi), + \varepsilon(Y), \qquad 5\text{-}3$$

where "F(Y)" is overpressure value at the reference point, "f(X)" the regression function for overpressure value without the channel's effect, "gg(zi)" is effect of two collapsed channels, which, from the response surface regression result, "h(zj)", is the effect of a single channel (which has insignificant fluid interaction with other channels which analysis in chapter 4) on overpressure. The expression "ε(Y)" is total error relative to the LT effect (f(X)) in this system. It consists: ε(gg), regression error between "G(Zi)" (overall effect of two collapsed channels on overpressure) and "gg(zi)", "ε(f)" (shown in 5.1) for which the values are less than 30% of the LT effect (f(X)) and ε(h), the regression difference between "G(Zj)" and "h(zj)". If the system only has two collapsed channels in the cluster, the total error will not include "ε(h)", because the difference between "G(Zi)" and "h(zi)" has been included in the process of the response surface methodology which calculated values for the function "gg(zi)". The main consideration in this section is to apply response surface regression results (gg(z)) to all simulation cases which have a large degree of interaction between two channels and to assess whether the error ("ε(gg)" and "ε(Y)") is within the acceptable range.

From the results of the response surface methodology, expressions of "gg(z)" are shown in Figure 5-8 a which was shown in Chapter 4, and the results of residual normal plots are shown in Figure 5-8 b. From results shown in Figure 5-8, it can be seen that the regression function from response surface methodology is a cube equation which has two arguments ("h(z1), h(z2)"), and the residual normal plots show that the results could be well fitted on basic simulations of a response surface. The function "gg(z)" is applied to all of the involved models (i.e. the 80 models satisfy the condition that interaction between the two channels cannot be ignored) which have two combined channel-levee systems cluster, to view the importance of relative error "ε (gg)" on the LT effect. The detailed results are shown in Appendix D, and the graph of relative error scattering is shown in Figure 5-9. FromFigure 5-9, for all of the simulations relative error "ε (gg)" is less than 10%t of LT effect ("f(X)"), and for over 88% of the models, relative error was less than 5% of the LT effect. That means the difference between the regression function "gg(z)" and the objective function "G(Z)" is in the acceptable range and not important in this study.

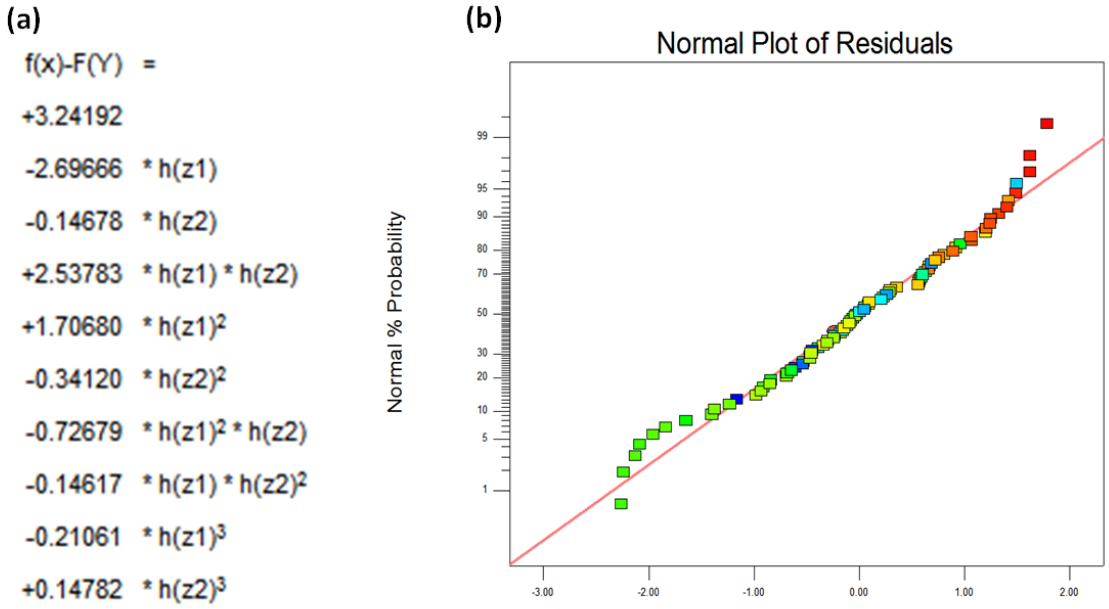

Figure 5-8 a) Response surface regression results for two channel's upscaled effect. The function is a cube function and has two arguments. In this study, cube simulation could better meet the accuracy requirements within the established framework. b) Residual normal plots for simulation results and predicted results, showing that the results could be well fitting in basic simulations of the response surface.

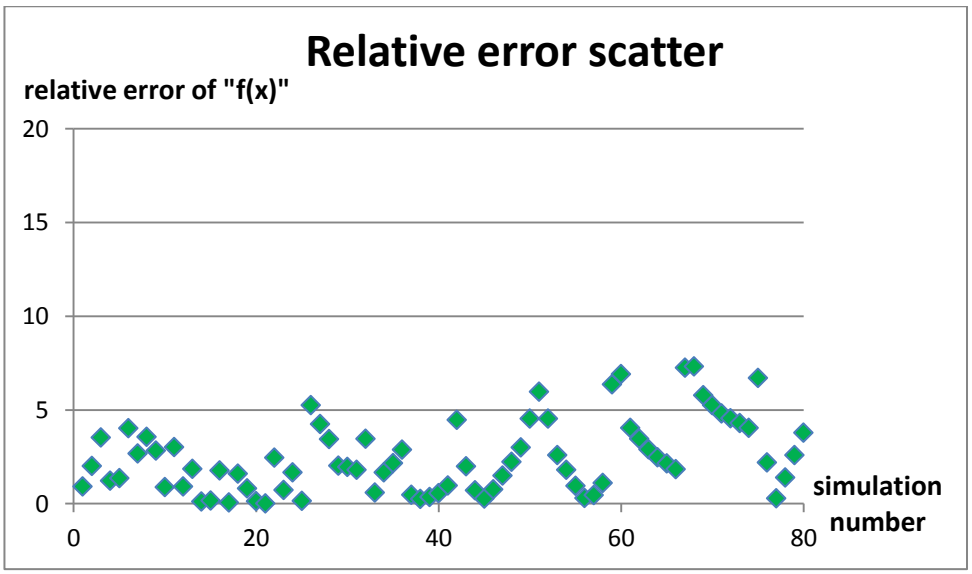

Figure 5-9 Relative error scatter for regression difference and LT effect. From the results, it can be seen that relative error for all of involved models is less than 10% of LT effect, and for most of them it is less than 5%. Only 9 models (11%) have relative error above5% of LT effect ("f(X)"). This means the difference between the 'two channels overall effect ("G(Z)") and the fitting results ("gg(z)") is in the acceptable range and is not important in this study.

If the difference between the regression function "gg(z)" and the objective function "G(Z)" is found to be in the acceptable range after analysis, then the importance of total error "ε(Y)" will also be considered in models which a cluster only has two channel-levee systems. In section 5.1, the importance of the relative error "ε(f)" was assessed, which was less than 30% of the LT effect ("f(X)"), and the regression error "ε(gg)" was less than 10% of LT effect ("f(X)"); Considering their vectors, the total relative error value should be less than 40% of the LT effect ("f(X)"). The total relative error of the LT effect was analyzed, to find out whether this is the in acceptable range (in previous studies, the upper limit of total error was established as 30% of the LT effect). The relative error scatter is shown in Figure 5-10. From the results, for all of the simulations which satisfy the condition that interaction between the two channels cannot be ignored, the total relative error of the LT effect was less than 20%, which is because of the two parts of the relative error vector. That means the total error results for predictions of overpressure value in a basin that has a cluster with two collapsed channels are ideal and in the acceptable range. Moreover, the relative error is 20% of the LT effect, which is ideal applying as the results of the LT effect ("f(X)") and single channel effect ("h(z)"), where relative error is less than 30% of the LT effect.

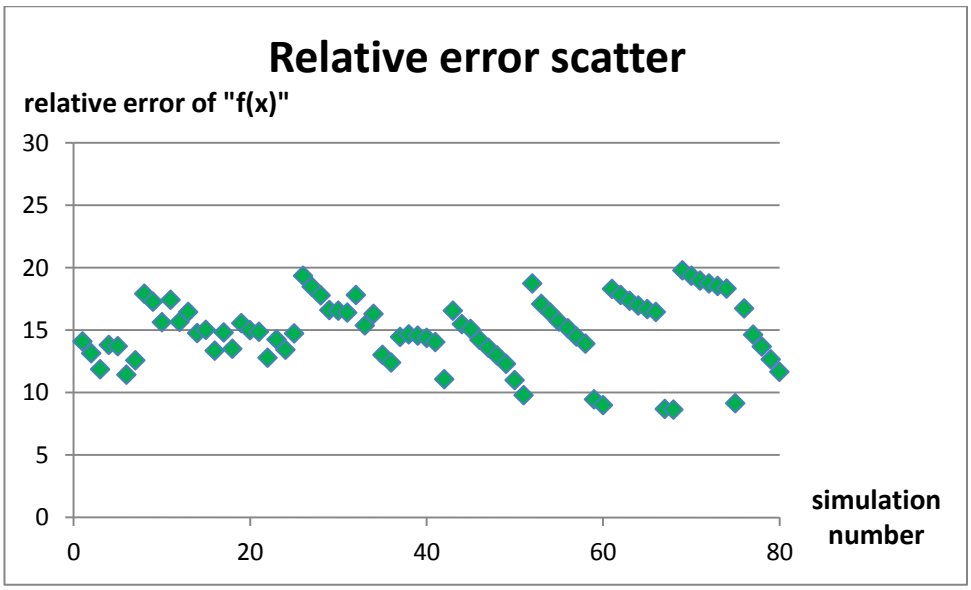

Figure 5-10 Relative error scatter graph: in all of the cases involved, total error for the basin with a two collapsed channels cluster is less than 20% of the LT effect. The total error in inacceptable range which is less than 30% of the LT effect, in this study.

In summary, the response surface regression results for the effect of two collapsed channel-levee systems appears to be well fitted on all the involved simulations, and the relative error was also in the acceptable range (less than 30% of the LT effect). In the study in section 5.2 and 5.3, the response surface results for the LT effect ("f(X)") and single channel effect ("h(z)") are also all well-fitting on the simulations involved, and according to these results above, the relative error of each of the three parts can be ignored in this study, and could be used to upscale multiple CLs fluid interaction effect on overpressure in next section (as it is in the acceptable range). And it is obvious to see that some parts of Figure 5-9 and 5-10 show repeated patterns, that because the most of examine models in this section were from Section 4.4.2, which have constant value on f(X) (R,C,D,H). Most of models in this section have same ε(f), that's the reason of Figure 5-9 and 5-10 showed some repeated patterns.

5.5 Applying upscaling to complex cases

As shown in previous sections, if a basin has multiple scattered CLSs, their overall effect on overpressure at the aquifer crest can be expressed by a sum of all effects of individual CLSs if they are scatter, whereas if more than two of them collapse to form a cluster near the aquifer, their overall effect could be expressed by the effect of an upscaled super CLS of one channel nearest to the aquifer and the channel which is closest to it, and individual effects of all remaining CLSs as a decomposition, approximated in the forms of gg(z) and Σh(z), respectively. The single channel effect

function “h(z)” and two collapsed channels upscale function “gg(z)” were successfully applied in the simulations involved in the previous study. In this section, additional 20, more realistic, cases are created to further validate the finding and to verify the work flow in terms of the predictive accuracy with respect to the variability of the relative errors relative to estimated LT effect, i.e. f(X), and the adaptability of the workflow As pointed in Chapter 4, the total error in the system comprise many elements, arisen from regression (or fitting), parameter dimensional reduction, simplification of interactions among CLSs in upscaled and decomposition forms for example.. Moreover, the total error is not simply additive, by combining these, and it is necessary to consider their value vector (in a similar way to the cases in sections 5.3 and 5.4). As shown in those sections, for most of cases the relative error are small and far less than the threshold value of 10% as ‘acceptable’. Due to the complexity of the total error, a detailed study of it is deferred in a future study. Thus, the main work of this section is to follow the previously established methods to calculate overpressure value (“F(Y)”), view the total relative error on the LT effect, and establish whether it is in the appropriate range (30% of LT effect f(X)), and subsequently describe an effective workflow for analysis of overpressure value in multiple channel-levee systems in a sedimentary basin.

Appendix F details the settings and the simulation results of all 20 cases each of which contains multiple irregular CLSs. Four of the cases are shown in Figure 5-11.

In Figure 5-11a) five CSLs with different characteristics are distributed above a sandstone aquifer, and the sedimentation rate of the over-burden mud is 100 m/Ma, clay content is 0.1, aquifer depth and relief are both 2000 metres. There is a cluster of 3 CLSs (1,2,3): CLSs 1 and 3 are the closest in the cluster and to the dipping aquifer. Based on the findings in previous Sections the effect of this cluster on overpressure could be expressed in terms of their upscaled effect plus decomposition of the single effect of CLS 2, the second closet to the cluster, and the overall impact of all remaining CLSs as the decomposition of their individual effects (channel 4 and 5 are the result of a long geological sedimentation time after the aquifer was formed, and thus their interaction with other channels could be ignored). The simulated overpressure at the aquifer crest, i.e. F(Y), is 5.97 MPa. The predicted value using developed formula (f(X) + h(z2)+h(z4)+h(z5) + gg(z1,z2) is 5.89 MPa, and this gives a total error of just 0.65% of the LT effect f(X), equal to 12.51 MPa. In Figure 5-11 b, there are five channels above the dipping aquifer, sedimentation rate of over-burden mud is 300 m/Ma, clay content is 0.3, aquifer depth and relief are all 2000 metres. CLSs 1 ,3 and 5 form a

cluster, similarly, the predicted effect on overpressure at the aquifer crest is h(z2)+h(z4)+h(z5) + gg(z1,z3). The simulated overpressure is 8.73 MPa, while the predicted value is is 7.61 MPa, giving a total error of just 8.76% relative to the LT effect of 12.73 MPa). In Figure 5-11 c) there are six channels above the dipping aquifer, sedimentation rate of over-burden mud is 100 m/Ma, clay content is 0.5, aquifer depth and relief are each 2000 metres. In this case, CLS 1 is separated from all other CLSs. There are 2 channel clusters, comprising CLSs 2 and 3 and CLSs 4, 5 and 6, respectively. The overall impact of the first cluster is modelled as gg(z2&z3) . Because CLSs 4, 5, 6 are much newer sediments after the aquifer deposited at a much slow rate, as shown in previous sections, they play a very small and negligible role in terms of fluid interactions, and the overall impact could be expressed as h(z4)+h(z5)+h(z6). Therefore, the predicted overpressure is expressed as f(X) + h(z1)+ h(z4)+h(z5)+h(z6) + gg(z2,z3) and is equal to 8.79 MPa, while the simulated one is 9.74 MPa, giving a a total error is 7.2% relative to the LT effect of 13.11 MPa. In Figure 5.10 d, there are five CLSs which form a big cluster. The sedimentation rate of over-burden mud is 100 m/Ma, clay content is 0.1, aquifer depth and relief are all 2000 metres. In the cluster, CLSs 1 and 3 are nearest to each other and CLS 1 is the closest to the dipping aquifer deposited 2 Ma after the aquifer. Again, the predicted overall effect of the cluster may be expressed as (f(X) + h(z2)+h(z4)+h(z5) + gg(z1,z3) equal to 8.61 MPa, while the simulated one is 8.56 MPa, giving a total error of just 0.4% relative to the LT effect equal to 12.51 MPa.

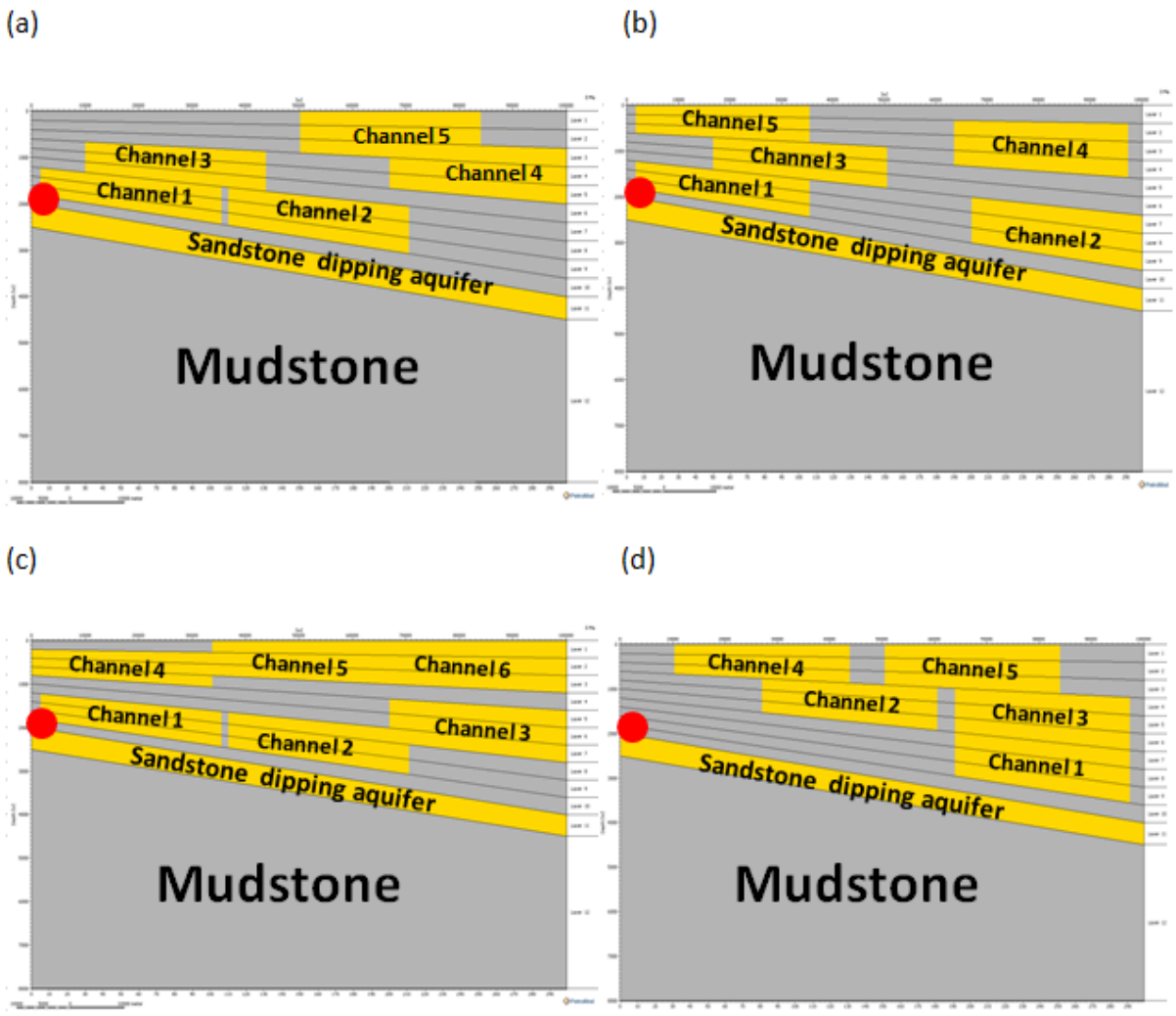

Figure 5-11 a) the overall effect of the five channels above the aquifer can be expressed as channel 1 and channel 3's upscaled effect added to the others 3 channels' respective single effects. The overpressure value at the reference point (red region) from the simulation output ("F(Y)") is 5.97 MPa. Predicted the value from previous study and method is 5.89 MPa, which has MPa difference of 0.08 from the result from the simulation output. Totally error is just 0.65% of the LT effect (12.51 MPa). b) The overall effect of the five channels above the aquifer can be expressed as channel 1 and channel 3's upscaled effect, to which is added the other 3 channels' respective single effects. The overpressure value at the aquifer crest from the simulation output ("F(Y)") is 8.73 MPa. Predicted value from the previous study and method is 7.61 MPa, 1.12 MPa below the result from the simulation output. The total error is just 8.76% of the LT effect (12.73 MPa). c) The overall effect of the six channels above the aquifer can be expressed as channel 2 and channel 3's upscaled effect, added to the single effect of the other 4 channels. The overpressure value at the aquifer crest from the simulation output ("F(Y)") is 9.74 MPa. Predicted value from the previous study and method is 8.79 MPa, which has a difference of from the simulation output result. The total error is just 7.2% of LT effect (13.11 MPa). d) the five channel cluster's overall effect on overpressure at the aquifer crest can be expressed as the upscaled effect of channel 1 and channel 3 and the decomposition of the other three channel's single effect; , the simulation output of overpressure value at the reference point is 8.56, and the predicted result from the previous study is 8.61, which has a difference of 0.06 MPa from the result from simulation output; the total error is only 0.4% of the LT effect (12.51 MPa). In

summary, the methods and results studied in previous can be successfully applied in the four random synthetic cases, and total error was also limited to within the ideal range.

For the remaining 16 cases, the results show the similar patterns (see Appendix F); the highest total error is less than 30%. This means that the approach tested on simpler cases could well be applied to complex cases with the total error to fall within a satisfactory range.

5.6 A workflow for analysing and predicting the effects of GUs on overpressure for LT-type basins

From the cases applied here, the methods used in the previous analyses of overpressure value at the aquifer crest could well be applied in almost all of the cases involved in the simulations. That means CLs fluid interaction understanding on overpressure is correct. In next step, a workflow for upscaling multiple CLs fluid effect on overpressure prediction used fluid interaction understanding which studied before will be summarized.

The analysis of the applicability of the Response Surface regression results in terms of three aspects (lateral Transfer effect, single channel effect and two collapsed channels effect on overpressure distribution at the aquifer crest) has been carried out, and demonstrated that all of them could be well-fitting and suitable. In this section, a workflow for the analysis of a sedimentary basin with multiple channel-levee systems in different geological conditions and overpressure prediction used fluid interaction effects upscaling were worked out, and applied in synthetic simulation cases to assess its applicability and accuracy.

If sedimentary basin cases satisfy the conditions that they have a lateral-fluid-transferring sedimentary base and it is overlaid by multiple channel-levee systems, the over-burden rock property is nearly homogeneous and the bulk is fine-grain, the following workflow for analysis of overpressure at the aquifer crest could be applied. Firstly: the basin sedimentation type (fast or slow) and rock properties (clay content) should be considered in terms of the following conditions:

(1) Their over-burden sedimentation rates and rock properties are as follows:

Sedimentation rate is higher than 1000 m/Ma, clay content is higher than 0.1.

Sedimentation rate is higher than 800 m/Ma, clay content is higher than 0.3.

Sedimentation rate is higher than 500 m/Ma, clay content is higher than 0.5

Overpressure value on crest of aquifer "F(Y)" could be expressed by the following equation (for which data for sedimentation rate, clay content, aquifer depth, relief and bending are needed):

$$F(Y) = f(X) + \varepsilon(f); X = (D, H, C, R, B), \quad 5\text{-}4$$

in which "f(X)" is the adopted function from Figure 5.1, and the "Ɛ(f)" value should be less than 30%of the value of function "f(X)".

(2) Their over-burden sedimentation rate and rock properties are as follows:

Sedimentation rate is less than 1000 m/Ma, clay content is 0.1.

Sedimentation rate is less than 800 m/Ma, clay content is less than 0.3.

Sedimentation rate is less than 500 m/Ma, clay content is less than 0.5

Relationships between each GU should be considered, and the condition will be divided into two parts:

[1] Relative distances between each channel-levee systems are scattered, or all the channels are located far away from the lateral sand layer (geological time of deposition is more than 2 million years).

Overpressure value at the crest of the aquifer ("F(Y)") can be expressed by the following equation (for which data about sedimentation rate, clay content, aquifer depth, relief and each channel-levee systems relative size, location and depth ("z") are needed):

$$F(Y) = f(X) + \sum_{0}^{i} h(zi) + \varepsilon(Y); X = (D, H, C, R), Z = (S, L, d) \quad 5\text{-}5$$

in which "f(x)" is the adopted function from Figure 5.1, "h(z)" is the adopted function from Figure 5.4, and the value of total system relative error "Ɛ(Y)" should be less than 30% of the value of function "f(X)".

[2]: The basin has two or more channel-levee systems which form a cluster (collapsed together and having a vertical overlap area), and one of them is located near the lateral sand layer (geological time is at less than or equal to 2 million years).

The effect of the two nearest channels which satisfy the condition above in the cluster (za, zb) could be upscaled, and overpressure value at the crest of the aquifer F(Y) can be expressed by the following equation (for which data about sedimentation rate, clay content, aquifer depth, relief and each channel-levee systems relative size, location and depth ("z") are needed)

$$F(Y) = f(X) + \sum_{0}^{i} h(zi) + gg(za, zb) + \varepsilon(Y); \mathrm{X} = (D, H, C, R), Z = (S, L, D) \qquad 5\text{-}6$$

(Note that "i" does not include a and b, as the function was assumed for a case with one cluster. If cases have two or more clusters, each cluster's effect on overpressure will be expressed in this form)

In the equation "f(X)" is the function adopted in Figure 5.1, "h(z)" is the adopted function in Figure 5.4, and gg(za,zb) is the adopted function in Figure 5.7. The value of the totally system relative error "Ɛ (Y)" should be less than 30% of the value of function "f(X)".

5.7 A workflow for developing the role of GUs in a deep-water basin

This thesis provides a workflow to develop the understanding of GU fluid interaction and upscaling relative to predicting overpressure in deep-water basin, which was used on LT reference cases to assess the role of GUs (chosen as channel-levee systems). This result forms the basis for follow-on research that can seek to further generalise the approach to a wider set of systems and their associated descriptive parameters.

The main approach of the work flow can be divided into four parts:

1. Depending on the circumstances, it is necessary to establish a reference model to demonstrate that quick method can be developed based on well-established scientific methodologies.

2. Estimating overpressure at the chosen reference point by screening and analysing a set of mainly geometric parameters that describe the reference case, AND including the presence of additional GUs and accordingly assessing their interaction relative to predicting overpressure. As the number of geometric parameters could be high, the approach adopted here is one in which the task is simplified to assess whether it is possible under plausibly realistic model arrangements , to find ways to reduce the system complexity to a small number of "key" parameters, while still making a

sufficiently accurate prediction of overpressure. The methodology used here for prediction could adopt a response surface to define relationships between overpressure and the key parameters in their considered range.

3. Demonstrating the target function, which is the prediction of overpressure at a certain reference location, which can be estimated with sufficient accuracy over a wide range of parameters of the system, while examining the results concerning the role of GU interaction in overpressure prediction.

4. Define in which conditions of such a reference case, the complex structure of the GU could be simplified relative to predicting overpressure and how, according to the analysis of the results. Reach the goal of simplifying the heterogeneity of the architecture in overpressure prediction in a deep-water basin.

5.8 Summary

This chapter mainly proved that the prediction of overpressure value on chosen reference point is accuracy that has acceptable range of relative error which means the LT and LT + CLs systems overpressure character assessment and GU interaction on overpressure research is effective in this reference case. According the workflow which developed in these study, the initial understanding of GU role on overpressure character were obtained in LT reference case, which has so much potential on academic and industry aspects. At first, the workflow could be extended to others reference cases and focusing their GU role on overpressure by analysing their parameters, and get understand of GU interaction on overpressure, which could helping for simplifying complexity and heterogeneity deep-water basin modelling cases on overpressure character in industry. As in LT cases, if there are several channel-levee systems has small size and far away from dipping aquifer, their influence on overpressure could be ignored which were researched in thesis, and such CLs data don't need to be collected in overpressure prediction. Secondly, if the there is a particular real case with multiple CLs and overpressure prediction is a concern, the results can be used to better assess the system overpressure quickly. But real cases have more complex factors and simulation tools and results cannot handle these problems well. At least, the results can be undertaken to better understand the overpressure issues in such cases. The results were summarized below:

1. Analysis of the results of synthetic cases and all of the involved simulations found that these could be well fitted, and the difference between predicted and

simulation output values (system total error) can also be maintained within an acceptable range (less than 30% of the LT effect). A workflow for developing a representation of GU interaction relative to predicting overpressure was also summarized.

2. The conclusions demonstrated that the workflow could be successfully used on the LT reference case. The results could accurately predict overpressure at the aquifer crest without constructing full scale models and carrying out seismic measurements. The methods provide an effective way to simplify the complex structure that brings about the effect of CLSs on overpressure distribution, and to understand the importance of fluid interaction between the GUs. These ideas could provide much insight and potential focus on the significance of fluid properties and the use of upscaling and simplified methods in investigating the effects of multiple GUs in deep-water basin.

Chapter 6. CONCLUSIONS AND FUTURE WORK

6.1 Summary of the workflow for developing GU interaction

This thesis has developed and analysed a workflow to identify GU interactions relative to predicting overpressure in deep-water basins. The approach used the classic LT reference case to assess the role of GU arrangements, which here use channel-levee systems as the GU type, due to the fact that they are individually spatially-limited "objects" that present the most challenge to the multi-GU upscaling task. The work proves that there is a basis for follow-on research that can seek to further generalise the approach to a wider set of systems and their associated descriptive parameters. This follow-on could, in principle, create a framework in which overpressure could be estimated simply from a geometric model with ages and lithology types (given as rough averages). Such an estimate would allow a quick assessment of an unknown basin to be undertaken, enabling the available analysis time to be focused on detailed numerical simulations of specific cases to give the most value in terms of deriving understanding of enabling how the specifics of that particular basin have influenced overpressure distribution. The workflow could be used for simplifying project basin modelling processing and heterogeneity GUs fluid complexity effect on overpressure distribution, which could reflect on saving time and financial costs on complexity full-scale modelling building and seismic data collection...

The main approach of the workflow can be divided into four parts:

1. Depending on the circumstances, it is necessary to establish a reference model to demonstrate that such a quick method can be developed based on well-established scientific methodologies. The LT model captures the role of a progressively-tilting aquifer, which is the key characteristic of many subsurface situations.
2. Estimating overpressure at a chosen reference point by screening and analysing a set of mainly geometric parameters that describe the reference case, and identifying the presence of additional GUs to assess their interaction relative to predicting overpressure. The number and complexity of geometric parameters can be high, so the approach adopted here is one in which the task is simplified such that it can be assessed whether it is possible, under plausibly realistic model arrangements, to find ways to reduce the system's complexity to a small number of "key" parameters while still making a sufficiently accurate prediction

of overpressure. Here, the methodology for prediction can adopt a response surface to define the relationships between overpressure and the key parameters in the range being considered.

3. Demonstrating the target function, the prediction of overpressure at a certain reference location, which can be estimated with sufficient accuracy over a wide range of parameters of the system, while examine the results regarding the role of GU interaction on overpressure prediction.
4. Define in which condition of such a reference case the complex structure of the GU could be simplified relative to predicting overpressure and how, according to the analyse results. This is to reach the goal of simplifying the effect of the heterogeneity of the architecture on overpressure prediction in a deep-water basin.

This thesis supports a novel workflow to predict overpressure in LT reference cases with a dipping aquifer and deposits of multiple channel-levee systems. It provides methods of analysis and a ready-developed target function step by step in different geological conditions. It identified in which conditions the complex architecture of CLSs can be simplified for overpressure prediction and in which conditions this complex architecture needs to be more explicitly detailed and how this can be achieved.

The fluid interaction and flow effect upscaling method on OP on LT reference cases is summarized below:

1. The influences of overpressure on a dipping aquifer crest in basin modelling have been parameterized. The important influencing factors on overpressure and the sensitivity of their influence were obtained and summarized: these are over-burden mud sedimentation rate, clay content, aquifer depth and relief, which are proportional to overpressure at the aquifer crest. The other influencing parameter is aquifer bending, which has an inverse influence on overpressure.
2. The relationship between overpressure and the influencing factors was obtained using response surface D-optimal methodology (see equation in section 3.7). The results could accurately predict overpressure at the aquifer crest when the basin has only a dipping aquifer.
3. Channel-levee systems can influence fluid migration from the aquifer crest to the CLs and thus reduce overpressure at the dipping aquifer crest in the basin formation process. Their degree of influence was found to be only an additional part of the existing LT base (less than 30% of LT).

4. The area of the CLS needs to be considered first: if it accounts for a small proportion (less than 0.1) of the over-burden sediments, the effect of the interaction between the aquifer and the CLS or clusters on overpressure distribution can be ignored.
5. There are seven important controlling factors for the influence of a single CLS on overpressure distribution:, over-burden sedimentation rate, over-burden mud clay-content, aquifer relief, location of the CLS, and depth of the CLS which inversely impacts the system's influence, and additionally, aquifer depth, and the area of the CLS can also have a proportional impact on the influence of the CLS on overpressure.
6. When a basin has deposition of two or more CLSs, the fluid interaction between them also needs to be considered. When their positions are scattered or far from each other in the vertical direction, the fluid interaction between them is not obvious and its effect on overpressure can be ignored. In this case the overall influence on overpressure could be regarded as the decomposition of the single influence of each of them on overpressure (calculated by equation in section 4.6).
7. When a basin has two or more CLSs deposited, and at least two of these form a cluster (touching each other or with a small vertical distance, close to the aquifer and with an overlapping area in the vertical direction), the cluster can be seen as a whole. In these cases, the overall influence of such a cluster on overpressure in the aquifer crest could be expressed as its influence after upscaling (calculated by the equation in section 4.7.5) which satisfies the conditions of being closest to each other, closest to the aquifer and having an overlapping area in the vertical direction in the cluster; single influence of any other CLSs (calculated by the equation in section 4.6) is then added to predict overpressure at the aquifer crest.

If a sedimentary basin case satisfies the conditions that it has lateral-fluid-transferring sediments at the base and is overlaid by multiple channel-levee systems, its over-burden rock property is nearly homogeneous and the bulk is fine-grained, then the workflow for the analysis of overpressure at the aquifer crest can then be applied. First, the basin sedimentation type (fast or slow) and rock properties (clay content) should be considered:

(1) When the over-burden sedimentation rate and rock properties are as follows:

Sedimentation rate is higher than 1000 m/Ma, clay content is higher than 0.1.

Sedimentation rate is higher than 800 m/Ma, clay content is higher than 0.3.

Sedimentation rate is higher than 500 m/Ma, clay content is higher than 0.5.

In these cases overpressure value at the crest of aquifer "F(Y)" could be expressed by (for which we which we need to obtain data for sedimentation rate, clay content, aquifer depth, relief and bending):

$$F(Y) = f(X) + \varepsilon(f); X = (D, H, C, R, B)$$

in which "f(X)" is the adopted function in Figure 5.1, and the value "Ɛ(f)" should be less than 30 percent of the value of function "f(X)".

(2) Relationships between each GUs should be considered when their over-burden sedimentation rate and rock property are as follows:

Sedimentation rate is less than 1000 m/Ma, clay content is 0.1.

Sedimentation rate is less than 800 m/Ma, clay content is less than 0.3.

Sedimentation rate is less than 500 m/Ma, clay content is less than 0.5.

In these cases, the condition will be divided into two parts:

[1] Each channel-levee system's relative distances are scattered, or all the channels stay far away from the lateral sand layer (geological times are more than 2 million years).

Overpressure value on the crest of aquifer ("F(Y)") could be expressed by the following eaquation, for which it is necessary to obtain data about sedimentation rate, clay content, aquifer depth, relief and each channel-levee systems relative size, location and depth ("z")):

$$F(Y) = f(X) + \sum_{0}^{i} h(zi) + \varepsilon(Y); X = (D, H, C, R), Z = (S, L, d),$$

in which "f(X)" is the adopted function shown in Figure 5.1, "h(z)" is the adopted function shown in Figure 5.4, and the value of the total system relative error "Ɛ(Y)" should be less than 30 % of the value of function "f(X)".

[2]: The basin has two or more channel-levee systems which form a cluster (collapsed together and having a vertical overlap area), and one of them is located near the lateral sand layer (geological time is at least less than 2 million years)

The two nearest channels which satisfy the condition above in cluster (za, zb) can be upscaled, and overpressure value at the crest of of the aquifer, F(Y), can be expressed by the following equation, for which it is necessary to obtain data about sedimentation rate, clay content, aquifer depth, relief and each channel-levee system's relative size, location and depth ("z")):

$$F(Y) = f(X) + \sum_{0}^{i} h(zi) + gg(za, zb) + \varepsilon(Y); X = (D, H, C, R), Z = (S, L, D)$$

(Note that "i" does not include a and b; the function was assumed to have one cluster. If cases have two or more clusters, each cluster's effect on overpressure will be expressed in this form)

in which "f(X)" is the adopted function shown in Figure 5.1, "h(z)" is the adopted function shown in Figure 5.4, and gg(za,zb) is the adopted function shown in Figure 5.7. The value of the total system relative error "Ɛ(Y)" should be less than 30% of the value of function "f(X)".

According the workflow which developed in these study, the initial understanding of GU role on overpressure character were obtained in LT reference case, which has so much potential on academic and industry aspects. At first, the workflow could be extended to others reference cases and focusing their GU role on overpressure by analysing their parameters, and get understand of GU interaction on overpressure, which could helping for simplifying complexity and heterogeneity deep-water basin modelling cases on overpressure character in industry. As in LT cases, if there are several channel-levee systems has small size and far away from dipping aquifer, their influence on overpressure could be ignored which were researched in thesis, and such CLs data don't need to be collected in overpressure prediction. Secondly, if the there is a particular real case with multiple CLs and overpressure prediction is concern, the results can be used to better assess the system overpressure quickly. But real cases have more complexity factors aspect and simulation tools and results cannot handle these problems well. At least, the results can be undertaken to better understand the overpressure issues in such cases.

6.2 Future work

- Find more complete parameter space of influencing factors in both the LT model and the LT+CLS model, to enable more accurate prediction of overpressure in each condition.
- Extend the adopted range of each influencing parameter in the design of the simulation and analysis in order to increase the integrity and breadth of predictions.
- If basin has four or more channel-levee systems cluster, the understanding of overall impact on overpressure at the aquifer crest should also be developed by systematic simulation: the purpose is to show every configuration in parameter space to view their fluid interaction and upscale scheme for predicting the cluster's impact on overpressure. If possible, an attempt should be made to find a general upscale formula with new parameters which could suitable in all different cases for upscaling and overpressure prediction.
- Apply the results and workflow to others possible cases which have different GU types and key geological parameters to develop the understanding of their GUs role on overpressure prediction.

Appendix

Appendix A

For catching lateral transfer model physical interaction, the 5 key parameters relationships with overpressure on chosen reference point were calculated. 360 models which were created by experimental design and value range review for assessing the system. In the table, overpressure value in sixth column means F(Y), predict value means f(X) which from response surface methodology, and error is a percentage which means “100* (f(X)-F(Y)) / f(X)”. Simulations setting and results detail are showed below:

Height (m)	"a"	Rate (m/Ma)	Clay content	Depth (m)	Overpressure (MPa)	Predict (MPa)	Error %	Simulation Number
1000	0.00	100	0.1	2000	9.05	10.56	14.31	1
2000	0.00	100	0.1	2000	12.04	12.51	3.79	2
3000	0.00	100	0.1	2000	14.36	14.47	0.75	3
3000	0.33	100	0.1	2000	10.67	12.71	16.04	4
2000	0.50	100	0.1	2000	9.32	10.28	9.32	5
3000	0.67	100	0.1	2000	9.71	10.95	11.32	6
1000	1.00	100	0.1	2000	7.49	6.89	8.66	7
2000	1.00	100	0.1	2000	8.38	8.04	4.21	8
3000	1.00	100	0.1	2000	8.9	9.19	3.15	9
1000	0.00	300	0.1	2000	14	11.86	18.07	10
2000	0.00	300	0.1	2000	11.57	13.76	15.94	11
3000	0.00	300	0.1	2000	19.77	15.67	26.16	12
3000	0.33	300	0.1	2000	15.81	13.94	13.41	13
2000	0.50	300	0.1	2000	14.23	11.57	22.97	14
3000	0.67	300	0.1	2000	14.62	12.21	19.73	15
1000	1.00	300	0.1	2000	10.62	8.28	28.29	16
2000	1.00	300	0.1	2000	12.02	9.38	28.15	17

3000	1.00	300	0.1	2000	11.72	10.48	11.82	18
1000	0.00	500	0.1	2000	16.47	13.15	25.21	19
2000	0.00	500	0.1	2000	18.8	15.01	25.23	20
3000	0.00	500	0.1	2000	21.61	16.87	28.08	21
3000	0.33	500	0.1	2000	18.17	15.17	19.76	22
2000	0.50	500	0.1	2000	16.51	12.87	28.33	23
3000	0.67	500	0.1	2000	16.83	13.47	24.93	24
1000	1.00	500	0.1	2000	12.01	9.66	24.29	25
2000	1.00	500	0.1	2000	13.13	10.72	22.51	26
3000	1.00	500	0.1	2000	14.78	11.77	25.56	27
1000	0.00	1000	0.1	2000	18.92	16.39	15.41	28
2000	0.00	1000	0.1	2000	20.99	18.14	15.74	29
3000	0.00	1000	0.1	2000	23.51	19.88	18.27	30
3000	0.33	1000	0.1	2000	20.33	18.25	11.39	31
2000	0.50	1000	0.1	2000	18.83	16.10	16.96	32
3000	0.67	1000	0.1	2000	19.14	16.63	15.13	33
1000	1.00	1000	0.1	2000	15.72	13.13	19.77	34
2000	1.00	1000	0.1	2000	17.43	14.06	23.95	35
3000	1.00	1000	0.1	2000	17.98	15.00	19.87	36
1000	0.00	2000	0.1	2000	20.95	22.87	8.41	37
2000	0.00	2000	0.1	2000	24	24.38	1.56	38
3000	0.00	2000	0.1	2000	23.73	25.89	8.34	39
3000	0.33	2000	0.1	2000	21.94	24.41	10.12	40
2000	0.50	2000	0.1	2000	20.57	22.57	8.85	41
3000	0.67	2000	0.1	2000	20.8	22.93	9.30	42
1000	1.00	2000	0.1	2000	18.64	20.05	7.03	43
2000	1.00	2000	0.1	2000	19.34	20.75	6.80	44

3000	1.00	2000	0.1	2000	19.96	21.45	6.96	45
1000	0.00	100	0.3	2000	8.92	10.05	11.25	46
2000	0.00	100	0.3	2000	9.08	11.60	21.73	47
3000	0.00	100	0.3	2000	10.91	13.15	17.05	48
3000	0.33	100	0.3	2000	8.58	11.77	27.11	49
2000	0.50	100	0.3	2000	8.12	9.93	18.25	50
3000	0.67	100	0.3	2000	7.36	10.39	29.16	51
1000	1.00	100	0.3	2000	6.91	7.52	8.09	52
2000	1.00	100	0.3	2000	5.25	8.26	36.47	53
3000	1.00	100	0.3	2000	6.72	9.01	25.41	54
1000	0.00	300	0.3	2000	8.95	10.86	17.56	55
2000	0.00	300	0.3	2000	11.45	12.36	7.36	56
3000	0.00	300	0.3	2000	13.64	13.86	1.61	57
3000	0.33	300	0.3	2000	10.09	12.51	19.36	58
2000	0.50	300	0.3	2000	8.68	10.74	19.15	59
3000	0.67	300	0.3	2000	9.04	11.16	19.00	60
1000	1.00	300	0.3	2000	6.94	8.41	17.50	61
2000	1.00	300	0.3	2000	7.67	9.11	15.82	62
3000	1.00	300	0.3	2000	8.17	9.81	16.72	63
1000	0.00	500	0.3	2000	10.48	11.66	10.13	64
2000	0.00	500	0.3	2000	13.58	13.12	3.52	65
3000	0.00	500	0.3	2000	15.36	14.58	5.38	66
3000	0.33	500	0.3	2000	11.98	13.25	9.61	67
2000	0.50	500	0.3	2000	10.55	11.54	8.57	68
3000	0.67	500	0.3	2000	10.89	11.93	8.73	69
1000	1.00	500	0.3	2000	8.83	9.31	5.12	70
2000	1.00	500	0.3	2000	9.53	9.96	4.30	71

3000	1.00	500	0.3	2000	10.04	10.61	5.37	72
1000	0.00	1000	0.3	2000	12.88	13.68	5.82	73
2000	0.00	1000	0.3	2000	15.71	15.02	4.63	74
3000	0.00	1000	0.3	2000	17.09	16.35	4.50	75
3000	0.33	1000	0.3	2000	14.26	15.11	5.60	76
2000	0.50	1000	0.3	2000	12.86	13.55	5.06	77
3000	0.67	1000	0.3	2000	13.25	13.86	4.39	78
1000	1.00	1000	0.3	2000	11.09	11.54	3.92	79
2000	1.00	1000	0.3	2000	11.58	12.08	4.11	80
3000	1.00	1000	0.3	2000	12.17	12.61	3.50	81
1000	0.00	2000	0.3	2000	15.05	17.70	14.99	82
2000	0.00	2000	0.3	2000	17.44	18.81	7.27	83
3000	0.00	2000	0.3	2000	18.64	19.91	6.39	84
3000	0.33	2000	0.3	2000	16.02	18.81	14.84	85
2000	0.50	2000	0.3	2000	14.84	17.56	15.49	86
3000	0.67	2000	0.3	2000	15.15	17.71	14.47	87
1000	1.00	2000	0.3	2000	13.03	16.01	18.64	88
2000	1.00	2000	0.3	2000	13.67	16.31	16.21	89
3000	1.00	2000	0.3	2000	14.29	16.61	13.98	90
1000	0.00	100	0.5	2000	7.21	9.54	24.42	91
2000	0.00	100	0.5	2000	8.56	10.69	19.91	92
3000	0.00	100	0.5	2000	10.1	11.84	14.67	93
3000	0.33	100	0.5	2000	8.35	10.83	22.93	94
2000	0.50	100	0.5	2000	7.25	9.59	24.38	95
3000	0.67	100	0.5	2000	7.64	9.83	22.29	96
1000	1.00	100	0.5	2000	6.07	8.14	25.45	97
2000	1.00	100	0.5	2000	6.54	8.49	22.93	98

3000	1.00	100	0.5	2000	7.33	8.83	16.98	99
1000	0.00	300	0.5	2000	9.34	9.86	5.23	100
2000	0.00	300	0.5	2000	11.84	10.96	8.06	101
3000	0.00	300	0.5	2000	13.24	12.06	9.81	102
3000	0.33	300	0.5	2000	10.67	11.08	3.74	103
2000	0.50	300	0.5	2000	9.47	9.90	4.34	104
3000	0.67	300	0.5	2000	9.65	10.11	4.57	105
1000	1.00	300	0.5	2000	7.72	8.55	9.67	106
2000	1.00	300	0.5	2000	8.35	8.84	5.57	107
3000	1.00	300	0.5	2000	8.85	9.14	3.16	108
1000	0.00	500	0.5	2000	10.79	10.17	6.09	109
3000	0.00	500	0.5	2000	13.81	12.28	12.47	110
								111
3000	0.33	500	0.5	2000	11.78	11.34	3.92	112
2000	0.50	500	0.5	2000	10.73	10.21	5.07	113
3000	0.67	500	0.5	2000	11.03	10.39	6.14	114
1000	1.00	500	0.5	2000	9.11	8.95	1.79	115
2000	1.00	500	0.5	2000	9.74	9.20	5.88	116
3000	1.00	500	0.5	2000	10.12	9.45	7.11	117
1000	0.00	1000	0.5	2000	12.06	10.96	10.06	118
2000	0.00	1000	0.5	2000	13.23	11.89	11.23	119
3000	0.00	1000	0.5	2000	12.28	12.83	4.30	120
3000	0.33	1000	0.5	2000	12.82	11.96	7.17	121
2000	0.50	1000	0.5	2000	11.92	10.99	8.43	122
3000	0.67	1000	0.5	2000	12.19	11.09	9.89	123
1000	1.00	1000	0.5	2000	10.61	9.96	6.53	124
2000	1.00	1000	0.5	2000	11.02	10.09	9.20	125

3000	1.00	1000	0.5	2000	11.4	10.22	11.51	126
1000	0.00	2000	0.5	2000	11.88	12.53	5.21	127
2000	0.00	2000	0.5	2000	12.28	13.24	7.22	128
3000	0.00	2000	0.5	2000	12.19	13.94	12.53	129
3000	0.33	2000	0.5	2000	12.81	13.22	3.07	130
2000	0.50	2000	0.5	2000	12.03	12.56	4.18	131
3000	0.67	2000	0.5	2000	12.38	12.49	0.91	132
1000	1.00	2000	0.5	2000	11.03	11.98	7.92	133
2000	1.00	2000	0.5	2000	11.3	11.88	4.85	134
3000	1.00	2000	0.5	2000	11.68	11.77	0.79	135
1000	0.00	100	0.7	2000	9.08	9.03	0.56	136
2000	0.00	100	0.7	2000	10.63	9.78	8.74	137
3000	0.00	100	0.7	2000	10.91	10.52	3.70	138
3000	0.33	100	0.7	2000	9.9	9.90	0.03	139
2000	0.50	100	0.7	2000	9.03	9.24	2.29	140
3000	0.67	100	0.7	2000	9.16	9.27	1.21	141
1000	1.00	100	0.7	2000	7.82	8.77	10.80	142
2000	1.00	100	0.7	2000	8.15	8.71	6.41	143
3000	1.00	100	0.7	2000	8.56	8.65	1.02	144
1000	0.00	300	0.7	2000	10.57	8.85	19.38	145
2000	0.00	300	0.7	2000	10.1	9.55	5.73	146
3000	0.00	300	0.7	2000	9.33	10.25	8.99	147
3000	0.33	300	0.7	2000	10.98	9.66	13.70	148
2000	0.50	300	0.7	2000	10.37	9.06	14.41	149
3000	0.67	300	0.7	2000	10.42	9.06	14.98	150
1000	1.00	300	0.7	2000	9.42	8.68	8.52	151
2000	1.00	300	0.7	2000	9.79	8.57	14.18	152

3000	1.00	300	0.7	2000	9.96	8.47	17.62	153
1000	0.00	500	0.7	2000	10.74	8.68	23.75	154
2000	0.00	500	0.7	2000	9.39	9.33	0.64	155
3000	0.00	500	0.7	2000	9.31	9.98	6.73	156
3000	0.33	500	0.7	2000	10.25	9.42	8.84	157
2000	0.50	500	0.7	2000	10.4	8.89	17.05	158
3000	0.67	500	0.7	2000	9.69	8.85	9.47	159
1000	1.00	500	0.7	2000	9.94	8.59	15.67	160
2000	1.00	500	0.7	2000	10.11	8.44	19.78	161
3000	1.00	500	0.7	2000	10.29	8.29	24.17	162
1000	0.00	1000	0.7	2000	9.03	8.24	9.59	163
2000	0.00	1000	0.7	2000	11.4	8.77	29.93	164
3000	0.00	1000	0.7	2000	9.36	9.31	0.55	165
3000	0.33	1000	0.7	2000	9.33	8.82	5.81	166
2000	0.50	1000	0.7	2000	9.22	8.44	9.24	167
3000	0.67	1000	0.7	2000	9.5	8.33	14.09	168
1000	1.00	1000	0.7	2000	9.07	8.38	8.27	169
2000	1.00	1000	0.7	2000	9.37	8.11	15.59	170
3000	1.00	1000	0.7	2000	9.32	7.84	18.95	171
1000	0.00	2000	0.7	2000	8.63	7.36	17.21	172
2000	0.00	2000	0.7	2000	9.34	7.66	21.90	173
3000	0.00	2000	0.7	2000	9.32	7.96	17.07	174
3000	0.33	2000	0.7	2000	8.85	7.62	16.17	175
2000	0.50	2000	0.7	2000	8.57	7.55	13.51	176
3000	0.67	2000	0.7	2000	8.49	7.28	16.70	177
1000	1.00	2000	0.7	2000	8.18	7.94	2.98	178
2000	1.00	2000	0.7	2000	8.21	7.44	10.38	179

3000	1.00	2000	0.7	2000	8.25	6.93	19.01	180
1000	0.00	100	0.1	3000	15.37	19.90	22.76	181
2000	0.00	100	0.1	3000	18.76	21.92	14.40	182
3000	0.00	100	0.1	3000	21.51	23.93	10.12	183
3000	0.33	100	0.1	3000	17.41	22.16	21.43	184
2000	0.50	100	0.1	3000	16.59	19.66	15.61	185
3000	0.67	100	0.1	3000	16.39	20.39	19.60	186
1000	1.00	100	0.1	3000	13.72	16.19	15.26	187
2000	1.00	100	0.1	3000	14.67	17.40	15.70	188
3000	1.00	100	0.1	3000	15.61	18.61	16.14	189
1000	0.00	300	0.1	3000	23.43	21.35	9.73	190
2000	0.00	300	0.1	3000	27.14	23.32	16.37	191
3000	0.00	300	0.1	3000	29.81	25.29	17.87	192
3000	0.33	300	0.1	3000	25.21	23.55	7.06	193
2000	0.50	300	0.1	3000	23.62	21.11	11.89	194
3000	0.67	300	0.1	3000	24.49	21.80	12.32	195
1000	1.00	300	0.1	3000	21.15	17.73	19.27	196
2000	1.00	300	0.1	3000	22.24	18.90	17.69	197
3000	1.00	300	0.1	3000	23.25	20.06	15.90	198
1000	0.00	500	0.1	3000	26.35	22.81	15.54	199
2000	0.00	500	0.1	3000	30.16	24.73	21.97	200
3000	0.00	500	0.1	3000	30.53	26.65	14.56	201
3000	0.33	500	0.1	3000	28.26	24.94	13.33	202
2000	0.50	500	0.1	3000	26.57	22.56	17.78	203
3000	0.67	500	0.1	3000	27.22	23.22	17.22	204
1000	1.00	500	0.1	3000	24.18	19.27	25.45	205
2000	1.00	500	0.1	3000	25.25	20.39	23.83	206

3000	1.00	500	0.1	3000	26.12	21.51	21.44	207
1000	0.00	1000	0.1	3000	30.01	26.44	13.52	208
2000	0.00	1000	0.1	3000	32.69	28.24	15.75	209
3000	0.00	1000	0.1	3000	34.31	30.05	14.19	210
3000	0.33	1000	0.1	3000	31.55	28.41	11.07	211
2000	0.50	1000	0.1	3000	30.09	26.18	14.92	212
3000	0.67	1000	0.1	3000	30.37	26.77	13.46	213
1000	1.00	1000	0.1	3000	27.69	23.13	19.73	214
2000	1.00	1000	0.1	3000	28.53	24.13	18.25	215
3000	1.00	1000	0.1	3000	29.4	25.13	17.01	216
1000	0.00	2000	0.1	3000	32.72	33.70	2.91	217
2000	0.00	2000	0.1	3000	35.3	35.27	0.09	218
3000	0.00	2000	0.1	3000	37.02	36.84	0.49	219
3000	0.33	2000	0.1	3000	33.15	35.35	6.22	220
2000	0.50	2000	0.1	3000	31.99	33.43	4.32	221
3000	0.67	2000	0.1	3000	32.14	33.86	5.07	222
1000	1.00	2000	0.1	3000	30.47	30.83	1.18	223
2000	1.00	2000	0.1	3000	31.16	31.60	1.39	224
3000	1.00	2000	0.1	3000	31.19	32.36	3.63	225
1000	0.00	100	0.3	3000	15.34	18.25	15.94	226
2000	0.00	100	0.3	3000	15.26	19.86	23.17	227
3000	0.00	100	0.3	3000	15.74	21.48	26.71	228
3000	0.33	100	0.3	3000	14.3	20.08	28.79	229
2000	0.50	100	0.3	3000	13.55	18.17	25.44	230
3000	0.67	100	0.3	3000	13.23	18.69	29.20	231
1000	1.00	100	0.3	3000	10.6	15.68	32.38	232
2000	1.00	100	0.3	3000	10.69	16.48	35.15	233

3000	1.00	100	0.3	3000	11.24	17.29	35.00	234
1000	0.00	300	0.3	3000	16.69	19.21	13.13	235
2000	0.00	300	0.3	3000	20.17	20.78	2.93	236
3000	0.00	300	0.3	3000	22.48	22.34	0.61	237
3000	0.33	300	0.3	3000	18.52	20.98	11.72	238
2000	0.50	300	0.3	3000	16.81	19.13	12.14	239
3000	0.67	300	0.3	3000	17.45	19.61	11.04	240
1000	1.00	300	0.3	3000	14.71	16.73	12.06	241
2000	1.00	300	0.3	3000	15.7	17.49	10.23	242
3000	1.00	300	0.3	3000	16.34	18.25	10.47	243
1000	0.00	500	0.3	3000	19.49	20.17	3.39	244
2000	0.00	500	0.3	3000	22.83	21.69	5.24	245
3000	0.00	500	0.3	3000	25.07	23.21	8.00	246
3000	0.33	500	0.3	3000	20.94	21.88	4.28	247
2000	0.50	500	0.3	3000	19.42	20.09	3.35	248
3000	0.67	500	0.3	3000	20.06	20.54	2.35	249
1000	1.00	500	0.3	3000	17.53	17.78	1.39	250
2000	1.00	500	0.3	3000	18.44	18.49	0.28	251
3000	1.00	500	0.3	3000	19	19.21	1.08	252
1000	0.00	1000	0.3	3000	22.84	22.58	1.16	253
2000	0.00	1000	0.3	3000	25.8	23.98	7.59	254
3000	0.00	1000	0.3	3000	27.41	25.38	7.99	255
3000	0.33	1000	0.3	3000	24.28	24.12	0.66	256
2000	0.50	1000	0.3	3000	22.76	22.49	1.19	257
3000	0.67	1000	0.3	3000	23.21	22.86	1.53	258
1000	1.00	1000	0.3	3000	20.65	20.41	1.20	259
2000	1.00	1000	0.3	3000	21.38	21.00	1.80	260

3000	1.00	1000	0.3	3000	22.25	21.60	3.01	261
1000	0.00	2000	0.3	3000	25.43	27.39	7.15	262
2000	0.00	2000	0.3	3000	28.08	28.56	1.67	263
3000	0.00	2000	0.3	3000	29.51	29.72	0.72	264
3000	0.33	2000	0.3	3000	26.55	28.61	7.20	265
2000	0.50	2000	0.3	3000	25.23	27.29	7.55	266
3000	0.67	2000	0.3	3000	25.45	27.50	7.44	267
1000	1.00	2000	0.3	3000	23.28	25.66	9.27	268
2000	1.00	2000	0.3	3000	23.99	26.02	7.81	269
3000	1.00	2000	0.3	3000	24.44	26.38	7.37	270
1000	0.00	100	0.5	3000	12.57	16.60	24.27	271
2000	0.00	100	0.5	3000	15.3	17.81	14.09	272
3000	0.00	100	0.5	3000	17.29	19.02	9.10	273
3000	0.33	100	0.5	3000	13.97	18.00	22.41	274
2000	0.50	100	0.5	3000	12.69	16.69	23.96	275
3000	0.67	100	0.5	3000	13.08	16.99	23.01	276
1000	1.00	100	0.5	3000	10.9	15.16	28.10	277
2000	1.00	100	0.5	3000	11.53	15.57	25.93	278
3000	1.00	100	0.5	3000	12.16	15.97	23.87	279
1000	0.00	300	0.5	3000	17.39	17.07	1.87	280
2000	0.00	300	0.5	3000	19.98	18.23	9.57	281
3000	0.00	300	0.5	3000	21.55	19.40	11.09	282
3000	0.33	300	0.5	3000	18.54	18.41	0.70	283
2000	0.50	300	0.5	3000	17.48	17.16	1.88	284
3000	0.67	300	0.5	3000	17.78	17.43	2.03	285
1000	1.00	300	0.5	3000	15.52	15.72	1.28	286
2000	1.00	300	0.5	3000	16.31	16.08	1.43	287

3000	1.00	300	0.5	3000	16.69	16.44	1.53	288
1000	0.00	500	0.5	3000	19.15	17.54	9.17	289
2000	0.00	500	0.5	3000	21.56	18.66	15.55	290
3000	0.00	500	0.5	3000	22.73	19.78	14.94	291
3000	0.33	500	0.5	3000	20.22	18.82	7.44	292
2000	0.50	500	0.5	3000	19.08	17.63	8.25	293
3000	0.67	500	0.5	3000	19.32	17.86	8.16	294
1000	1.00	500	0.5	3000	17.41	16.28	6.93	295
2000	1.00	500	0.5	3000	18.08	16.59	8.96	296
3000	1.00	500	0.5	3000	18.43	16.91	9.02	297
1000	0.00	1000	0.5	3000	20.78	18.72	11.00	298
2000	0.00	1000	0.5	3000	22.35	19.72	13.33	299
3000	0.00	1000	0.5	3000	18.7	20.72	9.75	300
3000	0.33	1000	0.5	3000	21.77	19.84	9.74	301
2000	0.50	1000	0.5	3000	20.66	18.80	9.90	302
3000	0.67	1000	0.5	3000	20.97	18.95	10.63	303
1000	1.00	1000	0.5	3000	19.17	17.68	8.41	304
2000	1.00	1000	0.5	3000	19.51	17.88	9.14	305
3000	1.00	1000	0.5	3000	20.27	18.07	12.17	306
1000	0.00	2000	0.5	3000	19.57	21.08	7.16	307
2000	0.00	2000	0.5	3000	19.84	21.84	9.17	308
3000	0.00	2000	0.5	3000	19.03	22.61	15.83	309
3000	0.33	2000	0.5	3000	21.06	21.87	3.72	310
2000	0.50	2000	0.5	3000	20.03	21.14	5.27	311
3000	0.67	2000	0.5	3000	20.53	21.14	2.88	312
1000	1.00	2000	0.5	3000	18.7	20.48	8.71	313
2000	1.00	2000	0.5	3000	19.42	20.44	5.01	314

3000	1.00	2000	0.5	3000	19.92	20.40	2.37	315
1000	0.00	100	0.7	3000	16.11	14.95	7.77	316
2000	0.00	100	0.7	3000	17.7	15.76	12.33	317
3000	0.00	100	0.7	3000	18.96	16.57	14.46	318
3000	0.33	100	0.7	3000	16.81	15.93	5.54	319
2000	0.50	100	0.7	3000	15.93	15.20	4.78	320
3000	0.67	100	0.7	3000	16.12	15.29	5.43	321
1000	1.00	100	0.7	3000	14.65	14.65	0.03	322
2000	1.00	100	0.7	3000	15.16	14.65	3.49	323
3000	1.00	100	0.7	3000	15.34	14.65	4.69	324
1000	0.00	300	0.7	3000	18.18	14.93	21.77	325
2000	0.00	300	0.7	3000	17.99	15.69	14.65	326
3000	0.00	300	0.7	3000	14.78	16.45	10.17	327
3000	0.33	300	0.7	3000	18.59	15.84	17.33	328
2000	0.50	300	0.7	3000	17.88	15.18	17.78	329
3000	0.67	300	0.7	3000	17.97	15.24	17.94	330
1000	1.00	300	0.7	3000	16.8	14.72	14.17	331
2000	1.00	300	0.7	3000	17.06	14.67	16.28	332
3000	1.00	300	0.7	3000	17.1	14.63	16.90	333
1000	0.00	500	0.7	3000	17.87	14.91	19.85	334
2000	0.00	500	0.7	3000	14.86	15.63	4.90	335
3000	0.00	500	0.7	3000	14.51	16.34	11.20	336
3000	0.33	500	0.7	3000	18.21	15.76	15.54	337
2000	0.50	500	0.7	3000	17.77	15.16	17.22	338
3000	0.67	500	0.7	3000	17.97	15.18	18.36	339
1000	1.00	500	0.7	3000	17.07	14.79	15.45	340
2000	1.00	500	0.7	3000	17.31	14.69	17.80	341

3000	1.00	500	0.7	3000	17.04	14.60	16.68	342
1000	0.00	1000	0.7	3000	15.23	14.86	2.47	343
2000	0.00	1000	0.7	3000	14.05	15.46	9.12	344
3000	0.00	1000	0.7	3000	14.13	16.06	12.00	345
3000	0.33	1000	0.7	3000	14.27	15.55	8.25	346
2000	0.50	1000	0.7	3000	15.81	15.11	4.66	347
3000	0.67	1000	0.7	3000	16.24	15.05	7.92	348
1000	1.00	1000	0.7	3000	15.48	14.96	3.48	349
2000	1.00	1000	0.7	3000	15.88	14.75	7.65	350
3000	1.00	1000	0.7	3000	15.94	14.54	9.60	351
1000	0.00	2000	0.7	3000	13.89	14.77	5.95	352
2000	0.00	2000	0.7	3000	14.02	15.13	7.34	353
3000	0.00	2000	0.7	3000	14.09	15.49	9.05	354
3000	0.33	2000	0.7	3000	14.05	15.14	7.17	355
2000	0.50	2000	0.7	3000	13.98	15.00	6.79	356
3000	0.67	2000	0.7	3000	14.05	14.78	4.93	357
1000	1.00	2000	0.7	3000	13.86	15.31	9.46	358
2000	1.00	2000	0.7	3000	13.74	14.87	7.57	359
3000	1.00	2000	0.7	3000	13.83	14.42	4.11	360

From the results, “f(x)” could applicable better use in most of cases, over 85% cases which relative error were less than 20%, and over 66% cases which relative error were less than 15% We can find relative error in most of simulations could less than 20% (detail in section 5.2). Cases which relative error was bigger than 20% have common features: most of their clay content is 0.3 or 0.5, sedimentation rate are small in parameter space and most of their bending degree value are “1”.

Appendix B

To examine importance of the seven key parameters in function G(Z), 12 groups of models, which have different channel-levee systems size and position, were created. In each group, the four parameters in function f(X) were different. These systematic simulations are mainly to test at what conditions the importance of the four factors could be ignored in function G(Z).

In simulations, g(X*, z) is the CLS effects when sedimentation rate, over-burden clay content, aquifer depth and relief (100 m/Ma, 0.1, 2000m, 2000m) are held constant. So if the results could show that g(X*, z) make little difference with each G(Z) relative to f(X), the four factors (R, P, D, H) can be 'ignored' in the sense they are fixed. Last column is relative error on LT effect which is a percentage: 100* (G(Z)-g(X*,z)) / f(X).

Group 1											
Burial Rate (R)	**Clay content (P)**	**RP Depth (D)**	**Relief (H)**	**CLS Size (S)**	**CLS Location (L)**	**CLS Depth (d)**	**f(X)**	**F(Y)**	**G(Z)**	**G(Z)-g(X*z)**	**Error %**
100	0.1	2000	2000	0.1	0.3	0.1	12.19	9.98	2.21	0	0.00
500	0.1	2000	2000	0.1	0.3	0.1	19.71	17.64	2.07	0.14	0.71
800	0.1	2000	2000	0.1	0.3	0.1	21.21	19.5	1.71	0.5	2.36
1000	0.1	2000	2000	0.1	0.3	0.1	21.78	20.29	1.49	0.72	3.31
100	0.3	2000	2000	0.1	0.3	0.1	7.92	6.29	1.63	0.58	7.32
500	0.3	2000	2000	0.1	0.3	0.1	14.32	12.6	1.72	0.49	3.42
800	0.3	2000	2000	0.1	0.3	0.1	15.87	14.37	1.5	0.71	4.47
100	0.5	2000	2000	0.1	0.3	0.1	9.41	7.95	1.46	0.75	7.97
100	0.1	3000	2000	0.1	0.3	0.1	19.02	16.08	2.94	0.73	3.84
500	0.1	3000	2000	0.1	0.3	0.1	30.37	27.72	2.65	0.44	1.45
800	0.1	3000	2000	0.1	0.3	0.1	31.92	30.4	1.52	0.69	2.16
1000	0.1	3000	2000	0.1	0.3	0.1	32.87	31.18	1.69	0.52	1.58
100	0.3	3000	2000	0.1	0.3	0.1	14.27	11.88	2.39	0.18	1.26
500	0.3	3000	2000	0.1	0.3	0.1	23.9	21.84	2.06	0.15	0.63
800	0.3	3000	2000	0.1	0.3	0.1	26.03	24.33	1.7	0.51	1.96
100	0.5	3000	2000	0.1	0.3	0.1	16.36	14.32	2.04	0.17	1.04
100	0.1	2000	3000	0.1	0.3	0.1	14.55	12.32	2.23	0.02	0.14
500	0.1	2000	3000	0.1	0.3	0.1	21.67	20.34	1.33	0.88	4.06
800	0.1	2000	3000	0.1	0.3	0.1	22.87	21.91	0.96	1.25	5.47
1000	0.1	2000	3000	0.1	0.3	0.1	23.42	22.55	0.87	1.34	5.72
100	0.3	2000	3000	0.1	0.3	0.1	9.82	8.13	1.69	0.52	5.30
500	0.3	2000	3000	0.1	0.3	0.1	16.31	15.04	1.27	0.94	5.76
800	0.3	2000	3000	0.1	0.3	0.1	17.61	16.68	0.93	1.28	7.27
100	0.5	2000	3000	0.1	0.3	0.1	11.17	9.85	1.32	0.89	7.97
100	0.1	3000	3000	0.1	0.3	0.1	21.55	18.38	3.17	0.96	4.45
500	0.1	3000	3000	0.1	0.3	0.1	31	30.39	0.61	1.6	5.16

800	0.1	3000	3000	0.1	0.3	0.1	33.16	32.01	1.15	1.06	3.20
1000	0.1	3000	3000	0.1	0.3	0.1	34.37	32.89	1.48	0.73	2.12
100	0.3	3000	3000	0.1	0.3	0.1	16.45	13.9	2.55	0.34	2.07
500	0.3	3000	3000	0.1	0.3	0.1	25.95	24.23	1.72	0.49	1.89
800	0.3	3000	3000	0.1	0.3	0.1	27.76	26.55	1.21	1	3.60
100	0.5	3000	3000	0.1	0.3	0.1	18.27	16.25	2.02	0.19	1.04
Group 2											
Burial Rate (R)	**Clay content (P)**	**RP Depth (D)**	**Relief (H)**	**CLS Size (S)**	**CLS Location (L)**	**CLS Depth (d)**	**f(X)**	**F(Y)**	**G(Z)**	**G(Z)-g(X*z)**	**Error %**
100	0.1	2000	2000	0.2	0.3	0.1	12.19	8.03	4.16	0	0.00
500	0.1	2000	2000	0.2	0.3	0.1	19.71	15.91	3.8	0.36	1.83
800	0.1	2000	2000	0.2	0.3	0.1	21.21	18.06	3.15	1.01	4.76
1000	0.1	2000	2000	0.2	0.3	0.1	21.78	19	2.78	1.38	6.34
100	0.3	2000	2000	0.2	0.3	0.1	7.92	5.17	2.75	1.41	17.80
500	0.3	2000	2000	0.2	0.3	0.1	14.32	11.47	2.85	1.31	9.15
800	0.3	2000	2000	0.2	0.3	0.1	15.87	13.41	2.46	1.7	10.71
100	0.5	2000	2000	0.2	0.3	0.1	9.41	7.15	2.26	1.9	20.19
100	0.1	3000	2000	0.2	0.3	0.1	19.02	13.55	5.47	1.31	6.89
500	0.1	3000	2000	0.2	0.3	0.1	30.37	25.91	4.46	0.3	0.99
800	0.1	3000	2000	0.2	0.3	0.1	31.92	29.01	2.91	1.25	3.92
1000	0.1	3000	2000	0.2	0.3	0.1	32.87	30.31	2.56	1.6	4.87
100	0.3	3000	2000	0.2	0.3	0.1	14.27	10.37	3.9	0.26	1.82
500	0.3	3000	2000	0.2	0.3	0.1	23.9	20.83	3.07	1.09	4.56
800	0.3	3000	2000	0.2	0.3	0.1	26.03	23.64	2.39	1.77	6.80
100	0.5	3000	2000	0.2	0.3	0.1	16.36	13.46	2.9	1.26	7.70
100	0.1	2000	3000	0.2	0.3	0.1	14.55	10.21	4.34	0.18	1.24
500	0.1	2000	3000	0.2	0.3	0.1	21.67	18.9	2.77	1.39	6.41
800	0.1	2000	3000	0.2	0.3	0.1	22.87	20.91	1.96	2.2	9.62
1000	0.1	2000	3000	0.2	0.3	0.1	23.42	21.7	1.72	2.44	10.42
100	0.3	2000	3000	0.2	0.3	0.1	9.82	6.89	2.93	1.23	12.53
500	0.3	2000	3000	0.2	0.3	0.1	16.31	14.09	2.22	1.94	11.89
800	0.3	2000	3000	0.2	0.3	0.1	17.61	15.99	1.62	2.54	14.42
100	0.5	2000	3000	0.2	0.3	0.1	11.17	9.1	2.07	2.09	18.71
100	0.1	3000	3000	0.2	0.3	0.1	21.55	15.61	5.94	1.78	8.26
500	0.1	3000	3000	0.2	0.3	0.1	31	28.7	2.3	1.86	6.00
800	0.1	3000	3000	0.2	0.3	0.1	33.16	30.88	2.28	1.88	5.67
1000	0.1	3000	3000	0.2	0.3	0.1	34.37	32.12	2.25	1.91	5.56
100	0.3	3000	3000	0.2	0.3	0.1	16.45	12.24	4.21	0.05	0.30
500	0.3	3000	3000	0.2	0.3	0.1	25.95	23.34	2.61	1.55	5.97
800	0.3	3000	3000	0.2	0.3	0.1	27.76	26.02	1.74	2.42	8.72
100	0.5	3000	3000	0.2	0.3	0.1	18.27	15.37	2.9	1.26	6.90
Group 3											
Burial Rate (R)	**Clay content (P)**	**RP Depth (D)**	**Relief (H)**	**CLS Size (S)**	**CLS Location (L)**	**CLS Depth (d)**	**f(X)**	**F(Y)**	**G(Z)**	**G(Z)-g(X*z)**	**Error %**
100	0.1	2000	2000	0.1	0.7	0.1	12.19	11.4	0.79	0	0.00

500	0.1	2000	2000	0.1	0.7	0.1	19.71	19.11	0.6	0.19	0.96
800	0.1	2000	2000	0.1	0.7	0.1	21.21	20.78	0.43	0.36	1.70
1000	0.1	2000	2000	0.1	0.7	0.1	21.78	21.44	0.34	0.45	2.07
100	0.3	2000	2000	0.1	0.7	0.1	7.92	7.3	0.62	0.17	2.15
500	0.3	2000	2000	0.1	0.7	0.1	14.32	13.74	0.58	0.21	1.47
800	0.3	2000	2000	0.1	0.7	0.1	15.87	15.39	0.48	0.31	1.95
100	0.5	2000	2000	0.1	0.7	0.1	9.41	8.84	0.57	0.22	2.34
100	0.1	3000	2000	0.1	0.7	0.1	19.02	17.64	1.38	0.59	3.10
500	0.1	3000	2000	0.1	0.7	0.1	30.37	29.32	1.05	0.26	0.86
800	0.1	3000	2000	0.1	0.7	0.1	31.92	31.28	0.64	0.15	0.47
1000	0.1	3000	2000	0.1	0.7	0.1	32.87	32.39	0.48	0.31	0.94
100	0.3	3000	2000	0.1	0.7	0.1	14.27	13.14	1.13	0.34	2.38
500	0.3	3000	2000	0.1	0.7	0.1	23.9	23.04	0.86	0.07	0.29
800	0.3	3000	2000	0.1	0.7	0.1	26.03	25.34	0.69	0.1	0.38
100	0.5	3000	2000	0.1	0.7	0.1	16.36	15.39	0.97	0.18	1.10
100	0.1	2000	3000	0.1	0.7	0.1	14.55	14.05	0.5	0.29	1.99
500	0.1	2000	3000	0.1	0.7	0.1	21.67	21.44	0.23	0.56	2.58
800	0.1	2000	3000	0.1	0.7	0.1	22.87	22.37	0.5	0.29	1.27
1000	0.1	2000	3000	0.1	0.7	0.1	23.42	23.36	0.06	0.73	3.12
100	0.3	2000	3000	0.1	0.7	0.1	9.82	9.36	0.46	0.33	3.36
500	0.3	2000	3000	0.1	0.7	0.1	16.31	15.99	0.32	0.47	2.88
800	0.3	2000	3000	0.1	0.7	0.1	17.61	17.37	0.24	0.55	3.12
100	0.5	2000	3000	0.1	0.7	0.1	11.17	10.78	0.39	0.4	3.58
100	0.1	3000	3000	0.1	0.7	0.1	21.55	20.5	1.05	0.26	1.21
500	0.1	3000	3000	0.1	0.7	0.1	31	30.62	0.38	0.41	1.32
800	0.1	3000	3000	0.1	0.7	0.1	33.16	32.91	0.25	0.54	1.63
1000	0.1	3000	3000	0.1	0.7	0.1	34.37	34.16	0.21	0.58	1.69
100	0.3	3000	3000	0.1	0.7	0.1	16.45	15.56	0.89	0.1	0.61
500	0.3	3000	3000	0.1	0.7	0.1	25.95	25.43	0.52	0.27	1.04
800	0.3	3000	3000	0.1	0.7	0.1	27.76	27.4	0.36	0.43	1.55
100	0.5	3000	3000	0.1	0.7	0.1	18.27	17.56	0.71	0.08	0.44
Group 4											
Burial Rate (R)	**Clay content (P)**	**RP Depth (D)**	**Relief (H)**	**CLS Size (S)**	**CLS Location (L)**	**CLS Depth (d)**	**f(X)**	**F(Y)**	**G(Z)**	**G(Z)-g(X*z)**	**Error %**
100	0.1	2000	2000	0.2	0.7	0.1	12.19	10.15	2.04	0	0.00
500	0.1	2000	2000	0.2	0.7	0.1	19.71	18.29	1.42	0.62	3.15
800	0.1	2000	2000	0.2	0.7	0.1	21.21	20.21	1	1.04	4.90
1000	0.1	2000	2000	0.2	0.7	0.1	21.78	20.98	0.8	1.24	5.69
100	0.3	2000	2000	0.2	0.7	0.1	7.92	6.64	1.28	0.76	9.60
500	0.3	2000	2000	0.2	0.7	0.1	14.32	13.2	1.12	0.92	6.42
800	0.3	2000	2000	0.2	0.7	0.1	15.87	14.97	0.9	1.14	7.18
100	0.5	2000	2000	0.2	0.7	0.1	9.41	8.38	1.03	1.01	10.73
100	0.1	3000	2000	0.2	0.7	0.1	19.02	15.81	3.21	1.17	6.15
500	0.1	3000	2000	0.2	0.7	0.1	30.37	28.26	2.11	0.07	0.23
800	0.1	3000	2000	0.2	0.7	0.1	31.92	31.08	0.84	1.2	3.76
1000	0.1	3000	2000	0.2	0.7	0.1	32.87	31.88	0.99	1.05	3.19

100	0.3	3000	2000	0.2	0.7	0.1	14.27	12.16	2.11	0.07	0.49
500	0.3	3000	2000	0.2	0.7	0.1	23.9	22.44	1.46	0.58	2.43
800	0.3	3000	2000	0.2	0.7	0.1	26.03	24.91	1.12	0.92	3.53
100	0.5	3000	2000	0.2	0.7	0.1	16.36	14.81	1.55	0.49	3.00
100	0.1	2000	3000	0.2	0.7	0.1	14.55	12.93	1.62	0.42	2.89
500	0.1	2000	3000	0.2	0.7	0.1	21.67	21.01	0.66	1.38	6.37
800	0.1	2000	3000	0.2	0.7	0.1	22.87	22.43	0.44	1.6	7.00
1000	0.1	2000	3000	0.2	0.7	0.1	23.42	23.04	0.38	1.66	7.09
100	0.3	2000	3000	0.2	0.7	0.1	9.82	8.78	1.04	1	10.18
500	0.3	2000	3000	0.2	0.7	0.1	16.31	15.63	0.68	1.36	8.34
800	0.3	2000	3000	0.2	0.7	0.1	17.61	17.13	0.48	1.56	8.86
100	0.5	2000	3000	0.2	0.7	0.1	11.17	10.41	0.76	1.28	11.46
100	0.1	3000	3000	0.2	0.7	0.1	21.55	18.76	2.79	0.75	3.48
500	0.1	3000	3000	0.2	0.7	0.1	31	30.31	0.69	1.35	4.35
800	0.1	3000	3000	0.2	0.7	0.1	33.16	32.64	0.52	1.52	4.58
1000	0.1	3000	3000	0.2	0.7	0.1	34.37	33.89	0.48	1.56	4.54
100	0.3	3000	3000	0.2	0.7	0.1	16.45	14.67	1.78	0.26	1.58
500	0.3	3000	3000	0.2	0.7	0.1	25.95	25	0.95	1.09	4.20
800	0.3	3000	3000	0.2	0.7	0.1	27.76	27.12	0.64	1.4	5.04
100	0.5	3000	3000	0.2	0.7	0.1	18.27	17.05	1.22	0.82	4.49
Group 5											
Burial Rate (R)	**Clay content (P)**	**RP Depth (D)**	**Relief (H)**	**CLS Size (S)**	**CLS Location (L)**	**CLS Depth (d)**	**f(X)**	**F(Y)**	**G(Z)**	**G(Z)-g(X*z)**	**Error %**
100	0.1	2000	2000	0.1	0.3	0.2	12.19	10.74	1.45	0	0.00
500	0.1	2000	2000	0.1	0.3	0.2	19.71	18.55	1.16	0.29	1.47
800	0.1	2000	2000	0.1	0.3	0.2	21.21	20.3	0.91	0.54	2.55
1000	0.1	2000	2000	0.1	0.3	0.2	21.78	21.01	0.77	0.68	3.12
100	0.3	2000	2000	0.1	0.3	0.2	7.92	6.97	0.95	0.5	6.31
500	0.3	2000	2000	0.1	0.3	0.2	14.32	13.48	0.84	0.61	4.26
800	0.3	2000	2000	0.1	0.3	0.2	15.87	15.18	0.69	0.76	4.79
100	0.5	2000	2000	0.1	0.3	0.2	9.41	8.76	0.65	0.8	8.50
100	0.1	3000	2000	0.1	0.3	0.2	19.02	17.16	1.86	0.41	2.16
500	0.1	3000	2000	0.1	0.3	0.2	30.37	28.93	1.44	0.01	0.03
800	0.1	3000	2000	0.1	0.3	0.2	31.92	31.33	0.59	0.86	2.69
1000	0.1	3000	2000	0.1	0.3	0.2	32.87	31.9	0.97	0.48	1.46
100	0.3	3000	2000	0.1	0.3	0.2	14.27	12.99	1.28	0.17	1.19
500	0.3	3000	2000	0.1	0.3	0.2	23.9	23.01	0.89	0.56	2.34
800	0.3	3000	2000	0.1	0.3	0.2	26.03	25.35	0.68	0.77	2.96
100	0.5	3000	2000	0.1	0.3	0.2	16.36	15.56	0.8	0.65	3.97
100	0.1	2000	3000	0.1	0.3	0.2	14.55	13.14	1.41	0.04	0.27
500	0.1	2000	3000	0.1	0.3	0.2	21.67	20.98	0.69	0.76	3.51
800	0.1	2000	3000	0.1	0.3	0.2	22.87	22.34	0.53	0.92	4.02
1000	0.1	2000	3000	0.1	0.3	0.2	23.42	22.91	0.51	0.94	4.01
100	0.3	2000	3000	0.1	0.3	0.2	9.82	8.88	0.94	0.51	5.19
500	0.3	2000	3000	0.1	0.3	0.2	16.31	15.72	0.59	0.86	5.27
800	0.3	2000	3000	0.1	0.3	0.2	17.61	17.2	0.41	1.04	5.91

100	0.5	2000	3000	0.1	0.3	0.2	11.17	10.62	0.55	0.9	8.06
100	0.1	3000	3000	0.1	0.3	0.2	21.55	19.61	1.94	0.49	2.27
500	0.1	3000	3000	0.1	0.3	0.2	31	30.74	0.26	1.19	3.84
800	0.1	3000	3000	0.1	0.3	0.2	33.16	32.6	0.56	0.89	2.68
1000	0.1	3000	3000	0.1	0.3	0.2	34.37	33.53	0.84	0.61	1.77
100	0.3	3000	3000	0.1	0.3	0.2	16.45	15.14	1.31	0.14	0.85
500	0.3	3000	3000	0.1	0.3	0.2	25.95	25.26	0.69	0.76	2.93
800	0.3	3000	3000	0.1	0.3	0.2	27.76	27.31	0.45	1	3.60
100	0.5	3000	3000	0.1	0.3	0.2	18.27	17.53	0.74	0.71	3.89
Group 6											
Burial Rate (R)	**Clay content (P)**	**RP Depth (D)**	**Relief (H)**	**CLS Size (S)**	**CLS Location (L)**	**CLS Depth (d)**	**f(X)**	**F(Y)**	**G(Z)**	**G(Z)-g(X*z)**	**Error %**
100	0.1	2000	2000	0.2	0.3	0.2	12.19	9.58	2.61	0	0.00
500	0.1	2000	2000	0.2	0.3	0.2	19.71	17.61	2.1	0.51	2.59
800	0.1	2000	2000	0.2	0.3	0.2	21.21	19.53	1.68	0.93	4.38
1000	0.1	2000	2000	0.2	0.3	0.2	21.78	20.32	1.46	1.15	5.28
100	0.3	2000	2000	0.2	0.3	0.2	7.92	6.44	1.48	1.13	14.27
500	0.3	2000	2000	0.2	0.3	0.2	14.32	13.02	1.3	1.31	9.15
800	0.3	2000	2000	0.2	0.3	0.2	15.87	14.83	1.04	1.57	9.89
100	0.5	2000	2000	0.2	0.3	0.2	9.41	8.65	0.76	1.85	19.66
100	0.1	3000	2000	0.2	0.3	0.2	19.02	15.71	3.31	0.7	3.68
500	0.1	3000	2000	0.2	0.3	0.2	30.37	27.96	2.41	0.2	0.66
800	0.1	3000	2000	0.2	0.3	0.2	31.92	30.66	1.26	1.35	4.23
1000	0.1	3000	2000	0.2	0.3	0.2	32.87	31.21	1.66	0.95	2.89
100	0.3	3000	2000	0.2	0.3	0.2	14.27	12.33	1.94	0.67	4.70
500	0.3	3000	2000	0.2	0.3	0.2	23.9	22.68	1.22	1.39	5.82
800	0.3	3000	2000	0.2	0.3	0.2	26.03	25.17	0.86	1.75	6.72
100	0.5	3000	2000	0.2	0.3	0.2	16.36	15.59	0.77	1.84	11.25
100	0.1	2000	3000	0.2	0.3	0.2	14.55	11.9	2.65	0.04	0.27
500	0.1	2000	3000	0.2	0.3	0.2	21.67	20.25	1.42	1.19	5.49
800	0.1	2000	3000	0.2	0.3	0.2	22.87	21.86	1.01	1.6	7.00
1000	0.1	2000	3000	0.2	0.3	0.2	23.42	22.43	0.99	1.62	6.92
100	0.3	2000	3000	0.2	0.3	0.2	9.82	8.3	1.52	1.09	11.10
500	0.3	2000	3000	0.2	0.3	0.2	16.31	15.37	0.94	1.67	10.24
800	0.3	2000	3000	0.2	0.3	0.2	17.61	16.98	0.63	1.98	11.24
100	0.5	2000	3000	0.2	0.3	0.2	11.17	10.3	0.87	1.74	15.58
100	0.1	3000	3000	0.2	0.3	0.2	21.55	18.08	3.47	0.86	3.99
500	0.1	3000	3000	0.2	0.3	0.2	31	30.64	0.36	2.25	7.26
800	0.1	3000	3000	0.2	0.3	0.2	33.16	32.25	0.91	1.7	5.13
1000	0.1	3000	3000	0.2	0.3	0.2	34.37	33.07	1.3	1.31	3.81
100	0.3	3000	3000	0.2	0.3	0.2	16.45	14.46	1.99	0.62	3.77
500	0.3	3000	3000	0.2	0.3	0.2	25.95	25.03	0.92	1.69	6.51
800	0.3	3000	3000	0.2	0.3	0.2	27.76	27.23	0.53	2.08	7.49
100	0.5	3000	3000	0.2	0.3	0.2	18.27	17.6	0.67	1.94	10.62
Group 7											

Burial Rate (R)	Clay content (P)	RP Depth (D)	Relief (H)	CLS Size (S)	CLS Location (L)	CLS Depth (d)	f(X)	F(Y)	G(Z)	G(Z)-g(X*z)	Error %
100	0.1	2000	2000	0.1	0.7	0.2	12.19	11.61	0.58	0	0.00
500	0.1	2000	2000	0.1	0.7	0.2	19.71	19.32	0.39	0.19	0.96
800	0.1	2000	2000	0.1	0.7	0.2	21.21	20.94	0.27	0.31	1.46
1000	0.1	2000	2000	0.1	0.7	0.2	21.78	21.58	0.2	0.38	1.74
500	0.3	2000	2000	0.1	0.7	0.2	14.32	13.97	0.35	0.23	1.61
800	0.3	2000	2000	0.1	0.7	0.2	15.87	15.59	0.28	0.3	1.89
100	0.5	2000	2000	0.1	0.7	0.2	9.41	9.1	0.31	0.27	2.87
100	0.1	3000	2000	0.1	0.7	0.2	19.02	18.08	0.94	0.36	1.89
500	0.1	3000	2000	0.1	0.7	0.2	30.37	29.77	0.6	0.02	0.07
800	0.1	3000	2000	0.1	0.7	0.2	31.92	31.59	0.33	0.25	0.78
100	0.3	3000	2000	0.1	0.7	0.2	14.27	13.62	0.65	0.07	0.49
500	0.3	3000	2000	0.1	0.7	0.2	23.9	23.46	0.44	0.14	0.59
800	0.3	3000	2000	0.1	0.7	0.2	26.03	25.69	0.34	0.24	0.92
100	0.5	3000	2000	0.1	0.7	0.2	16.36	15.9	0.46	0.12	0.73
100	0.1	2000	3000	0.1	0.7	0.2	14.55	14.11	0.44	0.14	0.96
500	0.1	2000	3000	0.1	0.7	0.2	21.67	21.49	0.18	0.4	1.85
800	0.1	2000	3000	0.1	0.7	0.2	22.87	22.77	0.1	0.48	2.10
1000	0.1	2000	3000	0.1	0.7	0.2	23.42	23.35	0.07	0.51	2.18
100	0.3	2000	3000	0.1	0.7	0.2	9.82	9.49	0.33	0.25	2.55
500	0.3	2000	3000	0.1	0.7	0.2	16.31	16.09	0.22	0.36	2.21
800	0.3	2000	3000	0.1	0.7	0.2	17.61	17.45	0.16	0.42	2.39
100	0.5	2000	3000	0.1	0.7	0.2	11.17	10.93	0.24	0.34	3.04
100	0.1	3000	3000	0.1	0.7	0.2	21.55	20.77	0.78	0.2	0.93
500	0.1	3000	3000	0.1	0.7	0.2	31	30.77	0.23	0.35	1.13
800	0.1	3000	3000	0.1	0.7	0.2	33.16	33	0.16	0.42	1.27
1000	0.1	3000	3000	0.1	0.7	0.2	34.37	34.25	0.12	0.46	1.34
100	0.3	3000	3000	0.1	0.7	0.2	16.45	15.91	0.54	0.04	0.24
500	0.3	3000	3000	0.1	0.7	0.2	25.95	25.66	0.29	0.29	1.12
800	0.3	3000	3000	0.1	0.7	0.2	27.76	27.56	0.2	0.38	1.37
100	0.5	3000	3000	0.1	0.7	0.2	18.27	17.9	0.37	0.21	1.15
Group 8											
Burial Rate (R)	**Clay content (P)**	**RP Depth (D)**	**Relief (H)**	**CLS Size (S)**	**CLS Location (L)**	**CLS Depth (d)**	**f(X)**	**F(Y)**	**G(Z)**	**G(Z)-g(X*z)**	**Error %**
100	0.1	2000	2000	0.2	0.7	0.2	12.19	10.94	1.25	0	0.00
500	0.1	2000	2000	0.2	0.7	0.2	19.71	18.93	0.78	0.47	2.38
800	0.1	2000	2000	0.2	0.7	0.2	21.21	20.68	0.53	0.72	3.39
1000	0.1	2000	2000	0.2	0.7	0.2	21.78	21.37	0.41	0.84	3.86
100	0.3	2000	2000	0.2	0.7	0.2	7.92	7.23	0.69	0.56	7.07
500	0.3	2000	2000	0.2	0.7	0.2	14.32	13.75	0.57	0.68	4.75
800	0.3	2000	2000	0.2	0.7	0.2	15.87	15.43	0.44	0.81	5.10
100	0.5	2000	2000	0.2	0.7	0.2	9.41	8.95	0.46	0.79	8.40
100	0.1	3000	2000	0.2	0.7	0.2	19.02	17.13	1.89	0.64	3.36
500	0.1	3000	2000	0.2	0.7	0.2	30.37	29.27	1.1	0.15	0.49
800	0.1	3000	2000	0.2	0.7	0.2	31.92	31.37	0.55	0.7	2.19

1000	0.1	3000	2000	0.2	0.7	0.2	32.87	32.42	0.45	0.8	2.43
100	0.3	3000	2000	0.2	0.7	0.2	14.27	13.22	1.05	0.2	1.40
500	0.3	3000	2000	0.2	0.7	0.2	23.9	23.23	0.67	0.58	2.43
800	0.3	3000	2000	0.2	0.7	0.2	26.03	25.54	0.49	0.76	2.92
100	0.5	3000	2000	0.2	0.7	0.2	16.36	15.79	0.57	0.68	4.16
100	0.1	2000	3000	0.2	0.7	0.2	14.55	13.52	1.03	0.22	1.51
500	0.1	2000	3000	0.2	0.7	0.2	21.67	21.3	0.37	0.88	4.06
800	0.1	2000	3000	0.2	0.7	0.2	22.87	22.61	0.26	0.99	4.33
1000	0.1	2000	3000	0.2	0.7	0.2	23.42	23.19	0.23	1.02	4.36
100	0.3	2000	3000	0.2	0.7	0.2	9.82	9.23	0.59	0.66	6.72
500	0.3	2000	3000	0.2	0.7	0.2	16.31	15.94	0.37	0.88	5.40
800	0.3	2000	3000	0.2	0.7	0.2	17.61	17.36	0.25	1	5.68
100	0.5	2000	3000	0.2	0.7	0.2	11.17	10.8	0.37	0.88	7.88
100	0.1	3000	3000	0.2	0.7	0.2	21.55	19.89	1.66	0.41	1.90
500	0.1	3000	3000	0.2	0.7	0.2	31	30.55	0.45	0.8	2.58
800	0.1	3000	3000	0.2	0.7	0.2	33.16	32.88	0.28	0.97	2.93
1000	0.1	3000	3000	0.2	0.7	0.2	34.37	34.13	0.24	1.01	2.94
100	0.3	3000	3000	0.2	0.7	0.2	16.45	15.55	0.9	0.35	2.13
500	0.3	3000	3000	0.2	0.7	0.2	25.95	25.49	0.46	0.79	3.04
800	0.3	3000	3000	0.2	0.7	0.2	27.76	27.46	0.3	0.95	3.42
100	0.5	3000	3000	0.2	0.7	0.2	18.27	17.78	0.49	0.76	4.16
Group 9											
Burial Rate (R)	**Clay content (P)**	**RP Depth (D)**	**Relief (H)**	**CLS Size (S)**	**CLS Location (L)**	**CLS Depth (d)**	**f(X)**	**F(Y)**	**G(Z)**	**G(Z)-g(X*z)**	**Error %**
100	0.1	2000	2000	0.1	0.3	0.4	12.19	11.41	0.78	0	0.00
500	0.1	2000	2000	0.1	0.3	0.4	19.71	19.08	0.63	0.15	0.76
800	0.1	2000	2000	0.1	0.3	0.4	21.21	20.7	0.51	0.27	1.27
1000	0.1	2000	2000	0.1	0.3	0.4	21.78	21.34	0.44	0.34	1.56
500	0.3	2000	2000	0.1	0.3	0.4	14.32	14.04	0.28	0.5	3.49
100	0.1	3000	2000	0.1	0.3	0.4	19.02	18.07	0.95	0.17	0.89
500	0.1	3000	2000	0.1	0.3	0.4	30.37	29.58	0.79	0.01	0.03
1000	0.1	3000	2000	0.1	0.3	0.4	32.87	32.3	0.57	0.21	0.64
100	0.3	3000	2000	0.1	0.3	0.4	14.27	13.87	0.4	0.38	2.66
100	0.1	2000	3000	0.1	0.3	0.4	14.55	13.8	0.75	0.03	0.21
500	0.1	2000	3000	0.1	0.3	0.4	21.67	21.3	0.37	0.41	1.89
800	0.1	2000	3000	0.1	0.3	0.4	22.87	22.54	0.33	0.45	1.97
1000	0.1	2000	3000	0.1	0.3	0.4	23.42	23.07	0.35	0.43	1.84
100	0.3	2000	3000	0.1	0.3	0.4	9.82	9.49	0.33	0.45	4.58
500	0.3	2000	3000	0.1	0.3	0.4	16.31	16.12	0.19	0.59	3.62
100	0.1	3000	3000	0.1	0.3	0.4	21.55	20.58	0.97	0.19	0.88
500	0.1	3000	3000	0.1	0.3	0.4	31	30.48	0.52	0.26	0.84
1000	0.1	3000	3000	0.1	0.3	0.4	34.37	33.82	0.55	0.23	0.67
100	0.3	3000	3000	0.1	0.3	0.4	16.45	16.07	0.38	0.4	2.43
Group 10											
Burial Rate	**Clay content**	**RP Depth**	**Relief**	**CLS Size**	**CLS Location**	**CLS Depth (d)**	**f(X)**	**F(Y)**	**G(Z)**	**G(Z)-g(X*z)**	**Error %**

(R)	(P)	(D)	(H)	(S)	(L)						
100	0.1	2000	2000	0.2	0.3	0.4	12.19	10.66	1.53	0	0.00
500	0.1	2000	2000	0.2	0.3	0.4	19.71	18.34	1.37	0.16	0.81
800	0.1	2000	2000	0.2	0.3	0.4	21.21	20.04	1.17	0.36	1.70
1000	0.1	2000	2000	0.2	0.3	0.4	21.78	20.73	1.05	0.48	2.20
100	0.3	2000	2000	0.2	0.3	0.4	7.92	7.4	0.52	1.01	12.75
500	0.3	2000	2000	0.2	0.3	0.4	14.32	13.83	0.49	1.04	7.26
800	0.3	2000	2000	0.2	0.3	0.4	15.87	15.48	0.39	1.14	7.18
100	0.1	3000	2000	0.2	0.3	0.4	19.02	17.1	1.92	0.39	2.05
500	0.1	3000	2000	0.2	0.3	0.4	30.37	28.71	1.66	0.13	0.43
800	0.1	3000	2000	0.2	0.3	0.4	31.92	31.11	0.81	0.72	2.26
1000	0.1	3000	2000	0.2	0.3	0.4	32.87	31.55	1.32	0.21	0.64
100	0.3	3000	2000	0.2	0.3	0.4	14.27	13.62	0.65	0.88	6.17
500	0.3	3000	2000	0.2	0.3	0.4	23.9	23.45	0.45	1.08	4.52
800	0.3	3000	2000	0.2	0.3	0.4	26.03	25.71	0.32	1.21	4.65
100	0.1	2000	3000	0.2	0.3	0.4	14.55	12.99	1.56	0.03	0.21
500	0.1	2000	3000	0.2	0.3	0.4	21.67	20.73	0.94	0.59	2.72
800	0.1	2000	3000	0.2	0.3	0.4	22.87	22.14	0.73	0.8	3.50
1000	0.1	2000	3000	0.2	0.3	0.4	23.42	22.63	0.79	0.74	3.16
100	0.3	2000	3000	0.2	0.3	0.4	9.82	9.29	0.53	1	10.18
500	0.3	2000	3000	0.2	0.3	0.4	16.31	15.97	0.34	1.19	7.30
100	0.1	3000	3000	0.2	0.3	0.4	21.55	19.56	1.99	0.46	2.13
800	0.1	3000	3000	0.2	0.3	0.4	33.16	32.42	0.74	0.79	2.38
1000	0.1	3000	3000	0.2	0.3	0.4	34.37	33.26	1.11	0.42	1.22
100	0.3	3000	3000	0.2	0.3	0.4	16.45	15.81	0.64	0.89	5.41
500	0.3	3000	3000	0.2	0.3	0.4	25.95	25.64	0.31	1.22	4.70
800	0.3	3000	3000	0.2	0.3	0.4	27.76	27.6	0.16	1.37	4.94
Group 11											
Burial Rate (R)	**Clay content (P)**	**RP Depth (D)**	**Relief (H)**	**CLS Size (S)**	**CLS Location (L)**	**CLS Depth (d)**	**f(X)**	**F(Y)**	**G(Z)**	**G(Z)-g(X*z)**	**Error %**
100	0.1	2000	2000	0.1	0.7	0.4	12.19	12.23	-0.04	0	0.00
100	0.1	3000	2000	0.1	0.7	0.4	19.02	18.5	0.52	0.56	2.94
500	0.1	3000	2000	0.1	0.7	0.4	30.37	30.07	0.3	0.34	1.12
100	0.1	2000	3000	0.1	0.7	0.4	14.55	14.27	0.28	0.32	2.20
100	0.1	3000	3000	0.1	0.7	0.4	21.55	21.11	0.44	0.48	2.23
Group 12											
Burial Rate (R)	**Clay content (P)**	**RP Depth (D)**	**Relief (H)**	**CLS Size (S)**	**CLS Location (L)**	**CLS Depth (d)**	**f(X)**	**F(Y)**	**G(Z)**	**G(Z)-g(X*z)**	**Error %**
100	0.1	2000	2000	0.2	0.7	0.4	12.19	11.41	0.78	0	0.00
500	0.1	2000	2000	0.2	0.7	0.4	19.71	19.17	0.54	0.24	1.22
800	0.1	2000	2000	0.2	0.7	0.4	21.21	20.82	0.39	0.39	1.84
1000	0.1	2000	2000	0.2	0.7	0.4	21.78	21.47	0.31	0.47	2.16
500	0.3	2000	2000	0.2	0.7	0.4	14.32	14.07	0.25	0.53	3.70
100	0.1	3000	2000	0.2	0.7	0.4	19.02	17.88	1.14	0.36	1.89
500	0.1	3000	2000	0.2	0.7	0.4	30.37	29.64	0.73	0.05	0.16

800	0.1	3000	2000	0.2	0.7	0.4	31.92	31.51	0.41	0.37	1.16
1000	0.1	3000	2000	0.2	0.7	0.4	32.87	32.53	0.34	0.44	1.34
100	0.3	3000	2000	0.2	0.7	0.4	14.27	13.86	0.41	0.37	2.59
500	0.3	3000	2000	0.2	0.7	0.4	23.9	23.64	0.26	0.52	2.18
800	0.3	3000	2000	0.2	0.7	0.4	26.03	25.84	0.19	0.59	2.27
100	0.1	2000	3000	0.2	0.7	0.4	14.55	13.89	0.66	0.12	0.82
500	0.1	2000	3000	0.2	0.7	0.4	21.67	21.44	0.23	0.55	2.54
100	0.3	2000	3000	0.2	0.7	0.4	9.82	9.55	0.27	0.51	5.19
100	0.1	3000	3000	0.2	0.7	0.4	21.55	20.56	0.99	0.21	0.97
500	0.1	3000	3000	0.2	0.7	0.4	31	30.7	0.3	0.48	1.55
100	0.3	3000	3000	0.2	0.7	0.4	16.45	16.11	0.34	0.44	2.67

Holding the four factors constant, the CLS effect may be expressed by three dimensional functions. This seems to be a good and effective method to reduce parameter order and function complexity. That is: $F(Y) = f(X) + G(Z) = f(X) + g(X^*, z)$ + error (from $g(X^*, z)$ to $G(Z)$ and LT error). From the 12 groups which have same the three variable factors, the four factors are: RP over-burden sedimentation rate is 100m/Ma, over-burden clay content is 0.1, aquifer depth is 2000 meters and relief is 2000 meters. In the parameter space, difference between "G(Zi)" and "g(X*,zi)" [$G(Zi) - g(X^*, zi)$] are all less than 8% of LT effect (f(Xi)), most of them are less than 5%: $[G(Z) - g(X^*, z)]/f(X) < 0.08$. So divide function G(Z) to two parts in thesis: $g(X^*, z)$ and error which value is less than 8% of LT effect.

Appendix C

This table presents the relationship between the three significant parameters (CLs size, location and depth) on CLs effect and overpressure change at the chosen reference point. As default in the Design Expert Package, the quadratic model was chosen. D-optimal design required 20 cases for the 3 factors. 108 models (detail as in Chapter 4.4, and Appendix B) simulated previously were used. These models are enough for quartic models which need 45 cases based on 3 factors. I used all results of 108 models as input to the D-optimal design, to get more accurate model determination and response surface results. In the table, column 7 means fitting result about g(X*, z) which from response surface, column 8 is error which is importance between g(X*, z) and h(z) on CLS fluid interaction g(X*,z), 100* (g(X*,z)-h(z))/g(X*z), the value is percentage. Column 9 is error which is importance between g(X*, z) and h(z) on LT effect f(X), 100* (g(X*,z)-h(z))/f(X), the value is percentage.

S	L	d	f(X) MPa	F(Y) MPa	CLS eff. g(X*,z)	h(z)	error with g(X*,z) %	error with f(x) %
0.1	0.2	0.1	12.19	9.37	2.82	2.37	16.04	3.71
0.1	0.2	0.2	12.19	10.3	1.89	1.96	3.84	0.60
0.1	0.2	0.3	12.19	10.86	1.33	1.56	17.09	1.86
0.1	0.2	0.4	12.19	11.16	1.03	1.15	11.84	1.00
0.1	0.2	0.6	12.19	11.35	0.84	0.34	59.35	4.09
0.1	0.35	0.1	12.19	10.24	1.95	1.80	7.69	1.23
0.1	0.35	0.2	12.19	10.92	1.27	1.51	18.75	1.95
0.1	0.35	0.3	12.19	11.3	0.89	1.22	36.66	2.68
0.1	0.35	0.4	12.19	11.61	0.58	0.92	59.37	2.83
0.1	0.35	0.6	12.19	11.6	0.59	0.34	42.27	2.05
0.1	0.5	0.1	12.19	10.86	1.33	1.23	7.35	0.80
0.1	0.5	0.2	12.19	11.3	0.89	1.05	18.39	1.34
0.1	0.5	0.3	12.19	11.56	0.63	0.88	38.93	2.01
0.1	0.5	0.4	12.19	11.7	0.49	0.70	42.19	1.70
0.1	0.5	0.6	12.19	11.73	0.46	0.34	26.14	0.99
0.1	0.6	0.1	12.19	11.16	1.03	0.85	17.12	1.45
0.1	0.6	0.2	12.19	11.48	0.71	0.75	5.74	0.33
0.1	0.6	0.3	12.19	11.67	0.52	0.65	24.59	1.05
0.1	0.6	0.4	12.19	11.78	0.41	0.54	32.93	1.11
0.1	0.6	0.6	12.19	11.79	0.4	0.34	15.20	0.50
0.1	0.7	0.1	12.19	11.4	0.79	0.48	39.86	2.58
0.1	0.7	0.2	12.19	11.61	0.58	0.45	22.79	1.08
0.1	0.7	0.3	12.19	11.75	0.44	0.42	4.42	0.16
0.1	0.7	0.4	12.19	11.84	0.35	0.39	12.35	0.35
0.1	0.7	0.6	12.19	11.83	0.36	0.34	5.93	0.18

0.15	0.2	0.1	12.19	8.24	3.95	3.04	22.92	7.43
0.15	0.2	0.2	12.19	9.62	2.57	2.43	5.57	1.17
0.15	0.2	0.3	12.19	10.35	1.84	1.81	1.67	0.25
0.15	0.2	0.4	12.19	10.73	1.46	1.19	18.39	2.20
0.15	0.2	0.5	12.19	10.91	1.28	0.57	55.17	5.79
0.15	0.35	0.1	12.19	9.29	2.9	2.50	13.88	3.30
0.15	0.35	0.2	12.19	10.39	1.8	1.99	10.72	1.58
0.15	0.35	0.3	12.19	10.93	1.26	1.49	18.15	1.88
0.15	0.35	0.4	12.19	11.2	0.99	0.98	0.57	0.05
0.15	0.35	0.5	12.19	11.29	0.9	0.48	46.66	3.44
0.15	0.5	0.1	12.19	10.08	2.11	1.95	7.58	1.31
0.15	0.5	0.2	12.19	10.88	1.31	1.56	19.02	2.04
0.15	0.5	0.3	12.19	11.27	0.92	1.17	26.98	2.04
0.15	0.5	0.4	12.19	11.46	0.73	0.78	6.47	0.39
0.15	0.5	0.5	12.19	11.51	0.68	0.39	43.19	2.41
0.15	0.6	0.1	12.19	10.48	1.71	1.59	7.30	1.02
0.15	0.6	0.2	12.19	11.11	1.08	1.27	17.58	1.56
0.15	0.6	0.3	12.19	11.42	0.77	0.95	23.96	1.51
0.15	0.6	0.4	12.19	11.58	0.61	0.64	4.78	0.24
0.15	0.6	0.5	12.19	11.6	0.59	0.32	45.11	2.18
0.15	0.7	0.1	12.19	10.8	1.39	1.22	12.21	1.39
0.15	0.7	0.2	12.19	11.28	0.91	0.98	7.75	0.58
0.15	0.7	0.3	12.19	11.53	0.66	0.74	12.24	0.66
0.15	0.7	0.4	12.19	11.66	0.53	0.50	5.46	0.24
0.15	0.7	0.5	12.19	11.66	0.53	0.26	50.69	2.20
0.2	0.2	0.1	12.19	8.5	3.69	3.72	0.85	0.26
0.2	0.2	0.2	12.19	9.39	2.8	2.89	3.26	0.75
0.2	0.2	0.3	12.19	10.07	2.12	2.06	2.77	0.48
0.2	0.2	0.4	12.19	10.78	1.41	1.23	12.69	1.47
0.2	0.2	0.5	12.19	11.58	0.61	0.40	34.28	1.72
0.2	0.35	0.1	12.19	9.16	3.03	3.19	5.44	1.35
0.2	0.35	0.2	12.19	9.93	2.26	2.48	9.64	1.79
0.2	0.35	0.3	12.19	10.6	1.59	1.76	10.77	1.40
0.2	0.35	0.4	12.19	10.91	1.28	1.04	18.41	1.93
0.2	0.35	0.5	12.19	11.75	0.44	0.33	25.54	0.92
0.2	0.5	0.1	12.19	9.83	2.36	2.67	13.05	2.53
0.2	0.5	0.2	12.19	9.94	2.25	2.06	8.24	1.52
0.2	0.5	0.3	12.19	10.97	1.22	1.46	19.77	1.98
0.2	0.5	0.4	12.19	11.36	0.83	0.86	3.34	0.23
0.2	0.5	0.5	12.19	12	0.19	0.25	33.88	0.53
0.2	0.6	0.1	12.19	9.94	2.25	2.32	2.96	0.55
0.2	0.6	0.2	12.19	10.28	1.91	1.79	6.34	0.99
0.2	0.6	0.3	12.19	10.83	1.36	1.26	7.27	0.81
0.2	0.6	0.4	12.19	11.48	0.71	0.73	3.29	0.19
0.2	0.6	0.5	12.19	11.96	0.23	0.21	10.63	0.20
0.2	0.7	0.1	12.19	10.15	2.04	1.97	3.65	0.61

0.2	0.7	0.2	12.19	10.94	1.25	1.51	21.06	2.16
0.2	0.7	0.3	12.19	11.04	1.15	1.06	7.73	0.73
0.2	0.7	0.4	12.19	11.41	0.78	0.61	21.94	1.40
0.2	0.7	0.5	12.19	12	0.19	0.16	17.52	0.27

The results showed that all cases "ε(h)" (the error does not contain ε(f), the total error will be analyzed later) is less than 10 percent of LT effect (f(x)), and over 80% cases have less than 5% error of LT effect. That means difference between the regression function "h (z)" and the objective function "g(X*,z)" is in an acceptable range.

Appendix D

For assessing CLSs interaction on overpressure on chosen reference point, a group of models with different CLSs position and size were created to investigate in which conditions, the two CLSs overall impact could be expressed as the individual impacts, in other words, the significance of difference between "G (Z)" and "h (z1) + h (z2)" compared with f(x). In the table, h(z1), h(z2) which in column 9 and 10 are means single CLS fluid interaction which from response surface. G(Z) in column 11 means 2 CLS overall fluid interaction on overpressure. Column 12 is difference between G(Z) and single CLS effect decomposition $\sum h(z)$, and column 13 is relative error between G(Z) and $\sum h(z)$ on LT effect f(X) "100*(G(Z)- $\sum h(z))/f(X)$", the value is percentage.

S1	L1	d1	S2	L2	d2	F(Y) MPa	f(X) MPa	h(z1)	h(z2)	G(Z)	G(Z) - (h(z1)+h(z2))	Error with f(X)%
0.1	0.2	0.1	0.1	0.35	0.4	7.49	12.19	2.37	0.92	4.70	1.41	11.55
0.1	0.2	0.1	0.1	0.2	0.6	8.27	12.19	2.37	0.34	3.92	1.21	9.93
0.1	0.6	0.4	0.1	0.7	0.1	9.97	12.19	0.54	0.48	2.22	1.20	9.84
0.1	0.35	0.1	0.1	0.6	0.4	8.68	12.19	1.80	0.54	3.51	1.17	9.56
0.1	0.6	0.1	0.1	0.7	0.4	9.78	12.19	0.85	0.39	2.41	1.16	9.54
0.1	0.2	0.4	0.1	0.35	0.1	8.13	12.19	1.15	1.80	4.06	1.11	9.09
0.1	0.2	0.1	0.15	0.35	0.5	8.17	12.19	2.37	0.48	4.02	1.17	9.62
0.1	0.2	0.1	0.15	0.2	0.4	6.72	12.19	2.37	1.19	5.47	1.91	15.67
0.1	0.2	0.1	0.15	0.35	0.4	6.98	12.19	2.37	0.98	5.21	1.86	15.24
0.1	0.2	0.6	0.15	0.2	0.1	7.09	12.19	0.34	3.04	5.10	1.71	14.06
0.1	0.35	0.1	0.15	0.7	0.4	8.23	12.19	1.80	0.50	3.96	1.66	13.61
0.1	0.2	0.1	0.15	0.2	0.5	7.62	12.19	2.37	0.57	4.57	1.63	13.36
0.1	0.35	0.1	0.15	0.6	0.4	8.16	12.19	1.80	0.64	4.03	1.59	13.05
0.1	0.35	0.1	0.15	0.2	0.4	7.66	12.19	1.80	1.19	4.53	1.54	12.62
0.1	0.35	0.1	0.15	0.35	0.4	7.89	12.19	1.80	0.98	4.30	1.52	12.43
0.1	0.7	0.1	0.15	0.7	0.4	9.72	12.19	0.48	0.50	2.47	1.49	12.25
0.1	0.7	0.1	0.15	0.35	0.4	9.25	12.19	0.48	0.98	2.94	1.48	12.15
0.1	0.7	0.1	0.15	0.6	0.4	9.62	12.19	0.48	0.64	2.57	1.46	11.94
0.1	0.6	0.1	0.15	0.7	0.4	9.39	12.19	0.85	0.50	2.80	1.45	11.86
0.1	0.6	0.1	0.15	0.6	0.4	9.32	12.19	0.85	0.64	2.87	1.38	11.30
0.1	0.6	0.1	0.15	0.35	0.4	8.98	12.19	0.85	0.98	3.21	1.37	11.25
0.1	0.35	0.6	0.15	0.2	0.1	7.5	12.19	0.34	3.04	4.69	1.30	10.70
0.1	0.35	0.1	0.15	0.35	0.5	8.72	12.19	1.80	0.48	3.47	1.19	9.76
0.1	0.35	0.1	0.15	0.2	0.5	8.69	12.19	1.80	0.57	3.50	1.13	9.24
0.1	0.35	0.6	0.15	0.35	0.1	8.25	12.19	0.34	2.50	3.94	1.10	9.04
0.15	0.2	0.1	0.15	0.35	0.5	6.4	12.19	3.04	0.48	5.79	2.27	18.58
0.15	0.6	0.4	0.15	0.7	0.5	9.23	12.19	0.64	0.26	2.96	2.06	16.90
0.15	0.2	0.5	0.15	0.35	0.1	7.23	12.19	0.57	2.50	4.96	1.89	15.50
0.15	0.6	0.4	0.15	0.6	0.5	9.44	12.19	0.64	0.32	2.75	1.79	14.66
0.15	0.35	0.1	0.15	0.7	0.5	7.69	12.19	2.50	0.26	4.50	1.74	14.28
0.15	0.35	0.1	0.15	0.6	0.5	7.63	12.19	2.50	0.32	4.56	1.74	14.26
0.15	0.2	0.1	0.15	0.35	0.4	6.65	12.19	3.04	0.98	5.54	1.51	12.39

0.15	0.35	0.5	0.15	0.7	0.1	9.04	12.19	0.48	1.22	3.15	1.45	11.89
0.15	0.35	0.5	0.15	0.6	0.1	8.68	12.19	0.48	1.59	3.51	1.44	11.85
0.15	0.35	0.1	0.15	0.7	0.4	7.91	12.19	2.50	0.50	4.28	1.28	10.51
0.15	0.35	0.1	0.15	0.6	0.4	7.86	12.19	2.50	0.64	4.33	1.19	9.79
0.15	0.6	0.1	0.15	0.7	0.4	8.93	12.19	1.59	0.50	3.26	1.17	9.63
0.15	0.2	0.1	0.15	0.3	0.1	7.95	12.19	3.04	2.31	4.45	-0.91	-7.46
0.15	0.2	0.1	0.15	0.4	0.1	7.74	12.19	3.04	2.13	4.52	-0.66	-5.39
0.15	0.2	0.1	0.15	0.45	0.1	7.67	12.19	3.04	1.95	4.59	-0.40	-3.32
0.15	0.2	0.1	0.15	0.5	0.1	7.6	12.19	3.04	1.77	4.64	-0.17	-1.41
0.15	0.2	0.1	0.15	0.55	0.1	7.55	12.19	3.04	1.22	4.49	0.23	1.85
0.15	0.2	0.1	0.15	0.7	0.1	7.7	12.19	3.04	2.43	4.68	-0.79	-6.49
0.15	0.2	0.1	0.15	0.2	0.2	7.51	12.19	3.04	2.14	4.65	-0.53	-4.37
0.15	0.2	0.1	0.15	0.3	0.2	7.54	12.19	3.04	1.99	4.67	-0.37	-3.02
0.15	0.2	0.1	0.15	0.35	0.2	7.52	12.19	3.04	1.85	4.62	-0.27	-2.24
0.15	0.2	0.1	0.15	0.4	0.2	7.57	12.19	3.04	1.70	4.61	-0.14	-1.14
0.15	0.2	0.1	0.15	0.45	0.2	7.58	12.19	3.04	1.56	4.60	0.00	-0.03
0.15	0.2	0.1	0.15	0.5	0.2	7.59	12.19	3.04	1.41	4.58	0.12	0.99
0.15	0.2	0.1	0.15	0.55	0.2	7.61	12.19	3.04	1.27	4.46	0.15	1.19
0.15	0.2	0.1	0.15	0.6	0.2	7.73	12.19	3.04	0.98	4.39	0.36	2.99
0.15	0.2	0.1	0.15	0.7	0.2	7.8	12.19	3.04	1.81	5.29	0.44	3.58
0.15	0.2	0.1	0.15	0.2	0.3	6.9	12.19	3.04	1.60	5.17	0.53	4.35
0.15	0.2	0.1	0.15	0.3	0.3	7.02	12.19	3.04	1.49	5.13	0.60	4.89
0.15	0.2	0.1	0.15	0.35	0.3	7.06	12.19	3.04	1.38	5.08	0.65	5.36
0.15	0.2	0.1	0.15	0.4	0.3	7.11	12.19	3.04	1.28	5.05	0.73	5.99
0.15	0.2	0.1	0.15	0.45	0.3	7.14	12.19	3.04	1.17	5.00	0.79	6.46
0.15	0.2	0.1	0.15	0.5	0.3	7.19	12.19	3.04	1.06	4.96	0.85	7.01
0.15	0.2	0.1	0.15	0.55	0.3	7.23	12.19	3.04	0.95	4.35	0.35	2.88
0.15	0.2	0.1	0.15	0.6	0.3	7.84	12.19	3.04	0.74	4.32	0.53	4.38
0.15	0.2	0.1	0.15	0.7	0.3	7.87	12.19	3.04	1.05	5.59	1.49	12.24
0.15	0.2	0.1	0.15	0.3	0.4	6.6	12.19	3.04	0.98	5.54	1.51	12.39
0.15	0.2	0.1	0.15	0.35	0.4	6.65	12.19	3.04	0.92	5.49	1.53	12.55
0.15	0.2	0.1	0.15	0.4	0.4	6.7	12.19	3.04	0.85	5.45	1.56	12.79
0.15	0.2	0.1	0.15	0.45	0.4	6.74	12.19	3.04	0.78	5.42	1.60	13.11
0.15	0.2	0.1	0.15	0.5	0.4	6.77	12.19	3.04	0.71	5.39	1.64	13.43
0.15	0.2	0.1	0.15	0.55	0.4	6.8	12.19	3.04	0.64	4.28	0.60	4.89
0.15	0.2	0.1	0.15	0.6	0.4	7.91	12.19	3.04	0.50	4.26	0.71	5.86
0.15	0.2	0.1	0.15	0.7	0.4	7.93	12.19	3.04	0.51	5.86	2.30	18.90
0.15	0.2	0.1	0.15	0.3	0.5	6.33	12.19	3.04	0.48	5.79	2.27	18.58
0.15	0.2	0.1	0.15	0.35	0.5	6.4	12.19	3.04	0.45	5.73	2.24	18.35
0.15	0.2	0.1	0.15	0.4	0.5	6.46	12.19	3.04	0.42	5.69	2.23	18.28
0.15	0.2	0.1	0.15	0.45	0.5	6.5	12.19	3.04	0.39	5.65	2.22	18.20
0.15	0.2	0.1	0.15	0.5	0.5	6.54	12.19	3.04	0.36	5.61	2.21	18.13
0.15	0.2	0.1	0.15	0.55	0.5	6.58	12.19	3.04	0.26	4.26	0.95	7.83
0.15	0.2	0.1	0.15	0.7	0.5	7.93	12.19	3.04	-0.03	5.15	2.14	17.52
0.15	0.2	0.1	0.15	0.3	0.6	7.04	12.19	3.04	-0.02	4.86	1.83	15.04

0.15	0.2	0.1	0.15	0.4	0.6	7.33	12.19	3.04	-0.01	4.73	1.70	13.92
0.15	0.2	0.1	0.15	0.45	0.6	7.46	12.19	3.04	0.00	4.59	1.55	12.71
0.15	0.2	0.1	0.15	0.5	0.6	7.6	12.19	3.04	0.00	4.45	1.40	11.51
0.15	0.2	0.1	0.15	0.55	0.6	7.74	12.19	1.96	1.96	0.00	-3.91	32.11

From the results, it is found that the parameter space was divided into two parts, one is that the overall effect of two CLSs on overpressure can be expressed as the effect of two single CLS: F(Yi)=f(Xi)+ $\sum_{o}^{i} \boldsymbol{g}(\boldsymbol{zi})$. In this condition, the relative distance of the two CLSs is generally large. The other one is that the effect of two CLSs overlay and need to be regressed with a single effect which is near to their overall effect on overpressures distribution: F(Yi)=f(Xi)+gg(zi), in which gg(zi) is "m1g(z1)+m2g(z2)", in this condition, two CLSs generally collapse together, or are very close in vertical distance and have a vertical overlap. The results also confirm: CLSs fluid interactions of CLSs changes by their relative distance.

Appendix E

This appendix sets the three squared channels near the aquifer, while LT parameters (R, C, D, H) are the same as previous. Because they have biggest fluid interaction by LT effect constant of all parameter space in this position, then setting one or two CLS in transitional position (figure 4-28 b) of the squared in condition of contact together (If the results are shared common feature in transition location and extreme positions, results of the CLS in others position of the squared should have the same feature). 44 cases were simulated in this section for viewing overall impact on overpressure expression; the parameter detail are showed in appendix E.

S1	L1	d1	S2	L2	d2	S3	L3	d3	F(Y)	f(X)
0.1	0.18	0.1	0.1	0.18	0.4	0.1	0.18	0.7	6.11	12.19
0.1	0.18	0.1	0.1	0.18	0.4	0.1	0.35	0.7	6.33	12.19
0.1	0.18	0.1	0.1	0.18	0.4	0.1	0.52	0.7	6.45	12.19
0.1	0.18	0.1	0.1	0.18	0.4	0.1	0.18	0.7	6.11	12.19
0.1	0.18	0.1	0.1	0.35	0.4	0.1	0.18	0.7	6.27	12.19
0.1	0.18	0.1	0.1	0.52	0.4	0.1	0.18	0.7	6.32	12.19
0.1	0.18	0.1	0.1	0.52	0.1	0.1	0.18	0.4	6.11	12.19
0.1	0.18	0.1	0.1	0.52	0.1	0.1	0.35	0.4	6.44	12.19
0.1	0.18	0.1	0.1	0.52	0.1	0.1	0.52	0.4	6.72	12.19
0.1	0.18	0.1	0.1	0.18	0.4	0.1	0.52	0.1	6.11	12.19
0.1	0.18	0.1	0.1	0.18	0.4	0.1	0.52	0.2	6.62	12.19
0.1	0.18	0.1	0.1	0.18	0.4	0.1	0.52	0.4	6.87	12.19
0.1	0.18	0.1	0.1	0.52	0.4	0.1	0.52	0.7	6.66	12.19
0.1	0.18	0.1	0.1	0.52	0.4	0.1	0.83	0.7	6.7	12.19
0.1	0.18	0.1	0.1	0.52	0.4	0.1	0.83	0.4	7.63	12.19
0.1	0.18	0.1	0.1	0.52	0.4	0.1	0.83	0.1	7.14	12.19
0.1	0.18	0.1	0.1	0.52	0.1	0.1	0.83	0.4	8.76	12.19
0.1	0.18	0.1	0.1	0.52	0.1	0.1	0.83	0.1	7.34	12.19
0.1	0.18	0.1	0.1	0.18	0.4	0.1	0.18	0.7	6.11	12.19
0.1	0.18	0.1	0.1	0.18	0.3	0.1	0.18	0.5	6.76	12.19
0.1	0.18	0.1	0.1	0.52	0.4	0.1	0.83	0.7	6.7	12.19
0.1	0.18	0.1	0.1	0.18	0.4	0.1	0.52	0.7	6.45	12.19
0.1	0.18	0.1	0.1	0.52	0.1	0.1	0.18	0.4	6.11	12.19
0.1	0.18	0.1	0.1	0.18	0.4	0.1	0.35	0.1	6.62	12.19
0.1	0.18	0.1	0.1	0.25	0.4	0.1	0.35	0.1	6.76	12.19
0.1	0.18	0.1	0.1	0.25	0.3	0.1	0.35	0.1	7.31	12.19
0.1	0.18	0.1	0.1	0.52	0.1	0.1	0.83	0.1	7.14	12.19
0.1	0.50	0.1	0.1	0.33	0.4	0.1	0.66	0.4	8.97	12.19
0.1	0.50	0.1	0.1	0.33	0.4	0.1	0.66	0.4	8.97	12.19

After analysis, all of the 44 cases showed the same feature that the overall impact of 3 CLS cluster on overpressure could be expressed as that of two of them being upscaled while the other is one impact decomposition. Hypothesis was proved correct and the simulation results showed the same feature with hypothesis.

Appendix F

A group of 20 synthetic cases containing multiple irregular channel-levee systems were created to investigate overpressure value on aquifer crest, analysis methods and results which studied in previous were used to predict overpressure value on reference point, and assessment applicability of the methods and results (systems character and GU interaction on overpressure on chosen reference point). The results were divided to two parts which are showed below:

Channel-levee systems position setting

S1	L1	D1	S2	L2	D2	S3	L3	D3	S4	L4	D4	S5	L5	D5	S6	L6	D6
0.1	0.18	0.1	0.1	0.26	0.4	0.1	0.53	0.1	0.1	0.67	0.7	0.1	0.83	0.5			
0.1	0.18	0.1	0.1	0.33	0.4	0.1	0.18	0.7	0.1	0.83	0.1	0.1	0.73	0.6			
0.1	0.18	0.1	0.1	0.16	0.6	0.1	0.53	0.1	0.1	0.5	0.7	0.1	0.83	0.3			
0.1	0.73	0.1	0.1	0.73	0.4	0.1	0.33	0.4	0.1	0.67	0.7	0.1	0.26	0.7			
0.1	0.18	0.1	0.1	0.26	0.4	0.1	0.53	0.1	0.1	0.67	0.7	0.1	0.83	0.5			
0.1	0.18	0.1	0.1	0.33	0.4	0.1	0.18	0.7	0.1	0.83	0.1	0.1	0.73	0.6			
0.1	0.18	0.1	0.1	0.16	0.6	0.1	0.53	0.1	0.1	0.5	0.7	0.1	0.83	0.3	0.1	0.83	0.7
0.1	0.73	0.1	0.1	0.73	0.4	0.1	0.33	0.4	0.1	0.67	0.7	0.1	0.26	0.7			
0.1	0.18	0.1	0.1	0.51	0.4	0.1	0.8	0.1	0.1	0.26	0.6						
0.1	0.18	0.1	0.1	0.51	0.4	0.1	0.8	0.1	0.1	0.26	0.6	0.1	0.77	0.7			
0.1	0.18	0.1	0.1	0.8	0.1	0.1	0.26	0.6	0.1	0.77	0.7						
0.1	0.18	0.1	0.1	0.8	0.1	0.1	0.26	0.6	0.1	0.77	0.7	0.1	0.51	0.1			
0.1	0.18	0.1	0.1	0.23	0.4	0.1	0.8	0.1	0.1	0.26	0.6	0.1	0.77	0.7			
0.1	0.18	0.1	0.1	0.36	0.3	0.1	0.8	0.1	0.1	0.26	0.6	0.1	0.77	0.7			
0.1	0.33	0.1	0.1	0.36	0.4	0.1	0.77	0.1	0.1	0.73	0.7						
0.1	0.33	0.1	0.1	0.36	0.4	0.1	0.77	0.1	0.1	0.73	0.7	0.1	0.23	0.7			
0.1	0.33	0.1	0.1	0.36	0.4	0.1	0.77	0.1	0.1	0.77	0.4	0.1	0.73	0.7			
0.15	0.21	0.1	0.15	0.35	0.5	0.15	0.75	0.1									
0.15	0.21	0.1	0.15	0.35	0.5	0.15	0.75	0.1	0.15	0.71	0.5						
0.15	0.21	0.1	0.15	0.35	0.5	0.15	0.75	0.1	0.15	0.71	0.5	0.1	0.2	0.7			
0.1	0.23	0.1	0.1	0.33	0.4	0.1	0.26	0.7	0.1	0.73	0.1	0.1	0.67	0.7			
0.1	0.23	0.1	0.1	0.33	0.4	0.1	0.26	0.7	0.1	0.73	0.1	0.1	0.77	0.6			
0.1	0.23	0.1	0.1	0.33	0.4	0.1	0.26	0.7	0.15	0.78	0.1	0.1	0.8	0.7			
0.1	0.23	0.1	0.1	0.33	0.4	0.1	0.26	0.7	0.15	0.78	0.1	0.15	0.75	0.5			

Analysis of results

F(Y)	h(z1)	h(z2)	h(z3)	h(z4)	h(z5)	h(z6)	h(z1,z2)	f(X) MPa	Total error %	F(Y) MPa
5.97	2.43	1.05	1.10	0.28	0.26		4.96	12.51	0.65	5.88
8.73	2.43	0.95	-0.07	-0.02	0.33		4.89	12.73	8.75	7.61
9.74	2.43	0.34	1.10	0.16	0.11		4.26	13.11	9.09	8.54
8.56	0.36	0.34	0.95	0.28	-0.01		2.67	12.51	0.40	8.61
5.97	2.43	1.05	1.10	0.28	0.26		4.96	12.51	0.65	5.88
8.73	2.43	0.95	-0.07	-0.02	0.33		4.89	12.73	8.75	7.61
9.74	2.43	0.34	1.10	0.16	0.11	0.41	4.26	13.11	9.09	8.54
8.56	0.36	0.34	0.95	0.28	-0.01		2.67	12.51	0.40	8.61

5.66	2.43	0.67	0.09	0.34			4.63	12.51	14.20	7.43
5.36	2.43	0.67	0.09	0.34	0.36		4.63	12.51	13.69	7.07
7.84	2.43	0.09	0.34	0.36				12.51	11.51	9.28
7.39	2.43	0.09	0.34	0.36	1.16			12.51	5.76	8.11
6.97	2.43	1.10	0.09	0.34	0.36		5.00	12.51	2.11	6.70
6.06	2.43	1.17	0.09	0.34	0.36		5.05	12.51	4.75	6.65
7.66	1.87	0.89	0.21	0.33			4.25	12.51	0.42	7.71
6.79	1.87	0.89	0.21	0.33	-0.04		4.25	12.51	7.78	7.75
6.68	1.87	0.89	0.21	0.28	0.33		4.25	12.51	12.62	5.10
6.23	2.98	0.48	1.03				5.09	12.51	1.23	6.38
5.34	2.98	0.48	1.03	0.25			5.09	12.51	6.34	6.13
5.34	2.98	0.48	1.03	0.25	-0.06		5.09	12.51	9.56	6.19
14.02	2.25	0.95	-0.01	0.36	0.28		4.73	15.01	19.02	11.16
12.15	2.25	0.95	-0.01	0.36	0.33		4.73	15.01	6.89	11.11
13.71	2.25	0.95	-0.01	0.91	0.38		4.73	15.01	21.31	10.51
13.30	2.25	0.95	-0.01	0.91	0.23		4.73	15.01	17.54	10.66

The simulations results were showed in second form, the biggest totally error on LT effect of them is also less than 30% which like previous single channel or cluster cases results. That means the methods of analysis GU interaction and system character on overpressure on chosen reference point could be well fit and correct in such random synthetic cases. The totally error, have not been increased by influence of their complexity, which still could maintain satisfactory range.

Reference Cited

1. N. T. T. Binnh, T.T., *Physical properties of the shallow sediments in late Pleistocene formations, Ursa Basin, Gulf of Mexico, and their implications for generation and preservation of shallow overpressures.* Marine and Petroleum Geology, 2009. 26: p. 474-486.
2. J. -C. Faugeres, A.F.L., L. Masse and S. Zaragosi, *The Columbia Channel-levee system: a fan drift in the southern Brazil Basin.* Geological Society, London, 2002. 22: p. 223-238.
3. E. D. SCOTT, F.G., S. J. JOLLEY, *Sedimentological control of fluid flow in deep marine turbidite reservoirs: Pierce Field, UK Central North Sea.* Geological Society, London, Special Publications, 2010. 347: p. 113-132.
4. Swarbrick, R.E., Osborne, M. J., Yardley, G. S., Macleod, G., Bigge, A., Grunberger, D., Aplin, A. C., & Larter, S., *Bean field-Integrated study of an overpressured Central North Sea oil/gas field.* Overpressure in Petroleum Exploration Workshop, 1998. 7-8 April Expanded Abstract.
5. Peter B. Flemings, B.B.S., Thomas Finkbeiner and Mark Zoback, *Flow focusing in overpressured sandstones: theory, observations, and applications.* American Journal of Science, 2002. 302: p. 827-855.
6. David N. Dewhurst, A.F.S., *Impact of stress and sedimentary anisotropies on velocity anisotropy in shale.* CSIRO Petroleum, 2004.
7. Barker, C., *Aquathermal pressuring: role of temperature in development of abnormal pressure zone.* Am. Ass. Petrol. Geol. Bull., 1972. 56: p. 2068-2071.
8. Powers, M.C., *Fluid-release mechanisms in compacting marine mudrocks and their importance in oil exploration.* Am. Ass. Petrol. Geol. Bull., 1967. 51: p. 1240-1245.
9. Magara, K., *Re-evaluation of montmorillonite dehydration as cause of abnormal pressure and hydrocarbon migration.* Am. Ass. Petrol. Geol. Bull., 1975. 59: p. 292-302.
10. Spencer, C.W., *Abnormal formational pressure caused by hydrocarbon generation-examples from the Rocky Mountain region.* Developments in Petroleum Science, 1994. 38: p. 343-372.
11. Wangen, M., *Pressure and temperature evolution in sedimentary basins.* Geophys. Int., 1992. 110: p. 601-613.
12. Ungerer, P., Bessis, D., Chenet, P. Y., Durand, B., Nogaret, E., Chianelli, A., Oudin, J. L. & Perrin, J. F., *Geological and geochematical models in oil exploration: principles and practical examples.* Petroleum Geochemistry and Basin Evaluation, 1984. 35: p. 53-77.
13. Dickinson, G., *Geological aspects of abnormal reservoir pressure in Gulf Coast Louisiana.* Am. Ass. Petrol. Geol. Bull., 1953. 37: p. 410-432.
14. Harrison, W.J.S., L. L., *Paleohydrology of the Gulf of Mexico Bain.* Am. Sci., 1991. 291: p. 109-176.
15. G. S. Yardley, R.E. Swarbrick., *Lateral transfer: a source of additional overpressure?* Marine and Petroleum Geology, 2000. 17: p. 523-537.
16. Science, I., *Geo-pressure Publications.* Ikon Science website. http://www.ikonscience.com/library/geopressure-publications.
17. kooi, H., *Insufficiency of compaction disequilibrium as the sole cause of high pore fluid pressure in pre-Cenozoic sediments* Bain Research, 1997. 9: p. 227-241.
18. S. M. Carmichael, S.A., J. K. Bennett, M. A. Fatimi, K. Hosein, R. W. Jones, M. B. Longacre, M. J. Osborne and R. S. J. Tozer, *Geology and hydrocarbon*

potential of the offshore Indus Basin, Pakistan. Petroleum Geoscience 2009, 2009. 15: p. 107-116.
19. Alam, T.D.a.Z., *Seismic stratigraphy of the offshore Indus Basin.* Geological Society, London, Special Publications, 2002. 195: p. 259-271.
20. F. Hadler-Jacobsen, M.H.G.a.J.M.B., *Seismic stratigraphic and geomorphic analysis of deep-marine deposition along the West African continental margin.* Geological Society, London, 2007. 277: p. 47-84.
21. Smith, R.I., Hodgson, N. & Fulton, M, *Salt control on Triassic reservoir distribution, UKCS Central North Sea.* Petroleum Geology of Northwest Europe,, 1993. 4: p. 547-558.
22. Hossack, J., *Geometric rules of section balancing.* American Association of Petroleum Geologists,, 1995. 65: p. 29-40.
23. Davison, I., Alsop, I., Birch, P., Elders, C., Evans, N., Nicholson, H., Rorison, P., Wade, D., Woodward, J., & Young, M., *Geometry and late-stage structural evolution of Central Graben salt diapirs, North Sea.* Marine and Petroleum Geology, 1999.
24. R.E Swarbrick, M.J.O., D Grunberger, G.S Yardley, *Integrated study of the Judy Field (Block 30/7a) — an overpressured Central North Sea oil/gas field.* Marine and Petroleum Geology, 2000. 17(9): p. 993-1010.
25. Posamentier, H.W., *Depositional elements associated with a basin floor channel-levee system: case study from the Gulf of Mexico.* Marine and Petroleum Geology, 2003. 20: p. 677-690.
26. Russell B. Wynn, B.T.C., Jeff Peakall, *Sinuous deep-water channels: Genesis, geometry and architecture.* Marine and Petroleum Geology, 2007. 24: p. 341-387.
27. J. N. Fowler, E.G., P. Sherwood, M. J. Smith, S. Algar, I. Busono, G.Goffey & A. Strong, *Depositional architectures of Recent deepwater deposits in the Kutei Basin, East Kalimantan.* The Geological Society of London, 2004. 29: p. 25-33.
28. Sawyer, D., Flemings, P.B., Dugan, B., Shipboard Scientific Party, IODP Expedition 308, *Lateral variations in core, log, and seismic attributes of a mass transport complex in the ursa region, IODP expedition 308, Northern Gulf of Mexico.* In: Proceedings of the Offshore Technology Conference, Houston, Texas, 2007b. April 30- May 3: p. OTC Paper 19098.
29. Kneller, B., *The influence of flow parameters on turbidite slope channel architecture.* Marine and Petroleum Geology, 2003. 20: p. 901-910.
30. Peakall, J., McCaffrey, W.D., Kneller, B.C., *A process model for the evolution, morphology, and architecture of sinuous submarine channels.* Journal of Sedimentary Research, 2000. 70: p. 434-448.
31. Peirmez, C., Imran, J., *Reconstruction of turbidity currents in Amazon Channel.* Marine and Petroleum Geology, 2003. 20: p. 823-849.
32. Clark, J.D., Pickering, K.T., *Submarine Channels: Process and Architecture.* Vallis Press, London, 1996. 231pp.
33. Athy, L.F., *Density, porosity and compaction of sedimentary rocks.* American Association of Petroleum Geologists Bulletin, 1930. 31: p. 241-287.
34. Smith, J.E., *The dynamics of shale compaction and evolution of pore fluid pressure.* Mathematical Geology, 1971. 3: p. 239-263.
35. Sharp, J.M.D., A., *Energy transport in thick sequences of compacting sediments.* Geological Society of America Bulletin, 1976. 87: p. 390-400.
36. Yukler, M.A., Cornford, C. & Welte, D.H., *One dimensional model to simulate geomogic, hydrodynamic and thermodynamic development of a sedimentary basin.* Geologiscbe Rundscbau, 1978. 67: p. 960-979.

37. Bethke, C.M., *A numerical model of compaction driven ground water flow and heat transfer and its application to the paleohydrology of intractratonic sedimentary basins.* Journal of Geophysical Research, 1985. 90: p. 6817-6828.
38. Lerche, I., *Basin Analysis. Quatitative methods.* Academic Press, 1990.
39. Ungerer, P., Burrus, J., Doligez, B., Chenet, J.Y. & Bessis, F., *Basin evaluation by integrated two-dimensional modeling of heat transfer, fluid-flow, hydrocarbon generation and migration.* American Association of Petroleum Geologists Bulletin, 1990. 74: p. 309-355.
40. Luo, X.V., G., *Contributions of compaction and aquathermal pressure to geopressure and the influence of enviormental conditions.* American Association of Petroleum Geologists Bulletin, 1992. 76: p. 1550-1559.
41. Hermanrud, C., *Basin modeling techniques - an overview.* Basin Modelling Advance and Applications, 1993. Special Publication, 3.: p. 1-34.
42. Schneider, F., Burrus, J. & Wolf, S., *Modelling overpressure by effective-stress/porosity relationships in low-permeability rocks: empirical artifice of physical reality?* Basin modelling: Advances and Applications., 1993. Norwegian Petroleum Society (NPF) Special Publication, 3.: p. 333-341.
43. Audet, M.D., *Compaction and overpressuring in Pleistocene sediments on the Luisian Shelf, Gulf of Mexico.* Journal of Geochemical Exploration, 1996. 78-79: p. 449-451.
44. Gibson, R.E., *The progress of consolidation in clay layer increasing in thickness with time.* Geotechnique, 1958. 8: p. 171-181.
45. Bredehoeft, J.D.H., B. B., *On the maintenance of anomalous fluid pressure-1, Thick sedimentary sequences.* Geol. Soc. Am. Bull., 1968. 79: p. 1097-1106.
46. B.B. Hanshaw, J.D.B., *On the maintenance of anomalous fluid pressures: II. Source layer at depth.* Bulletin of the Geological Society of America, 1968. 79: p. 1107–1122.
47. Terzaghi, K., *Theoretical soil mechanics.* Wiley, New York 1943.
48. Smith, J.E., *The dynamics of shale compaction and evolution of pore fluid pressure.* Mathematical Geology 1971. 3: p. 239-263.
49. Audet, D.M.M., J. D. C., *Forawrd modelling of porosity and pore pressure evolution in sedimentary basins.* Basin Res, 1992. 4: p. 147-162.
50. Gaarenstroom, L., Tromp, R. A. J., de, Jong, M. C., & Brandenburg, A. M., *Overpressure in the central North Sea: implications for trap integrity and drilling safety.* In petroleum Geol. of Northwest Europe: proceedings of the 4th Conference, 1993: p. 1305-1313.
51. Traugott, M., *The pore pressure Centroid Concept: reducing drilling risks.* In Abstract: Compaction and Overpressure Current Research, 1996. 9-10 December.
52. Traugott, M., *Pore/fracture pressure determinations in deep water.* Deepwater Technology, 1997. 218(8): p. 68-70.
53. Osborne, M.J., & Swarbrick, R. E., *Mechanisms for generating overpressure in sedimentary basins: a reevaluation.* American Association of Petroleum Geologists Bulletin, 1997. 81: p. 1023-1041.
54. Traugott, P.H., *Prediction of pore pressure before and after drilling—taking the risk out of drilling overpressured prospects.* AAPG Hedberg Conference, 1994.
55. Bowers, G.L., *Pore pressure estimation from velocity data: accounting for overpressure mechanisms besides undercompaction.* IADC/SPE conference dallas, 1994. paper 27488: p. 515-530.
56. Schneider, F., Bouteca, M., & Vasseur, G., *Validity of the porosity/effective-stress concept in sedimentary basin modelling.* First Break, 1994. 12(6): p. 321-326.

57. Mann, D.M., & Mackenzie, A. S., *Prediction of pore fluid pressures in sedimentary basins.* Marine and Petroleum Geology, 1990. 7: p. 55-65.
58. Doligez, B., Bessis, F., Burrus, J., Ungerer, P. & Chenet, P. Y., *Integrated numerical modelling of the sedimentation, heat transfer and fluid migration in a sedimentary basin: the Themis model.* Thermal Modeling of Sedimentary Basins, 1986: p. 567-596.
59. Hudson, J.D., *Sedimentation rates in relation to the Phanerozoic time-scale.* Geological Society, London, Special Publications, 1964. 1: p. 37-42.
60. Gorden, D.S., and Flemings, P. B., *Generation of overpressure and compaction-driven fluid flow in a Plio-Pleistocene growth-faulted basin, Eugene Island 330, offshore Louisiana.* Basin Research, 1998. 10: p. 177-196.
61. Yunlai Yang, A.C.A., *A permeability–porosity relationship for mudstones.* Marine and Petroleum Geology, 2010. 27: p. 1692-1697.
62. Y. Yang, A.C.A., *Definition and practical application of mudstone porosity-effective stress relationships.* Petroleum Geoscience, 2004. 10: p. 153-162.
63. PetroMod, *IES PetroMod release 4.0, technical aspects.* Intergated Exploration Systems, 1998.
64. K. Bjørlykke, K.H., *Effects of burial diagenesis on stresses, compaction and fluid flow in sedimentary basins.* Marine and Petroleum Geology, 1997. 14: p. 267-276.
65. Marte Gutierrez, M.W., *Modeling of compaction and overpressuring in sedimentary basins.* Marine and Petroleum Geology, 2005. 22: p. 351-363.
66. Wilson, G.E.P.B.a.K.B., *On the Experimental Attainment of Optimum Conditions.* Journal of the Royal Statistical Society. Series B (Methodological), 1951. 13, No. 1: p. 1-45.
67. ASA, C., *Design of Experiment (DoE).* http://www.camo.com/rt/Resources/design_of_experiment.html, 2002-2009.
68. Peng, C.Y.a.G., R., *Experimental Design in Deterministic Modeling: Assessing Significant Uncertainties.* SPE Asia Pacific Oil and Gas Conference and Exhibition, Jakarta, Indonesia, 2003: p. 9-11.
69. Jinaporn Prasanphanich, M.S.E., *Gas reserves Estimation by Monte Carlo Simulation and Chemical Flooding Optimization using Experimental Design and Response Surface Methodology.* The University of Texas at Austin, 2009.
70. Myers, R.H.a.M., D.C., *Response Surface: Process and Product Optimization Using Designed Experiments.* Second Edition, John Wiley & Sons, New Jersey, 2002.
71. NIST/SEMATECH, *e-handbook of statistical Methods.* http://www.itl.nist.gov/div898/handbook/.
72. Mason, R.L., Gunst, R.F., and Hess, J.L., *Statistical Design and Analysis of Experiments with Applications to Engineering and Science.* John Wiley & Sons, New York, 1989.
73. Montgomery, D.C., *Design and Analysis of Experiments.* Fifth Edition, John Wilety and Sons, New York, 2001: p. 170-387.
74. P.F. de Aguiar, Bourgucygnon. M.S. Khots, D.L. Massart, R. Phan-Than-Luu, *D-optimal designs.* Chemometrics and Intelligent Laboratory Systems, 1995. 30: p. 199-210.
75. Nachtsheim, R.D.C.a.C.J., *Technometrics.* 1980. 22: p. 315.
76. Draper, R.C.S.J.a.N.R., *Technomertrics.* 1975. 17: p. 15.
77. Fedorov, V.V., *Theory of Optimal Experiments.* Moscow Unversity, 1972.
78. Carlson, R., *Design and Optimization in Organic Synthesis.* Amsterdam, 1992. chapter 7.
79. Mitchell, T.J., *Technometrics.* 1974. 16: p. 203.

80. Schlomer, S., & Krooss, B. M., *Experimental characterisation of the hydrocarbon sealing efficiency of cap rocks.* Marine and Petroleum Geology, 1997. 14: p. 565-580.
81. D. W. WAPLES , G.D.C., *Some thoughts on porosity reduction- rock mechanics, overpressure and fluid flow.* Consultant, 9299 William Cody Drive, Evergreen, CO 80439 USA. Department of Geology and Applied Geology, University of Glasgow, Glasgow G12 8QQ, UK (Present address: Department of Petroleum Engineering, Heriot-Watt University, Edinburgh EH14 4AS, UK), 1998.
82. Sadler, D.R., *Intuitive data processing as a potential source of bias in naturalistic evaluations.* Educational Evaluation and Policy Analysis, 1981. 3(4): p. 25–31.
83. Holmes, A., *A revised geological time-scale.* Trans. Edinb. geol. Soc, 1959. 17: p. 183-216.
84. KULP, J.L., *Geologic time scale.* Science, 1961. 133.
85. J. Robertson, N.R.G.a.R.E.S., *Overpressure distribution in Palaegene reservoirs of the UK Central North Sea and implications for lateral and vertical fluid flow.* Petroleum Geoscience, 2013. 19: p. 223-236.
86. Stump, B.B., *Illuminating basinal fluid flow in Eugene Island 330 (Gulf of Mexico) through in situ observations.* Master of Science, 1998.
87. Swawyer, D.E., Flemings, P.B., Shipp, C., Winker, C., *Seismic geomorphology, lithology, and evolution of the late Pleistocene Mars0Ursa turbidite mini0basin, Northern Gulf of Mexico.* American Association of Petroleum Geologists Bulletin, 2007a. 91(2): p. 215-234.